MOLECULAR MECHANISMS UNDERLYING THE ACTION OF HISTONE DEACETYLASES INHIBITORS (HDACIs) IN OVARIAN CANCER

Fernanda Maria Gonçalves da Silva

Orientadora: Ana Maria Félix de Campos Pinto, Professora Associada

Co-orientadora: Jacinta Serpa, Professora Auxiliar

Tese para obtenção do grau de Doutor em Ciências da Vida

na Especialidade em Biomedicina

Dezembro, 2016

The result chapters presented in this thesis are manuscripts published or in preparation for subsequent publications. I clarify that I have participated fully in the conception and execution of the experimental work, interpretation of the results and manuscript drafting.

The work was approved by the Ethical Committee of Nova Faculty of Medicine (1/2015) and by the IPOLFG (UIC-938).

INDEX

ABSTRACT

Epithelial ovarian cancer (EOC) is the most lethal gynecological malignancy, despite advances in treatment. The most common histological type, high grade serous carcinoma (HGSC) is usually diagnosed at an advanced stage, and although this type of tumors frequently responds to surgery and platinum-based chemotherapy, they usually recur. Ovarian clear cell carcinoma (CCC) is an unusual histological type, which is known to be intrinsically chemoresistant and is associated with poor prognosis in advanced stages. Hence, the discovery of new therapeutic strategies urges and the fact that histone deacetylases (HDACs) expression is increased in ovarian cancer points out HDAC inhibitors (HDACIs) as an attractive approach.

Our hypothesis is that HDACIs are useful drugs to treat ovarian cancer. So, the main goal was to disclose the molecular mechanisms underlying the action of HDACIs in ovarian cancer.

We investigated the expression profile of HDAC, class I (HDAC1, 2, 3) and class II (HDAC4, 6 and phosphoHDAC4/5/7) in ovarian cancer. HDACs protein expression was analyzed by immunohistochemistry on tissue microarrays (TMA) from 64 patients with ovarian cancer (49 cases of HGSC and 15 cases of CCC). Our results showed that HGSC expressed HDAC1, 2, 3, 4, 6 and phosphoHDAC4/5/7 whereas CCC expressed HDAC1, 2 and 6. HDAC2, 3, 4 and pHDAC4/5/7 were associated with HGSC type. Kaplan-Meier curves showed that HDACs expression was not associated with survival. We also evaluated the association of HDACs expression profile with the cell cycle markers and we found that HDAC1 expression was statistically associated with p21 expression in HGSC.

In order to understand the effects of HDACIs we used cancer cell lines (OVCAR3 and ES2) exposed to HDACIs, butyric acid and vorinostat, 5-aza-2´-deoxycytidine (DNA methylation inhibitor) and carboplatin and paclitaxel (standard chemotherapy) alone and combined. Analysis of cell death, proliferation and migration in cancer cell lines was performed. Our results showed, that both HDACIs induced cell death, mainly through apoptosis in the two cell lines. This result was further confirmed in ES2 cell

line exposed to vorinostat, by the study of immunofluorescence of cleaved caspase 3 and the *ratio* of BAX/BCL-2 proteins, which increased after vorinostat exposure. Cell migration was decreased by vorinostat in both cancer cell lines. Our results also indicated that the association of different drugs were able to potentiate the effect of standard chemotherapy, mainly in ES2 cell line (CCC), supporting that EOC treatment can benefit from combined chemical and epigenetic therapy.

Considering that CCC is a unique clinical, histopathological and molecular entity within ovarian cancer and having HNF1β as a pivotal pro-survival gene we evaluate the role of HNF1β in cell cycle arrest and apoptosis in CCC upon vorinostat exposure. Our results showed that vorinostat induced increased levels of HNF1β and at the same time cell cycle arrest and apoptosis in ES2 cells. This effect on HNF1β is associated with increased acetylation load of HNF1β. This study confirms that epigenetic modulation affects not only the conformation of chromatin and gene expression, but also it may alter the function and the *turnover* of proteins other than histones.

Also, epigenetic modulation of signaling pathways have been reported in HGSC and CCC**,** including the overexpression of Notch pathway elements and we investigated the modulation of the Notch pathway by vorinostat in ovarian cancer. Using immunofluorescence and quantitative polymerase chain reaction, our results revealed that vorinostat activated the Notch pathway in CCC and HGSC cell lines, through different Notch ligands. The activation of Notch pathway by vorinostat, in CCC and HGSC cell lines, culminated in the increased expression of the same downstream transcription factors, hairy enhancer of split (*Hes1) 1 and 5, and Hes-related proteins 1* and *2.* Therefore, vorinostat modulates the expression of several downstream targets of the Notch pathway and independent Notch receptors and ligands that are expressed in HGSC and CCC. This upregulation of the Notch pathway may explain why vorinostat therapy fails in ovarian carcinoma treatment, as shown in certain clinical trials.

We also established a cell line from ascitic fluid from a patient with HGSC, who had been previously treated with neoadjuvant chemotherapy. The cell spontaneous immortalization was obtained on 2D cell culture and expansion was performed on 2D

and 3D cell cultures. Characterization studies confirmed that IPO-SOC43 cell line is of EOC origin and maintains morphological and molecular features of the primary tumor. The success of the cell line growth in a 3D systems, allows it to be used in more complex assays than those performed in 2D models. IPO-SOC43 is available for public research and we hope it can contribute to enrich the *in vitro* models addressing EOC heterogeneity, being useful to investigate EOC and to develop new therapeutic modalities.

In conclusion, the results *in vitro* proved that there is benefits of combined therapy, using drugs with action of epigenetic modulation and conventional therapy. This thesis also pave the path for future studies on the role of HDACs cancer cells pathophysiology, serving as markers for the design of personalized and specific therapeutic strategies.

Keywords: ovarian cancer, HDAC, HDACIs, HGSC, CCC

RESUMO

O carcinoma do ovário é a neoplasia ginecológica mais letal. Vários fatores são identificados como responsáveis pela baixa eficácia no tratamento do carcinoma do ovário. Assim, é postulado que a elevada taxa de mortalidade se deve principalmente, a dificuldades no diagnóstico da doença numa fase inicial e à resistência à terapêutica convencional. Deste modo, a investigação de novas estratégias terapêuticas é essencial e urgente.

A expressão aumentada das desacetilases de histonas (HDAC) identificada em carcinomas do ovário pode indicar que os inibidores de HDACs (HDACIs) possam ser uma alternativa terapêutica. Os HDACIs são uma classe de agentes anti-neoplásicos, que bloqueiam a desacetilação de histonas e outras proteínas, causando paragem do ciclo celular, diferenciação e/ou apoptose das células neoplásicas. Vários HDACIs estão a ser testados em ensaios clínicos, quer como agentes únicos quer em terapias combinadas, apresentando alguns resultados positivos no combate a vários tumores sólidos e hematológicos. Os mecanismos moleculares do efeito anti-tumoral dos HDACIs não estão completamente esclarecidos, nem a avaliação da sensibilidade e/ou resistência das células a fármacos com influência na regulação epigenética.

O cancro do ovário é um conjunto vasto de neoplasias distintas sendo os carcinomas o grupo mais prevalente. Atualmente, não é possível, de modo fiável prever o curso clínico da doença nem a resposta individual à quimioterapia. No entanto, a identificação morfológica do tipo de carcinoma do ovário tem valor prognóstico independente em análise multivariada, pelo que a avaliação de potenciais biomarcadores que possam constituir alvos terapêuticos deverá ser efetuada de modo independente, pois previsivelmente cada tipo histológico deverá ter uma resposta específica ao tratamento.

Por estas razões, a hipótese geral desta tese é que os HDACIs são fármacos úteis no tratamento do cancro do ovário, sendo o objetivo a avaliação de mecanismos subjacentes à ação destes fármacos em carcinomas de ovário de modo a permitir uma terapêutica mais eficaz.

Neste projeto foram estudados apenas dois tipos histológicos de carcinoma do ovário: seroso de alto grau (HGSC), que é o mais frequente e o carcinoma de células claras (CCC) que apesar de pouco frequente é atualmente resistente à terapia convencional.

Assim, um dos primeiros objetivos desta tese foi caracterizar o perfil de expressão das HDACs em carcinomas do ovário e validar a relevância de testar HDACIs como agentes de regulação epigenética, no tratamento do carcinoma do ovário. Os resultados em doentes com cancro do ovário mostram que o perfil de expressão das HDACs se associa ao tipo histológico. No HGSC verifica-se uma associação das HDACs 2, 3, 4 e das HDAC4/5/7 fosforiladas, enquanto que no carcinoma de células claras (CCC), as HDAC1, 2 e 6 apresentam níveis elevados de expressão e verifica-se uma diminuição da expressão da HDAC3, HDAC4 e das HDAC4/5/7 fosforiladas. A expressão das HDACs 2, 3, 4 e das HDAC4/5/7 fosforiladas estão associadas ao tipo histológico sendo mais expressas no HGSC. A expressão da HDAC3 está ainda associada a parâmetros clínicos, nomeadamente ao estádio mais avançado e à metastização; bem como a HDAC4c e a HDAC4/5/7 fosforiladas.

Considerando que as HDACs estão sobre-expressas nestes tipos histológicos de carcinomas do ovário, seguidamente, pretendemos avaliar o efeito epigenético dos HDACIs em modelos *in vitro* de carcinoma de ovário e compreender as alterações decorrentes da exposição aos HDACIs, bem como perceber o efeito destes na dinâmica molecular e viabilidade celular. Para tal, usamos duas linhas celulares, de dois tipos histológicos já avaliados, uma linha de HGSC - OVCAR3 e uma linha celular de CCC - ES2.

Os resultados indicam que os HDACI induzem a morte celular em ambas as linhas celulares, principalmente através da apoptose, avaliada por citometria de fluxo. Este resultado foi evidenciado na linha celular ES2 exposta ao vorinostat, pelo estudo da imunofluorescência da caspase 3 clivada e da avaliação da razão das proteínas BAX/BCL-2, que aumentou após a exposição ao vorinostat. Os resultados também indicam que a associação de diferentes tipos de fármacos potencia o efeito da quimioterapia convencional e os HDACIs, em particular o vorinostat, tendo um efeito

cumulativo na morte celular, principalmente na linha celular ES2 (CCC). A migração celular também é afetada pelo vorinostat em ambas as linhas celulares de carcinoma de ovário.

Os resultados mostram também que o vorinostat induz aumento do HNF1β e ao mesmo tempo paragem do ciclo celular e apoptose nas células ES2. O aumento da expressão do HNF1β é acompanhado pelo aumento dos seus níveis da acetilação.

Este estudo confirma que a modulação epigenética afeta a conformação da cromatina e da expressão genética, mas também pode alterar a função e o *turnover* de outras proteínas além das histonas. Pela primeira vez é observado que a proteína HNF1β pode ser acetilada, contudo serão necessários mais estudos para validar o papel da acetilação na função e degradação da proteína HNF1β.

Nesta tese foi avaliado também a modulação de outras vias de sinalização importantes no carcinoma do ovário, como por exemplo a via Notch através da exposição a HDACIs, nomeadamente vorinostat e ácido butírico. E os nossos resultados mostram que o vorinostat ativa a via Notch nas linhas celulares de CCC e HGSC, através de diferentes ligandos da via Notch. No CCC, a ativação da via Notch parece ocorrer através dos ligandos Delta (Dll) 1, 2 e 3, enquanto nos HGSC, os ligandos Dll1, Jagged 1 e 2 são os mais expressos. A ativação da via Notch pelo vorinostat, em ambas linhas celulares, culminou na expressão aumentada dos mesmos genes alvo da via Notch, Hes1 e 5 e Hey 1 e 2.

Assim, o vorinostat modula a expressão de vários fatores de transcrição da via Notch, independentemente do painel de receptores e dos ligandos expressos nas linhas de HGSC e CCC. Esta redundância da via Notch pode explicar porque a terapêutica isolada com vorinostat falha no tratamento do carcinoma do ovário, como observado em vários ensaios clínicos.

Por fim, no decorrer dos trabalhos apresentados, e considerando a importância das linhas celulares na compreensão da biologia do cancro e nos mecanismos de sensibilidade e resistência das células aos fármacos, foi estabelecida uma linha celular, IPO-SOC43 a partir de líquido ascítico de uma doente com HGSC que havia sido previamente tratada com quimioterapia neoadjuvante.

Foram efetuados estudos de caracterização desta linha que demonstram que a linha celular IPO-SOC43 é de origem epitelial e que mantém características morfológicas e moleculares do tumor primário. As células mantêm-se em cultura em monocamada (2D) e em agregados em 3D, com taxas de proliferação e viabilidade dentro do esperado para uma linha neoplásica maligna. O sucesso da viabilidade em culturas 3D permite o seu uso em ensaios mais complexos, nomeadamente, na análise da contribuição dos vários componentes do microambiente tumoral na progressão da doença e resposta à terapêutica.

A linha celular IPO-SOC43 está disponível para ser utilizada experimentalmente e esperamos que possa contribuir para enriquecer os modelos *in vitro* que abordam a heterogeneidade dos EOC e desenvolver novas modalidades terapêuticas.

Em suma, os resultados contribuem para a implementação racional de novas e diferentes abordagens terapêuticas. Os resultados mostram que *in vitro* há benefício de terapêutica combinada, utilizando fármacos com ação de modelação epigenética e terapia convencional. Esta tese também abre caminho para estudos futuros mais detalhados sobre a função das HDACs na dinâmica celular e não só na regulação epigenética, bem como também na análise de mecanismos subjacentes à ação de proteínas codificadas por genes relevantes em cada tipo histológico de carcinoma do ovário.

Espera-se assim, que a compreensão dos mecanismos subjacentes à ação dos fármacos envolvidos na regulação epigenética possa fornecer orientações para estratégias terapêuticas mais específicas e personalizadas.

Palavras-chave: carcinoma ovário, HDAC, HDACIs, HGSC, CCC

FIGURE INDEX

TABLE INDEX

ACKNOWLEDGMENTS

This PhD thesis would not be possible without a large number of contributions, and for this reason I would like to express my gratitude to my supervisors, Ana Félix, for all the precious mentoring, guidance and motivation and to Jacinta Serpa for guiding me in the field of molecular biology, teaching me professional attitude towards designing, conducting and evaluating laboratory experiments. Both of them generously shared their time and expertise with me, were always open to answer my questions and discuss my ideas and were critical and supportive at the same time. I am deeply indebted to them for helping me.

I am also thankful for all former and present members of the UIPM with a very special thanks to Leonor Remédio, Francisco Caiado, Germana Domingues, Lídia Silva, Sofia Gouveia and Filipa Coelho for all the good work environment, great friendship and helpful discussions.

I would like to thank to the director José Cabeçadas, doctors and all colleagues of the Pathology Department of IPOLFG, especially to Teresa Pereira, Sónia Araújo, Filipa Areia, Cátia Teixeira, Arsénia Manhita and Filipa Antunes for creating a motivating and pleasant working atmosphere. From IPOLFG, I also thank Carmo Martins for her precious help with CGH and to António Guimarães for the valuable clinical data.

I would like to thank to Vitor Espírito Santo and Catarina Brito, from IBET for sharing your knowledge of 3D cultures.

Last, but not least, I would like to thank my parents and my family for their continuous support and encouragement. To my husband, for his patience and caring attention during my study and to my sons Pedro and Tiago for the endless love and kindness.

LIST OF PUBLICATIONS

The author declares that has designed and performed research, collected and analyzed data, and wrote the text of the published paper, and the manuscripts in preparation, which are part of this dissertation.

Published original paper:

Silva, F., Félix, A. & Serpa, J. Functional redundancy of the Notch pathway in ovarian cancer cell lines. *Oncol. Lett.* **12,** 2686–2691 (2016).

Published in proceedings (Poster):

Silva, F., Serpa, J., Domingues, G., Silva, G., Almeida, A., Félix, A. Cell death induced by HDACS inhibitors in ovarian cancer cell lines (serous and clear cells carcinomas) – role of NOTCH, TP53 and FN1. BMC Proceedings, 4(Suppl 2):P36 (2010).

Silva, F., Serpa, J., Fernandes, S., Dias, S., Félix, A. HDACS inhibitors effects in Ovarian Clear Cell Carcinoma. SINAL, 6th National Meeting, April, UMinho (2012).

Silva, F., Fernandes, S., Félix, A., Serpa, J., Vorinostat Increases ARID1A splicing variant expression which may regulate HNF1β and cell survival, in Ovarian Clear Cell Carcinoma (CCC). International Journal of Gynecological Cancer, 23 (8) (2013)

Silva, F., Coelho, F., Fernandes, S., Félix, A., Serpa, J., Vorinostat induces HNF1β expression and latency in ovarian clear cell carcinoma (OCCC) and resistance in ovarian serous carcinoma (OSC), EACR-AACR-SIC, Anticancer Drug Action and Drug Resistance: from Cancer Biology to the Clinic, (2015)

ABBREVIATIONS

ARID1A	adenine thymine-rich interactive domain 1A gene
AKT	akt serine/Threonine kinase
ATCC	American Type Culture Collection
BAX	BCL-2 associated X protein
BCL-2	B-cell lymphoma 2
BAD	BCL-2 associated agonist of cell death
BRAF	v-Raf murine sarcoma viral oncogene homolog B1
BRCA1	breast cancer 1 gene
BRCA2	breast cancer 2 gene
CA125	cancer antigen 125
CCNE1	cyclin E1
CDKN1A	cyclin dependent kinase inhibitor 1A
CTNNB1	catenin beta 1
EOC	epithelial ovarian cancer
ER	estrogen receptor
FACS	fluorescence-activated cell sorting
FBS	fetal bovine serum
FIGO	Féderation Internationale de Gynécologie et d'Obstétrique
FITC	fluorescein isothiocyanate
FOXM1	forkhead box M1
GSH	glutathione peroxidase
HAT	histone acetyltransferases
HDAC	histone deacetylases
HDACI	histone deacetylases inhibitors
HES	human hairy and enhancer of split
HEY	hairy/enhancer of split related with YRPW motif
HER-2	human epidermal growth factor receptor 2
HPRT	hypoxanthine-guanine phosphoribosyl transferase
HNF1β	hepatocyte nuclear factor 1β
γ-H2AX	gamma-H2A histone family member X

LOH	heterozygosity
MAPK	mitogen-activated protein kinase
MLH1	mutL homolog 1
MSH2	mutS homolog 2
MSH6	mutS homolog 6
IHC	immunohistochemistry
KRAS	kirsten rat sarcoma viral oncogene homolog
MAPK	mitogen-activated protein kinase
mTOR	mammalian target of rapamycin
NICD	notch intracellular domain
NF1	neurofibromin 1
PAX	paired box 2
$p16^{INK4A}$	cyclin-dependent kinase inhibitor 2A
p21	cyclin-dependent kinase inhibitor 1A
p53	tumor protein/suppressor p53
PBS	phosphate-buffered saline
PCR	polymerase chain reaction
PFA	paraformaldehyde
PIK3CA	phosphatidylinositol-4,5-bisphosphate 3-kinase catalytic subunit alpha
PMS2	PMS1 homolog 2, mismatch repair endonuclease
PPP2R1A	protein phosphatase 2, regulatory subunit A
PTEN	phosphatase and tensin homolog
ROMA	risk of ovarian malignancy algorithm
ROS	reactive oxygen species
RB1	retinoblastoma transcriptional corepressor 1
RSF1	remodeling and spacing factor 1
SAHA	suberoylanilide hydroxamic acid
TCGA	The Cancer Genome Atlas
TMA	tissue microarray
TP53	gene encoding tumor protein p53
WHO	World Health Organization
WT1	wilm's tumor 1 factor

CHAPTER 1

INTRODUCTION

Cancer is a group of distinct diseases in which cells proliferate out of control and invade other tissues. Cancer cells no longer respond to genes that regulate cell cycle, function, differentiation and death. Tumor cell invasion of surrounding tissues and distant organs is the main cause of morbidity and mortality for most cancer patients[1]. The biological process by which normal cells are transformed into malignant cancer cells has been the subject of a large research in the biomedical sciences for many decades[1]. Cancer is the leading cause of mortality worldwide, being responsible for 8.2 million cancer related deaths in 2012[2].

1.1 Epithelial ovarian cancer (EOC)

1.1.1 Epidemiology and Risk factors

Epithelial ovarian cancer (EOC) is the most lethal gynecology malignancy[3–5] and the seventh most common in women worldwide. Nearly 240,000 women[6] were estimated to have been diagnosed with ovarian cancer in 2012 with incidence rates varying across the world. Although ovarian cancer accounts for only 4% of all cancers in women[7], it has one of the highest death-to-incidence ratios, due to difficulties in detection, diagnosis and therapy of the disease[8]. Like most cancers, the risk of ovarian cancer rises with age: the median age of patients at diagnosis is 60 years, and the average lifetime risk for women in developed countries is around one in 70[9,10].

Most ovarian carcinomas occur after menopause when the ovaries have little or no physiological role. As a consequence of the absence of abnormal ovarian function associated with major symptoms and the anatomical location (deep in the pelvis) about 70% of the patients are diagnosed with advanced-stage (extra-ovarian) disease and 5-years survival rates are between 20-40%[11,12]. Although most advanced stage cancers respond to standard therapy, relapse occurs in over 70% of patients, with progression associate with resistance to therapy and fatal disclosure[13].

In Portugal, the incidence of ovarian cancer is 490/100.000 (2008) and 5-year survival rate is 40%. Every year, in Portugal, the disease accounts for more than 371 deaths[12].

There are several factors that can affect the risk of developing ovarian cancer and therefore ensuring a primary prevention, screening and early detection. One important risk factor is the familial history of ovarian or breast cancer, present in only 10–15% of patients and mainly associated with germline mutations in *BRCA1* and *BRCA2* (breast cancer 1, 2 gene) genes[14], and also with Lynch syndrome (a group of hereditary nonpolyposis colorectal cancer), having germline mutations in DNA missmatch repair genes *MLH1* (MutL homolog1), *MSH2* (MutS homolog 2), *MSH6* (MutS homolog 6) and *PMS2* (PMS1 homolog 2*)*[15,16]. Women with a *BRCA1* mutation, the risk of epithelial ovarian cancer is 39–46%[17], and with a *BRCA2* mutation is between 12–20%[9,14]. Whereas, for women with Lynch syndrome a 3-14% risk of ovarian cancer is estimated. The management of women with genetic predisposition for ovarian cancer includes surveillance and risk-reducing surgery[18].

Moreover, nulliparity, early menarche, late menopause, and increasing age are associated with increased risk, whereas oral contraceptive use, pregnancy, lactation, and tubal ligation are associated with reduced risk[19]. Several studies have demonstrated that the use of oral contraceptives for more than five years decreases the risk of ovarian cancer by 20%[19]. The prophylactic salpingo-oophorectomy may reduce the risk of ovarian cancer by 80 to 95% and can be recommended for women with high risk of developing the disease[20]. Survival of ovarian cancer patients has improved due to the increased use of platinum-based therapy and a greater determination to treat recurrent disease. As mentioned above, the majority of patient firstly respond to chemotherapy, but most will relapse, contributing to around 152,000 deaths in 2012 all over the world[6].

1.1.2 Histological Types

Ovarian tumors mainly arise from three different cell types; epithelial, germ, and sex cord stromal cells[21] and several studies have contributed to confirm the heterogeneous nature of EOC based on their clinicopathological and molecular features and possible putative precursor lesions[22–24]. EOC represent 90% of ovarian malignant tumors[21] and is a very heterogeneous group of neoplasms that exhibit a wide range of tumor morphology, clinical manifestations and underlying genetic alterations[25].

Current investigations support the general view that serous tumors develop, at least in 50%, from the fallopian tube; endometrioid and clear cell tumors are postulated to arise from endometrial tissue in the ovary (most probably by passing through the fallopian tube) that results in endometriosis and tumors[23,24].

According to the latest classification by World Health Organization[2] in 2014 and based on histopathology, immunohistochemistry, and molecular genetic analysis, ovarian epithelial tumors are grouped into seven different types. Low grade tumors include low grade serous carcinoma (LGSC<5%), endometrioid carcinomas (EC; 10%), mucinous carcinomas (MC; 3%), and a subset of clear cell carcinomas (CCC; 10%)[26–29]. These tumors develop slowly and in general are confined to the ovary[30], genetically stable, and each histological type has a distinct genetic profile[27,29,30]. In contrast, high grade tumors progress rapidly and include high grade serous carcinoma (HGSC), seromucinous tumors (probably), undifferentiated carcinoma and some clear cell carcinomas[28] (Figure 1.1). HGSC is the most prevalent type and it is characterized by a very homogenous genetic profile characterized by tumor protein p53 (*TP53*) mutations and exhibit widespread DNA copy number alterations[27–31].

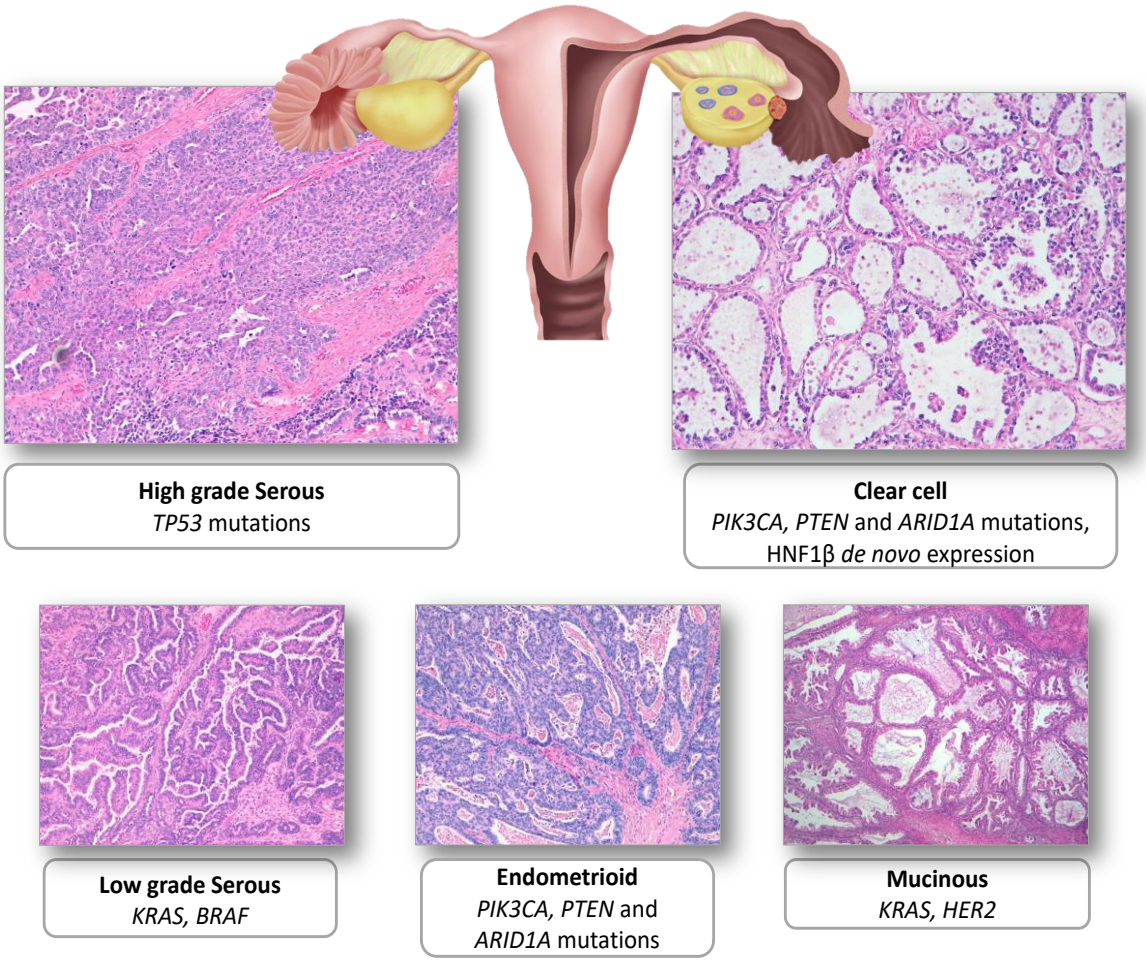

Figure 1. 1 - **Representative examples of the five main types of ovarian carcinoma stained with hematoxylin and eosin (H&E)**
High grade serous carcinoma, clear cell carcinoma, low grade serous carcinoma, endometrioid carcinoma and mucinous carcinoma. Scheme adapted from Jones & Drapkin[32] and Karst & Drapkin[33].

1.1.2.1 Serous carcinoma

Serous histology is the most common, representing 70% of EOC[34]. It is accepted that LGSC and HGSC are fundamentally different tumor types, and consequently, different diseases[2].

1.1.2.1.1 Low grade serous carcinomas (LGSC)

LGSC are rare and account for <5% of all cases of ovarian carcinomas[35]. They frequently have a noninvasive serous borderline component (with or without micropapillary pattern) and probably they represent tumor progression of serous borderline tumors beyond microinvasion. Although the presence of small foci of LGSC

in an ovarian borderline tumor is associated with a good prognosis, patients with advanced stage disease fare less favorably. Typically, present as large masses that are confined to one ovary (stage Ia), are indolent, and have good prognosis[2,28]. They show a relative genetic stability and usually display a variety of somatic alterations that include mutations in v-Raf murine sarcoma viral oncogene homolog B1 *(BRAF)* or kirsten rat sarcoma viral oncogene homolog (*KRAS)* genes, in 33-50% and 27-36%[36], respectively.

Microscopically, LGSC has small papillae of tumor cells exhibiting uniform nuclei within hyalinized stroma, which often contains psammoma bodies. Distinction of LGSC from HGSC relies on cell atypia and mitotic activity. Ki-67 immunoreaction differs between the two tumor types, being the median Ki-67 labeling index lower (2.5%) in LGSC than in HGSC (22.4%)[37]. The most useful immunomarker is p53 as this tumor type shows a *wild type* positivity in the nuclei in contrast with HGSC[2].

1.1.2.1.2 High grade serous carcinomas (HGSC)

HGSC are aggressive tumors that are usually diagnosed at an advanced stage, and although they frequently respond to surgery and platinum-based chemotherapy, they eventually recur. Microscopically, HGSC show neoplastic cells displaying papillary and solid growth with slit-like glandular lumens. The tumor cells are usually of intermediate size, with spotted bizarre mononuclear giant cells exhibiting prominent nucleoli[26]. In contrast to LGSC, these tumors show more than threefold variation in nuclear size[26,38].

In contrast to LGSCs, HGSCs are not associated with serous borderline tumors and typically exhibit *TP53* mutations and *BRCA* alterations[39], and most of these tumors show immunoexpression for p53, BRCA1, WT1 (Wilm's tumor 1 factor), p16 and have estrogen receptors (ER) in approximately two-thirds of HGSC cases[40].

HGSC show considerable genetic instability, harbor mutations and show an association of *TP53* mutations with increased expression of gamma-H2A histone family member X (γ-H2AX), a marker of DNA damage, expression of Ki-67, a proliferation marker and also potential alterations in *BRCA1* and *BRCA2* genes. In addition,

overexpression/amplification of HER2/neu, AKT (AKT serine/ threonine kinase) and loss of heterozygosity (LOH) on chromosomes 7q and 9q are common[4]. Profiling of *mRNA* and miRNA (micro RNA) of 489 Type II tumors, in particular HGSC, performed by The Cancer Genome Atlas (TCGA)[31] revealed that almost all samples comprised *TP53* mutations (in almost 98% of the cases) and significant recurring somatic mutations in *NF1 (*neurofibromin 1*), BRCA1, BRCA2, RB1* (RB transcriptional corepressor 1), *CDK12*[27–31] (cyclin dependent kinase 12), *CCNE1* (cyclin E1), *AKT2* (AKT serine/ threonine kinase 2), *RSF1* (remodeling and spacing factor 1) and *PIK3CA (*phosphatidylinositol-4,5-bisphosphate 3-kinase catalytic subunit alpha*)*[31,41]*. KRAS* mutations are rare and *BRAF* mutations have not been described in HGSC[36]. In addition, *Notch3* and *FoxM1* (forkhead box M1) were found to be involved in HGSC pathophysiology. More recently, the results of the TCGA study were highlighted in another genome-wide report[42].

As a result of the chromosomal instability, HGSC are typically aneuploid, with very complex karyotypes. The aCGH (array Comparative Genomic Hybridization) findings of the TCGA study[31] reveal gains/amplifications of 1q, 3q 6p 7q, 8q, 12p, 20p and 20q; and losses of 4p, 4q, 5q, 6q, 8p, 9p, 9q, 11p, 11q ,13q, 14q, 15q, 16p, 16q, 17p, 17q, 18p, 18q, 19p, 19q and 22q some of them already reported in other studies[43]. Other genetic alterations observed, suggest a co-operative effect, for example, associations have been found between *CCNE1* (cyclin E1) and 12p amplification[41], and between *MYC* (V-Myc Avian Myelocytomatosis viral oncogene homolog) and 20q amplification by fluorescence *in situ* hybridization (FISH). Also, positive associations were identified between gains on 19 and 20q, gain of 20q and loss of X, and between the loss of several regions, particularly 17q.

1.1.2.2 Endometrioid carcinomas (EC)

After HGSC, EC and clear cell carcinomas (CCC) are the most frequent types of EOC accounting for approximately 10-15% of all ovarian carcinomas[23]. The molecular and genetic alterations that underlie the development of these tumors are beginning to emerge. It has been recognized that endometriosis is the precursor lesion of EC and

CCC and a direct transition from ovarian atypical endometriosis to EC or CCC, in 15%-32% of cases[44].

EC occur most frequently in women of perimenopausal age, and most of them are found at an early stage[45]. These ovarian tumors are bilateral in 28% of cases and are associated in 15%–20% of cases with a carcinoma of the endometrium[45,46]. In the former presentation, both tumors are endometrioid in type in the majority of cases[2]. Up to 42% of cases, evidences of bilateral ovarian or pelvic endometriosis is present. Squamous differentiation inside the tumor occurs in 50% of cases[45]. Somatic mutations in *CTNNB1* (β-catenin) and *PTEN (*phosphatase and tensin homolog) genes are the most common genetic alterations identified in ECs, being *CTNNB1* mutations associated with a favorable disease outcome[47,48]. Also *PTEN* is mutated in 20% of cases and its inactivation results in the lack of inhibition of PI3K-AKT signaling pathway that inhibits apoptosis and activates proliferation. The finding of LOH at 10q23 and somatic *PTEN* mutations in endometriotic cysts, adjacent to ECs with similar genetic alterations, provides additional evidence of the precursor role of endometriosis in ovarian carcinogenesis[47]. An alternative mechanism for the activation of PI3K signaling in EC is activating mutations of *PIK3CA*, which encodes the p110 catalytic subunit of PI3K. EC is the most frequently encountered type in patients with hereditary Lynch syndrome[49]. The reported frequency of microsatellite instability (MI) in ovarian ECs ranges from 12.5% to 19%[50,51].

Recent discovery of *ARID1A* mutations in ovarian EC as well as in adjacent endometriosis, is considered a particular feature of these tumors[52]**,** although it appears to be a late event in endometrial carcinoma[53]. EC have expression of vimentin, cytokeratins (CK7, 97%; CK20, 13%), epithelial membrane antigens (EMA), estrogen and progesterone receptors by immunohistochemical studies[54].

1.1.2.3 Clear cell carcinomas (CCC)

CCC is a rare type known to be intrinsically chemoresistant and associate with very poor prognosis in advanced stages[55]. Tumors are commonly unilateral. As EC, they are also associated with endometriosis, and those tumors next to endometriotic lesions seem to have a more favorable prognosis[56]. The diagnosis of CCC is based

predominantly in the architectural findings: solid, tubule-cystic and papillary areas mixed in varied proportions. Cytological features are characterized most commonly for polygonal to flattened cells with pale or clear cytoplasm, which is attributed to the accumulation of glycogen and lipids. Densely hyaline basement membrane material expanding the cores of the papillae or deposit between cells is a common feature. Mitoses are less frequent than in other types of EOC[55].

Based on genome-wide mutational analysis, the most common mutations identified in CCC include *ARID1A* mutation in nearly half of the CCC (46%-57%) and loss of BAF250a expression (protein encoded by *ARID1A*)[44]. *ARID1A* gene has been identified as a novel tumor suppressor[44,57] and acts as a chromatin remodeling modifier, which stimulates cell signaling that can lead to cell cycle arrest and cell death in the event of DNA damage, consequently the dysfunction of *ARID1A* may result in susceptibility to CCC carcinogenesis through a defect in the repair or replication of damaged DNA[58]. A recent study indicated that the loss of *ARID1A* protein expression is related to short disease-free survival and chemoresistance in CCC[59].

Activating mutations of *PIK3CA* and deletion of *PTEN*, are found respectively in about 50% and 20% of tumors[47], supporting the role of an aberrant PI3K/PTEN pathway in CCC[60]. In addition, the overexpression of Notch pathway elements has also been reported in these tumors[61,62]. In contrast to various other human tumor types, *TP53* and *Rb* (retinoblastoma protein) mutations are rarely detected in CCC, but these cell cycle regulatory proteins may be involved in the carcinogenesis of CCC through inactivation by *ARID1A*[58] for example. In CCC, no *BRCA* alterations, chromosomal instability, nor complex karyotypes as seen in HGSC[63] have been reported, however epigenetic modulation of signaling pathways have been described[64–66].

Molecular alterations in CCC are mainly unknown and this histological type represent a distinct challenge with a unique and different histology, with *de novo* expression of HNF1β (hepatocyte nuclear factor 1β transcription factor).

HNF1β is involved in the glycogen synthesis[67] and regulates several specific genes, including those encoding dipeptidyl peptidase IV (protein degradation), osteopontin (bone remodeling), angiotensin converting enzyme 2 (ferritin induction,

iron deposition, and antiapoptosis), annexin 4 (calcium ion binding, epithelial cell differentiation), and UDP Glucuronosyltransferase 1 Family, Polypeptide A Complex (*UGT1A1*) (detoxifycation)[68]. It is postulated that HNF1β plays an important role in the pathogenesis and behavior of CCC[69]. Promoter hypomethylation of *HNF1β*, and active transcription, was previously reported in CCC[70,71]. Moreover, recently, we showed the role of HNF1β in the intrinsic chemoresistance exhibited by CCC[72].

CCC tumor cells are usually positive for HNF1β (>90%) and are negative for ER and WT1 in >95% of cases[37,40]. In addition to its presence in CCC, HNF1β is also expressed in the majority of tumors with cytoplasmic clearing, including renal CCC, endometrial CCC[69] and ovarian and endometrial carcinomas of mixed histology.

1.1.2.4 Mucinous carcinomas (MC)

Mucinous tumors account, approximately, for 3% of EOC. The cells of MC resemble cells of the gastric pylorus, or intestine[45,46,73], showing gastrointestinal differentiation in the majority of these tumors. Primary MC of the ovary are large, unilateral and usually confined to the ovary, without ovarian surface involvement or pseudomyxoma peritonei, while mucinous ovarian metastases are typically small (<10 cm) and bilateral. Malignant mucinous ovarian tumors are often heterogeneous, showing the coexistence of benign-appearing, borderline, noninvasive carcinoma, and invasive components. This morphology suggests a step-wise progression from benign to borderline and from borderline to carcinoma[74]. The category of mucinous borderline tumor with intraepithelial carcinoma is used for those tumors that lack obvious stromal invasion but show unequivocally malignant areas[75]. Mucinous borderline tumors with intraepithelial carcinoma have a very low risk of recurrence (<5%)[76].

The gene expression profile of MC differs from the HGSC, EC and CCC[77]. *KRAS* mutations are frequent, (up to 75% of primary MC), and seems to be an early tumorigenic event[78]. Using *KRAS* as a molecular marker, laser capture microdissection studies have shown the identical *KRAS* mutation in MC and adjacent mucinous cystadenomas and borderline tumors[74] supports the morphological continuum of tumor progression.

1.1.2.5 Other types of ovarian carcinomas

Seromucinous carcinomas (SMC), Brenner carcinomas (BC) and Undifferenciated carcinomas (UC)

Seromucinous carcinomas (SMC) are composed predominantly of serous and endocervical-type mucinous epithelium. These tumors are quite uncommon and data on the epidemiology is still insufficient[2].

Brenner carcinomas (BC) are extremely rare but Brenner benign tumor accounts for 5% of benign ovarian epithelial tumors[2]. BC histogenesis is not well characterized nor the genetic and molecular events.

Another uncommon histological type is undifferentiated carcinomas (UC), usually appear as solid masses with extensive necrosis, and a deficient mismatch repair proteins have been found in almost half of the tumors[2].

In summary, each histological type of EOC is associated with a distinct profile of clinical, morphological, genetic and molecular alterations, which for the most common low-grade tumors are shared with their respective precursor lesions (borderline tumors and endometriosis) supporting their stepwise progression. In contrast, the high grade tumors, aside from a very high frequency of *TP53* mutations and molecular alterations of *BRCA1/2*, are characterized by marked genetic instability.

1.1.3 Clinical presentation

Ovarian cancer is often described as a 'silent killer'[79] because the symptoms are non-specific and common to other diseases. Symptoms such as abdominal discomfort, bloating, gas, nausea, and urinary urgency, frequently lead to misdiagnosis[80,81], and contribute for the high percentage of cases that are diagnosed at an advanced stage. In addition, there is no routine and reliable screening for ovarian cancer[82], hence the majority of women are diagnosed at advanced stage exhibiting extraovarian and metastatic (mainly peritoneal) disease.

Approximately 70% of women with ovarian cancer are diagnosed at stage III or IV of the disease[82]. Ovarian cancer usually spreads to the opposite ovary/fallopian tube, and the uterus, and then intraperitoneally. Distant metastases are rare, but may occur in the liver, lungs, pleura, adrenal glands, and spleen[76]. The histological grade of tumors can affect treatment and prognosis. Low grade tumors have a more favorable prognosis than high grade tumors.

Cancer spread can greatly cause the accumulation of fluid in the abdomen, called ascites, which is a common complication of ovarian cancer that can cause swelling, fatigue and shortness of breath[82].

CA125, the serum tumor marker carbohydrate antigen 125 also known as mucin 16 (MUC16) is a secreted and membrane-associated glycoprotein expressed by coelomic and müllerian-derived epithelia, including the epithelium of the fallopian tube, endometrium and endocervix[83].

CA125 levels are low (< 35 U/mL) in the serum of healthy individuals, and CA125 elevation is commonly associated with HGSC, the most common histological type of ovarian carcinoma[83]. CA125 can be used for monitoring disease recurrence[84]. Although it is elevated in only 50-60% of ovarian cancer patients it can also be elevated in other non-cancerous gynecological complications such as benign ovarian neoplasms, endometriosis, pelvis inflammatory disease, liver disease or other malignant conditions, including cancers of the pancreas, breast, lung and colon[85]. Nevertheless, CA125 cannot be used as a unique parameter in the prediction of malignancy. Usually, a combination of a patient's medical history, clinical examination results, imaging data and tumor marker profile is used to clinically differentiate malignant ovarian masses from their benign counterparts and perform a histological exam for diagnosis confirmation. However, CA125 assay detects circulating MUC16, is one of the most widely used cancer biomarkers for the follow-up of ovarian carcinoma.

Recently Ricardo et al.[86] demonstrated that detection of aberrant cancer-associated glycoforms (Tn, STn, and T) of MUC16 as well as MUC1 in circulation, in ovarian cancer tissue using Proximity Ligation Assays (PLA), can improve the yield of serum assays and they have the capacity to distinguish borderline and malignant

serous tumors from benign lesions with a specificity of 100% and a sensitivity of 70-80% on tissues. In fact, serous ovarian carcinomas selectively express Tn and STn glycoforms of MUC16 and MUC1, and these glycomucin profiles are likely to serve as more cancer-specific biomarkers than the mucins themselves. This study provides strong support for the use of PLAs to detect aberrant glycoforms of mucins and thereby improve cancer specificity of biomarker assays[86].

The *human epididymis secretory protein 4* (*HE4*) gene was found to be overexpressed in ovarian cancer[87] and is used as a potential serum biomarker. HE4 belongs to the family of whey acidic four-disulfide core (WFDC) proteins with suspected trypsin inhibitor properties. HE4 was first determined in the epithelium of the distal epididymis[88].

Biomarker HE4 has very low expression in the epithelia of respiratory and female reproductive tissues including ovary, but high secreted levels can be found in the serum of ovarian cancer patients[89] and also in ovarian cancer tissue[88]. Recently, Moore at al.[90,91] published a series of papers that used a combination of CA125, HE4 and menopausal status to predict the presence of a malignant ovarian tumor. Originally, nine potential biomarkers were evaluated, from which HE4 was the most effective in detecting ovarian cancer. When CA125 was combined with HE4, the prediction rate was higher, showing a sensitivity for detecting malignant disease of 76.4% at a specificity of 95%[90,92] in ovarian carcinoma *vs* endometriotic cysts. Measured values of HE4 and CA125 can be combined in an algorithm called ROMA (Risk of Ovarian Malignancy Algorithm), which additionally includes the menopausal status. Several published studies[91,92] show that ROMA helps in the triage of pre and postmenopausal women suspected for ovarian cancer. This high accuracy helps to stratify patients into low-and-high risk groups and therefore contributes to better diagnosis, treatment and outcome.

Non-invasive screening tools have been studied to help screening this cancer, such as transabdominal and transvaginal ultrasonography (TVS), since it is able to estimate ovarian size, detects masses as small as 1 cm and distinguishes solid lesions from cysts. Besides its important role in differentiating between benign and malignant

adnexal masses[93], the specificity of ultrasonography is not adequate for its use as a single screening modality[94].

The majority of ovarian tumors are surgically staged to determine the presence of extraovarian disease, classified according to the terms of the staging scheme (I to IV) developed by the Fédération Internationale de Gynécologie et d'Obstétrique (FIGO) and the classification system prognosis helps to define treatment (Table 1.1). Staging is performed by examining histological sections of tissue samples and cytological assessment of fluid samples[95].

1.1.4 Treatment of ovarian cancer

Ovarian cancer is highly curable when it is confined to the ovaries, with an expected 80–95% in 5-year survival[73]. Only about 20% of affected patients are found at this stage, and the diagnosis is often made incidentally during the study of another medical condition. Current therapies for advanced ovarian carcinomas are limited and not curative and the search for new therapeutic agents in the treatment of the disease and recurrence, have been disappointing[22].

The standard treatment for ovarian cancer patients includes cytoreductive surgery, during which adequate staging is performed by pathological examination of ovarian and other tissues to define the histological nature of the tumor and its stage. In patients diagnosed with early disease, surgery alone may be sufficient but in advanced disease, debulking surgery followed by chemotherapy is recommended[96].

Chemotherapy after surgery is referred to as 'first-line' treatment and involves a combination of a platinum and taxane-based chemotherapy (usually six cycles of carboplatin and paclitaxel) delivered intravenously (IV) or intraperitonealy (IP)[97,98]. Patients with advanced ovarian cancer who aren't initially able to undergo surgery due to unressectable tumors can be treated with chemotherapy, being considered for surgery (neoadjuvant treatment)[9] and then followed by platinum-based combination of chemotherapy, or not. Although initially the majority of patients become tumor free, the disease will recur and inevitably progress under treatment[99].

Table 1. 1 - **TNM and FIGO classifications for Ovarian, Fallopian Tube and Peritoneal Cancer Staging System**
Adapted from the Fédération Internationale de Gynécologie et d'Obstétrique[2], 2014.

Primary tumor (T)		
TNM	**FIGO**	
TX		Primary tumor cannot be assessed
T0		No evidence of primary tumor
T1	I	Tumor limited to the ovaries (one or both) or fallopian tubes
T1a	IA	Tumor limited to one ovary (capsule intact) or fallopian tube; no tumor on ovarian or fallopian tube surface; no malignant cells in the ascites or peritoneal washings.
T1b	IB	Tumor limited to both ovaries (capsules intact) or fallopian tubes; no tumor on ovarian or fallopian tube surface; no malignant cells in the ascites or peritoneal washings.
T1c	IC	Tumor limited to one or both ovaries or fallopian tubes, with any of the following: IC1: Surgically spill intraoperatively. IC2: Capsule ruptured before surgery or tumor on ovarian or fallopian tube surface. IC3: Malignant cells present in the ascites or peritoneal washings.
T2	II	Tumor involves one or both ovaries or fallopian tubes with pelvic extension or peritoneal cancer.
T2a	IIA	Extension and/or implants on the uterus and/or fallopian tubes and/or ovaries.
T2b	IIB	Extension to other pelvic intraperitoneal tissues.
T3	III	Tumor involves one or both ovaries, or fallopian tubes, or primary peritoneal cancer, with cytologically or histologically confirmed spread to the peritoneum outside of the pelvis and/or metastasis to the retroperitoneal lymph nodes.
T3a	IIIA	Metastasis to the retroperitoneal lymph nodes with or without microscopic peritoneal involvement beyond the pelvis.
T3b	IIIB	Macroscopic peritoneal metastases beyond the pelvic ≤2 cm in greatest dimension, with or without metastasis to the retroperitoneal lymph nodes.
T3c	IIIC	Macroscopic peritoneal metastases beyond the pelvic >2 cm in greatest dimension, with or without metastasis to the retroperitoneal lymph nodes.
T4	IV	Distant metastasis excluding peritoneal metastases.
T4c	IVA	Pleural effusion with positive cytology.
T4b	IVB	Metastases to extra-abdominal organs (including inguinal lymph nodes and lymph nodes outside of the abdominal cavity)

Regional lymph nodes (N)		
NX		Regional lymph nodes cannot be assessed
N0		No regional lymph node metastasis
N1	IIIC	Regional lymph node metastasis

Distant metastasis (M)		
M0		No distant metastasis
M1	IV	Distant metastasis (excludes peritoneal metastasis)

Similar to other malignancies, the management of ovarian cancer has evolved from single agent to combination of chemotherapy agents. The most frequently used combination as the first-line chemotherapy for ovarian cancer patients is the combination of platinum and taxane drugs.

Two platinum compounds are most commonly used, cisplatin and carboplatin. Cisplatin is one of the most potent antitumor agent known, displaying clinical activity against a wide variety of solid tumors[100,101]. The toxic side effects associated with the use of this drug was the motion for the development of the second-generation platinum chemotherapeutic agent, carboplatin[102,103].

Besides their chemical similarity, cisplatin and carboplatin operate by same mechanisms: the formation of protein and DNA adducts (covalent bounds) and the generation of reactive oxygen species (ROS). Labile ligands in the coordination sphere, chloride for cisplatin and 1,1-cyclobutanedicarboxylate (CBDCA) for carboplatin, are displaced by water or other biological nucleophiles, and the activated *cis*-diammineplatinum(II) moiety bind to purine bases in nuclear DNA[104]. The resulting platinum-DNA adducts, mainly 1,2-intrastrand cross-links, leads to death of cancer cells through the induction of errors in DNA, transcription inhibition and subsequent downstream effects[105]. Because cisplatin and carboplatin have the same NH_3 non-leaving group ligands, the resulting DNA adducts are identical[106] and therefore the drugs exhibit the same spectrum of activity[107]. Its cytotoxic mode of action is mediated by its interaction with DNA to form DNA adducts, primarily intra-strand crosslink adducts, which activate several signal transduction pathways, including those involving ATR (serine/threonine-protein kinase ATR), p53, p73 and MAPK, ending with the activation of apoptosis[100].

Carboplatin, however, is significantly less toxic than cisplatin. The typical patient dose for carboplatin is approximately ten times greater than cisplatin (400 mg/m^2 *versus* 40 mg/m^2), and the dose-limiting toxic side effect of carboplatin is myelosuppression in contrast to nephrotoxicity for cisplatin[102].

Taxanes are hydrophobic mitotic inhibitors and paclitaxel is one of the taxanes in clinical use. Paclitaxel is highly protein bound, with large volumes of distribution and

poor penetration into the central nervous system[108] and is eliminated via hepatic metabolism. Despite the initial effectiveness of the response to paclitaxel in most cases patients in due course become resistant and relapse[109]. At a higher dose, paclitaxel is known to suppress microtubule minus ends detachment from centrosomes[110–112]. The taxanes can also induce apoptosis and have anti-angiogenic properties[113]. In various studies it is showed as an effective anticancer agent against lung, breast, ovarian, leukemia and liver cancer[114].

Regarding the mechanism of action of taxanes, they bind to the β-subunit of tubulin, resulting in the formation of stable, non-functional microtubule bundles and thus interfering with mitosis, inducing a cell cycle arrest in G2 for paclitaxel and in S-phase for docetaxel[115]. Recent studies showed that taxanes are also able to induce ROS production in cancer cells, and hydrogen peroxide (H_2O_2) was found to be involved in induced cancer cell death *in vitro* and *in vivo*[116,117].

Tumor resistance to chemotherapy may be present at the beginning of treatment, can develop during treatment, or become apparent on recurrence of disease[118]. Patient response to chemotherapy for ovarian cancer is in fact heterogeneous and there are no tools to aid the prediction of sensitivity or resistance to chemotherapy, treatment stratification and current use in clinical setting[119].

Resistance mechanisms that limit the extent of DNA damage associated with chemotherapy include decrease of intracellular drug accumulation, increased drug inactivation and increased DNA damage repair or inhibition of transmitted DNA damage recognition[100]. Increased glutathione levels is also a mechanism of resistance, since thiols are highly nucleophilic and besides being ROS scavengers they also react with platinum derived drugs as carboplatin and cisplatin[72].

ROS are naturally produced by cells through aerobic metabolism, and high levels of ROS in the cells are associated with many diseases including cancer[120]. However, under certain conditions, ROS increase proapoptotic molecules such as p53 and p38 MAP kinase[121]. ROS-sensitive signaling pathways are persistently elevated in many types of cancers, where they participate in cell growth/proliferation, differentiation, protein synthesis, glucose metabolism, cell survival and inflammation[122]. ROS can act

as second messengers in cellular signaling[123]. H_2O_2 regulates protein activity through reversible oxidation of its targets including protein tyrosine phosphatases, protein tyrosine kinases, receptor tyrosine kinases and transcription factors[122,123]. The formation of ROS upon chemotherapy depends on the concentration of chemotherapeutic agents and the duration of exposure[124]. The efficiency of several chemotherapeutic agents depends on the alteration of redox state through the generation of ROS, inducing cell death[125].

One main explanation on tumor cell resistance to paclitaxel is the overexpression of P-glycoprotein (P-gp, MDR-1), which works as a drug efflux pump. However, clinical utility of P-gp inhibitors are often ineffective or toxic at the doses required to attenuate P-gp function[126,127]. Other possible mechanisms of resistance involve alterations in the drug-binding affinity of the microtubules[128], changes in tubulin structure and cell cycle deregulation[129]. Thus, paclitaxel-resistant mechanisms are complicated and still not entirely clear.

Summing up, ovarian cancer usually responds to chemotherapy, (the combination of carboplatin and paclitaxel is the most used) but, in the majority of cases the cancer recurs resulting in the death of eventually half of patients[77] as a consequence of the development of drug resistance[99]. Therapeutic resistance can arise from tumor cells that are intrinsically resistant as well as those that have acquired resistance during treatment[130]. To date, there are no reliable clinical factors that can properly stratify patients for suitable chemotherapy strategies.

1.2 Molecular features of ovarian cancer

Alterations in cell cycle regulatory genes, mainly tumor suppressor genes and proto-oncogenes induce an unrestrained growth of cells and serve as precursors of immortality. Of the many regulators, tumor suppressor proteins play a pivotal role in the cell cycle regulation process and are highly deregulated in ovarian carcinomas[131]. Besides some cases integrated in hereditary cancer syndromes, most mutations seen in EOC are somatic mutations affecting cells by interfering with several signaling pathways and cell mechanisms.

1.2.1 Pathways involved in ovarian cancer

1.2.1.1 Notch Signaling Pathway

Notch signaling pathway is an evolutionary conserved pathway that is required for embryonic development, and in adult tissues acts in homeostasis[132]. Notch signaling is a justacrine pathway that has been found to be deregulated in human hematological malignancies and solid tumors[133,134]. It has multiple roles in cell fate determination through regulation of proliferation, differentiation, survival and apoptosis[135,136]. Notch receptors (Notch1-4) as well as their ligands Delta-like (Dll1, 3 and 4) and Serrate-like Jagged1 and 2[137–140] are single-pass transmembrane proteins with extracellular domains that consist of multiple epidermal growth factor (EGF)-like repeats. The extent of EGF-like repeat fucosylation by the fucosyltransferases, such as Fringe, determines the affinity strength between the receptors and their ligands. Notch receptors are synthesized in the endoplasmic reticulum as an inactive single peptide precursor[141].

Notch signaling is initiated by the binding of Notch Delta/Jagged ligands to Notch receptors (Figure 1.2). This interaction induces a first cleavage (S1) in the Notch receptor by furin-like convertases producing an extracellular N-terminal fragment and a transmembrane C-terminal fragment that also includes the Notch intracellular domain (NICD). A second cleavage (S2) occurs catalyzed by a member of disintegrin and metalloproteases (ADAM) family (ADAM17 or ADAM10), also known as the metalloproteinase tumor necrosis factor-α-converting enzyme (TACE). The remaining Notch fragment is then accessible to the presenilin-dependent γ-secretase protease complex and this complex carries out the third and final cleavage (S3) of the Notch protein[135,142]. This final cleavage event releases the active NICD into the cytoplasm and after translocation into the nucleus, binds to ubiquitous transcription factor CSL (CBF1/Suppressor of Hairless, and Longevity-Assurance Gene-1), and converts a large co-repressor complex into a transcriptional activating complex. The complex contains NICD, CSL, mastermind-like protein (MAML; a transcriptional coactivator), SKIP (Ski-interacting protein as a CBF1 binding protein) and p300, and activates the transcription of Notch target genes. The Notch target genes are transcription factors of the Hairy

Enhancer of Split (*HES*) family proteins, HES related proteins (*HEY*)[143] as well as cell cycle regulators such as p21, cyclin D1 and 3[144], c-myc[145], and HER2[146].

The Notch pathway has also been implicated as interacting with the EGFR/HER2 tyrosine kinase receptor family, as well as phosphatidylinositol 3-kinase/AKT/mTOR signaling, two central growth pathways in the physiological and neoplastic setting[147]. Although interaction of Notch signaling with other pathways has been a focus of investigation, the exact mechanisms of this crosstalk remain largely unknown. It is evident that the interaction of Notch signaling with other pathways highly depends on the cellular context, and differs from one cellular microenvironment to another[140].

Elements of the Notch pathway are altered in more than 20% of HGSC, mostly as amplifications in the ligand Jagged 1 and 2 and Notch 3[31]. Notch3 (mRNA and protein) was found to be overexpressed especially in serous ovarian carcinomas compared with the normal ovarian surface epithelium[148] and correlation with aggressive tumors with poor prognosis[148,149] have been described.

Notch 3 was found to be active in some ovarian cancer cell lines, but according to observations by Hopfer and colleagues[150] there were no differences in the expression of extracellular Notch3 between ovarian cancers and benign ovarian adenomas. Park et al.[151] demonstrated that Notch3 expression is associated with post chemotherapy recurrence, probably as a result of upregulation of the ATP Binding Cassette Subfamily B Member 1 (*ABCB1)* that acts as a pump of xenobiotics. Chemoresistance to platinum-based therapy was also associated with Notch3 activation[152]. In ovarian cancer cell lines Notch1 overexpression has also been shown to promote tumor cell proliferation[153,154].

Targeting the Notch pathway either with small molecule inhibitors primarily with γ-secretase inhibitors (GSIs) or monoclonal antibodies (mAbs) to Notch ligands and Notch receptors are currently in clinical development[136].

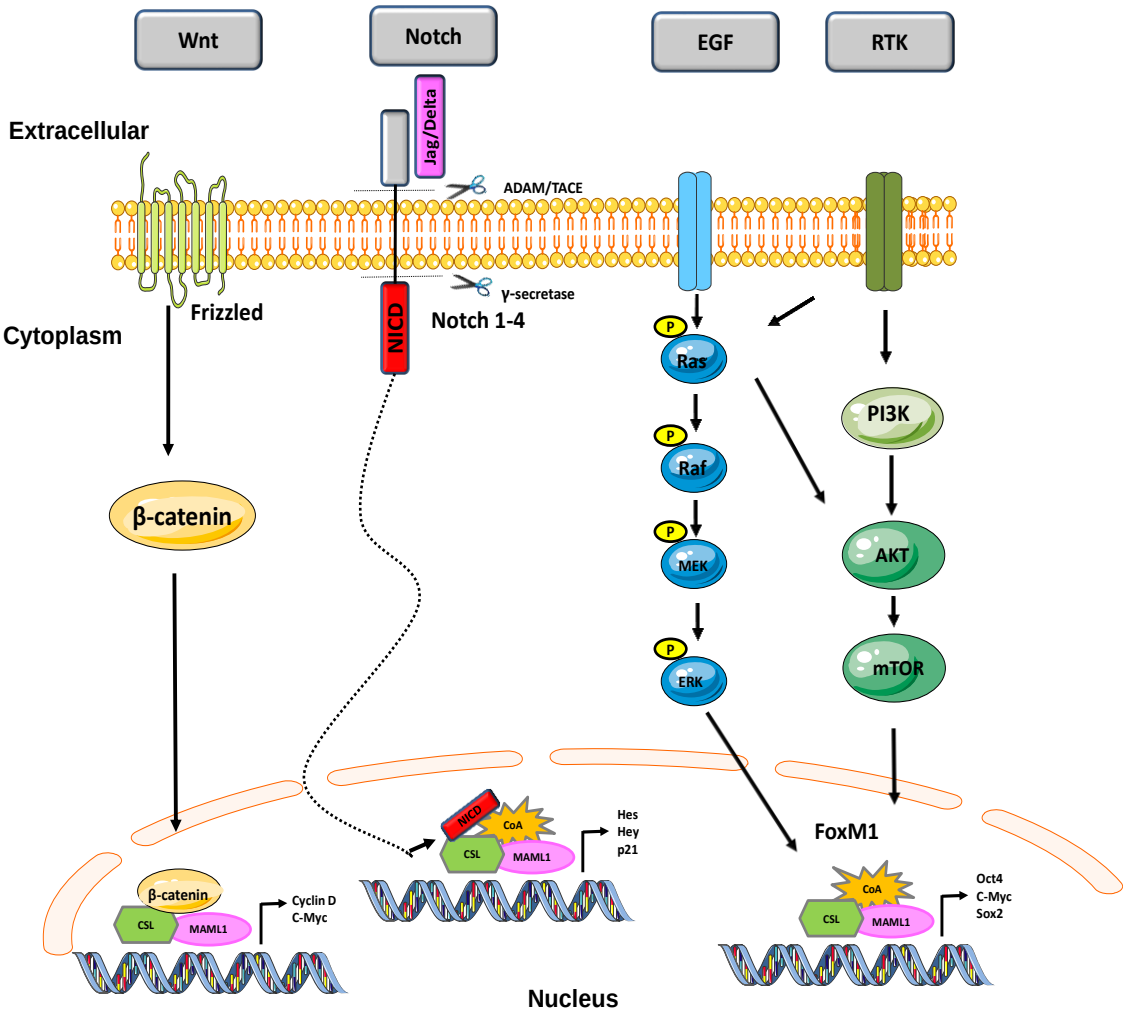

Figure 1. 2 - **Ovarian cancer signaling pathways scheme**

Scheme adapted from Yap, 2013; Longuespée et al., 2012 and Toss et al., 2013 [155–157].

1.2.1.2 Mitogen-activated protein kinases (MAPK) pathway

MAPK/ERK pathway activation and subsequent interactions are highly regulated events that become deregulated in cancer cells. The pathway begins with the activation of Kirsten rat sarcoma oncoprotein (KRAS), which initiates a multistep phosphorylation events that leads to the activation of RAF/MEK and MAPK pathways, and in conjunction with mammalian target of rapamycin (mTOR), a target of the protein AK strain thymoma (AKT) pathway, which ultimately regulate the transcription of molecules that are involved in mitogenesis[158–160] (Figure 1.2).

Point mutations in *KRAS* provide an advantage for the survival and progression of tumors[161–163]. *KRAS* somatic mutations have been implicated in the genesis of LGSC, inducing a mitogenic phenotype[164].

Patients with ovarian cancer frequently present activation of the MAPK/ERK pathway due to somatic mutations of *KRAS* or *BRAF*, which seem to occur early in malignant transformation[36]. *KRAS* and *BRAF* mutations are found in respectively 27-36% and 33-50% of LGSC. In contrast, a study conducted on 489 HGSC, TCGA[31] showed that in 45% of cases that contained altered PI3K/RAS signaling, less than 1% was due to mutations and only 11% were due to amplifications. Also, *BRAF* was mutated in 0.5% of HGSC cases. These mutations enhance kinase activity, becoming the mutated protein independent of the activation of the tyrosine kinase receptor, and hyperactivating the MAPK pathway during the initiation and progression of tumorigenesis[158].

1.2.1.3 PI3K/PTEN/AKT pathway

The PI3K pathway is activated through transmembrane tyrosine kinase receptors (RTK). PI3K is a heterodimeric protein comprised of a regulatory subunit, p85, and a catalytic subunit, p110[165,166]. The p110 catalytic subunits exit as several isoforms α, β, γ and δ[166]. Recruitment of the PI3K complex to the inner surface of the plasma membrane juxtaposes it with its substrate phosphatidylinositol-4,5 diphosphate (PIP_2) located in the inner lamina of the cell membrane. PIP_2 is then phosphorylated by the p110 subunit to form phosphatidylinositol-3,4,5 trisphosphate (PIP_3). The conversion of PIP_3 to PIP_2, and the subsequent inactivation of PI3K downstream signaling, is facilitated by the tumor suppressor *PTEN* located on chromosome 10[167] (Figure 1.2).

PTEN is a tumor suppressor gene, whose mutations promote the loss of function of the protein and are present in many cancers, including in ovarian cancer[4,160,168–171].

AKT activation is generally associated with processes of cell survival, growth, and proliferation[172]. Cell survival is regulated by inhibitory phosphorylation of the forkhead box O (FoxO) transcription factor family by AKT, and thus attenuation of their pro-

apoptotic target gene *Bim* as well as by direct inactivation by phosphorylation of BAD[173].

Cell proliferation is regulated by activation of mTOR thereby promoting protein synthesis[174]. mTOR promotes cell growth and proliferation in association with the PI3K/AKT pathway[166] through the phosphorylation of AKT at the serine residue 473 by the mTOR complex 2 (mTORC2). The mTOR complex 1 (mTORC1) element raptor, and the mTORC2 element rictor, differ from each other in composition by a few elements that make up the respective complexes, accounting for the difference in resistance to rapamycin[175]. mTORC1 promotes proliferation by the activation of molecules involved in protein synthesis, mTORC2 promotes cell survival and proliferation through AKT activation[176].

Cell proliferation is stimulated via a number of mechanisms including inhibition of the FoxO-mediated transcription of the cyclin-dependent kinase inhibitor $p27^{Kip1}$[177]. AKT also inhibits both $p27^{Kip1}$ and p21 function by phosphorylation[178] as well as by regulating D-type cyclins[179].

The FoxO factors function as downstream elements of the PI3K/AKT/PTEN signaling pathway and are essential for cell proliferation, differentiation, DNA damage repair and apoptosis[180,181]. Upon activation of the PI3K/AKT signaling pathway, FoxO proteins undergo AKT-mediated phosphorylation. Under conditions of stress or in the absence of growth or survival factors, the PI3K/AKT pathway is inhibited and FoxO3a proteins translocate to the cell nucleus, where they execute their transcriptional functions. By contrast, the dephosphorylation of activated FoxO3a induces cell cycle arrest and apoptosis.

The cytostatic and cytotoxic effects of a variety of anti-cancer drugs[182], such as paclitaxel[183,184] doxorubicin[185], lapatinib[186], gefitinib[187], imatinib[188,189], and cisplatin[190], are mediated through the activation of FoxO, particularly FoxO3a. The phosphorylation of FoxO3a induces FoxM1 upregulation, which in turn promotes cell proliferation and survival[190,191].

A number of studies have revealed FoxM1 to be a key cell cycle regulator in the transition from G1 to S phase and in the progression to mitosis[192–194] and have demonstrated overexpression of the FoxM1 gene in human cancer cells and tissues, including in ovarian cancer[31,195]. In the study by TCGA[31], 87% of the cases studied showed that elements of the FoxM1 pathway, such as baculoviral inhibitor of apoptosis repeat-containing 5 (BIRC5/survivin), cyclin B1 (CCNB1), aurora kinase-B (AURKB), cell division cycle 25 homolog B (CDC25B) and polo-like kinase 1 (PLK1) were consistently overexpressed but not altered by DNA copy number changes[31]. Inactivation of FoxO or overexpression of FoxM1 is associated with tumorigenesis and cancer progression.

The integrated genomic analysis study of HGSC[31] showed that at least 45% of the cases contained alterations in the PI3K and RAS signaling pathways, whereas *PTEN* deletions were found in 7%. *PI3KCA* amplifications (18%) and mutations (<1%), AKT isoform amplifications AKT 1 and AKT 2 (3 and 6% respectively), were observed in conjunction with *KRAS* amplification (11%)[31]. KRAS, independently, controls survival through BRAF but it can also activate PI3K, that induces activation of AKT, and cell cycle progression. Similarly, in the PI3K/AKT/mTOR signaling, a study by Kinross et al.[196] using a mouse model demonstrated that *PTEN* double deletions with *PI3K* activation was necessary for HGSC and granulosa cell tumors development[166]. Therefore, a single event does not appear to influence ovarian tumorigenesis but multiple hits in the pathways that regulate growth, proliferation, and survival are required for tumorigenesis and progression.

PI3K mutations in ovarian tumors are rare, but an increase in gene copy number has been observed more frequently. The amplifications are more pronounced in HGSC than LGSC tumors along with AKT phosphorylation contributing to survival, and progression of the disease[197,198].

1.2.2 Genes involved in ovarian cancer

1.2.2.1 Tumor protein 53 (TP53)

The *TP53* gene codifies a *sui generis* tumor suppressor protein whose normal function is essential for cell normal physiology but when mutated p53 can exhibit oncogenic properties. Normal p53 function is anti-cancer and oncogenic p53 function is pro-cancer[199]. Hence, *TP53* is a multifunctional tumor suppressor gene that is often altered in ovarian and other cancers[199,200], plays a major role in regulating the cellular response to environmental and genotoxic stress, through cell cycle inhibition and promotion of programmed cell death and senescence.

Mutation of the *TP53* gene at the locus 17p13.1 is the most common single genetic alteration in sporadic human EOC. The p53 protein contains four functional domains – a transcriptional activation domain, a tetramerization domain and two DNA binding domains. In addition to possessing transcriptional activating properties, transcriptional repression has been described, although binding sites are less well characterized[201,202].

It has been estimated that the gene encoding p53 (*TP53*) is mutated in more than 50% of human cancers[203]. It appears that the loss of p53 normal function, by mutation or by other means, is highly advantageous and perhaps an absolute requirement for some cancers progression. This gene interacts with a variety of proteins involved in transcriptional regulation, DNA repair, cell cycle progression, apoptosis, and proteosome-mediated protein degradation[204]. De Graeff *et al.*[205] recently determined a prognostic value of p53 in ovarian cancer through a meta-analysis of 62 previously published studies using a total of 9448 patients. The p53 status was analyzed by IHC or mutational analysis. Out of 62 studies, 25 reported an association with poor survival while 4 were associated with improved survival. When the meta-analysis was restricted to serous tumors only, there was a significant association with poor prognosis[205]. Although, histotype heterogeneity and chemotherapeutic treatment were not taken into account and the analysis showed that the FIGO stage may influence the outcome predictive value of p53 and the prognostic significance of p53 seems also to be more restricted to low stage tumors[205].

Some other studies suggested a correlation between p53 status and response to platinum-based chemotherapy, while strong discrepancies are noticed in clinical studies with paclitaxel-based treatment. These inconsistencies are likely due to different antibodies utilized, chemotherapeutic regimen and heterogeneity of histotypes, which render the interpretation of all these studies difficult[206,207].

TP53 is a canonical exception to Knudson hypothesis[208], since a single mutation in one allele is enough to alter p53 tumor suppressor function, becoming advantageous for tumor survival. The majority of *TP53* mutations are missense mutations that cause single residue changes, largely occurring in the DNA binding domain[209]. Mutant p53 protein has the ability to form a tetramer with wild type p53, acting as a dominant negative to repress normal physiological processes of p53, possibly by inducing an inactive conformation of the DNA binding domain and reducing the ability to transactivate/repress target genes[210–212].

The relevance of the normal function of p53 in a cell is showed up by the p53 regulatory network, consisting of negative and positive feedback loops that modulate down and up p53 expression and activity[213]. The negative feedback loop established by p53 with MDM2 tightly controls both p53 and MDM2 levels in the cell. Tumor suppressor p53 activates targets in the *MDM2* gene to be transcribed, ultimately causing production of the MDM2 protein, which then inhibits p53[214,215]. This negative feedback loop is vital for controlling p53 activity to prevent detrimental pathogenic effects of excessive p53 activity.

Although *TP53* mutations have been detected in all histological types of EOC, a number of studies have demonstrated higher frequencies of such mutations in HGSC. Point mutations, missense mutations and truncations have been observed, resulting in the overexpression of the p53 protein that has been detected in many of the immunohistochemical studies performed[216,217]. The accumulation of mutated and oncogenic p53 has been shown to affect the expression and interaction of the pro-apoptotic *BAX* with the anti-apoptotic B-cell lymphoma 2 (*BCL-2)*[218,219].

The expression of mutated p53 results in the accumulation of the altered protein within the cell that has a negative effect on BAX, a transcriptional target of p53[220]. It

seems that p53 alterations in HGSC reduce BAX expression allowing the progression of solid tumors. However, immunohistochemistry studies in tumor tissue have not provided a definitive conclusion of a positive correlation with p53 expression and tumor prognosis and survival[221,222]. The expression of p53 *vs* BCL-2 and BCL-2 *vs* BAX have been shown to have a strong association with tumor grade and histopathological subtyping, factors that could be vital for identifying the specific epithelial ovarian carcinoma for adjuvant or combined therapies[223]. What has been observed is that the majority of ovarian tumors are initially very responsive to treatment but later become chemoresistant. Possibly the treatment itself may cause the selection of few cells within the tumor mass, harboring mutations in *TP53* that, in addition to epigenetic silencing of promoter regions of apoptotic favorable genes such as *p16* or *Rb*, may account for the relapse and progression of the tumor[131].

As previous described, mutations in *TP53* are a common event in ovarian tumorigenesis, being particularly frequent in HGSC but are uncommon in CCC (10%)[224]. This implies that other anti-apoptotic mechanisms are likely to be involved in the development of CCC. HNF1β, a diagnosis marker for CCCs[40], has been implicated in mediating apoptotic escape in tumor cells[225].

1.2.2.2 Hepatocyte nuclear factor 1β (HNF1β)

Hepatocyte nuclear factor 1β (HNF1β) was originally described as a novel homeodomain-containing transcription factor isolated from a human liver library and found to be essential during organogenesis of the liver, kidney, and pancreas[226]. HNF1β gene (formerly known as TCF2) is located on 17q21.3, contains 9 exons[227] and its expression is often altered in cancer[228]. CCC are usually positive for HNF1β (>90%)[37,40]. In addition, HNF1β is expressed in the majority of tumors with cytoplasmic clearing, including renal CCC and endometrial CCC[69].

HNF1β was found to be the most upregulated transcription factor in a gene expression analysis of four ovarian CCC cell lines when compared to non-CCC cell lines[228]. It was also subsequently reported to be positive in areas of endometriosis or endometriotic epithelium in a study of ovarian CCC lending molecular support for the

hypothesis that the concurrent endometriosis seen in CCC may be linked as a precursor lesion[67,229].

HNF1β is involved in the glycogen synthesis[67] and is also expressed in mid-to-late secretory and gestational endometrium (Arias-Stella reaction) and in atypical and inflammatory endometriosis. Studies confirm the identification of HNF1β as a susceptibility gene for CCC development and disclosed that promoter methylation plays a role in the regulation of *HNF1*β expression[229].

Immunohistochemistry (IHC) analysis for HNF1β protein expression comparing CCC and HGSC in 1,149 ovarian tumors from the Ovarian Tumor Tissue Analysis Consortium, and DNA-methylation analysis on 269 of these tumors, revealed that the majority of CCC expressed the HNF1β protein, and were unmethylated at the *HNF1*β promoter, whereas the majority of HGSC lacked HNF1β protein expression and displayed frequent *HNF1*β promoter methylation[228,229]. This epigenetic inactivation of *HNF1*β seen in ovarian HGSC has also been detected in colorectal, gastric and pancreatic cancer cell lines[70].

*HNF1*β promoter hypomethylation has recently been detected in additional clear cell histology, including endometrial, cervical and renal clear cell cancers, suggesting HNF1β expression and promoter hypomethylation to be a general biomarker of cytoplasmic clearing[69]. HNF1β overexpression in immortalized endometriosis epithelial cells (putative precursors of CCC) led to altered morphology and multinucleation of cells[228] while siRNA knock-down of *HNF1*β led to the induction of apoptosis in CCC cells lines[229].

1.2.2.3 Cyclins and Cyclin-dependent-Kinase inhibitors

The cyclin and cyclin dependent kinase (CDK) elements, activators and inhibitors that have a major role in ovarian cancer are cyclin D1, p16INK4A, $p27^{Kip1}$ and p21[230–232]. Their regulation and function have been shown to be controlled in part by the tumor suppressor gene TP53, which is predominantly mutated in HGSC[230,232].

CDK activators and inhibitors are major co-regulatory proteins in the cell cycle along with the p16, p53 and retinoblastoma (Rb)[233], being p21 a direct transcriptional

target of p53[234]. In the presence of wild-type (WT) p53, p21 induction is followed by the inhibition of cyclin E/CDK2 preventing the G1-S transition, encouraging the quiescent or apoptotic phenotype of cells[235].

Although the roles of p21 and p27 have been discussed in many cancers, they appear to have secondary roles in the etiology of ovarian cancer rather than in the genesis[236,237]. Loss of function or accumulation of these proteins in ovarian cancers has not been reported. In some cases, the absence or low expression of p21 in p53 expressing tumors appears to place patients at a higher risk for disease recurrence[238]. Studies have also shown that high p21 expression correlates with early stage ovarian tumors and that only high p27 expression was necessary for disease free survival[239].

1.3 Epigenetics and ovarian cancer

Epigenetic mechanisms are essential for normal development and maintenance of tissue-specific patterns of gene expression in mammals[240]. Epigenetics is defined as a heritable change in gene expression without alteration of the primary DNA sequence. So, disruption of epigenetic processes can lead to altered gene function and malignant cellular transformation[240,241]. The current status of epigenomic research shows that epigenetic modifications among cancer cells result in aberrant gene expression via DNA methylation, histone modifications and post-transcriptional gene regulation by microRNAs (miRNAs)[242,243]. These modifications are also associated with initiation and progression of ovarian cancers[241,244].

In the last years, the importance of biomedical research towards epigenetics has increased, with the aim to discover the mechanisms that underlie the epigenetic regulation of cell physiology. From these studies the reversibility of epigenetic mechanisms showed promising targets to treat several diseases, through epigenetic targeted therapy.

The structure of chromatin is complex, made up of DNA, histones, and non-histones proteins[245], these last two are primary targets of epigenetic regulation[246]. Chromatin is made of repeating units of nucleosomes, which consist of 146 base pairs of DNA wrapped around an octamer composed by 2 copies of four core histone

proteins (H3, H4, H2A and H2B). This assembly is allowed by the negative charge of DNA and the positive charge of histone tails[247]. The histone octomer plays an important role in establishing interactions between the nucleosomes and within the nucleosome particle itself[248]. The N-terminal tails of core histones are flexible and unstructured, but the rest are predominantly globular and well structured. Depending on the epigenetic modifications that occur in DNA and in histone tails, chromatin can adopt different conformational changes that control the activation or repression of gene transcription.

There are at least eight distinct types of histone post-translational modifications, namely acetylation, methylation, phosphorylation, ubiquitylation, sumoylation, ADP ribosylation, deamination and proline isomerization[131]. They can be viewed as a regulatory code that resides in the pattern of post-translational modifications for which the histone amino terminal tails are the target[248]. In this brief introduction we will mentioned the two main modifications: DNA methylation and histone acetylation.

1.3.1 DNA methylation

DNA methylation is the most studied epigenetic modification with regard to carcinogenesis, and has also been the major focus of pharmacological interventions in clinical trials. In normal cells, the human genome is not methylated uniformly, containing unmethylated segments interspersed with methylated regions. DNA methylation occurs on the cytosine residues of CpG dinucleotides, CpG enriched regions are so-called CpG islands that are usually regions greater than 200 bp in length[249], that have more than 50 percent of CG content[250] and frequencies above 0.6% predominantly in the 5' promoter regions of the genes[251]. Enzymes known as DNA methyltransferases (DNMTs) catalyze the addition of a methyl group (CH_3) to the 5'-carbon of cytosine in CpG-3' (Figure 1.3)[252].

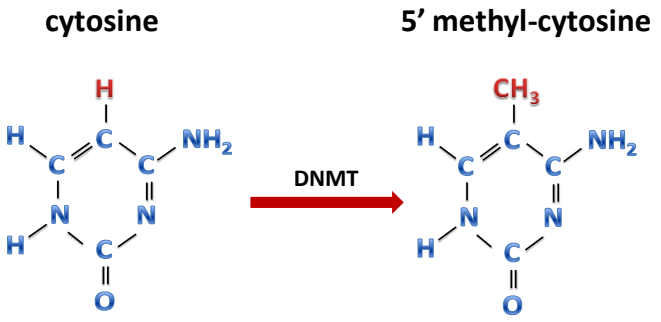

Figure 1. 3 – **Cytosine metylation**
Chemical structure of cytosine base unmethylated and methylated.

The methylation of CpG islands in gene promoters has been correlated with gene silencing, as it is an alternative pathway to the loss of tumor suppressor genes function, due to the lack of gene expression[253]. The epigenetic silencing of tumor suppressor genes has been associated with mechanisms such as uncontrolled cell division, the ability to infiltrate surrounding tissues, metastasis, avoiding apoptosis or sustaining angiogenesis, all of which are responsible for promoting tumor development. In ovarian cancer, a large number of tumor suppressor genes have been found to undergo promoter hypermethylation[254].

BRCA1 gene, as previous mentioned is one of the most studied genes, due to its role in inherited and sporadic forms of ovarian carcinomas[255,256]. It has been shown that promoter hypermethylation is a cause for *BRCA1* silencing[257] and has been reported in 15% of sporadic ovarian carcinomas[255,258].

In a study comparing the methylation status of *BRCA1* among tumor samples obtained from patients with benign ovarian tumors, borderline tumors and carcinomas, promoter methylation of *BRCA1* was detected in 31% of carcinomas but in none of the benign or borderline tumors[259]. Hypermethylation of *BRCA1* was significantly higher in serous carcinomas than in tumors of other histological type[260]. Methylation of *BRCA1*, while frequent in sporadic ovarian cancer, has not been reported in the hereditary type of the disease, nor in samples from women with a germline *BRCA1* mutation[261,262].

BRCA2 does not exhibit a similar methylation profile in ovarian cancer[263]. According to Chan et al.[264] methylated CpGs at the *BRCA2* promoter were either absent or at very low levels in tumor DNA compared to normal tissues[264].

Tumor suppressor genes involved in DNA mismatch repair (MMR) have a distinct carcinogenic mechanism in ovarian tumors. MMR is an endogenous molecular mechanism that corrects replication errors that escape the proof reading system of replicative DNA polymerases. In MMR-defective cells with methylation of promoters of MMR genes, base-to-base mismatches and insertion/deletion loops, are left uncorrected[265]. This results in increased spontaneous somatic mutations, being particularly obvious in non-expressed sequences comprising multiple simple repeats (microsatellites)[266]. Approximately 10% of ovarian cancers are related to this molecular pathway[267]. Defective MMR is often a consequence of germline mutations in the *MLH1*, *MSH2*, or, occasionally, *MSH6* or *PMS2* genes. Hypermethylation of the *MLH1* gene accompanied by loss of the gene expression has been reported in 10–30% of ovarian malignancies. This phenomenon is more frequently found in cases with acquired resistance to platinum-based chemotherapy (56%)[268,269]. The methylation frequency of *MSH2* promoters has also been reported to be as high as 57% in ovarian carcinomas, being higher in EC compared to other histological types[268]. Methylation grade of *MSH2* has been correlated with tumor grade and lymphatic metastasis.

Hypermethylation of tumor suppressor genes such as *PTEN* and $p16^{INK4A}$ have been observed contributing to the loss of function of these proteins in EOCs[260,270] and the absence of these proteins contribute to deregulate pathways.

DNA methyltransferases inhibitors have been proposed to be a promising strategy for epigenetic therapy in cancer treatment. The most commonly used DNMT inhibitors in clinical setting are nucleoside analogues, including 5-aza-2'-deoxycytidine (5-aza-dC)[240,246]. They are converted to deoxynucleotide triphosphates intracellularly and may be incorporated into replicating DNA instead of cytosine.

These inhibitors act by different actions, namely the loss of DNA methylation resulting in the re-expression of the tumor suppressor genes; the inhibition of tumor cell growth or by inducing cancer cell death[240,246].

In ovarian cancer, the recurrence of malignancy or the resistance to current therapies is one of the concerns in the treatment of these tumors. Epigenetic inhibitors hold the promise for overcoming chemoresistance through restoration of drug response genes and pathways[246]. Two clinical trials[271,272] provided evidences that DNA hypomethylation agents can reverse platinum resistance in ovarian cancer patients, suggesting the clinical benefits of epigenetic drugs in the treatment of chemoresistant or recurrent advanced cancer.

In summary, epigenetic alterations such as DNA methylation are involved in ovarian cancer initiation and progression. Hypermethylation has been found to be associated with the inactivation of almost every pathway involved in ovarian cancer development, including DNA repair, cell cycle regulation and apoptosis.

1.3.2 Histone acetylation

Histone modifications can alter histone-DNA interactions and consequent transcriptional activity due to changes in accessibility of the DNA to the transcriptional machinery. Histone tails are positively charged due to lysine and arginine amino acids. These positive charges allows the interaction and binding of the histone tails to the negatively charged phosphate groups on the DNA backbone[273].

Acetylation and deacetylation of histones play an important role in controlling chromatin activity and consequently transcription in eukaryotic cells[273]. The acetylation of histones and non-histone proteins is determined by the opposing activities of histone deacetylases (HDACs) and histone acetyltransferases (HATs). The balance between histone acetylation and deacetylation, mediated by HATs and HDACs, respectively, is usually tightly regulated, but this balance is often disturbed in diseases such as cancer[273].

Acetylation neutralizes the positive charges on the histone by changing amines into amides and decreasing the ability of the histones to bind to DNA. This decreased binding allows chromatin expansion, and genetic transcription takes place.

On the contrary, histone deacetylases remove those acetyl groups, retrieving the positive charge of histone tails and encouraging high-affinity binding between the

histones and DNA backbone[274]. The increased histone and DNA binding condenses chromatin structure and prevents transcription.

HDACs are a class of enzymes that remove acetyl groups ($O=C-CH_3$) from an ε-N-acetyl lysine amino acid on a histone, allowing the histones to wrap the DNA more tightly. A total of eighteen human HDACs enzymes are classified into four main groups depending on the homology of their catalytic domain[245,275], their subcellular localization and their enzymatic activity[276].

Classes I, II, and IV require a zinc molecule as an essential cofactor in their active site and are inhibited by Zn^{2+}-binding HDAC inhibitors[277]. Class I, includes HDAC1, HDAC2, HDAC3 and HDAC8. Class II, based on their sequence homology and domain organization, can be further subdivided into subclass IIa enzymes (HDACs 4, 5, 7 and 9) and subclass IIb enzymes (HDAC6 and HDAC10).

HDAC11 is the only member of the forth HDACs class, localized in the nucleus. Besides sharing the homology with class I and class II HDACs[278] and being a Zn^{2+}-dependent enzyme it does not have strong enough identity to be placed in either class. Class I HDACs are localized within the nucleus and are the most abundant and ubiquitously-expressed HDACs, whereas Class II localize between nucleus and cytoplasm depending upon the phosphorylation status, and their expression is tissue-specific (Table 1.2)[279–282].

Unlike conventional HDACs, class III HDACs are composed of seven mammalian sirtuins (SIRT1-7)[283]. They use nicotinamide adenine dinucleotide (NAD^+) as a cofactor instead of Zn^{2+}, therefore; they are not inhibited by Zn^{2+}-binding HDAC inhibitors. They are localized in the nucleus (SIRT1, SIRT6, and SIRT7), mitochondria (SIRT2, SIRT4, and SIRT5), and cytoplasm (SIRT2). The role of sirtuins in tumorigenesis is still controversial because some SIRTs have dual roles as oncoproteins and as tumor suppressor proteins[284,285].

Table 1. 2 - **Classes of histone deacetylases; localization in the cell, length, chromosomal localization and function**

HDAC family member	Cellular localization		Length (aa)	Chromosomal localization	Physiological function
Class I Zn^{2+} dependent	HDAC1	nucleus	483	1p34	Resistance to chemotherapy, proliferation, cell survival
	HDAC2	nucleus	488	6p21	Proliferation
	HDAC3	nucleus/cytoplasm	423	5q31	Proliferation, cell survival
	HDAC8	nucleus	377	Xq31	Proliferation
Class IIa Zn^{2+} dependent	HDAC4	nucleus/cytoplasm	1084	2q37	Angiogenesis, gluconeogenesis
	HDAC5	nucleus/cytoplasm	1122	17q21	Differentiation
	HDAC7	nucleus/cytoplasm	855	12q13	Differentiation
	HDAC9	nucleus/cytoplasm	1011	7p15-21	Angiogenesis
Class IIb Zn^{2+} dependent	HDAC6	cytoplasm	1215	Xp11	Migration
	HDAC10	cytoplasm	669	22q13	Migration
Class III NAD^{+} dependent	SIRT1	nucleus	747	--------	Differentiation, glucose metabolism, cell survival
	SIRT2	nucleus/cytoplasm mitochondria	389	--------	Cell cycle control, lipid synthesis
	SIRT3	nucleus	399	--------	ATP production, metabolism, apoptosis
	SIRT4	mitochondria	314	--------	Insulin secretion, metabolism, apoptosis
	SIRT5	mitochondria	310	--------	Urea cycle, metabolism, ATP regulation
	SIRT6	nucleus	355	--------	DNA repair, chromosome stability, metabolic regulation
	SIRT7	nucleus	400	--------	RNA pol I ,apoptosis transcription
Class IV Zn^{2+} dependent	HDAC11	nucleus	347	3p25	DNA replication

_____ not identified

Information retrieved from[245,275276].

1.3.3 HDAC inhibitors

Epigenetic alterations, as described above, are involved in the repression of tumor suppressor genes and promotion of tumorigenesis in ovarian cancers, thus drugs with histone deacetylase inhibitory activity are an attractive therapeutic approach[286].

HDAC inhibitors (HDACI) are chemical compounds that inhibit HDAC enzymes activity, leading to an increased acetylation of histones, and consequently to an increased transcription activity and subsequently upregulation of specific genes

involved in various cellular pathways including cell cycle, differentiation, DNA damage and repair, redox signaling, and apoptosis[276,279,287,288].

However, the complexity of the molecular network affected by the action of HDACIs does not allow the design of molecular pathways that may be predictive of therapeutic response. Hence, it remains unclear the molecular mechanisms underlying the response to HDAC inhibitors in cancer patients.

HDACIs undergoing evaluation for the treatment of cancer can be divided into four classes based on their chemical structure.

The classes include the short chain fatty acids (e.g., valproate and phenylbutyrate) that inhibit class I/IIa; hydroxamic acid derivatives (e.g., vorinostat, belinostat) that inhibit both class I and II enzymes; benzamides (e.g., entinostat,) that selectively inhibit a subset of class I enzymes and cyclic tetrapeptides (e.g., romidepsin)[245,275,289].

1.3.3.1 Mechanisms of action of HDACI

HDACI induce cell cycle arrest in both normal and transformed cells[287] and kill both proliferating and non-proliferating cells[290]. *In vitro*, the time of culture, concentration and type of HDACI used affect the number of genes detected with altered transcription *in vitro*. Short time points[291,292] and low concentrations[293] cause fewer changes in gene transcription and predominantly induce G_1 arrest, while increased time of exposure in culture and concentration of HDACI induces several changes in genes and induces both G_1 and G_2/M arrests[294].

G_1 and G_2 arrests are largely associated with induction of cyclin-dependent kinase (CDK) inhibitor p21, which blocks cyclin E/CDK2 complexes, leading to cell cycle arrest and inhibiting differentiation[294,295]. HDACI-induced expression of p21 is independent of p53 and correlates with an increase in the acetylation of histones associated with p21 promoter region[294,296]. In cells cultured with HDACI, the increase of CDK inhibitors and the decrease of cyclins may act together to account for the reduced CDK activity, causing dephosphorylation of Rb protein, which blocks cell cycle

through the inhibition of E2F activities in the transcription of genes for G_1 progression and G_1/S transition[279].

The action of HDACI cell cycle arrest in all cells is in contrast to the action of many chemotherapeutic drugs, which are only effective on proliferating cells. In some cells, the G_1 arrest is associated with terminal differentiation[294]. Transformed cells sensitive to HDACI induced cell death are usually in a cell growth-arrested state with increase of p21 expression[297]. Loss of p21 abolishes HDACI-induced G_1 arrest[297,298], as observed in HCT116 cells without p21 expression[299]. In some cases, HDACI may induce other CDK inhibitors that may cause cell cycle arrest. For example, TSA induces G_1 arrest in human colon HCT116 p21-/- cells associated with the induction of p15 (INK4b), which is an inhibitor of the cyclin D-dependent kinases[299].

HDAC inhibition also modulates the balance between pro- and anti-apoptotic proteins, causing cell death[300]. Hyperacetylation stabilizes the p53 protein, promoting both cell cycle arrest and the expression of proapoptotic genes[301]. HDAC inhibition upregulates the intrinsic and extrinsic apoptosis pathways through the induction of the proapoptotic genes, *Bmf* and *Bim*[302], and TRAIL and DR5, respectively[279].

HDACI activates the extrinsic apoptotic pathway by increasing expression of death receptors, including Fas (Apo-1 or CD95), tumor necrosis factor (TNF) receptor-1 (TNFR-1), TNF-related apoptosis-inducing ligand (TRAIL or Apo2-L) receptors (DR-4 and -5), DR-3 (Apo3) and DR-6, and their ligands, such as FasL, TNF, TRAIL and TL1A (Apo3L), leading to activation of caspase-8 and caspase-10[303]. HDACI induces this pathway *in vitro* and *in vivo*, in transformed cells, but not in normal cells[304,305]. Upregulation of death receptors and/or reducing the inhibitory regulators of death receptors pathway by HDACI sensitize tumor cells to TRAIL[279].

HDACI activates the intrinsic apoptotic pathways through the release of mitochondrial proteins, such as cytochrome *c*, apoptosis inducing factor (AIF) and Smac, with the consequent activation of caspase-9[279,281]. These mechanisms are regulated, in part, by pro- and antiapoptotic proteins of BCL-2 family[306]. Overexpression of Bcl-2 or BCL-XL, which protect mitochondria, inhibits HDACI-induced apoptosis. HDACI increase the proapoptotic proteins of BCL-2 family, such as BIM,

BMF, BAX, BAK and BIK[297,302] and decrease antiapoptotic proteins of Bcl-2 family, such as Bcl-2, BCL-XL, BCL-w and MCL-1[297,307]. The mechanism of this effect is not completely understood. It has been shown that vorinostat and TSA increase BIM transcription by increasing the activity of E2F1[302].

HDACI are also able to induce autophagy and at this process is expected to originate cell death and senescence[308].

The HDACI have shown synergistic or additive antitumor effects with a wide range of antitumor reagents, including chemotherapeutic agents such as antimetabolites 5-fluorodeoxyuridine and gemcitabine, antitubule agents paclitaxel and docetaxel, topoisomerase (Topo) II inhibitors doxorubicin, epirubicin, etoposide[309] and DNA crosslinking agent cisplatin[279,281,307]. The synergistic effects *in vitro* may depend on the sequence of drug administration.

Butyric acid and vorinostat (suberoylanilide hydroxamic acid or SAHA), two HDACIs will be further detailed. Vorinostat[310], which was FDA approved in 2006 for the treatment of cutaneous T-cell lymphoma has shown interesting results in *in vitro* models of ovarian cancer[311].

1.3.3.2 Butyric acid

Short chain fatty acids, in which butyrate (butyric acid) and valproate (valproic acid) are included, are carboxylate compounds that induce hyperacetylation through inhibition of HDAC, resulting in relaxation of chromatin, making DNA more accessible to transcription factors.

Butyric acid is a product resulting from fibers degradation in colon by bacteria and the natural synthesis and breakdown of longer chain fatty acid *in vivo*. But, in addition of being a part of the metabolic fatty acid cycle[312,313], butyric acid also functions as HDACI of class I and II enzymes to control cell proliferation and apoptosis in cancer cells[314]. Because cells are able to metabolize butyric acid, it is assumed that butyric acid has a weak effect as HDACI.

1.3.3.3 Vorinostat

Vorinostat is a small molecular weight (<300) linear hydroxamic acid compound that inhibits the enzymatic activity of a subset of class I HDACs, (HDAC1, HDAC2 and HDAC3) and the class II HDAC (HDAC6) at low nanomolar concentrations (half maximal inhibitory concentration < 86 nM)[245,281].

The molecular mechanisms of vorinostat-induced cell cycle arrest, differentiation, apoptosis and autophagy are not fully understood but are believed to be due to the inhibition of HDAC activity. Inhibition of HDAC activity by vorinostat causes an increase in acetylation of all the four core nucleosomal histones[245,281], induces the subsequent opening of DNA chain and promotes the expression of anti-proliferation and pro-apoptotic genes.

Many studies have found that the expression of approximately 5–10% genes is altered following exposure to vorinostat[245,275]. The genes regulated by vorinostat are dependent on the cell line under study and the study design (e.g, duration of vorinostat exposure and dose of vorinostat).

Vorinostat also causes an increase in acetylation of other chromatin modifying proteins, including members of the SWI/SNF family.

The exact molecular mechanisms how vorinostat induces apoptosis have yet to be fully clarified. It appears to occur through the interference in the intrinsic apoptotic pathway, characterized by the release of mitochondrial membrane proteins such as cytochrome C and the subsequent activation of caspases[275,315], but several studies have demonstrated that both caspase-dependent and independent cell death[275,308] can occur.

Vorinostat may affect cancer growth independently of its direct action on tumor cell proliferation and survival by regulating the expression of genes involved in tumor angiogenesis[316].

Vorinostat has demonstrated anti-tumor activity in a variety of *in vivo* rodent tumor models whether administered by the IP, IV or oral route in carcinogen-induced tumors[317], xenograft tumor models[318] and genetic mouse models[319,320]. Tumor growth

inhibition is observed at doses of vorinostat that do not produce toxic side effects. Vorinostat has also been evaluated in preclinical safety studies and the identified toxicities are reversible and easily monitored in clinical studies[321].

Vorinostat induces cell cycle arrest, differentiation, apoptosis and autophagy in transformed cell lines derived from hematological malignancies and solid tumors as monotherapy and in combination with cancer chemotherapies[322]. Vorinostat is well tolerated as both monotherapy and combined therapy with the most common toxicity symptoms including fatigue, nausea, diarrhea, anorexia and thrombocytopenia[323].

Vorinostat can be given orally, with a maximum tolerated dose (MTD) of 400 mg once daily or 200 mg twice daily, for hematological malignancies, but the dose level can be increased up to 600 mg in solid tumors[324].

In summary, HDACs catalyze the removal of acetyl groups from lysine residues of proteins, including the core nucleosomal histones. HDACIs have anti-tumor activity in preclinical and clinical studies. Non-neoplastic cells are relatively resistant to HDACI-induced cell death. The cell death pathways identified in mediating HDACI-induced transformed cell death include apoptosis by the intrinsic and extrinsic pathways, mitotic catastrophe/cell death, cell death as a consequence of autophagy, senescence and ROS-facilitated cell death.

Although a large number of investigations carried out in the last years have made possible a broad knowledge about HDACIs, the molecular basis for the antitumoral effects of HDACIs is not completely understood as well as the mechanisms underlying the sensitivity and resistance of cancer cells to drugs with epigenetic regulatory activity. Further research to understand the mechanism(s) of action of vorinostat and other HDACIs may reveal the way to developing rational combinations with other chemotherapeutic agents and perhaps ultimately to optimizing chemotherapy regimens for cancer patients.

AIM AND THESIS OUTLINE

Epithelial ovarian cancer (EOC) is the most lethal gynecological malignancy mainly due to late diagnosis, lack of specific therapy and resistance to conventional chemotherapy, based on platinum salts and taxanes. Hence, the discovery of new therapeutic strategies urges and the fact that histone deacetylases (HDACs) expression is increased in ovarian cancer points out HDAC inhibitors (HDACIs) as an attractive alternative.

The identification of ovarian cancer biomarkers that serve as indicators of cell sensitivity for HDACs inhibitors will allow the design of a more effective therapy. Furthermore, the understanding of the mechanisms underlying the action of drugs involved in epigenetic regulation can give us guidelines for new and more specific therapeutic strategies.

Our hypothesis is that HDACIs are useful drugs to treat ovarian cancer.

So, the main goal of this study was to disclose the mechanisms underlying the effect of HDACIs, in ovarian cancer. In order to accomplish this, five specific aims were addressed:

- To evaluate HDACs expression profiles in order to support the use of HDACIs in ovarian cancer (Chapter 2);
- To access *in vitro* alterations in proliferation and cell death in EOC cell lines, due to exposure to HDACIs (butyric acid and vorinostat) alone and in combination with 5-aza-dC, a DNA methyltransferase inhibitor, and conventional chemotherapy (carboplatin and paclitaxel) (Chapter 3);
- To evaluate the role of HNF1β in cell cycle arrest and apoptosis in CCC upon vorinostat exposure (Chapter 4);
- To study the modulatory effect of vorinostat in Notch signaling pathway (Chapter 5); and
- To establish human primary ovarian carcinoma cell lines, to be used as a tool to study EOC (Chapter 6).

The expression of HDACs was evaluated in EOC tissues samples. The effects of HDACI in ovarian cancer were evaluated *in vitro* by analyzing the general effects of HDACIs (butyric acid and vorinostat) alone and in combination with a DNA methyltransferase inhibitor, 5-aza-deoxycytidine (5-aza-dC), and with conventional therapy (carboplatin and paclitaxel) in cell behavior. In depth it was also addressed the effect of vorinostat, in cell cycle and apoptosis and in the expression of key genes in ovarian cancer such as HNF1β and Notch elements. Considering the importance of cell lines in cancer research, we also established a human ovarian cancer cell line of HGSC.

This thesis outline is organized in seven sections. In the 1st chapter there is a general introduction presenting all subjects and theoretical concepts concerning the thesis theme. The following sections include the results obtained in this PhD project (Chapter 2-6). Each chapter contains an abstract, a short introduction, methods, results and discussion. In the final chapter (chapter 7) the main conclusions enclosing all chapters are summarized and integrated, highlighting the major achievements that will contribute to improve the knowledge in ovarian cancer oncobiology.

CHAPTER 2

Protein expression profile of histone deacetylases (HDAC) 1, 2, 3, 4, 6 and PhosphoHDAC4/5/7 in ovarian cancer

Manuscript in preparation

Abstract

In cancer, histone acetylation was recognized has being involved in carcinogenesis and histone deacetylases (HDACs) play an important role in chromatin remodeling, gene repression, cell cycle progression, differentiation and therapy.

The present study aimed to investigate the expression profile of histone deacetylases (HDAC), Class I (HDAC1, 2, 3) and class II (HDAC4, 6 and phosphoHDAC4/5/7) in ovarian cancer, in order to support the evaluation of HDACIs in ovarian cancer. HDACs expression was analyzed by immunohistochemistry on tissue microarrays (TMA) from 64 patients with ovarian cancer. HDACs expression was evaluated and correlated with clinicopathological parameters and cell cycle markers.

Our results report that expression profile of HDACs were significantly associated with histological types of ovarian cancer. By immunohistochemistry, we found a high expression of HDAC1, 2, 3, 4, 6 and phosphoHDAC4/5/7 that was significantly associated with HGSC. The most expressed HDACs in CCC were HDAC1, 2 and 6.

HDAC3 was associated with stage and metastasis, HDAC4c and pHDAC4/5/7 were associated with metastasis in EOC. Kaplan-Meier curves showed that HDACs expression was not associated with survival.

Regarding the correlation with the cell cycle markers, we found that in HGSC HDAC1 expression was statistically associated with p21 expression, and HDAC3, HDAC4c and pHDAC4/5/7 were associated with p53 expression.

In addition, our results show that HDAC2, 3, 4 and phosphoHDAC4/5/7 were differentially expressed in HGSC and CCC.

In conclusion, the panel of HDACs expressed in HGSC and CCC supports the use of HDACIs as an alternative to treat ovarian cancer.

Keywords: HDACs, ovarian cancer, TMA, immunohistochemistry, HGSC, CCC.

Introduction

Epigenetic alterations including modifications of the acetylation status of histones in the development of human cancer have been recognized[246,325]. In the last years, several studies have highlighted the role of histone deacetylases (HDACs) in tumor progression and invasion and their potential use as therapeutic targets for cancer therapy and prognostic factors are recently emerging[326].

HDACs are regulators of gene expression by allowing the histones to wrap the DNA more tightly[274]**.** Histone acetylation is generally associated with increased transcription, while deacetylated histones are often associated with gene repression. Through these mechanisms, HDACs act as regulators of cell growth, differentiation and apoptotic programs and may favor neoplastic growth by allowing the aberrant transcription of key genes[327].

A total of eighteen human HDACs enzymes, classified in four main groups depending on the homology of their catalytic domain[245,275], their subcellular localization and their enzymatic activities[276] have been characterized in the literature and in Table 1.2, in Chapter 1.

Class I HDACs has been the most systematically investigated group with respect to function and relevance for tumor formation. In general, class I HDACs (HDACs 1-3 and 8) are primarily located in the nucleus and are associated with transcriptional repressors and cofactors, although there might be exceptions such as HDAC3, which are reported to be also located in the cytoplasm[328]. Class II HDACs (HDACs 4-7, 9 and 10) are large proteins that shuttle between the cytoplasm and the nucleus depending upon the phosphorylation status[279,282,287]**.**

In the last years, the expression of HDACs and its prognostic value has been analyzed in different kinds of human cancers[329–331]. HDAC expression seems to be associated with cell proliferation, angiogenesis, migration and invasion in cancer[329]. Based on these effects of HDAC new and different therapies were developed[332,333]. *In vitro* and *in vivo* assays showed that HDAC inhibition can limit growth of cancer cells and the differential expression of the various HDACs suggests that these enzymes play

unique roles in different cell types and tumors. At the present, HDACI in research and clinical use target class I and class II HDACs.

In 2006, the HDAC inhibitor suberoylanilide hydroxamic acid–vorinosat (SAHA) was the first HDACI to be approved for cutaneous T-cell lymphoma[334] therapy. In the last decade, different HDACI have being investigated in different types of cancers[335–337]. These drugs have been more intensively studied in cancer types with poor prognosis.

Epithelial ovarian cancers (EOC) are the leading cause of death in gynecological malignancies[3–5] and the high mortality is mainly due to advanced disease at diagnosis[5,13,338] and the lack of specific therapy. It is not clear which HDACs are active in these cancers and there is scarce information in the current literature about the expression profile of HDACs in ovarian carcinomas[325,339].

Our aim in this study was to evaluate expression profile of HDAC in human samples of ovarian carcinomas by immunohistochemistry and to find its potential relationship with tumor histology, clinical behavior and regulation of cell cycle proteins (p21, p16, p53 and cyclin D1). We also aimed to evaluate if its expression could help in the selection of HDACI.

Material and Methods

Patients and tissue samples

Representative cases of high grade serous ovarian carcinoma (HGSC) and clear cell carcinomas (CCC) were retrieved from the archives of the Department of Pathology of the Instituto Português de Oncologia de Lisboa de Francisco Gentil (IPOLFG). Only tumors treated with primary surgery were selected. All cases were reevaluated to confirm the histopathological diagnosis and 49 cases of HGSC and 15 cases of CCC were selected to construct a tissue microarray with 64 tumor samples of ovarian carcinoma and 2 commercial cell lines of ovarian carcinoma: OVCAR3 (a cell line derived from a HGSC) and ES2 (a derived cell line from a clear cell carcinoma).

The study protocol was approved by the Ethics Committee of IPOLFG (reference number UC-938/2013) and approved by NOVA Medical School University Ethics Committee (reference number 01/2015).

Cell lines

Clear cell carcinoma (CCC) cell line ES2 (CRL-1978) and high grade serous carcinoma (HGSC) cell line OVCAR3 (HTB-161) were obtained from American Type Culture Collection (Manassas, VA, USA). The cells were incubated at 37°C in a humidified atmosphere containing 5% CO2 in McCoy's 5A Modified Medium (Sigma-Aldrich, St. Louis, MO, USA) supplemented with 10% fetal bovine serum (FBS, S 0615, Invitrogen™, Thermo Fisher Scientific, Inc., Waltham, MA, USA) and 1% antibiotic-antimycotic (AA) (Invitrogen™; Thermo Fisher Scientific, Inc., Waltham, MA, USA). The cells were cultured to 80-100% confluence prior to detachment by incubation with 1X 0.05% trypsin-EDTA (Invitrogen™; Thermo Fisher Scientific, Inc.) at room temperature. Cells lines were collected and cytoblock was performed (according to manufacturer's instructions).

Tissue Microarray (TMA)

Representative hematoxylin and eosin (H&E) stained slides of ovarian cancer cases were selected for tissue microarray construction and three cores of each case were collected. Four cores from each commercial cell line cytoblocks were included.

Briefly, tissue cylinders with a diameter of 1.4 mm were punched from tumor areas of each donor tissue block and brought into a recipient paraffin block (tissue microarray–TMA), using a manual Tissue Puncher/Arrayer (Beecher Instruments, Silver Spring, MD, USA). Sections with normal (ovary, fallopian tube, tonsil, kidney) and cancer tissues (breast cancer, prostate cancer, mantle cell lymphoma) known to be positive for the different antibodies were used as positive controls. As negative controls, adjacent sections were processed as described above except that they were incubated without the primary antibody.

Immunohistochemistry

TMA sections (4μm) were cut for immunohistochemical analysis and sections were deparaffinized in xylene and dehydrated through graded concentrations of ethanol. Antigen retrieval was performed by PT Link (Dako), with target retrieval solution high pH, for 20 min at 95ºC. Formalin-fixed paraffin sections were incubated for 1h at room temperature with the following antibodies described in Table 2.1: mouse anti-HDAC1, mouse anti- HDAC2, rabbit anti-HDAC6, mouse anti-p21, mouse anti-p53, anti-CINTec p16, rabbit anti-cyclin D1 and were visualized by EnVision/HRP rabbit/mouse (ChemMate Envision Kit, Dako, K5007, USA). The visualization signal was developed with 3,3'-diaminobenzidine (DAB) solution, and all the slides were counterstained with Mayer's hematoxylin.

Immunohistochemical staining of sections of TMA for HDAC3, HDAC4 and phosphoHDAC 4/5/7 was performed using the Ventana Ultra BenchMark Automatic staining platform (Ventana Medical Systems, Tuscon, Az, USA). The slides were automatically deparaffinized and rehydrated using an EZ Prep solution. Antigen retrieval was achieved with ULTRA CC1 solution for 92 min of incubation. Sections were then incubated in primary antibody for 20 min for both mouse anti-HDAC3 and rabbit phosphoHDAC4/5/7. For the antibody rabbit anti-HDAC4, antigen retrieval was achieved with ULTRA CC1 for 40 min and incubated for 12 min. For antibodies p53, p16 and cyclinD1, antigen retrieval was achieved with ULTRA CC1 for 30 min and incubated for 20 min. The Benchmark platform uses a polymer detection system called OptiView to stain the antigen site brown. The sections were counterstained using Mayer´s Hematoxylin for staining contrast. Slides were then removed from the automated system, dry, covered, and analyzed by light microscopy.

Evaluation of Immunohistochemistry

The immunohistochemical evaluation was done by a pathologist and analyzed the nuclear and cytoplasmic expression of HDAC1, 2 and 3 (negative or positive) and the nuclear, cytoplasmic and/or membrane expression of HDAC4, 6 and phosphoHDAC4/5/7. A total of 64 cases of EOC and the two cell lines for HDACs with expression data were included in the final analysis.

Tissue microarrays were assessed for HDAC1, HDAC2, HDAC3, HDAC4, HDAC6 and phosphoHDAC4/5/7 staining. A two score system was used: 0 for negative cases, and 1 for positive cases. In all cores, at least some non-neoplastic cells, such as endothelial cells, lymphocytes or fibroblasts showed a weak and faint positivity with all HDAC antibodies. In total, only one case (2 %) of clear cell carcinoma was not interpretable for one marker. The staining for p53, p21, p16 and cyclin D1 was considered to be positive when there was a strong and widespread staining (>10%) of the nucleus of the tumor cells was found. Regarding p53 expression, three patterns were registered: positivity in >75% of tumor cells were stained; positive in ≤ 75% of cells; and the null pattern: when 0% of the neoplastic cells were positive.

Table 2. 1 - **Antibodies used for imunohistochemical study**

Antibody, clone, catalog number, company	**Dilution**	**Positive control**
Anti-Cyclin D1 SP4, 241R, Cell Marque	1:30	mantle cell lymphoma
Anti-HDAC1, clone 10E2, 5356 Cell Signaling Technology	1:2500	tonsil
Anti-HDAC2, clone 3F3, 5113 Cell Signaling Technology	1:500	tonsil
Anti-HDAC3, clone 7G6C5, 3949 Cell Signaling Technology	1:500	tonsil
Anti-HDAC4, clone 10E2, 7628, Cell Signaling Technology	1:500	breast cancer
Anti-HDAC6, clone D2E5, 7558 Cell Signaling Technology	1:500	prostate cancer
Anti-phosphoHDAC4/5/7, clone D2E5, 3443 Cell Signaling Technology	1:200	breast cancer
Anti-CINtec p16 clone E6H4, 725-4713 Ventana Medical System	predilute	cervical cancer
Anti-p21, clone SX118, M7202, Dako	1:40	tonsil
Anti-p53 clone DO7, 453M, Cell Marque	1:150	colon cancer

Statistical evaluation

For statistical analysis, IBM SPSS, version 21 (IBM Inc., Armonk, USA) was used. Associations between HDACs expression and clinical and pathological parameters were assessed by contingency tables and Fisher´s exact test to evaluate the distribution and the association of HDAC expression across tumors and by generalized linear models. Chi-square test was used to assess the associations of HDACs proteins expression with clinicopathological variables and cell cycle proteins.

Univariate survival analysis was performed by the generation of Kaplan-Meier curves, and differences between groups were compared by the log-rank test.

Multivariable survival analysis was performed using the Cox proportional hazards model. A *p*-value of 0.05 or less was considered statistically significant. Results were presented as hazard ratio (HR) and 95% confidence interval (CI).

Clinical and pathological characteristics

The main clinicopathological characteristics of ovarian cancer patients are presented in Table 2.2.

The median age of patients diagnosed as HGSC was 62 years old (range 35 and 82). Tumors stage was done using FIGO classification and 12% (6) of carcinomas were classified at stage I, 23% (11) were at stage II and the remaining 65% (32) patients were at stage III (table 2.2). The follow-up period was defined as the time interval between the surgery and last medical appointment or death. The median follow-up time was 58 months (range, 1 to 167 months). All cases were treated with adjuvant chemotherapy but two cases. Recurrences were diagnosed in all but 2 patients, 31 (63%) were local recurrences and metastases were found in 96% of patients (47/49). At the end of the follow up a total of 37 patients died (37/49, 88 %) of disease progression, 3 patients were lost for follow up, 4 died from other causes and only 5 (12%) patients remain alive of which 2 were alive without disease and 3 patients were alive with disease.

Table 2. 2 - **Clinical and pathological characteristics of the EOC patients**

Clinicopathological parameters	**HGSC (n=49)** **No. of patients (%)**	**CCC (n=15)** **No. of patients (%)**
Age		
≤ 61.5 years	22 (45)	8 (53)
> 61.5 years	27 (55)	7 (47)
median	62	61
Stage (FIGO)		
I	6 (12)	14 (93)
II	11 (23)	0
III	32 (65)	1(7)
Metastasis		
absent	2 (4)	12 (80)
present	47 (96)	3(20)
Status		
alive	5 (12)	9 (64)
died of disease	37 (88)	4 (31)
others*	7	2

* lost for follow-up, died of other causes

Regarding CCC, the median age of patients at the time of diagnosis was 61 (range, 31-81 years). All tumors were stage I, except one diagnosed at stage IIIC (Table 2.1). Follow up data was obtained and mean follow up was 56 months ranging from 17 months to 140 months. All cases were treated with surgery and chemotherapy. Recurrences occurred in 5 patients and metastases occur in 3 of 15 patients (20%). At the end of follow up, 9 (64%) of patients were alive being one alive with disease; 4(31%) patients died of disease's progression; 1 died of another cause, and one was lost for follow up.

Evaluating all cases included in this cohort, the median overall survival of patients was 56 months with a confidence interval between 45 to 67 months.

Results

HDACs expression in EOC

Immunostains were evaluated in all tissue cores of the TMA that included controls (normal and cancer tissues), tumor cases and cores from the commercial cell lines. HDAC1, HDAC2 staining was only present in the nucleus of cells. Regarding HDAC3, a nuclear staining was seen except in three cases diagnosed as HGSC, whereas HDAC3 had also a faint cytoplasmic expression in tumor cells. In all the previous TMA core samples, HDAC4 was expressed in the cytoplasm and in the membrane and phosphoHDAC4/5/7 and HDAC6 expression were present only in the cytoplasm.

As regard to commercial cell lines HDAC1, 2, 3 and 6 was expressed in the nucleus of OVCAR3 cells (high grade serous carcinoma cell line) and ES2 (clear cell carcinoma cell line). Both cell lines cells did not exhibit HDAC4 or phosphoHDAC4/5/7 staining, although rare ES2 cells exhibited phosphoHDAC4/5/7.

Regarding the results of HDACs in the ovarian carcinoma's samples, most cores showed an intermediate or high expression of the analyzed enzymes. The results of HDACs expression were registered in Figures 2.1., 2.2 and in Tables 2.3 to 2.6.

Table 2. 3 - **Expression of HDACs in EOC commercial lines**

Cell lines	HDAC1	HDAC2	HDAC3	HDAC4m	HDAC4c	HDAC6	pHDAC4/5/7
OVCAR3	1	1	1	0	0	1	0
ES2	1	1	1	0	0	1	rare

0= negative; 1=positive;
HDAC4m: membrane; HDAC4c: cytoplasm; pHDAC4/5/7: phosphoHDAC4/5/7

Table 2. 4 - **Expression of HDACs in EOC samples and its association with the histological type**

HDACs	HGSC			CCC			Total	
	positive	%	95% CI	positive	%	95% CI	patients	p-value
HDCA1	38	78	0.641-0.869	15	100	0.796-1.000	64	0.0540
HDAC2	49	100	0.927-1.000	12	80	0.548-0.929	64	**0.0109**
HDAC3	44	90	0.782-0.955	5	33	0.151-0.582	64	**0.0001**
HDAC4m	27	55	0.413-0.681	3	21	0.704-0.451	63	**0.0349**
HDAC4c	44	90	0.782-0.955	3	21	0.704-0.451	63	**0.0001**
HDAC6	41	84	0.709-0.914	13	87	0.621-0.962	64	1.000
phosphoHDAC4/5/7	45	92	0.808-0.967	6	43	0.198-0.642	63	**0.0003**

HDAC4m: membrane; HDAC4c: cytoplasm

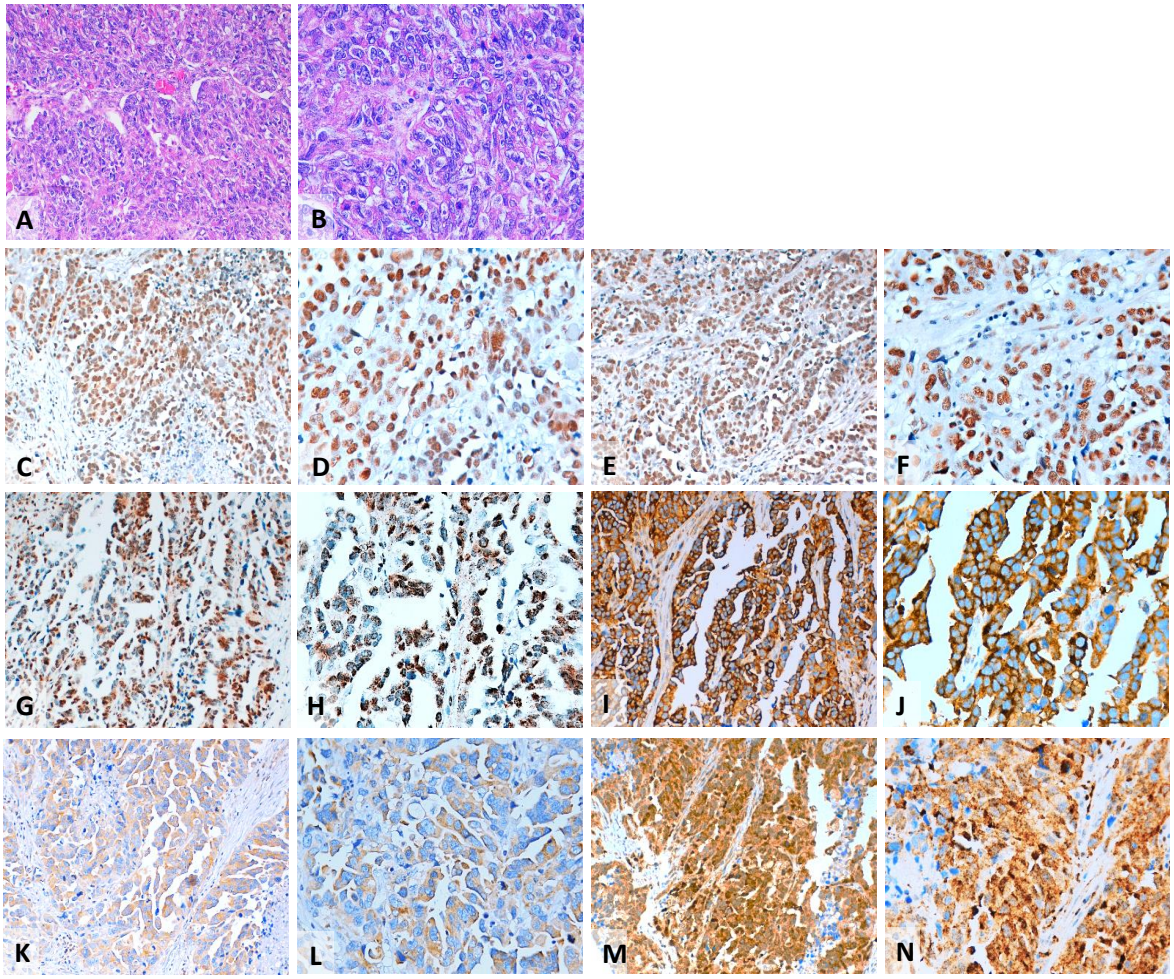

Figure 2. 1- **Representative pattern of HDACs protein expression in HGSC in tissue microarray (TMA) sections.**
Hematoxylin (H&E) and immunohistochemical stains for HDACs in TMA sections of HGSC. A, B- H&E; C, D- HDAC1; E, F- HDAC2; G, H- HDAC3; I, J- HDAC4; K, L- HDAC6; M, N- pHDAC4/5/7. Two magnifications (200x and 400x) are presented for each antibody.

In HGSC cases, a very high expression of HDACs was found (Table 2.4). HGSC expressed high levels of class I HDAC: 78% (38/49) for HDAC1; 100% (49/49) for HDAC2 and 90% (44/49) for HDAC3. Regarding class II HDACs, HDAC4 expression in HGSC cases in the cytoplasm was more frequent than in the membrane, 90% (44/49) *vs* 55% (27/49), respectively. Cytoplasmic expression of HDAC6 and phosphoHDAC4/5/7 was also found in this tumor type in 84% (41/64) and 92% (45/49), respectively.

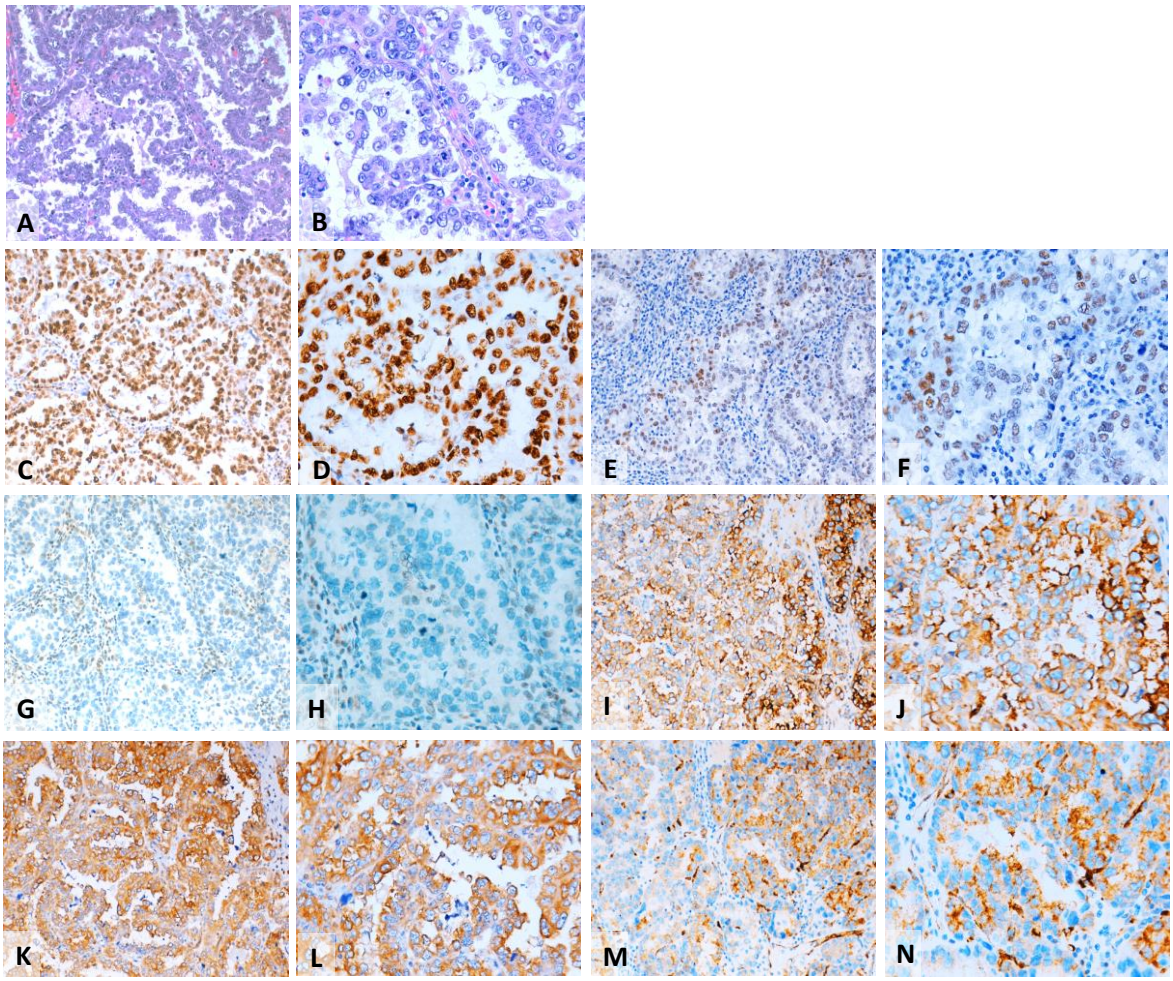

Figure 2. 2 - **Representative pattern of HDACs protein expression in CCC in tissue microarray (TMA) sections**
Hematoxylin (H&E) and immunohistochemical stains for HDACs in TMA sections of HGSC. A, B- H&E; C, D- HDAC1; E, F- HDAC2; G, H- HDAC3; I, J- HDAC4; K, L- HDAC6; M, N- pHDAC4/5/7. Two magnifications (200x and 400x) are presented for each antibody.

In CCC cases (Table 2.4), HDAC1, 2 and 6 were strikingly expressed, 100% (15/15), 80% (12/15) and 87% (13/15), respectively. However, HDAC3 expression was moderate, being only present in 33% (5/15) of cases, and HDAC4 even lower in the membrane and in the cytoplasm, only 21% (3/15) of cases expressed. PhosphoHDAC4/5/7 expression was observed in 43% (6/15) of cases.

The different expression of the HDACs and the tumor type were significant regarding HDAC2, HDAC3, HDAC4 and phosphoHDAC4/5/7 immunodetection, being more expressed in HGSC than in CCC. HDAC2 was present in all HGSC and only present in 80% of CCC being this difference significant with a p=0.0109 (CI=0.548-1.000). Nuclear HDAC3 expression was higher in HGSC compared to CCC, being this difference also significant (p<0.0001). Both membrane (p=0.0349) and cytoplasmic (p<0.0001) HDAC4 expression were associated with HGSC cases. PhosphoHDAC4/5/7 expression was also significantly associated (p=0.0003) with HGSC type as reported in Table 2.4.

HDACs expression and clinicopathological parameters in EOC

We analyzed the expression profile of HDACs and the clinicopathological data in separate groups for histological type and the all EOC.

In univariate analysis of all cases of EOC the expression of some of these enzymes was correlated with the clinicopathological parameters as reported in Table 2.5.

Table 2. 5 - **Association of HDACs expression and clinicopathological parameters in EOC** (Univariate analysis).

	HGSC n=49			CCC n=15			HGSC+CCC n=64		
	HDAC1 expression		**p value**	**HDAC1 expression**		**p value**	**HDAC1 expression**		**p value**
	negative n (%) 11	positive n (%) 38		negative n (%) 0	positive n (%) 15		negative n (%) 11	positive n (%) 53	
Age									
≤61.5	5 (45)	17 (45)	1.000	0	9 (60)		5 (45)	26 (49)	1.0000
>61.5	6 (55)	21 (55)		0	6 (40)		6 (55)	27 (51)	
Histological Type									
HGSC							11 (100)	38 (72)	**0.054**
CCC							0	15 (28)	
Stage									
I-II	3 (27)	14 (37)	0.725	0	14 (93)		3 (27)	28 (53)	0.186
III	8 (73)	24 (63)		0	1 (7)		8 (73)	25 (47)	
Metastasis									
absent	1 (9)	1 (3)	0.402	0	12 (80)		1 (9)	13 (25)	0.431
present	10 (91)	37 (97)		0	3 (20)		10 (91)	40 (75)	
	HDAC2 expression		**p value**	**HDAC2 expression**		**p value**	**HDAC2 expression**		**p value**
	negative n (%) 0	positive n (%) 49		negative n (%) 3	positive n (%) 12		negative n (%) 3	positive n (%) 61	
Age									
≤61.5	0	27 (55)		1 (33)	8 (67)	0.525	1 (33)	30 (49)	1.000
>61.5	0	22 (45)		2 (67)	4 (33)		2 (67)	31 (51)	
Histological Type									
HGSC	0						0	49 (20)	0.010
CCC	0						3	12 (80)	
Stage									
I-II	0	17 (35)		2 (67)	12 (100)	0.200	2 (67)	29 (48)	0.607
III	0	32 (65)		1 (33)	0		1 (33)	32 (52)	
Metastasis									
absent	0	2 (4)		2 (67)	10 (88)	0.516	2 (67)	12 (20)	0.118
present	0	47 (96)		1 (33)	2 (12)		1 (33)	49 (80)	
	HDAC3 expression		**p value**	**HDAC3 expression**		**p value**	**HDAC3 expression**		**p value**
	negative n (%) 5	positive n (%) 44		negative n (%) 10	positive n (%) 5		negative n (%) 15	positive n (%) 49	
Age									
≤61.5	0	4 (5)	1.000	5 (50	4 (80)	0.580	7 (47)	24 (49)	1.000
>61.5	5 (100)	42 (95)		5 (50)	1 (20)		8 (53)	25 (51)	
Histological Type									
HGSC							5 (33)	44 (90)	**0.0001**
CCC							10 (67)	5 (10)	
Stage									
I-II	5 (100)	12 (27)	**0.0032**	9 (90)	5 (100)	1.000	14 (93)	17 (35)	**0.0001**
III	0	32 (73)		1 (10)	0		1 (7)	32 (65)	
Metastasis									
absent	0	2 (5)	1.000	8 (80)	4 (80)	1.000	8 (47)	6 (12)	**0.002**
present	5 (100)	42 (95)		2 (20)	1 (20)		7 (53)	43 (88)	

	HGSC n=49			CCC n=15			HGSC+CCC n=64		
	HDAC4c expression			**HDAC4c expression**			**HDAC4c expression**		
	negative n (%) 5	positive n (%) 44	**p value**	negative n (%) 12	positive n (%) 3	**p value**	negative n (%) 16	positive n (%) 47	**p value**
Age									
≤61.5	4 (40)	18 (41)	0.160	5 (45)	2 (67)	0.209	9 (44)	21 (45)	0.564
>61.5	1 (20)	26 (59)		6 (55)	1 (33)		7 (56)	26 (55)	
Histological Type									
HGSC							5 (31)	44 (94)	**0.0001**
CCC							11 (69)	7 (6)	
Stage									
I-II	1 (20)	16 (36)	0.646	10 (91)	3 (100)	1.000	11 (69)	19 (40)	0.081
III	4 (80)	28 (64)		1 (9)	0		5 (31)	28 (60)	
Metastasis									
absent	1 (20)	1 (2)	0.196	10	1	0.093	11 (69)	2 (4)	**0.0001**
present	4 (80)	43 (98)		1	2		5 (31)	45 (96)	

	HDAC4m expression			**HDAC4m expression**			**HDAC4m expression**		
	negative n (%) 22	positive n (%) 27	**p value**	negative n (%) 11	positive n (%) 3	**p value**	negative n (%) 33	positive n (%) 30	**p value**
Age									
≤61.5	9 (40)	13 (48)	0.774	5 (45)	2 (67)	1.000	15 (45)	15 (50)	0.803
>61.5	13 (59)	14 (52)		6 (55)	1 (33)		18 (55)	15 (50)	
Histological Type									
HGSC							22 (67)	27 (90)	**0.034**
CCC							11 (33)	3 (10)	
Stage									
I-II	10 (45)	7 (26)	0.228	10 (91)	3 (100)	1.000	20 (39)	10 (33)	**0.044**
III	12 (55)	20 (74)		1 (9)	0		13 (61)	20 (67)	
Metastasis									
absent	0	2 (7)	0.495	9 (82)	2 (67)	1.000	9 (27)	4 (13)	0.221
present	22 (100)	25 (93)		2 (18)	1 (33)		24 (73)	26 (87)	

	HDAC6 expression			**HDAC6 expression**			**HDAC6 expression**		
	negative n (%) 8	positive n (%) 41	**p value**	negative n (%) 2	positive n (%) 13	**p value**	negative n (%) 10	positive n (%) 54	**p value**
Age									
≤61.5	5 (62)	17 (41)	0.440	0	9 (69)	0.143	5 (50)	26 (48)	1.000
>61.5	3 (38)	24 (59)		2 (100)	4 (31)		5 (50)	28 (52)	
Histological Type									
HGSC							8 (80)	41 (76)	1.000
CCC							2 (20)	13 (24)	
Stage									
I-II	1 (12)	16 (39)	0.233	2 (100)	12 (92)	1.000	3 (30)	28 (52)	0.305
III	7 (88)	25 (61)		0	1 (8)		7 (70)	26 (48)	
Metastasis									
absent	0	2 (5)	1.000	2 (100)	10 (77)	1.000	2 (20)	12 (22)	1.000
present	8 (100)	39 (95)		0	3 (23)		8 (80)	42 (78)	

	pHDAC expression			**pHDAC expression**			**pHDAC6expression**		
	negative n (%) 4	positive n (%) 45	**p value**	negative n (%) 8	positive n (%) 6	**p value**	negative n (%) 12	positive n (%) 51	**p value**
Age									
≤61.5	3 (75)	19 (42)	0.314	5 (63)	3 (50)	1.000	8 (67)	22 (43)	0.202
>61.5	1 (25)	26 (58)		3 (37)	3 (50)		4 (33)	29 (57)	
Histological Type									
HGSC							4 (33)	45 (88)	**0.0001**
CCC							8 (67)	6 (12)	
Stage									
I-II	1 (25)	16 (36)	1.000	7 (88)	6 (100)	1.000	8 (67)	22 (43)	0.202
III	3 (75)	29 (64)		1 (12)	0		4 (33)	29 (57)	
Metastasis									
absent	1 (25)	1 (2)	0.471	6 (75)	5 (83)	1.000	7 (58)	6 (12)	**0.001**
present	3 (75)	44 (98)		2 (25)	1 (17)		5 (42)	45 (88)	

In summary, HDAC3 expression was associated with stage (p=0.001), being present in high stage HGSC at presentation (p=0.002) and HDAC3, HDAC4c and phosphoHDAC4/5/7 expression was associated with the presence of metastasis (p=0.002), (p=0.001) and (p=0.001), respectively. No prognostic value of HDACs in overall survival (OS) was found using Kaplan-Meier method and log-rank test.

Subsequently, we performed multivariate analysis and the results indicated that there is a trend of association between the histological type and metastasis and in our cohort the histological type is an independent factor.

Table 2. 6 - **Multivariate analysis of HDAC3, HDAC4c and phosphoHDAC4/5/7 expression for histological type and metastasis**

Parameters	HDAC3			HDAC4c			pHDAC4		
	OR	95% CI	p value	OR	95% CI	p value	OR	95% CI	p value
Histological type (HGSC vs CCC)	0.045	0.004-0.494	0.011	0.149	0.19-1.148	0.68	0.112	0.013-0.956	0.045
Metastasis (absent vs present)	0.738	0.63-8.633	0.809	14.465	1.7-121.6	0.14	2.046	0.232-18.04	0.519

HDAC4c: cytoplasm, pHDAC4/5/7: phosphoHDACs/5/7, OR, odds ratio; CI, confidence interval

HDACs expression and cell cycle markers in EOC

The results of the immunohistochemical study of cell cycle markers performed on commercial cell line and EOC samples are registered in figure 2.3 and table 2.7 and 2.8.

Concerning the EOC cell lines, OVCAR3 expressed p53 and cyclin D1, and no expression for p16 and p21 was observed. ES2 exhibited p16, p53, Cyclin D1, however p21 was not present.

Table 2. 7 - **Expression of cell cycle markers in EOC commercial cell lines**

Cell lines	p16	p21	p53	Cyclin D1
OVCAR3	0	0	1*	1
ES2	1	0	1*	1

0= negative; 1=positive;
1*= overexpressed

Table 2. 8 - **Expression of cell cycle markers in EOC samples**

	HGSC			CCC			Total	p-value
	negative	positive	% positive	negative	positive	% positive	patients	
p16	11	38	78	4	11	73	64	0.737
p21	26	23	47	4	11	73	64	0.085
p53	15	34	69	3	12	80	64	0.528
Cyclin D1	40	9	18	13	2	13	64	1.000

	HGSC			CCC			
	negative <75% *	positive >75%	% positive #	Negative <75% *	positive >75%	% positive #	p value
p53	4	45	92	11	4	27	0.001

p53***Negative** – cases that show positive p53 stain in <75%; **Positive** - cases that show positive p53 stain in more than 75% of cells (overexpressed) or are completely negative (null)

In ovarian carcinoma cases, p21 was confined to the nucleus and was positive in 23 (47%) of HGSC and in 11 (73%) of CCC. In spite of a higher p21 expression in clear cell carcinomas, the p21 status was not associated to the histological subtype. Regarding p16 and cyclin D1 a very similar nuclear expression was found in both tumor types. In this cohort, the p53 status was related to histological type (p=0.001).

We analyzed expression of cell cycle markers in EOC (Table 2.9) and HDAC expression and we observed significant association between the expression of HDAC1 and p21 (p=0.002). We also observed significant association between p53 and some HDACs. We found that p53 positivity was correlated with HDAC3 (p=0.002), HDAC4c (p=0.033) and pHDAC4/5/7 (p=0.018). Cyclin D1 and p16 immunoexpression was not associated with any of the HDACs proteins studied in this series.

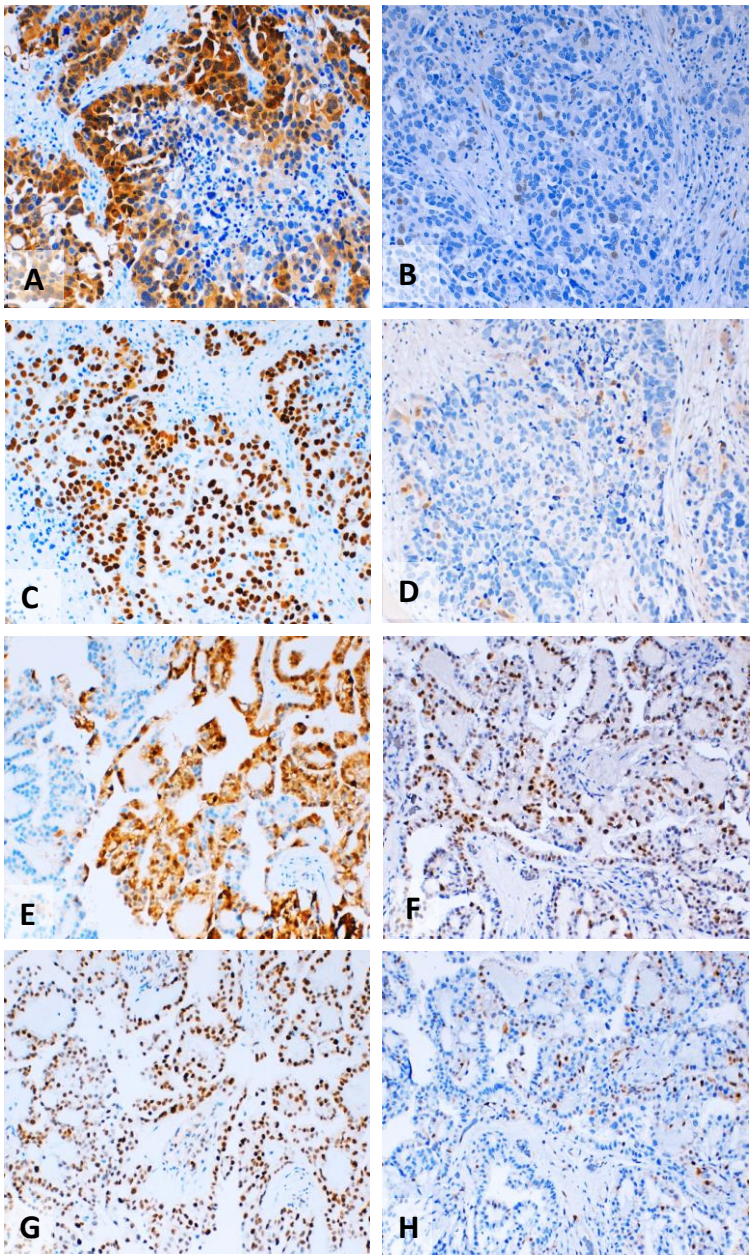

Figure 2. 3 - **Representative examples of immunostaining for p16, p21, p53 and cyclin D1 in different histological types of ovarian cancer**
Immunohistochemical stains for the cell cycle markers were performed in TMA sections. HGSC samples: A- p16, B- p21, C- p53, D- cyclinD1; CCC: E- p16, F- p21, G- p53, H- cyclinD1.

Table 2. 9 - **Expression of HDACs expression and cell cycle markers in EOC**

Cell cycle markers	HGSC n=49			CCC n=15			HGSC+CCC n=64		
	HDAC1 expression		p value	HDAC1 expression		p value	HDAC1 expression		p value
	negative n (%) 11	positive n (%) 38		negative n (%) 0	positive n (%) 15		negative n (%) 11	positive n (%) 53	
p16 expression									
negative	3 (27)	8 (21)	0.692	0	4 (27)		3 (27)	12 (23)	0.710
positive	8 (73)	30 (79)		0	11 (73)		8 (73)	41 (77)	
p21 expression									
negative	10 (91)	16 (42)	**0.006**	0	4 (27)		10 (91)	20 (38)	**0.002**
positive	1 (9)	22 (58)		0	11 (73)		1 (9)	33 (62)	
p53 expression									
overexpressed/null	9 (82)	36 (95)	0.214	0	5 (37)		9 (82)	41 (77)	1.000
"wild type"	2 (18)	2 (5)		0	10 (67)		2 (18)	12 (23)	
Cyclin D1 expression									
negative	10 (91)	30 (79)	0.662	0	13 (87)		10 (91)	43 (81)	0.672
positive	1 (9)	8 (21)		0	2 (13)		1 (9)	10 (19)	

	HDAC2 expression		p value	HDAC2 expression		p value	HDAC2 expression		p value
	negative n (%) 0	positive n (%) 49		negative n (%) 3	positive n (%) 12		negative n (%) 3	positive n (%) 61	
p16 expression									
negative	0	11(22)		1 (33)	3 (25)	1.000	1 (33)	14 (23)	0.558
positive	0	38 (78)		2 (67)	9 (75)		2 (67)	47 (77)	
p21 expression									
negative	0	26 (53)		1 (33)	3 (25)	1.000	1(33)	29 (48)	1.000
positive	0	23 (47)		2 (67)	9 (75)		2(67)	32 (52)	
p53 expression									
overexpressed/null	0	45 (92)		1 (33)	4 (33)	1.000	1(33)	49 (80)	0.118
"wild type"	0	4 (8)		2 (67)	8 (67)		2(67)	12 (20)	
Cyclin D1 expression									
negative	0	40 (82)		3 (100)	10 (83)	1.000	3 (100)	50 (82)	1.000
positive	0	9 (18)		0	2 (17)		0	11 (18)	

	HDAC3 expression		p value	HDAC3 expression		p value	HDAC3 expression		p value
	negative n (%) 5	positive n (%) 44		negative n (%) 10	positive n (%) 5		negative n (%) 15	positive n (%) 49	
p16 expression									
negative	2 (40)	9 (20)	0.311	3 (30)	1 (20)	1.000	5 (33)	10 (20)	0.315
positive	3 (60)	35 (80)		7 (70)	4 (80)		10 (67)	39 (80)	
p21 expression									
negative	3 (60)	23 (52)	1.000	4 (40)	0 (27)	0.231	7 (47)	23 (47)	1.000
positive	2 (40)	21 (48)		6 (60)	5 (73)		8 (53)	26 (53)	
p53 expression									
overexpressed/null	4 (80)	41 (93)	0.359	3 (30)	2 (40)	1.000	7 (47)	43 (88)	**0.002**
"wild type"	1 (20)	3 (7)		7 (70)	3 (60)		8 (53)	6 (12)	
Cyclin D1 expression									
negative	4 (80)	36 (82)	1.000	10 (100)	3 (60)	0.095	14 (93)	39 (80)	0.434
positive	1 (20)	8 (18)		0	2 (40)		1 (7)	10 (20)	

Cell cycle markers	HGSC n=49			CCC n=15			HGSC+CCC n=64		
	HDAC4c expression		p value	HDAC4c expression		p value	HDAC4c expression		p value
	negative n (%) 5	positive n (%) 44		negative n (%) 11	positive n (%) 3		negative n (%) 16	positive n (%) 47	
p16 expression									
negative	0	11 (25)	0.574	4 (36)	0	0.505	4 (25)	11 (23)	1.000
positive	5 (100)	33 (75)		7 (64)	3 (100)		12 (75)	36 (77)	
p21 expression									
negative	4 (80)	22 (50)	0.353	2 (18)	1 (33)	1.000	6 (62)	23 (49)	0.564
positive	1 (20)	22 (50)		9 (82)	2 (67)		10 (38)	24 (51)	
p53 expression									
overexpressed/null	5 (100)	40 (91)	1.000	4 (36)	0	0.505	9 (56)	40 (85)	**0.033**
"wild type"	0	4 (9)		7 (64)	3 (100)		7 (44)	7 (15)	
Cyclin D1 expression									
negative	4 (80)	36 (82)	1.000	9 (82)	3 (100)	1.000	13 (81)	39 (83)	1.000
positive	1 (20)	8 (18)		2 (18)	0		3 (19)	8 (17)	

	HDAC4m expression		p value	HDAC4m expression		p value	HDAC4m expression		p value
	negative n (%) 22	positive n (%) 27		negative n (%) 11	positive n (%) 3		negative n (%) 33	positive n (%) 30	
p16 expression									
negative	5 (23)	6 (22)	1.000	4 (36)	0	0.505	9 (73)	6 (20)	0.564
positive	17 (77)	21 (78)		7 (64)	3 (100)		24 (27)	24 (80)	
p21 expression									
negative	11 (50)	15 (56)	0.778	2 (18)	1 (67)	1.000	13 (39)	16 (53)	0.317
positive	11 (50)	12 (44)		9 (82)	2 (33)		20 (61)	14 (47)	
p53 expression									
overexpressed/null	20 (90)	25 (93)	1.000	4 (36)	0	0.505	24 (73)	25 (83)	0.373
"wild type"	2 (9)	2 (7)		7 (64)	3 (100)		9 (27)	5 (17)	
Cyclin D1 expression									
negative	16 (73)	24 (89)	0.266	9 (92)	3 (100)	1.000	25 (76)	27 (90)	0.189
positive	6 (27)	3 (11)		2 (18)	0		8 (24)	3 (10)	

	HDAC6 expression		p value	HDAC6 expression		p value	HDAC6 expression		p value
	negative n (%)8	positive n (%) 41		negative n (%) 2	positive n (%) 13		negative n (%) 10	positive n (%) 54	
p16 expression									
negative	2 (25)	9 (22)	1.000	2 (100)	2 (15)	0.057	4 (40)	11 (20)	0.226
positive	6 (75)	32 (78)		0	11 (85)		6 (60)	43 (80)	
p21 expression									
negative	4 (50)	22 (54)	1.000	0 (40)	4 (31)	1.000	4 (40)	26 (48)	0.738
positive	4 (50)	19 (46)		2 (60)	9 (69)		6 (60)	28 (52)	
p53 expression									
overexpressed/null	7 (86)	38 (93)	0.522	2 (100)	3 (23)	0.095	9 (90)	41 (76)	0.437
"wild type"	1 (12)	3 (7)		0	10 (77)		1 (10)	13 (24)	
Cyclin D1 expression									
negative	8 (100)	32 (78)	0.322	2 (100)	11 (85)	1.000	10 (100)	43 (80)	0.188
positive	0	8 (22)		0	2 (15)		0	11 (20)	

	pHDAC4/5/7 expression		p value	pHDAC4/5/7 expression		p value	pHDAC64/5/7 expression		p value
	negative n (%) 4	positive n (%) 45		negative n (%) 8	positive n (%) 6		negative n (%) 12	positive n (%) 51	
p16 expression									
negative	2 (50)	9 (20)	0.214	3 (37)	1 (17)	0.580	5 (42)	10 (20)	0.137
positive	2 (50)	36 (80)		5 (63)	5 (83)		7 (58)	41 (80)	
p21 expression									
negative	2 (50)	24 (53)	1.000	3 (37)	0	0.209	5 (42)	24 (47)	1.000
positive	2 (50)	21 (47)		5 (63)	6 (100)		7 (58)	27 (53)	
p53 expression									
overexpressed/null	4 (100)	41 (91)	1.000	2 (25)	2 (33)	1.000	6 (50)	43 (84)	**0.018**
"wild type"	0	4 (9)		6 (75)	4 (67)		6 (50)	8 (16)	
Cyclin D1 expression									
negative	4 (100)	36 (80)	1.000	8 (100)	4 (67)	0.165	12 (100)	40 (78)	0.104
positive	0	9 (20)		0	2 (33)		0	11 (22)	

Discussion

Ovarian carcinomas correspond to several different clinical and histological entities that are treated with the same therapeutic approach with very modest success[340]. Recently, genetic and molecular characterization of these entities, reinforced its individuality and the need to find more adequate therapeutics for each entity[34,37].

Over the 10 last years, HDACs have been reported to be involved in many human malignancies, including ovarian carcinomas[325,341] and their expression has been associated with clinicopathological parameters such as patients' survival and disease prognosis. The assessment of HDACs immunodetection profile and the biological and clinical significance of these markers in ovarian carcinomas remains scarce.

In the view of above considerations, the present study assessed the expression of class I and II HDACs in ovarian carcinomas, pursued to find their association with clinicopathological parameters and with the expression of cell cycle proteins. Also, to contribute for HDAC immuno-profile that might establishes a rational for the use of HDAC inhibitors in ovarian cancer.

Class I HDACs are mostly localized within the nucleus due to the lack of a nuclear export signal whereas class II HDACs shuttle between nucleus and cytoplasm in response to certain cellular signals[339].

In our panel of tumors, we observed a high expression of all HDACs in those cellular locations. All types of class I HDACs studied, HDAC1, 2 and 3, where present in the majority of HGSC and CCC cases. This result is in accordance with Hayashi et al.[325] that described an increased stepwise nuclear expression of HDAC1, HDAC2 and HDAC3 proteins from benign, borderline and malignant ovarian tumors.

In the analysis of our results, we observed a lower HDAC1 expression in HGSC (78%) than in CCC (100%), and a higher HDAC2 in HGSC (100%) than in CCC. These two HDACs have an opposite expression, being the HDAC2 significantly associated with the histological type (p=0.0109). The biological meaning of the different expression can be related with the biological redundancy of HDAC1 and 2. It is known that HDAC1 and

HDAC2 form homo-and heterodimers between each other[342,343], which allows them to act together or separately from each other, so HDAC1 in the absence of HDAC2 is still able to interact with Co-REST and Sin3a (this is also true vice versa), demonstrating that the integrity of known HDAC containing corepressor complexes Co-REST and Sin3a is not affected in the absence of one of these two enzymes. In fact, no association was found regarding these two HDACs and the clinical parameters evaluated.

HDAC3 protein expression in these two tumor type of ovarian carcinomas differs relevantly from the other two Class I HDACs proteins. The immunoexpression of HDAC3 in our set of CCC was low in comparison to previous reports[325,339]. HDAC3 in our series was highly express in the majority of HGSC (90%) and was seldom found in CCC (33%), being this difference statistically significant (p<0.0001). The low expression of HDAC3 in CCC might underlie different regulatory mechanisms of the three proteins in this tumor entity or might be dependent on the stage of disease. Hayashi et al.[325] found, in their series of cases of EOC, a correlation between HDAC3 expression on CCC and stage IV disease. In our series, all, but one case, were diagnosed at stage I and this might be the explanation for the lower expression of HDAC3 that we observed in our cohort of CCC. It is plausible that HDAC3 is associated with the biological aggressiveness. Although, we did not found an association between HDAC3 expression in CCC and stage or prognosis, in all the cohort of EOC cases, and in the HGSC group, HDAC3 was more frequently associated with advanced clinical stage (p=0.0001) and (p=0.0023), and presence of metastases (p=0.002) in EOC patients. Hayashi et al. also described the importance of HDAC3 expression for ovarian cancer cell migration[325]. Again, our cohort of CCC cases cannot be use to address this as only one case were at advance stage at presentation.

The study of the role of HDACs in cancer has been mainly focused on the potential contribution of members of the class I HDACs subfamily. However, in recent year's class II HDACs have started to be linked to several types of cancer[344–346]. Class II HDACs are regulated in part by shuttling the protein between the nucleus and cytoplasm. Cytoplasmic location of class II facilitates gene activation by removing HDACs from their target genes[248].

The HDAC4 nuclear localization seems to be important in cancer as HDAC inhibitors block its entrance to the nucleus[347]. In our series, we only found HDAC4 in the cytoplasm and/or in the cell membrane and was predominantly expressed in HGSC. Both membrane (p=0.0349) and cytoplasmic (p<0.0001) HDAC4 expression were associated with HGSC cases in comparison with CCC. The phosphorylation of HDAC4 generates binding sites for the 14-3-3 protein, an HDAC chaperon, and promotes its export from the nucleus to the cytoplasm[347]. This protein has been also found highly expressed in some cancers such as esophageal carcinoma[348] and breast cancer in comparison with others like renal, bladder and colorectal cancer[346]. HDAC4 has also been described in the cytoplasm of pancreatic adenocarcinoma[349]. In that series of pancreatic adenocarcinomas, the high cytoplasmic HDAC4 expression was associated with absence of metastasis. This is in contrast to our findings in ovarian carcinomas, where the HDAC4c was associated with the presence of metastasis (p=0.001). And also in contrast to Shen et al.[350] findings, that also reported that EOC at stage III/IV had higher HDAC4 expression when compared to initial stages. It might be relevant to mention that this HDAC is missing in both cell lines by immunohistochemical evaluation.

In our series of ovarian carcinomas phosphoHDAC4/5/7 expression was significantly associated with HGSC in comparison to CCC (p=0.003), corroborating the previous findings about HDAC4. The biological significant of this phospho-proteins is not clear in cancer but multiple cell stimuli, including VEGF-induced angiogenesis in endothelial cells, B cell and T cell activation, and differentiation of myoblasts into muscle fiber[248] are known to induce phosphorylation of highly conserved HDAC4 Ser632, HDAC5 Ser498 and HDAC7 Ser486 residues by CAMK and PKD kinases[248].

Among the HDACs family members, HDAC6 is overexpressed in many cancers[351] and has been implicated in cell migration and invasion[345,352,353]. HDAC6 is a cytoplasmic resident protein, that deacetylates tubulin and alter microtubule stability[354]. Tubulin deacetylation is required for disposal of misfolded proteins in aggresomes[355]. During the last decade, HDAC6 has emerged as a master regulator of the cellular protective response to cytotoxic accumulation of toxic bioproducts[351,356]. High levels of HDAC6 expression have been associated with tumorigenesis[357,358].

Importantly, there are small molecule inhibitors for HDAC6 currently being tested in advanced clinical trials for other tumor types (myeloma and lymphoid malignancies)[359]. Although high levels of HDAC6 in HGSC (84%) and CCC (87%) were found, no associations with the histological type of EOC, nor with clinicopathological features were observed. Nevertheless, it might be interesting to explore the molecular mechanisms of this therapeutic approach in these tumor types.

Because data from *in vitro* studies suggest a link between HDACs and cell cycle, we also aimed to verify the potential association to cell cycle markers in EOC[325,360]. HDAC1 and 2 act in concert to promote the G1-to-S progression[329]. And it has been observed that HDAC1 deacetylates p53 and modulates its effect on cell growth and apoptosis, and also mediates repression of p21 by deacetylating histones in the p21 promoter region, resulting in inhibition of p21 gene expression[329]. The p21 gene is the primary mediator of p53-induced cell cycle arrest, and cells lacking functional p53 express only low levels of p21.

In our set of cases, by immunohistochemistry we observed that the majority of HGSC cases express high HDAC1 and p21. These apparently unexpected result can be explain by other mechanisms of regulation of the expression of p21, independent of p53, as for example the hyperacetylation of histones 3 and 4[327,361]. Lagger et al.[362] suggest that interactions of p53 and HDACs, likely result in p53 deacetylation, thereby reducing its transcriptional activity and increasing its ubiquitination and degradation rate.

Recently, researchers reported that combination of HDACIs and anticancer agents, including conventional chemotherapeutic drugs, had synergistic effects[279]. In addition, HDAC3 has been associated with chemoresistance to etoposide[363] and to paclitaxel in melanoma cells[364]. Furthermore, it has been reported that HDAC inhibitors increased the efficacy of chemotherapy and that administering agents in sequence is important for ovarian cancer treatment[311].

The present study corroborates previous findings that showed that elevated HDACs expression were associated with clinicopathological parameters such as histopathological stage and presence of metastases, which are considered crucial for

ovarian carcinoma patient's management and prognosis. These findings provided evidence for a potential role of HDACs in the biological mechanisms of ovarian malignant disease. The potential implication of HDACs in ovarian carcinomas, point out the necessity for further studies in order to clarify the potential role of the molecules and their possible use in the established therapeutic regimens of this types of malignancy.

The elevated expression levels of HDAC1, 2 and 6 in ovarian carcinomas may reinforce the therapeutic utility of HDAC targeting in ovarian cancer, taking into consideration of HDACIs effect in cell proliferation and apoptosis. In this context, the cdk inhibitor p21 was shown to be the most commonly induced gene in various ovarian cancer cell lines by several HDACIs[296], because deacetylation of histones represses the transcription of these tumor suppressor genes.

Our study presents issues of strength and limitations in particular, it might be underpowered because of it is a small cohort and because it is not yet known if immunohistochemistry is useful to determine if HDAC protein expression as assessed by immunohistochemistry is a predictor of treatment response with HDACIs, Clearly, additional studies are needed to clarify this point. Although high rates of HDAC expression have been found to be prognostic markers in other tumor entities, in this cohort no survival value of these markers could be demonstrated but this study is useful to emphasize the difference between tumor types and the expression profile of HDACs.

In conclusion, we demonstrated that the class I and II HDACs enzymes are highly expressed in HGSC and CCC and it is correlated with ovarian histological type. Although HDAC expression was not correlated with patient survival, the expression patterns of HDACs could hypothetically be important to predict the response of EOC patients to epigenetic therapies alone or in combination with conventional chemotherapy.

Moreover, our results support the use of HDACIs as therapeutic agents to treat ovarian cancer.

CHAPTER 3

The *in vitro* effect of epigenetics regulatory drugs, isolated and combined with conventional chemotherapy, in epithelial ovarian cancer (EOC)

Manuscript in preparation

Abstract in proceddings:

Silva, F., Serpa, J., Domingues, G., Silva, G., Almeida, A., Félix, A. Cell death induced by HDACS inhibitors in ovarian cancer cell lines (serous and clear cells carcinomas) – role of NOTCH, TP53 and FN1. BMC Proceedings 2010, 4(Suppl 2):P36

Silva, F., Serpa, J., Fernandes, S., Dias, S., Félix, A. HDACS inhibitors effects in Ovarian Clear Cell Carcinoma. SINAL 2012, 6th National Meeting, April, UMinho.

Abstract

Epithelial ovarian cancer (EOC) is the most lethal gynecological malignancy. Standard treatment for ovarian cancer patients is cytoreductive surgery, and in advanced disease chemotherapy, after debulking surgery, is a usual procedure.

Our aim is to understand the effects of histone deacetylases inhibitors (HDACI) in ovarian cancer as well as the mechanisms underlying the sensitivity and resistance of cancer cells to drugs with epigenetic regulatory activity. Cancer cell lines (OVCAR3 and ES2) were used and exposed to HDACIs, butyric acid and vorinostat, 5-aza-2´-deoxycytidine (DNA methylation inhibitor) and carboplatin and paclitaxel (standard chemotherapy) alone and combined. Analysis of cell death, proliferation and migration in cancer cell lines was performed to evaluate the *in vitro* effects of the different therapeutic drugs.

Our results show, that the two distinct HDAC inhibitors, butyric acid and vorinostat induced cell death, mainly through apoptosis in the two cell lines. This result was further confirmed in ES2 cell line exposed to vorinostat, by the study of immunofluorescence of cleaved caspase 3 and the evaluation of the *ratio* of proteins BAX/BCL-2, which increased after vorinostat exposure. Cell migration is affected by vorinostat in both cancer cell lines. Our results also indicate that the association of different drugs types are able to potentiate the effect of standard chemotherapy, mainly in ES2 cell line (CCC), supporting that EOC treatment can benefit from combined chemical and epigenetic therapy.

Keywords: ovarian cancer, HDACI, vorinostat, chemotherapy.

Introduction

Epithelial ovarian cancer (EOC) is the most lethal gynecological malignancy[3–5]. Nearly 70% of patients present at advanced stage of ovarian cancer and the 5-year overall survival (OS) rates are around 20%[11]. The standard treatment for ovarian cancer patients includes cytoreductive surgery, during which adequate staging evaluation is performed, by pathological examination of ovarian and other abdominal tissues to define the nature of the tumor and its stage. In patients diagnosed with early cancer disease, surgery alone, or with adjuvant chemotherapy is usually sufficient, but in advanced disease, debulking surgery followed by chemotherapy is mandatory[96].

Current therapies for advanced ovarian cancer are limited and not curative and the search for new therapeutic agents to treat the primary disease and recurrences, have been disappointing[22]. New procedures of treatment based upon the knowledge of the mechanisms of carcinogenesis and new therapeutic targets are needed[242]. Recently, two new drugs have been introduced into the clinical practice as examples for the ‘‘proof-of-concept’’ approach to target cancers: Olaparib and Bevacizumab.

Olaparib, a Poly (ADP-ribose) polymerase (PARP) inhibitor was approved for patients[365] with inherent or acquired defects in DNA and Bevacizumab, a humanized monoclonal antibody that targets all isoforms of vascular endothelial growth factor (i.e. VEGF-A, VEGF-B, VEGF-C, VEGF-D, VEGF-E). Unfortunately, although promising results were expected, till present these two agents are not routinely used as first- or second-line treatment of EOCs[366].

A different approach can be developed targeting epigenetic changes, as they are crucial for the development and progression of cancer, including in EOC. Significant progress has been made to understand how various epigenetic changes such as DNA methylation, histone modification, miRNA expression and other modulators of chromatin structure, affect gene expression.

Histone acetyltransferases (HAT) and histone deacetylases (HDACs) are multifunctional enzymes that modify the acetylation status of both histone and nonhistone proteins, affecting a broad range of cellular processes (e.g., cell cycle,

apoptosis, and protein folding) and are often dysregulated in cancer[273]. HDACs (see Table 1.2 in Chapter 1) are classified into four main classes: I, II, III and IV.

HDAC inhibitors are small molecules that directly interact with HDAC catalytic sites preventing the removal of acetyl groups, thereby counteracting the action of HDACs (Figure 3.1), leading to an increased transcription activity and subsequently upregulation of specific genes involved in regulation of gene expression and in various cellular pathways including cell growth arrest, differentiation, DNA damage and repair, redox signaling, and apoptosis[276,279,287,288].

Short chain fatty acids, in which butyrate (butyric acid) and valproate (valproic acid) are included[312,313], also function as HDACI of class I and II enzymes to control cell proliferation and apoptosis in cancer cells[314]. Because cells are able to metabolize butyric acid, it is assumed as having a weak effect as HDACI.

Vorinostat, a HDAC inhibitor, is a small hydroxamic acid compound that inhibits the enzymatic activity of a subset of class I HDACs, (HDAC1, HDAC2 and HDAC3) and the class II (HDAC6) at low nanomolar concentrations, and shows anti-proliferative activity in a variety of pre-clinical tumor models[317,320] . It is currently in clinical use for the treatment of cutaneous T-cell lymphoma[367].

DNA methylation is another important process to regulate gene expression. DNA methylation occurs on cytosine residues of CpG dinucleotides. The methylation of CpG islands (regions greater than 200 bp in length, having more than 50 percent of CG content[250] and frequencies above 0.6%) found in gene promoters has been correlated with the loss of gene expression and gene silencing through DNA methylation[253].

The inhibition of DNA methylation can regulate gene expression by "opening" the chromatin structure detectable as increased nuclease sensitivity. This remodeling of chromatin structure allows transcription factors to bind to the promoter regions, assembly of the transcription complex, and gene expression[314]. Hence, DNA methylation is a mechanism that affects all the cell functions. The strong inhibitor of DNA-methyltransferases, 5-aza-2'-deoxycytidine (5-aza-dC), has also been a subject of several studies and clinical trials in cancer[368]. It is an analogue of cytosine, that when

incorporated into DNA, irreversibly binds the methyltransferase enzymes as they attempt to methylate the cytosine analogue[368].

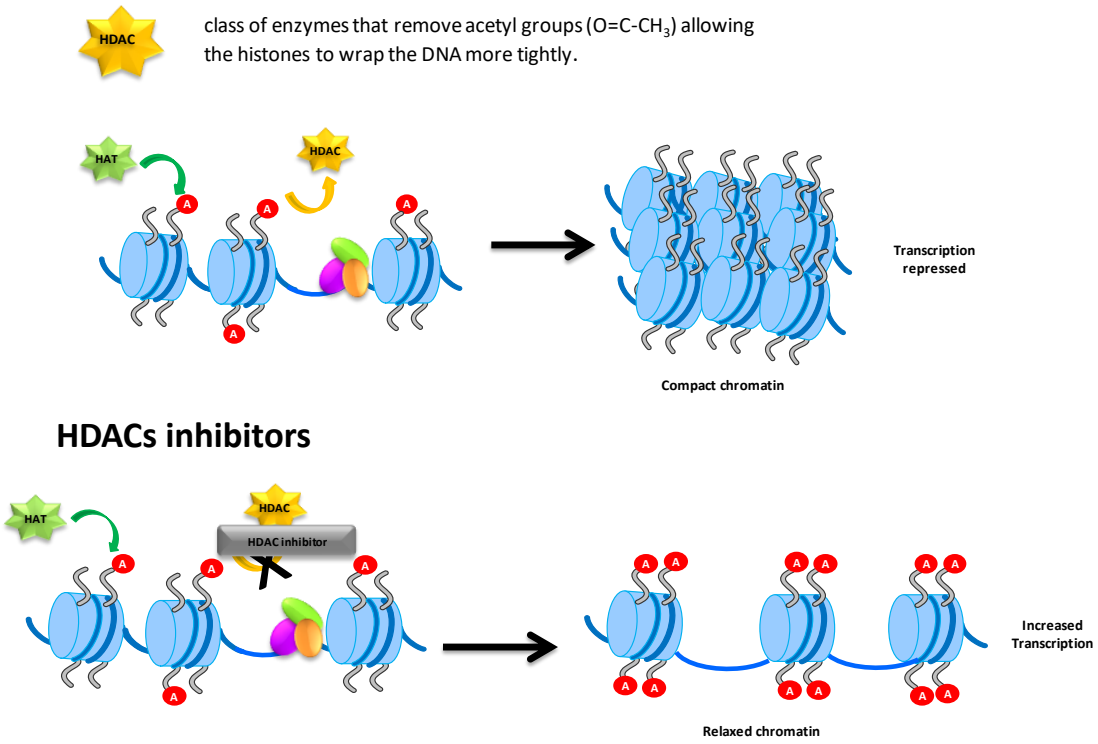

Figure 3. 1 - **Mechanism of action of HDAC inhibitors (HDACI)**
Acetylation of histone proteins is catalyzed by the action of HATs and is reversed by the action of HDACs. The tight coiling of DNA results from the deacetylation of histones that inhibits the transcription of important tumor suppressor genes (up). With histone deacetylases (HDACs) inhibited, high levels of acetylated histones cause DNA relaxation, allowing tumor suppressor genes to be accessible for transcription (down).

Our aim is to contribute to the study of the effects of HDACI in ovarian cancer cell lines as well as to disclose the mechanisms underlying the sensitivity and resistance of cancer cells to drugs with epigenetic regulatory activity. In this study we performed a set of experiments to evaluate the effect of HDACI and DNA methylation inhibitor alone or combined with conventional therapeutic agents in ovarian cancer cell lines.

Material and Methods

Cell lines and cell culture conditions

Clear cell carcinoma (CCC) cell line ES2 (CRL-1978) and high grade serous carcinoma (HGSC) cell line OVCAR3 (HTB-161) were obtained from American Type Culture Collection (Manassas, VA, USA). The cells were incubated at 37°C in a humidified atmosphere containing 5% CO2 in McCoy's 5A Modified Medium (Sigma-Aldrich, St. Louis, MO, USA) supplemented with 10% fetal bovine serum (FBS, S 0615, Invitrogen™, Thermo Fisher Scientific, Inc., Waltham, MA, USA) and 1% antibiotic-antimycotic (AA) (Invitrogen™; Thermo Fisher Scientific, Inc., Waltham, MA, USA). The cells were cultured to 80-100% confluence prior to detachment by incubation with 1X 0.05% trypsin-EDTA (Invitrogen™; Thermo Fisher Scientific, Inc.) at room temperature.

For the various assays, cell number was determined using a Bürker counting chamber. Prior to any experiment, cells were synchronized under starvation (culture medium without FBS), overnight at 37°C and 5% CO2. Preliminary assays were made to establish the concentrations of butyric acid, vorinostat and 5-aza-2´-deoxycytidine (5-aza-dC) based in literature. Cell lines ES2 and OVCAR3 cells were seeded onto 24 plates at a density of $1x10^4$, cultured with and without butyric acid, vorinostat and 5-aza-dC.

Chemicals and Reagents

Specifications on butyric acid, vorinostat, 5-aza-dC, paclitaxel (PTX) and carboplatin (CBP) are presented in Table 3.1. Vorinostat was dissolved in DMSO to produce a 50 mM stock solution and stored at -20°C. Paclitaxel and carboplatin were dissolved in sodium chloride and stored at room temperature and 4°C, respectively. All solutions were dilute in complete tissue culture medium immediately prior to use in an experiment.

Table 3. 1 - **Chemicals used in ovarian cancer cell lines**

Chemicals	Catalog no	Supplier	Dilution
Butyric acid	B10 350-0	Sigma-Aldrich	1mM
Vorinostat	CAS 149647-78-9	Cayman Chemical, Ann Arbor, MI, USA	5µM
5-Aza-2´-deoxycytidine	A3656	Sigma-Aldrich	5µM
Paclitaxel	Paclitaxel Kabi 6mg/ml, L AD0049	Fresenius Kabi Pharma	10µg/ml
Carboplatin	Carboplatin Hikma 10mg/ml, L 21LD0033	Hikma Pharmaceuticals	10µg/ml

Flow Cytometry analysis of cell death

Cells were collected, followed by centrifugation at 1200 rpm for 2 min, at designated times (0, 6, 18, 30 and 72h). The cell pellet was incubated with 1 µl annexin V- fluorescein isothiocyanate (FITC BD-Pharmigen) and 1 µl propidium iodide (PI) (50 µg/mL, Sigma-Aldrich, St. Louis, MO, USA) in 100 µl annexin V binding buffer 1X (10 mM HEPES (pH 7.4), 0.14M sodium chloride (NaCl), 2.5 mM calcium chloride ($CaCl_2$) at room temperature and in the dark for 15 min. After incubation, samples were rinsed with 0.1% (w/v) BSA (A9647, Sigma) in PBS 1X and centrifuged again at 1200 rpm for 2 min. Cells were suspended in 200 µl of annexin V binding buffer 1X.

Acquisition was performed in a FACScalibur flow cytometer (Becton Dickinson). A total of 10,000 cells per sample were acquired and data were analyzed with FlowJo software (http://www.flowjo.com/).

Immunofluorescence

Cells were cultured on glass slides with a 0.2% gelatin coating, until 80% of confluence and then fixed in 2% paraformaldehyde for 15 minutes at 4^{o}C. Blocking was performed with 0.1% (w/v) BSA in PBS 1X for 1 h at room temperature, and incubated with rabbit polyclonal anti-cleaved caspase 3 (catalog no. 9661S, Asp175, Cell Signaling) antibody, overnight at 4°C (diluted in 0.1% (w/v) BSA in PBS 1X, 1:100). Cells were incubated with secondary antibody for 2 h, at room temperature. Secondary

antibody used was Alexa Fluor®488 anti-rabbit (A-11008, Invitrogen). The slides were mounted in VECTASHIELD media with DAPI (4'-6-diamidino-2-phenylindole) (H-1200, Vector Labs) and examined by standard fluorescence microscopy using an Axio Imager.Z1 microscope (Zeiss). Images were acquired with AxioVision software and processed with ImageJ software (imagej.nih.gov/ij/version 1.44p).

Cell growth curves

Cells were seeded at a cell density of $1x10^4$ cells / well in a 12-well plate. Cell counting was determined by microscopy using the trypan blue exclusion method in a Bürker counting chamber at regular time intervals (0, 6, 18 and 30h). Each time point counting was performed in triplicate and growth curves were plotted. Prior to the experiment, cells were synchronized under starvation (culture medium without FBS) for eight hours at 37 °C and 5% CO_2.

Wound-healing assay

For wound-healing assay, cell lines were previously treated with 5µg/mL of Mitomycin-C (Sigma) an anti-proliferative agent, for 3 hours at 37°C 5% CO_2. A pipette tip was used to scratch a single wound in cells monolayer. Vorinostat (5µM) was added to medium and the plate was incubated at 5% CO_2 at 37°C. PBS 1X was used to washout the cell debris three times. The wound closure was monitored by photography when the scrape wound was introduced (0h) and at designated times after wounding (6, 18 and 30h).

Western blotting

Total protein extracts were obtained after cell lysis in Radio-Immunoprecipitation Assay (RIPA) lysis buffer (20mM/L Tris (pH 7.5), 150 mM/L NaCl, 5 mM/L KCl and 1% Triton X-100) previously supplemented with protease and phosphatase inhibitors to the cell pellet (Complete, Mini, EDTA-free Protease Inhibitor Cocktail Tablet (catalog no. 11836170001, Roche), 1 mM Orthovanadate (Na3VO4) (450243, Sigma) and 1 mM Sodium fluoride (NaF) (catalog no. 201154, Sigma). Whole protein lysates were quantified using standard Bradford protein assay, subsequently 100 µg protein

samples were then separated by electrophoresis in a 15% sodium dodecyl sulfate polyacrylamide gel (SDS-PAGE) and transferred to PVDF membranes (Bio-Rad).

For protein immunodetection, membranes were incubated with the specific primary antibodies: rabbit polyclonal anti-BCL2 (1:1000, catalog no. SAB4300340, Sigma-Aldrich); rabbit polyclonal anti-BAX (1:100; catalog no.HPA027878, Sigma-Aldrich) and mouse anti-β-actin (1:5000; catalog no., A5441, Sigma), overnight at 4°C, followed by incubation with peroxidase (HRP)-conjugated secondary antibodies (anti-mouse; catalog no. 31430, Thermo Scientific and anti-rabbit; catalog no. 31460, Thermo Scientific).

The peroxidase activity was detected by ECL method. Digital images were obtained in ChemiDoc XRS System (Bio-Rad) with Image Lab Software (imagej.nih.gov/ij/). Protein detection was quantified by digital analyses of the protein bands intensity that were normalized to β-actin, using ImageJ Software (http://rsbweb.nih.gov/ij/).

Reverse transcription-quantitative polymerase chain reaction (qPCR)

Total RNA was isolated from cells cultured with HDACI (butyric acid and vorinostat) or without HDACI (control condition), using RNeasy Mini Extraction Kit (catalog no., 74104, Qiagen, Inc., Valencia, CA, USA), according to manufacturer's protocol. cDNA synthesis was performed with 1 µg of total RNA, using random hexamers (catalog no. 11034731001; Roche Diagnostics, Indianapolis, IN, USA) and SuperScript II™ (200 U; catalog no. 18064-014, Invitrogen™, Thermo Fisher Scientific, Inc.), according to the manufacturer's protocol. The PCR amplifications conditions were as follows: 95°C for 2 min, 95°C for 10 min followed by 45 cycles of 95°C for 15 seconds, 60°C for 60 seconds. qPCR was performed using an ABI PRISM 7900HT Sequence Detection System (Applied Biosystems®; Thermo Fisher Scientific, Inc.) with Power SYBR Green PCR Master Mix (catalog no. 4367659, Applied Biosystems®, Thermo Fisher Scientific, Inc).

The primers sequences used were as follows: *BECLIN-1* GGCTGAGAGACTGGATCAGG (forward), CTTCAGCTTATCCAGCTGCG (reverse), *ATG-7* CGTCATTGCTGCAAGCAAGAG (forward), GATGAGCCCAGGAGGTCAG (reverse), *BAD*

AGGGAGGGCTGACCCAGAT (forward), GGCGGAAAACCCAAAACTTC (reverse), *BCL-2* ATGTGTGTGGAGAGCGTCAACC (forward), TGAGCAGAGTCTTCAGAGACAGCC (reverse). Data were analyzed in SDS 2.4.1 software (Applied Biosystems; Thermo Fisher Scientific, Inc.) and the relative expression of each gene was quantified by relative quantification (RQ) study module (ΔΔCt)[369] using hypoxanthine phosphorribosyltransferase gene (HPRT) as an endogenous reference gene.

Statistical analysis

Statistical analysis was performed using Student's t-test with GraphPad Prism software (GraphPad Software, Inc., La Jolla, CA, USA, version 5.03). $P<0.05$ was considered to indicate a statistically significant difference.

Results

Vorinostat induces cell death in ES2 and OVCAR3 cells, mainly through apoptosis

ES2 cells exposed to HDACI and 5-aza-dC, revealed increased levels of apoptosis at different timepoints in comparison to control condition (untreated cells) (Figure 3.2A). Butyric acid increased apoptosis in ES2 cells but in combination with 5-aza-dC apoptotic levels decreased (except for 18h). In contrast, vorinostat and 5-aza-dC showed a cumulative effect at 6, 30 and 72h of exposure and this was not observed for butyric acid and 5-aza-dC association.

Regarding necrosis, ES2 cells exposed to vorinostat showed increased levels in all conditions comparing to control at 30 and 72h of exposure (Figure 3.2B). A cumulative effect with the combination of HDACIs and 5-aza-dC was observed for butyric acid at 18, 30 and 72h, whereas for vorinostat it was observed only at 30h of exposure.

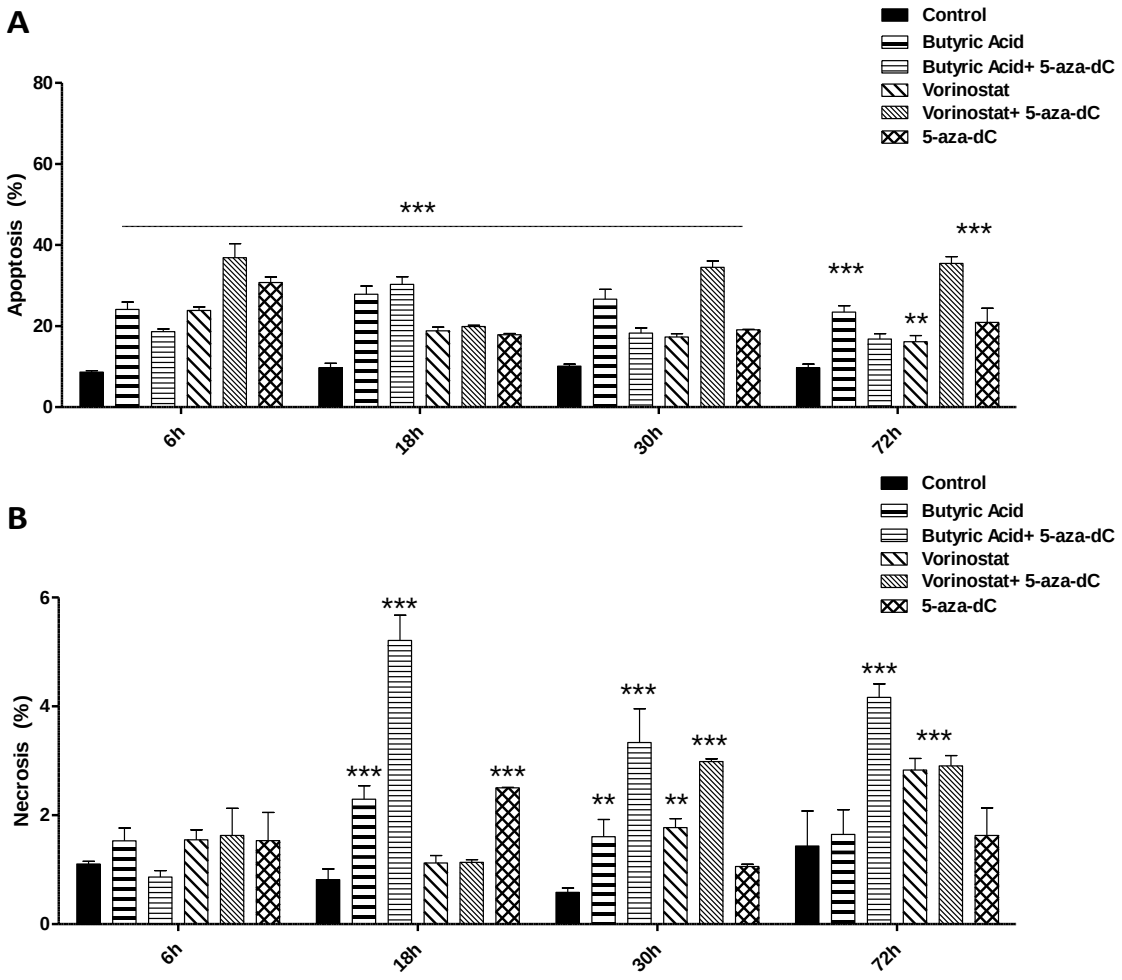

Figure 3. 2 - **Cell death in ES2 cell line exposed to HDACIs and 5-aza-dC**
Cells were cultured in control conditions and in the presence or absence of HDACs inhibitors and 5-aza-dC. Cells were analyzed by flow cytometry: **A.** apoptosis (annexin V positive cells), and **B.** necrosis (PI positive cells). Data were acquired after 6, 18, 30 and 72h after 16h of serum starvation. Data are mean ± standard deviation of triplicates. ***p ≤0.001

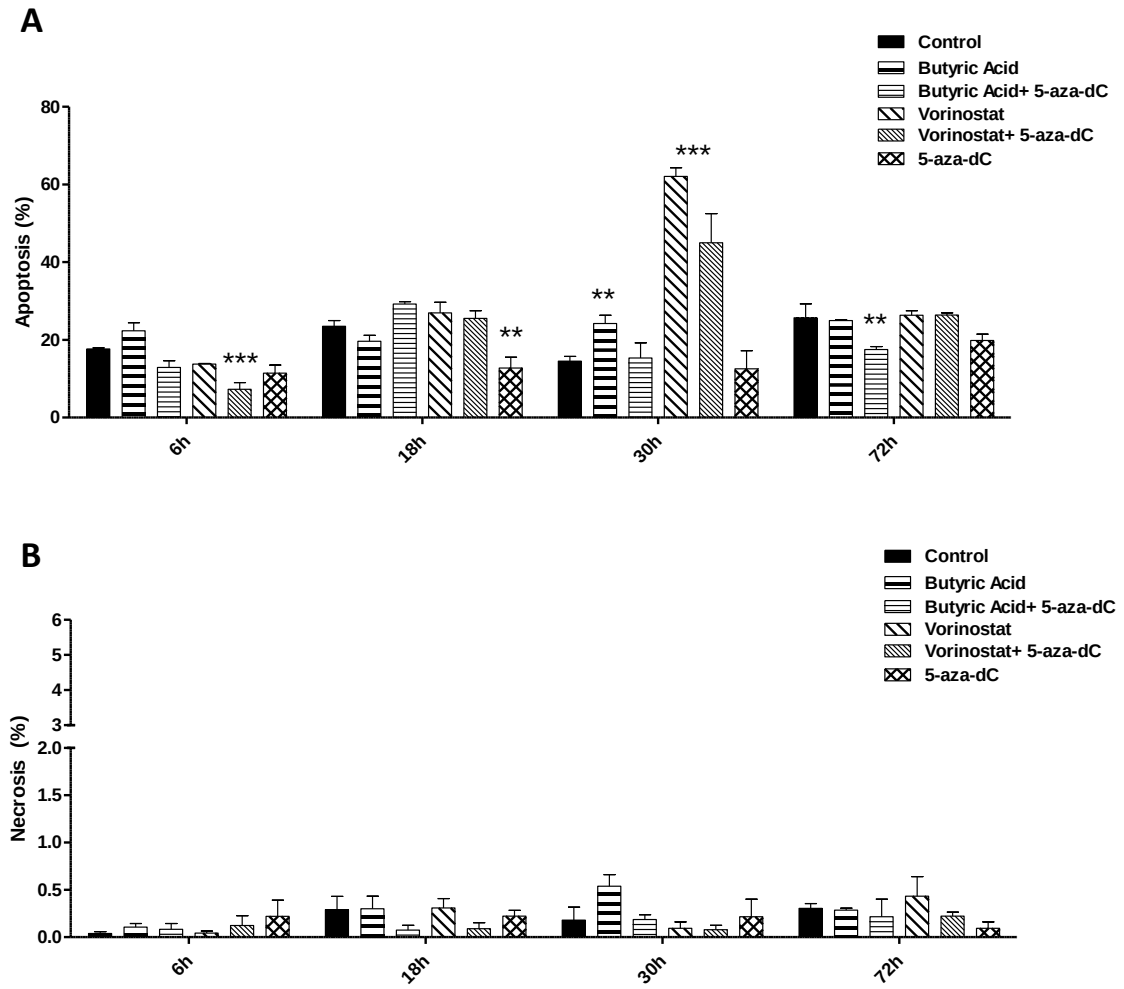

Figure 3. 3 - **Cell death in OVCAR3 cell line exposed to HDACIs and 5-aza-dC**
Cells were cultured in control conditions and in the presence or absence of HDACs inhibitors and 5-aza-dC. Cells were analyzed by flow cytometry: **A.** apoptosis (annexin V positive cells), and **B.** necrosis (PI positive cells). Data were acquired after 6, 18, 30 and 72h, after 16h of serum starvation. Data are mean ± standard deviation of triplicates. ***p ≤0.001

Regarding, the effects of HDACIs and 5-aza-dC in OVCAR3 cells, at different timepoints, we observed that only cells exposed to vorinostat alone and in combination with 5-aza-dC showed a high percentage of apoptosis at 30h when compared to control (Figure 3.3A). At 6h, apoptosis levels were decreased when compared to control cells but it was significant only upon the exposure to vorinostat and 5-aza-dC. The following timepoints also indicate a decrease of apoptosis when cells were exposed to 5-aza-dC at 18h, and at 30h and 72h. A decrease in apoptosis was also verified when cells were exposed to butyric acid and 5-aza-dC.

The necrosis levels in OVCAR3 cells in all conditions were very low, having no significant differences in the overall cell death (Figure 3.3B).

Vorinostat and 5-aza-dC decrease the expression of mRNA of *BCl-2* and vorinostat decreases *BAD* in ES2 cell line

In order to understand the mechanism through which vorinostat may exert cell death, we assessed the effect of vorinostat on the expression of genes related to apoptosis and autophagy in ES2 cell line. Two main pathways control apoptosis, the extrinsic and the intrinsic pathways. The extrinsic pathway was not evaluated because previous studies indicated that vorinostat induced apoptosis through the intrinsic pathway and the subsequent activation of caspases[275,315].

The intrinsic pathway is influenced by interactions between pro-apoptotic proteins such as BAX and BAD and anti-apoptotic proteins, such as BCL-2, BCL-X_L, or IAP proteins[370].

We investigated the levels of *BCL-2* and *BAD* mRNA expression in ES2 cell line exposed to HDACIs and 5-aza-dC.

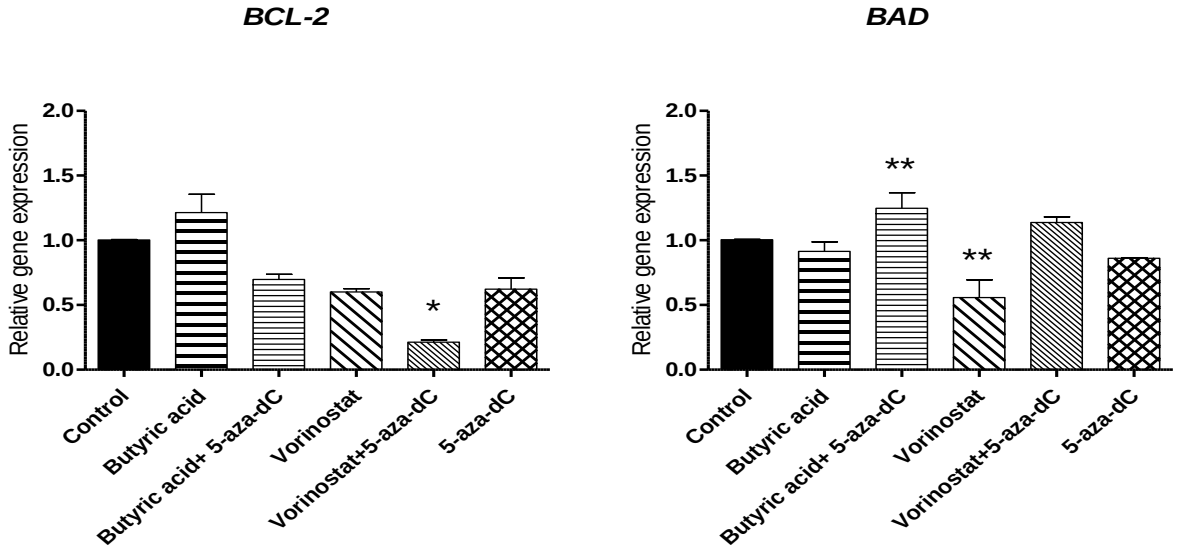

Figure 3. 4 - **mRNA expression of BCL-2 and BAD in ES2 cell line**
Cells were grown in control conditions, in the presence and absence of HDACs inhibitors and 5-aza-dC, and the expression of *BCL-2* and *BAD* were evaluated by RT-qPCR. *Hypoxanthine phosphoribosyltransferase* gene (HPRT) was used as endogenous control. Data are mean ± standard deviation of triplicates.***p ≤0.001

BCl-2 and *BAD mRNA* expression levels (Figure 3.4) in cells treated with vorinostat were both reduced when compared to cells without vorinostat exposure. In addition *BCL-2* expression also decreases when cells were exposed to vorinostat in combination with 5-aza-dC. Considering that there was no visible indications of effective apoptosis through mRNA, we used western blotting to examine the levels of expression of BAX and BCL-2 proteins to determine the changes in BAX:BCL-2 *ratio* (Figure 3.5) and in fact BAX/BCL-2 protein *ratio* was increased after vorinostat exposure indicating that vorinostat induces apoptosis in ES2 cells (Figure 3.5).

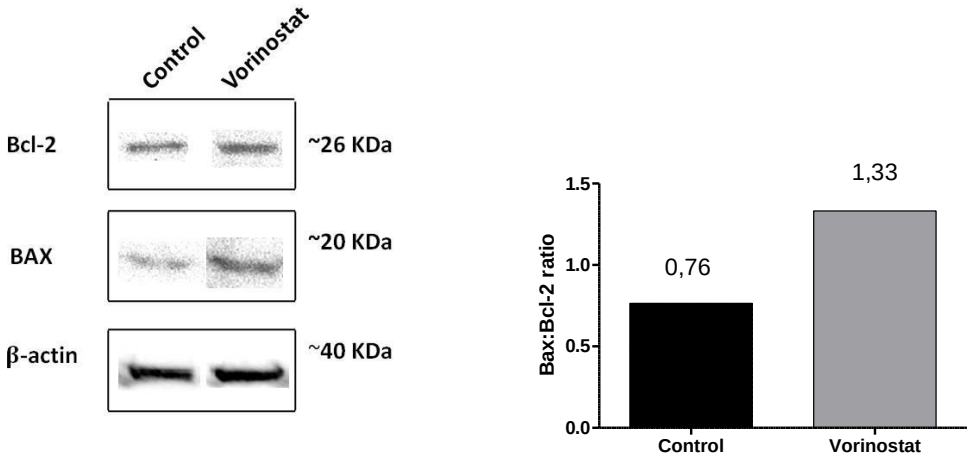

Figure 3. 5 - **Expression of BCl-2 and BAX by Western blot**
Cells were treated with and without vorinostat 5 µM. Cell extracts were analyzed in a 15% SDS-PAGE and β-actin served as endogenous control.

Vorinostat induce caspase activation in ES2 cell line

Finally, to validate apoptosis as the predominant cell death mechanism, the cleavage of caspase 3 was evaluated in ES2 cell line. Caspase 3 belongs to the cysteinyl aspartate-specific proteases family involved in death cascade. Moreover, caspase 3 is a common final step of the extrinsic and intrinsic pathways of apoptosis, being its cleavage a common sign that apoptosis is activated[371].

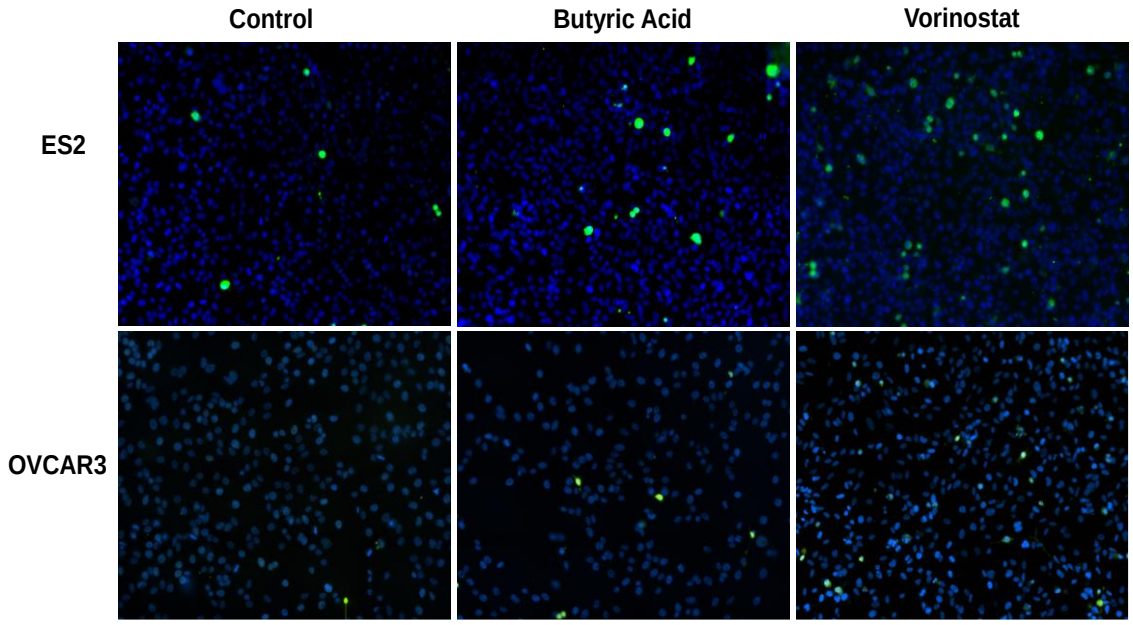

Figure 3. 6 - **Expression of cleaved caspase 3 by immunofluorescence in EOC cell lines**
Representative staining for cleaved caspase 3 (green) in ovarian cancer cells, grown in control conditions and in the presence of HDACs inhibitors exposure. The nuclei are stained with DAPI (blue).

Caspase 3 activation, evaluated by immunofluorescence staining for cleaved caspase 3, was induced by both HDACs inhibitors, being vorinostat more effective than butyric acid in caspase 3 cleavage when compared to control (Figure 3.6). Also, vorinostat induced higher expression of cleaved caspase 3 in ES2 cell line when compared to OVCAR3 cell line. This evaluation confirms that apoptosis occurs in ovarian cancer upon exposure to HDACI (butyric acid and vorinostat).

Vorinostat increases the expression of autophagy genes in ES2 cell line

Because autophagy besides being a survival mechanism, can promote cell death due to its extensive duration; the expression of autophagy genes *BECLIN-1* and *ATG-7* was evaluated in cells treated with HDACI.

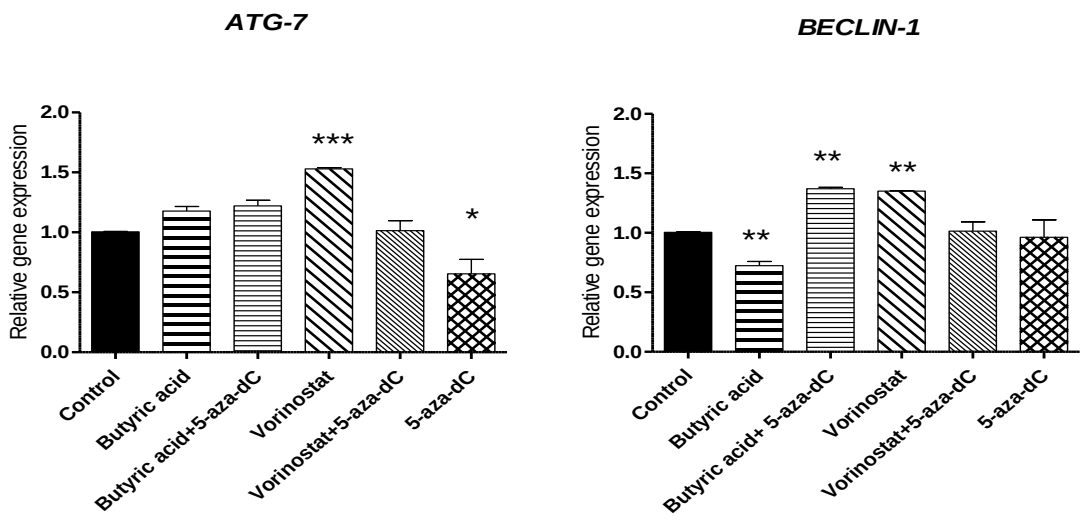

Figure 3. 7 - **mRNA expression of BECLIN-1 and ATG-7 in ES2 cell line**
Cells were grown in control conditions, in the presence and absence of HDACIs and 5-aza-dC and the expression of *ATG7* and *BECLIN*-1 were evaluated by RT-qPCR. *Hypoxanthine phosphoribosyltransferase* gene (*HPRT*) was used as endogenous control. Data are mean ± standard deviation of triplicates.***p ≤0.001

As shown in Figure 3.7, vorinostat induces the expression of *BECLIN*-1, required for the initiation of autophagy and *ATG-7,* which is necessary for the formation of autophagosomes. These transcripts are both upregulated in ES2 cells treated with vorinostat when compared with untreated cells (control). *BECLIN-1* expression is downregulated with butyric acid and there is no difference in these markers in cells treated with 5-aza-dC during the whole duration of treatment.

Effects of vorinostat and chemotherapy in ovarian cancer cell lines

Combined therapy with platinum agents (carboplatin or cisplatin) and taxane (paclitaxel) are used as standard postoperative chemotherapy for the majority of EOC[372]. Recently, some therapeutic approaches and clinical trials proposed the use of epigenetic regulatory drugs with standard chemotherapy[373,374]. So, we also studied the combinatory effects of vorinostat, 5-Aza-dC and conventional chemotherapy (carboplatin-CBP and paclitaxel-PTX) in EOC cells lines.

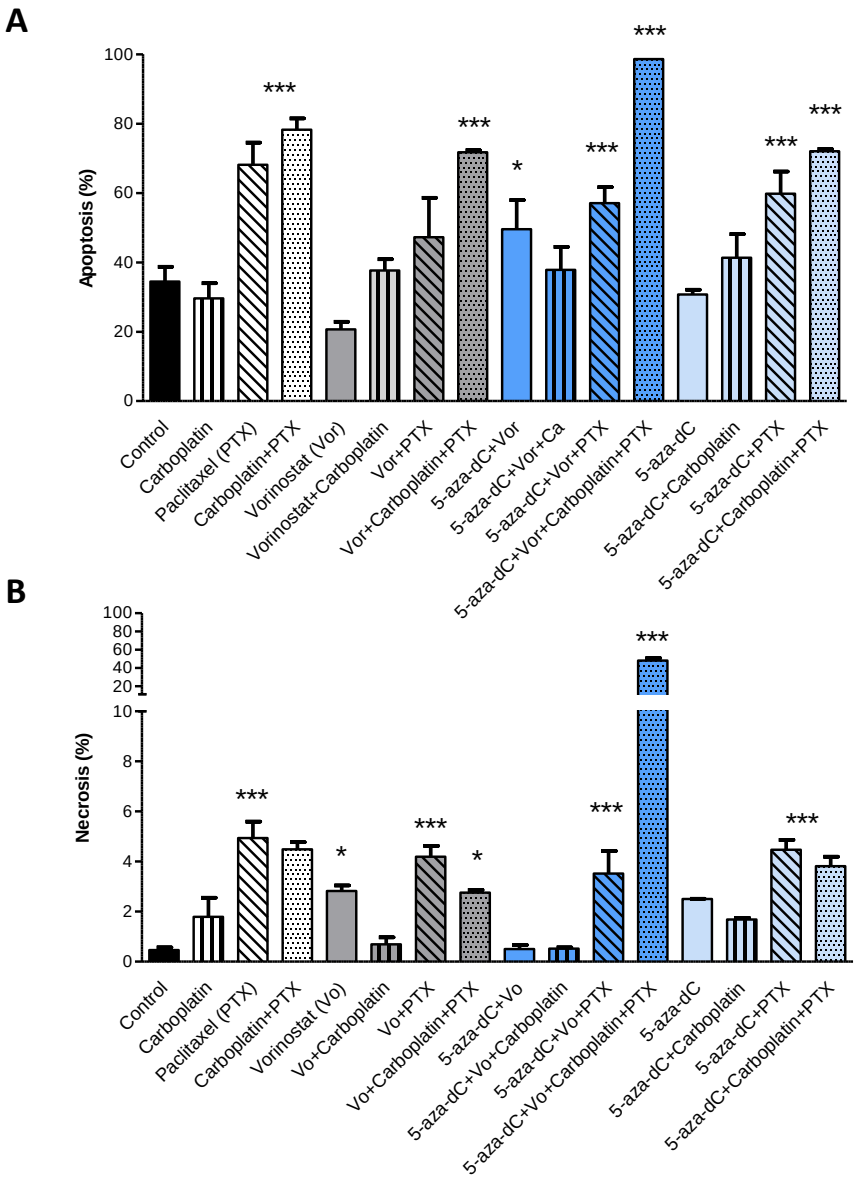

Figure 3. 8 - **Cell death in ES2 cell line exposed to vorinostat, 5-aza-dC, carboplatin and/or paclitaxel**
Cells were cultured in control conditions and in the presence of vorinostat, 5-aza-dC, carboplatin (CBP) and paclitaxel (PTX), alone or in combination, Cells were incubated for 30h with vorinostat and 5-aza-dC, and chemotherapy was added for 16h. Cells were analyzed by flow cytometry: **A.** apoptosis (annexin V positive cells), and **B.** necrosis (PI positive cells). Data are mean ± standard deviation of triplicates. ***p ≤0.001

In Figure 3.8A, flow cytometry analysis of apoptosis confirmed that in ES2 cells the combined effect of carboplatin (CBP) and paclitaxel (PTX) is cumulative, but mainly due to the contribution of paclitaxel. Vorinostat (Vo) and 5-aza-dC (in separate) improved the effect of CBP but they decreased the effect of PTX and no difference was

observed in the combinatory effect of CBP with PTX neither with the addition of vorinostat nor of 5-aza-dC. However, when the cells were exposed to all drugs together, cell death levels raised to 100%, both through apoptosis and necrosis (Figure 3.8).

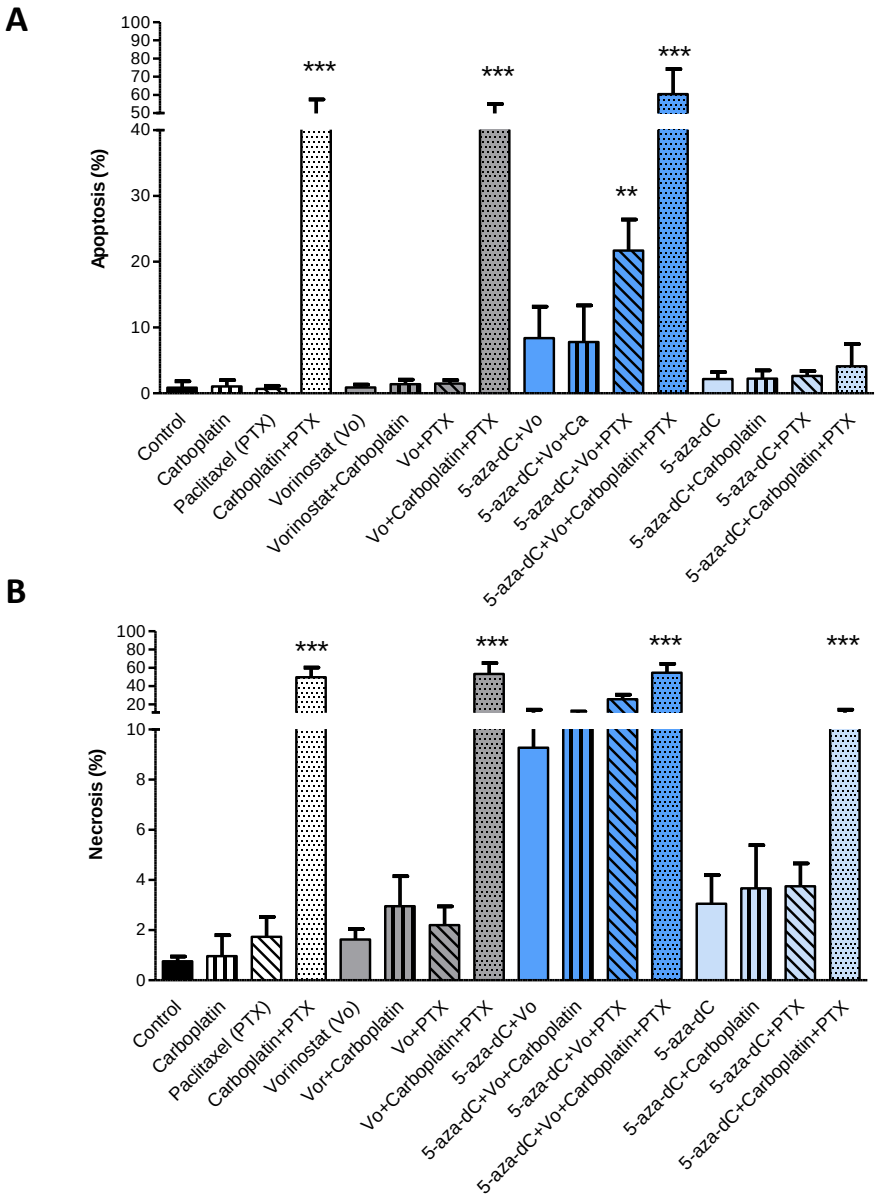

Figure 3. 9 - **Cell death in HGSC-OVCAR3 cell line exposed to vorinostat, 5-aza-dC, carboplatin and/or paclitaxel**

Cells were cultured in control conditions and in the presence of vorinostat, 5-aza-dC, carboplatin and paclitaxel, alone or in combination. Cells were incubated for 30h with vorinostat and 5-aza-dC, and chemotherapy was added for 16h. Cells were analyzed by flow cytometry: **A.** apoptosis (annexin V positive cells), and **B.** necrosis (PI positive cells). Data are mean ± standard deviation of triplicates. ***p ≤0.001

In Figure 3.9A, flow cytometry analysis of apoptosis and necrosis of OVCAR3 cells showed that the higher levels of cell death was associated with the combination of 5-aza-dC together with vorinostat when combined with the chemotherapeutic drugs alone or in combination, increased significantly the levels of apoptosis and necrosis (Figure 3.9B). Whereas 5-aza-dC without vorinostat did not alter the levels of apoptosis alone or in combination with CBP and/or PTX, so it seems that 5-aza-dC also potentiates the action of vorinostat.

HDACIs inhibit cell proliferation in ES2 (CCC) cell line

To investigate the effect of HDACs inhibitors and 5-aza-dC in cell proliferation, curves were done aiming to evaluate *in vitro* proliferation of the cells in the presence and absence of HDACIs and 5-aza-dC. Trypan blue exclusion assay was conducted to measure cell proliferation at 0, 6, 18 and 30 hours after seeding (Figure 3.10A and B).

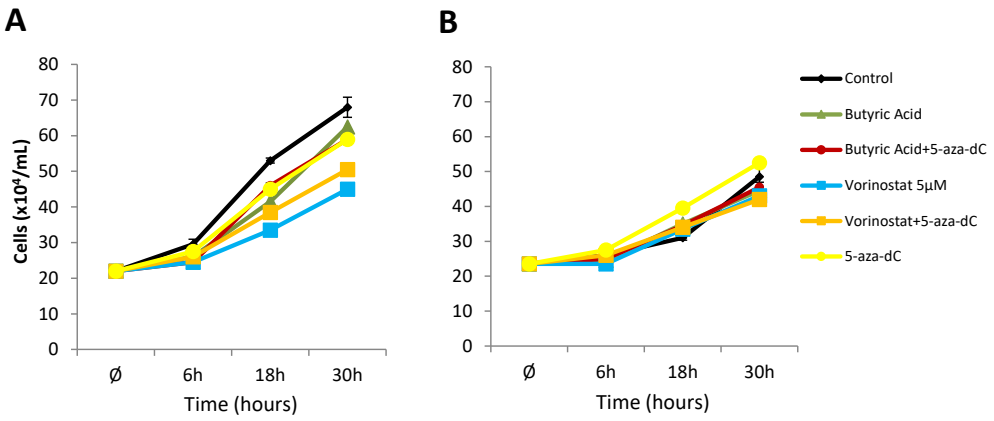

Figure 3. 10 - **Cell proliferation curve for ES2 and OVCAR3 cells exposed to HDACIs and 5-aza-dC**
Cells were grown in control conditions and in the presence and absence of HDACIs with and without 5-aza-dC. **A.** ES2 cell line and **B.** OVCAR3 cell line. Data were acquired at 0, 6, 18 and 30 hours after 16h of serum starvation and are mean ± standard deviation of three cell counts.

As shown in Figure 3.10A, the proliferation curve for ES2 cells treated with HDACI showed a decrease of proliferation rate; mainly in those cells under the exposure to vorinostat. In ES2 cells, the exposure to butyric acid, alone or in combination with 5-aza-dC showed high proliferation, similar to the proliferation rate when cells are exposed only to 5-aza-dC. However, when cells are exposed to vorinostat a decreased

of proliferation is verified even when there is a combined exposure with 5-aza-dC. Indeed, in this particular cell line, we verified that cells exposed in combined HDACI and 5-aza-dC have higher proliferation rate than when cells are exposed only to one.

In Figure 3.10B, the proliferation curve for OVCAR3 cells showed no differences in proliferation rate in all conditions. However, cells exposed to 5-aza-dC exhibit a tendency (but not significant) to proliferate more in comparison to control condition**.**

Vorinostat affects migration capacity mainly OVCAR3 cells

To test the effect of vorinostat on cell migration, wound healing assay was performed.

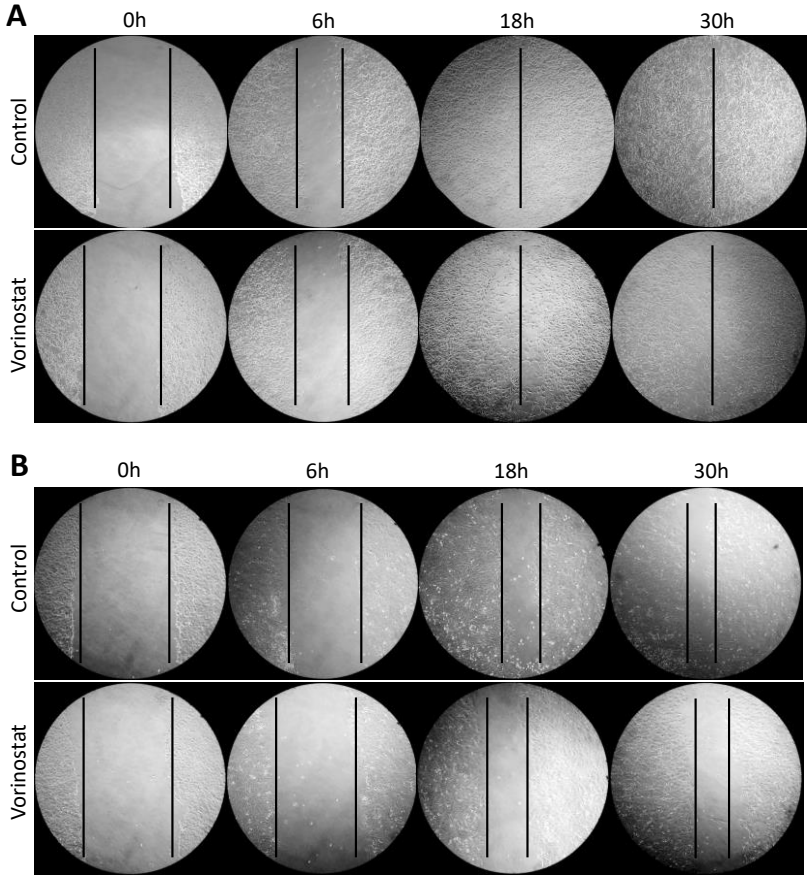

Figure 3. 11 - **Wound healing assay in ES2 cells and OVCAR3 cells exposed to vorinostat.** Mitomycin-C treated cells were grown in control conditions, with or without vorinostat. Wounds were made on monolayers of cells grown to 100% confluence. Effect of vorinostat on wound healing assays in **A.** ES2 cells and in **B.** OVCAR cells. Wound closure was photographed when the scratch wound was introduced (t=0 hours) and after 6h, 18h and 30h. Results presented here are representative of triplicate independent samples. Phase microscopy (original magnification: 200x).

As shown in Figure 3.11A, the wound healing assay showed that vorinostat inhibits cell migration in ES2 cell line after 6h. Despite the wound is almost completely closed at 30h in control and in vorinostat exposed cells, the cell density in control conditions is higher. Concerning OVCAR3 cell line (Figure 3.11B), the wound healing assay showed that vorinostat inhibits cell migration as seen at 18 and 30h after wounding.

Discussion

In clinical setting for the last 30 years, few improvements were done regarding treatment of ovarian cancer, being surgery and adjuvant chemotherapy the standard care in ovarian cancer patients. Many clinical trials have been testing different drugs and combined therapeutic schemes in advanced or recurrent disease, however, none of them proved to be better than the association of carboplatin and paclitaxel to increase overall survival and disease free survival[375]. Meanwhile, new therapeutic approaches, such as anti-VEGF and anti-PARP strategies[376,377] for treatment of ovarian cancer where found to be very useful in some clinical contexts.

As HDACs are overexpressed in cancer and represent a group of enzymes responsible for modifications of histones, conditioning epigenetic regulation, thus their action has been targeted in preclinical, clinical trials[322,378] and clinical settings[334,379,380]. HDACIs, appeared has promising drugs in the last decade as anticancer agents[332]. They are known to restore the expression of silenced tumor suppressor genes in cancer cells through their ability to block histone deacetylation.

HDACI have multiple actions in cells related to their ability of modulating gene expression, such as inducing programmed cell death in cancer cells through not very well understood mechanisms[381]. Other responses to these agents in cancer include cell cycle arrest, cell differentiation, autophagy and apoptosis, whereas normal cells are less affected[318]. HDACIs are currently in clinical use in the treatment of cutaneous T-cell lymphoma alone and in combination with other anticancer therapies[382]. *In vitro* vorinostat anti-tumor activity has been reported in several hematological and solid malignancies, including leukemia, mantle cell lymphoma, hepatocellular carcinoma,

pancreatic carcinoma, breast cancer, prostate cancer, colon cancer and ovarian cancer[335,372,383,384].

Our results allow us to confirm previous results in ovarian cancer cell lines regarding HDACIs[335,360]. We found that two distinct HDACIs, butyric acid and vorinostat, are able to induce cell death in ovarian cancer cell lines. Cell death is mainly through apoptosis, upon HDACIs exposure[335,360] as it was confirmed in our study in ES2 cell line, by the immunodetection of cleaved caspase 3 and the protein BAX/BCL-2 *ratio*, which increased after vorinostat exposure as Takai et al.[360] described. The same effect was reported in hematological malignancies[320].

Moreover, in ES2 cell line, we also study autophagy genes (*BECLIN-1* and *ATG-7*) and observed that the levels of these genes were increased with exposure to vorinostat. The results are in agreement with recent studies, that have demonstrated that tumor resistance to anticancer therapies can be overlapped through upregulation of autophagy in different tumor cell lines[385].

The potential role of autophagy in the therapeutic response to anticancer agents has been controversial, as opposing results were obtained from different cancer cell lines, suggesting that autophagy may function as a stress response, helping to promote cell survival or demonstrating that increased autophagy leads to apoptosis[385]. According to Wirawan *et al.*[371] in hematological cell lines, vorinostat induces autophagy that can change from a pro-apoptotic signal to a pro-survival function through acquired resistance. Autophagy is characterized by massive degradation of cellular contents, including essential organelles such as mitochondria, by means of complicated intracellular membrane/vesicle reorganization and lysosomal activity[371].

It has been purpose that autophagy allows the cell to survive in unfavorable conditions. It have been suggested, for example, that removal of apoptotic effectors (caspase 8), in the presence of which autophagy does not occur[386], by degradation of aggregated proteins and damage organelles, restores metabolic homeostasis by recycling metabolites and prevents ROS accumulation[387]. In fact, the increased levels of autophagy effectors observed with exposure to vorinostat in ES2 cancer cell line may function in this cell line as a mechanism of survival, because apoptosis and

autophagy regulators *BECLIN-1* e *ATG-7* are increased by vorinostat (Figure 3.2 and 3.7).

Concerning cell proliferation, our results indicate that exposure to HDACIs have different outcomes regarding the two cell lines. ES2 cell line showed a decrease of the proliferation rate mainly in cells exposed to vorinostat, but this effect was not observed in HGSC cell line (OVCAR3). Regarding the response to other drugs and their association (figure 3.10), we also obtained different results in these cell lines, being the most relevant the increased proliferation rate of ES2 cell line, when exposed to 5-aza dC or to the combination of HDACIs and 5-aza-dC. This results allow us to postulate that hypomethylation seems to be an important inducer of cell proliferation in this cell line, not rescued by HDACIs.

The cell line OVCAR3 behaves differently after the exposure to HDACIs and 5-aza-dC. The proliferation rate is similar in all conditions indicating that these cells are not affected by those agents. However, previous studies report that ovarian cancer cell lines treated with methylation inhibitor, as decitabine, produced synergistic inhibition of cell proliferation by apoptosis and cell cycle arrest[388].

Cell migration can be seen as a marker of cancer cells aggressive phenotype, since the ability of a cancer cell to invade the surrounding tissues and spread is determinant for disease progression and metastasis[389,390]. Our study on cell migration under HDACIs influence, demonstrated that vorinostat can diminished cell migration confirming previous reports[335] using other ovarian cancer cell lines. It is important to mention that this effect was not evident in ES2 cell line as it was in OVCAR3. This underline another difference on vorinostat effect between these two cell lines. We are convinced that proliferation might not influence the results of wound healing assay because cells were previously exposed to mitomycin C, an inhibitor of proliferation.

Previous studies have evaluated the action of vorinostat in ovarian cancer cell lines, and they have found that vorinostat suppress proliferation, migration and invasion in ovarian cancer cells, including cisplatin-resistant or highly-invasive ovarian cancer cells, by promoting histone acetylation[335]. Sonnemann et al.[391] also report that vorinostat activated caspase-3 in a concentration-dependent fashion in ovarian cancer

cell lines and in patient-derived ovarian cancer cells. However, no previous report showed differences between different histological types of ovarian cancer. We would like to emphasize that our results may be relevant and highlight the need of studying different cell lines to fully understand the modulating effects of this type of drug and its use may not be applied to all histological types of ovarian cancer.

Nevertheless, it is very important to remind that our results demonstrate that drugs commonly used in chemotherapy (carboplatin and paclitaxel) are still the most effective treatment to induce cell death, at least when applied in combination (carboplatin plus paclitaxel).

Finally, the most interesting results is however the demonstration, *in vitro*, that vorinostat and 5-aza-dC are able to potentiate the effect of these chemotherapeutic drugs, since the acquisition of therapy resistance is an important clinical problem[130]. Importantly, this effect of the drug association was more evident in ES2 cell line, supporting that CCC treatment can benefit from combined cytostatic, cytotoxic and epigenetic therapy. This particular histological type is recognized as being intrinsically resistant to platinum salt-based therapies and new therapeutic approaches are urgently need[72,392].

Our results are in agreement with other studies[72,393]. showing that ES2 cells are resistant to carboplatin induced cell death[72]. Resistance mechanisms that limit the extent of DNA damage associated with chemotherapy include decreased intracellular drug accumulation, increased drug inactivation, and increased DNA damage repair[100]. Increased glutathione (GSH) levels, a ROS scavenger are also a mechanism of resistance[72], since GSH reacts with carboplatin avoiding its contact with cell proteins and DNA and consequently decreasing carboplatin cytotoxic ability. According to Lopes-Coelho et al.[72], ES2 cells expressed more GSH, which synthesis is regulated by HNF1β, the key gene in CCC, and the abrogation of GSH synthesis increases ES2 sensitivity to carboplatin. Once carboplatin by itself does not induce cell death in ES2 cell line. This supports the use of epigenetic regulation in the treatment of this histological type**.**

Regarding OVCAR3 cells, we were able to document the benefit over the combination of carboplatin plus paclitaxel only if we submitted the cells in a tetra-combination, joining carboplatin plus paclitaxel with vorinostat plus 5-aza-dC. Our results are in agreement to other studies that have reported that a combination of 5-aza-dC or paclitaxel with vorinostat inhibited ovarian cancer growth while inducing apoptosis, cell cycle arrest and autophagy[394,395].

HDACI potentiate platinum effect in cancer cells, possibly mediated by increasing platinum adduct formation, facilitated by the open of DNA configuration, induced by HDAC inhibition[396,397] as well as by acetylation of other proteins such as transcription factors and tumor suppressor proteins. The synergy between HDACI, platinum agents and paclitaxel was also visible in HGSC cell lines, as reported in other studies[311,391]. But this effect was not observed in ES2 cells as previously discuss and it is another evidence of the heterogeneous nature of ovarian carcinomas.

Hence, ovarian cancer usually responds to chemotherapy but, in the majority of cases the cancer recurs resulting in the death of eventually half of patients[77] as a consequence of the development of drug resistance[99]. To date, there are no reliable clinical factors that can properly stratify patients for suitable chemotherapy strategies. Upon cancer relapse, the only currently available treatment option is further chemotherapy.

So, *in vitro,* the conjunction between conventional chemotherapy and epigenetic modulators can be a more effective therapeutic approach in EOC, and recent clinical studies report that combination of chemotherapeutic agents with vorinostat activity in relapsed platinum-sensitive ovarian cancer is more effective. We emphasize in our study the difference between cell lines of different histological types. It is important that studies consider that ovarian cancer is a heterogeneous entity and diverse histological types can respond differently to proposed therapies. Studies focusing on the histological type of ovarian cancer have never been made in previous approaches, which is a real limitation since each histological type constitute a molecular and clinical entity.

CHAPTER 4

HNF1β acetylation a possible path for Vorinostat impairment of ovarian clear cell carcinoma (CCC)

Manuscript in preparation

Abstract

Ovarian clear cell carcinoma (CCC) is an unique clinical, histopathological and molecular entity within ovarian cancer, having HNF1β as a pivotal pro-survival gene. Moreover, the extra-ovarian stage at the time of diagnosis and the resistance to conventional therapy accounts for the very poor prognosis of CCC.

Studies supporting the role of histone deacetylases (HDACs) in cancer progression, pointed out the use of HDAC inhibitors (HDACIs) as a promising therapeutic strategy.

The present study aimed to evaluate the effect of the HDACI vorinostat at the functional and at the molecular level in CCC cells.

Our results showed that vorinostat induced increased levels of HNF1β and at the same time cell cycle arrest and apoptosis in ES2 cells. This effect on HNF1β is associated with elevation on the acetylation load of HNF1β.

This study confirms that epigenetic modulation affects not only the conformation of chromatin and gene expression, but also it may alter the function and the turnover of proteins other than histones.

Keywords: clear cell carcinoma (CCC), vorinostat, HNF1β.

Introduction

Clinical, histopathological and genetic features prove that ovarian clear cell carcinoma (CCC) is a distinct entity within epithelial ovarian cancer (EOC)[398,399]. In most cases, CCC is associated with ovarian endometriosis[72,399]. Hepatocyte nuclear factor 1β (HNF1β) overexpression is a biological mark of CCC[400,401] and its considered to be responsible for cell survival, proliferation and chemoresistance[72,402]. As no mutations in HNF1β gene have been described to date in CCC, its overexpression in this tumor is thought to be probably under epigenetic control[72,399]. Resistance to standard treatment based in platinum salts and taxanes accounts for the very poor prognoses of advanced and recurrent CCC[398]. Hence, the discovery of therapeutic alternatives urges, target histone deacetylases (HDACs) seem to be a suitable and effective approach to treat cancer.

HDACs are often overexpressed in cancer and they induce chromatin compression and consequently gene silencing. Furthermore, their action is pointed out to be responsible for the silencing of tumor suppressor genes along cancer development[403–406], and the use of HDAC inhibitors (HDACIs) raised as new effective drugs. Previous studies show that HDACI action on the re-expression of certain silenced genes can result in cellular changes, including cell cycle arrest[407], DNA repair and damage assessment[408], and apoptosis[407,409–411]. This effect was mainly due to the restored expression of certain tumor suppressor genes supporting its use in cancer therapy. However, in most types of cancer the results of HDACIs application and trials fell short of expectations. Furthermore, most of the molecular mechanisms underlying the HDACIs failure remain not completely understood.

In the present paper we intended to depict how vorinostat, an HDACI, interferes with HNF1β expression and cellular behavior in CCC and its potential use in this tumor type. In order to achieve this, we evaluated the effect of vorinostat in two cancer cell lines representing ovarian serous carcinoma (HGSC), the most prevalent type of ovarian cancer, and CCC.

Material and Methods

Cell lines and cell culture

Cell lines from CCC, ES2 ovarian clear cell carcinoma (CRL-1978, ATCC) and HGSC, OVCAR3 ovarian serous carcinoma (HTB-161, ATCC) were obtained from American Type Culture Collection (ATCC). Cells were cultured in Dulbecco's modified Eagle's medium (DMEM) 1X (41965-039, Invitrogen) containing 4.5 g/L of D-glucose and 0.58 g/L of L-glutamine. Medium was supplemented with 10% Fetal Bovine Serum (FBS) (FBS, S 0615, Invitrogen, Thermo Fisher Scientific, Inc.) and 1% antibiotic-antimycotic (AA) (Invitrogen™; Thermo Fisher Scientific, Inc.) at 37°C in a humidified atmosphere containing 5% CO2 environment. Cells were grown to 75 - 100% optical confluence before they were detached by incubation with 1X 0.05% trypsin-EDTA (25300-054, Invitrogen™; Thermo Fisher Scientific, Inc.) at room temperature, and splited. The cell number was determined using a Bürker counting chamber. Prior to any experiment, cells were synchronized under starvation (FBS free culture medium), overnight at 37°C and 5% CO_2.

Cells were cultured with and without vorinostat at 5µM (suberoylanilide hydroxamic acid, Merck). For long time exposure, ES2 and OVCAR3 were stepwise exposed to vorinostat, first during 30 days, then vorinostat was removed for 20 days, which allows cells to proliferate again, and finally the cells were again exposed to vorinostat for more 20 days.

Flow cytometry analysis of total cell death (apoptosis and necrosis)

Cells were detached with trypsin, washed twice with cold PBS, and double stained with Annexin V- fluorescein isothiocyanate (FITC) (556420, BD-Pharmigen) and propidium iodide (PI) (P4864, Sigma-Aldrich) in Annexin-binding buffer, followed by analysis on FACSCalibur flow cytometer (Becton-Dickinson). All experiments were performed in triplicates. Data were analyzed using FlowJo software (http://www.flowjo.com/).

Flow cytometry analysis of cell cycle

Cells were collected, washed twice with cold PBS and fixed in 70% ethanol (100983, Merck) at 4°C. Cells were centrifuged at 1500 rpm for 5 min and then stained with 100 µl of 50 µg/ml of propidium iodide (PI) and incubated at 37°C for 40 min. Analysis was performed immediately after staining using FACSCalibur flow cytometer (Becton-Dickinson). All experiments were performed in triplicates. Data were analyzed using FlowJo software (http://www.flowjo.com/).

Reverse transcription-quantitative polymerase chain reaction (qPCR)

Ribonucleic acid (RNA) from ES2 and OVCAR3 was extracted using RNeasy Mini Extraction kit (74104, Qiagen, Inc.) according to the manufacturer's protocol. RNA concentration was determined by measuring the absorbance at 260 nm in a Nanodrop 2000 (Thermo Scientific). Reverse transcription polymerase chain reaction (RT-PCR) was performed with 1µg RNA and reversely-transcribed by SuperScript II Reverse Transcriptase (18080-44, 200 U; Invitrogen™, Thermo Fisher Scientific, Inc.), according to the manufacturer's protocol, in a T3000 thermocycler (Biometra). The PCR amplifications conditions were as follows: 95°C for 2 min, 95°C for 10 min followed by 45 cycles of 95°C for 15 seconds, 60°C for 60 seconds. qPCR was performed using an ABI PRISM 7900HT Sequence Detection System (Applied Biosystems®; Thermo Fisher Scientific, Inc.) with Power SYBR Green PCR Master Mix (4367659, Applied Biosystems®, Thermo Fisher Scientific, Inc).

The primers sequences used were as follows: *HNF1*β CCGACAATTCAACCAGACAG (forward), CAGAGCAGGCATCATCGGAC (reverse), *p21* GAGACTCTCAGGGTCGAAAACG (forward), ATTAGGGCTTCCTCTTGGAGAAG (reverse). Data were analyzed in SDS 2.4.1 software (Applied Biosystems; Thermo Fisher Scientific, Inc.) and the relative expression of each gene was quantified by relative quantification (RQ) study module (ΔΔCt)[369] using hypoxanthine phosphoribosyltransferase gene (HPRT) as an endogenous reference gene.

Automated Sanger sequencing analysis

Mutational analysis of TP53 was detected by polymerase chain reaction (PCR) for exon 7, followed by automated sequencing. PCR amplification was performed using specific primers (Forward: CCTCATCTTGGGCCTGTGTTA, Reverse: TGGAAGAAATCGGTA AGAGGTG) and DNA fragments with expected size were purified using Exonuclease I (20 U/µL) (EN0582, ThermoFisher)/FastAP Thermo-sensitive Alkaline Phosphatase (1 U/µL) (EF0651, ThermoFisher), according to the manufacturer's protocol. Sequencing reactions were performed using BigDye® Terminator v3.1 Cycle Sequencing kit, (catalog no. 4337456, Applied Biosystems) in a T3000 thermocycler (Biometra). Purification was executed with AutoSeq G-50 dye terminator removal kit (catalog no. 27-5340-02, GE Healthcare Life Sciences) according to manufacturer´s instruction and then evaluated in an ABI Prism™ 310 Genetic Analyzer (Applied Biosystems).

Western blotting

Total protein extracts were obtained after cell lysis in Radio-Immunoprecipitation Assay (RIPA) lysis buffer (20mM/L Tris (pH 7.5), 150 mM/L NaCl, 5 mM/L KCl and 1% Triton X-100) previously supplemented with protease and phosphatase inhibitors to the cell pellet (Complete, Mini, EDTA-free Protease Inhibitor Cocktail Tablet (catalog no. 11836170001, Roche), 1 mM Orthovanadate (Na3VO4) (450243, Sigma) and 1 mM Sodium fluoride (NaF) (catalog no. 201154, Sigma). Whole protein lysates were quantified using standard Bradford protein assay, subsequently 100 µg protein samples were then separated by electrophoresis in a 15% sodium dodecyl sulfate polyacrylamide gel (SDS-

For protein immunodetection, membranes were incubated with the specific primary antibodies: mouse monoclonal anti-p21 (1:1000; catalog no. 701151, Life technologies); mouse monoclonal anti-p53 (1:1000; catalog no. 453M-9, Sigma Aldrich); rabbit polyclonal anti-HNF1β (1:500; catalog no. HPA002083, Sigma-Aldrich); rabbit polyclonal anti-BCL-2 (1:1000; catalog no. SAB4300340, Sigma-Aldrich); rabbit polyclonal anti-BAX (1:100; catalog no. HPA027878, Sigma-Aldrich); rabbit polyclonal anti-acetyl-lysine (1:500; catalog no. AB3879, Millipore) and mouse monoclonal anti-β-actin (1:5000; catalog no., A5441, Sigma-Aldrich) and incubated overnight at 4°C,

followed by incubation with peroxidase (HRP)-conjugated secondary antibodies (anti-mouse; catalog no. 31430, Thermo Scientific and anti-rabbit; catalog no. 31460, Thermo Scientific).

The peroxidase activity was detected by ECL method. Digital images were obtained in ChemiDoc XRS System (Bio-Rad) with Image Lab Software (imagej.nih.gov/ij/). Protein detection was quantified by digital analyses of the protein bands intensity that were normalized to β-actin, and acetylation of HNF1β was quantified using total levels of HNF1β, by using ImageJ Software (http://rsbweb.nih.gov/ij/).

Immunoprecipitation

To obtained total protein extracts cells pellets were lysed using phosphate buffer (0.1M, pH 7) with 1% Triton X-100 (catalog no. T8787, Sigma) and protease and phosphatase inhibitors (Complete, Mini, EDTA-free Protease Inhibitor Cocktail Tablet (catalog no. 11836170001, Roche), 1 mM Orthovanadate (Na_3VO_4) (catalog no. 450243, Sigma) and 1 mM Sodium fluoride (NaF) (catalog no. 201154, Sigma)) followed by sonication (2 cycles of 10sec, 50% amplitude). Lysed cell pellets were incubated with anti-HNF1β (HPA002083, Sigma-Aldrich), overnight (ON) at 4°C followed by another incubation ON at 4°C with protein G-sapharose (51347800-EM, GE Healthcare). Samples (total protein extracts, anti-HNF1β and protein G-Sapharose) were then centrifuged and the pellet obtained ressuspended in glycine (0.1M) to obtain purified HNF1β and other proteins bound to HNF1β. HNF1β protein immunodetection were performed using western blotting (described above).

Immunofluorescence

Cells were cultured on glass slides coated with a 0.2% gelatin coating, until 80% of confluence and then fixed in 2% paraformaldehyde for 15 minutes at 4^{o}C. Blocking was performed with 0.2% (w/v) BSA in PBS 1X for 1 h at room temperature, and incubated with primary antibody overnight (diluted 1:100 in 0.2% (w/v) BSA in PBS 1X). The primary antibody was anti-HNF1β (HPA002083, Sigma-Aldrich). After PBS 1x washing, samples were incubated with secondary antibody (Alexa Fluor® 488 anti-rabbit, Invitrogen) for 2 h, at room temperature. The slides were mounted in

VECTASHIELD media with DAPI (4'-6-diamidino-2-phenylindole) (Vector Labs) and examined by standard fluorescence microscopy using a Nikon Instruments Eclipse Ti-S Inverted Microscope (Hamamatsu digital camera C10600 ORCA-R^2). Images were acquired and processed with NIS-Elements AR-3.2.

Statistical analysis

Data were analyzed using unpaired two-tailed student's test and one-way/two-way ANOVA with GraphPad Prim statistical software (San Diego, USA). A value of $p<0.05$ was considered statistically significant.

Results

Vorinostat effect in cancer cell proliferation, cell cycle status of EOC

The evaluation of the effect exerted by vorinostat on the proliferation rate and cell cycle status showed that ES2 cells proliferate at a lower rate in the presence of vorinostat which is consistent with the G0-G1 cell cycle arrest observed after 30h of exposure to vorinostat (Figure 4.1A and B). OVCAR3 cells showed no alterations in growth curve and in cell cycle status due to vorinostat exposure (Figure 4.1A and B). Accordingly, the expression of p21, which is a cyclin dependent kinase (CDK) inhibitor and a canonical HDACI gene target[412,413] is increased in ES2 cells exposed to vorinostat (Figure 4.1C).

Upon a long term exposure to vorinostat, ES2 cells exhibit again a G0/G1 cell cycle arrest, which is reversed by the removal of vorinostat (Figure 4.2A). The levels of p21 mRNA were in agreement with the observed dynamics of cell cycle activity (Figure 4.2B). In contrast, the OVCAR3 cells have no significant changes in cell cycle status after the long term vorinostat exposure as we observed in the 30h exposure (Figure 4.2A and 4.1B).

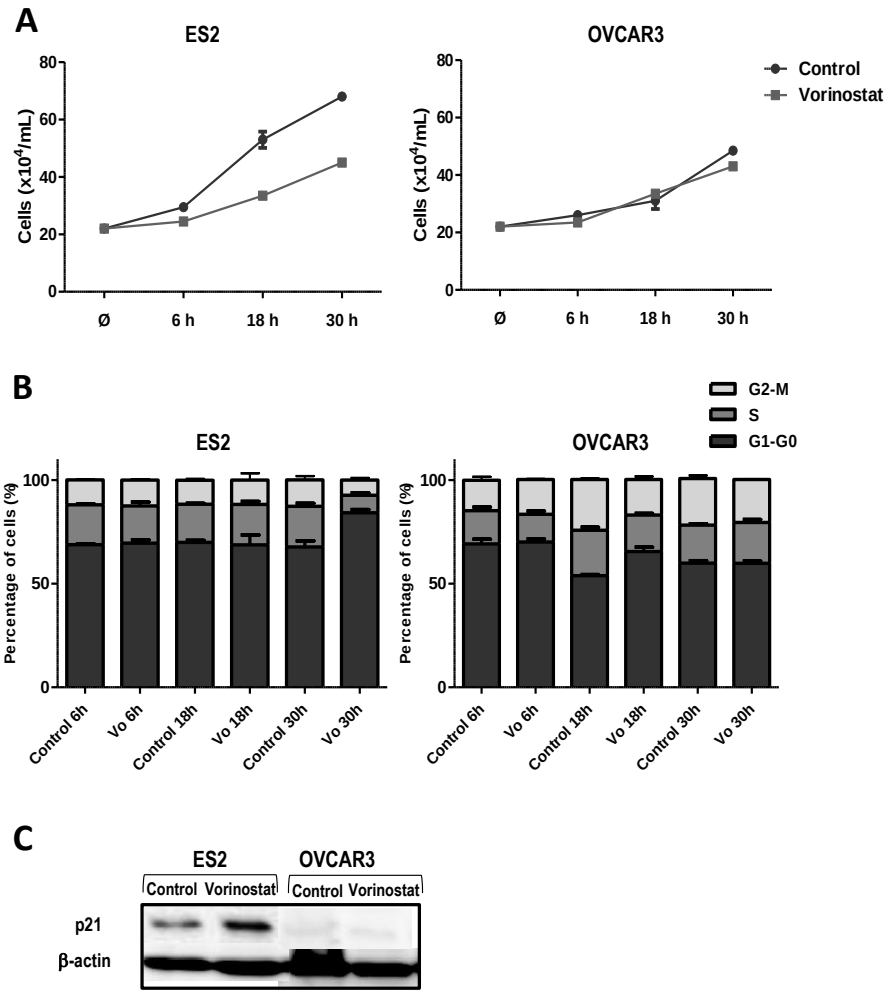

Figure 4. 1 - **Vorinostat affects cell proliferation of clear cell carcinoma (ES2) but not of serous carcinoma (OVCAR3)**

A. Vorinostat exposure induces a significant decrease in cell proliferation, in ES2 cell line; **B.** ES2 cells exposed to vorinostat show cell cycle arrest in G1-G0, at 30h, and **C.** In ES2 vorinostat also increases the levels of p21 in ES2 but not in OVCAR3.

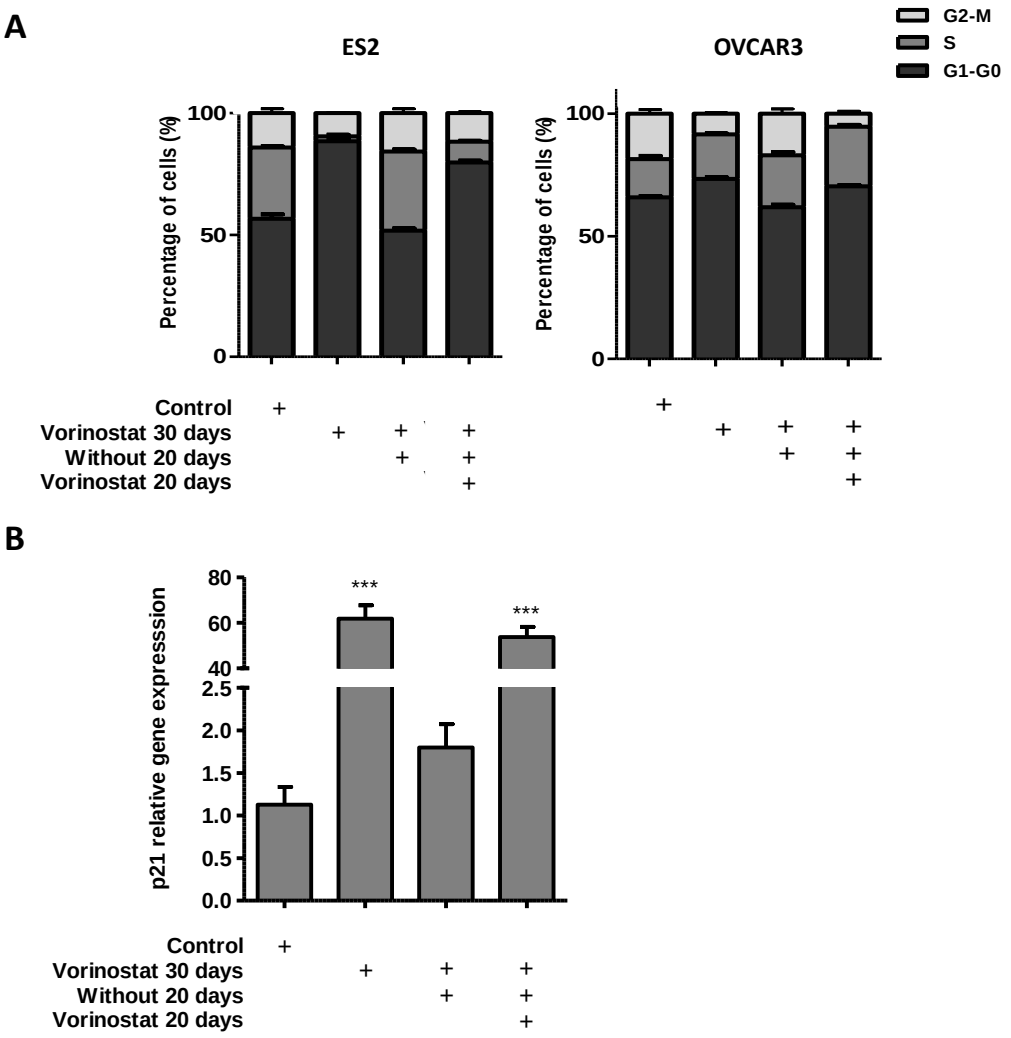

Figure 4. 2 - **Long term exposure of Vorinostat induces p21 expression and cell cycle arrest in clear cell carcinoma (ES2)**
A. Long term vorinostat exposure induces G0/G1 cell cycle arrest in ES2 cells but not in OVCAR3, and **B.** Vorinostat modulates the expression of p21 in clear cell carcinoma (ES2)

As p53 is one of the main responsible for cell cycle regulation and is frequently mutated in cancer as it is in the ES2 (C.722 C>T) and OVCAR3 (C.743 G>A) cell lines, we were prompted to evaluate the expression of p53 upon vorinostat exposure. The expression levels of p53 at vorinostat short term (30h) exposure remained unaltered in both cell lines (Figure 4.3A). It is interesting to state that these cell lines only expressed the mutated p53, and the wild type p53 (Figure 4.3B) was not detected. In a long term exposure of ES2 to vorinostat, p53 levels are maintained but its levels are significantly increased when after 30 days vorinostat is removed for 20 days (Figure 4.3C).

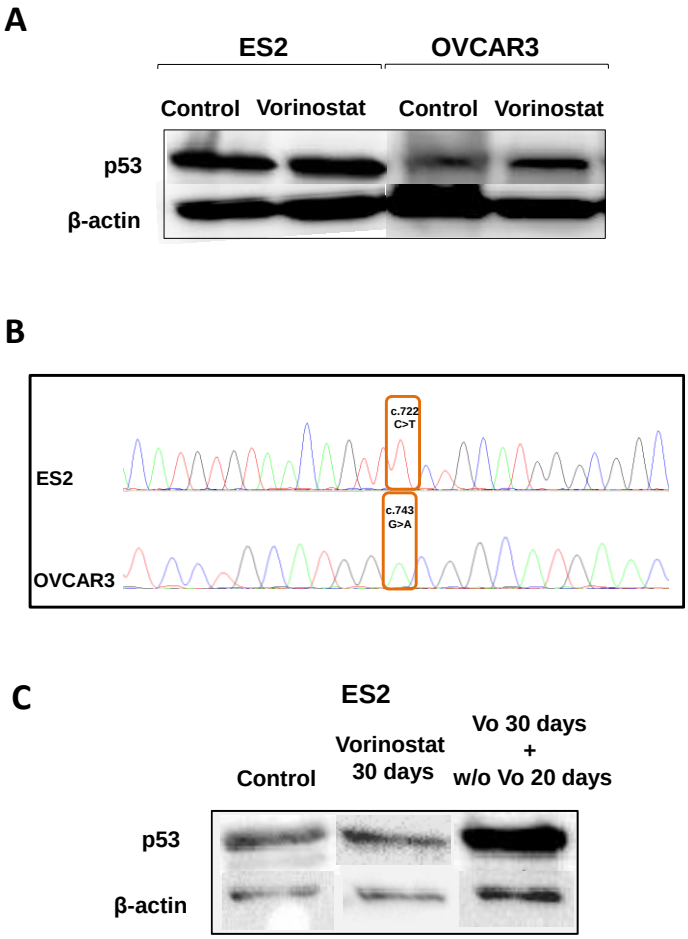

Figure 4. 3 - **The expression of mutant p53 increases in ES2 upon vorinostat removal, after long term exposure**
A. Exposure (30h) to vorinostat increases the levels of p53, in HGSC-OVCAR3 cells but nor in ES2 cells; **B.** p53 mRNA expressed in OVCAR3 and ES2 cells are mutated variants, having missense mutations in exon 7, respectively c.722 C>T and c.743 G>A, and **C.** Long term exposure (30 days) to vorinostat followed by 20 days without vorinostat increase the protein levels of p53 in ES2 cell line.

Vorinostat effect in cell viability and HNF1β expression in CCC

Vorinostat induces death of ES2 cells at 6, 18 and 30h of exposure as observed in figure 4.4A. This effect was also observed in OVCAR3 cells under vorinostat exposure, but only after 30h of treatment (Figure 4.4A). Moreover, the *ratio* of BAX (pro-apoptotic) versus BCL-2 (anti-apoptotic) expression is increased in ES2 but not in OVCAR3, after 30h of vorinostat exposure, confirming the pro-apoptotic effect of vorinostat in CCC (Figure 4.4B). The levels of cleaved caspase 3 are consistent with apoptosis in both cell lines (Figure 4.4C).

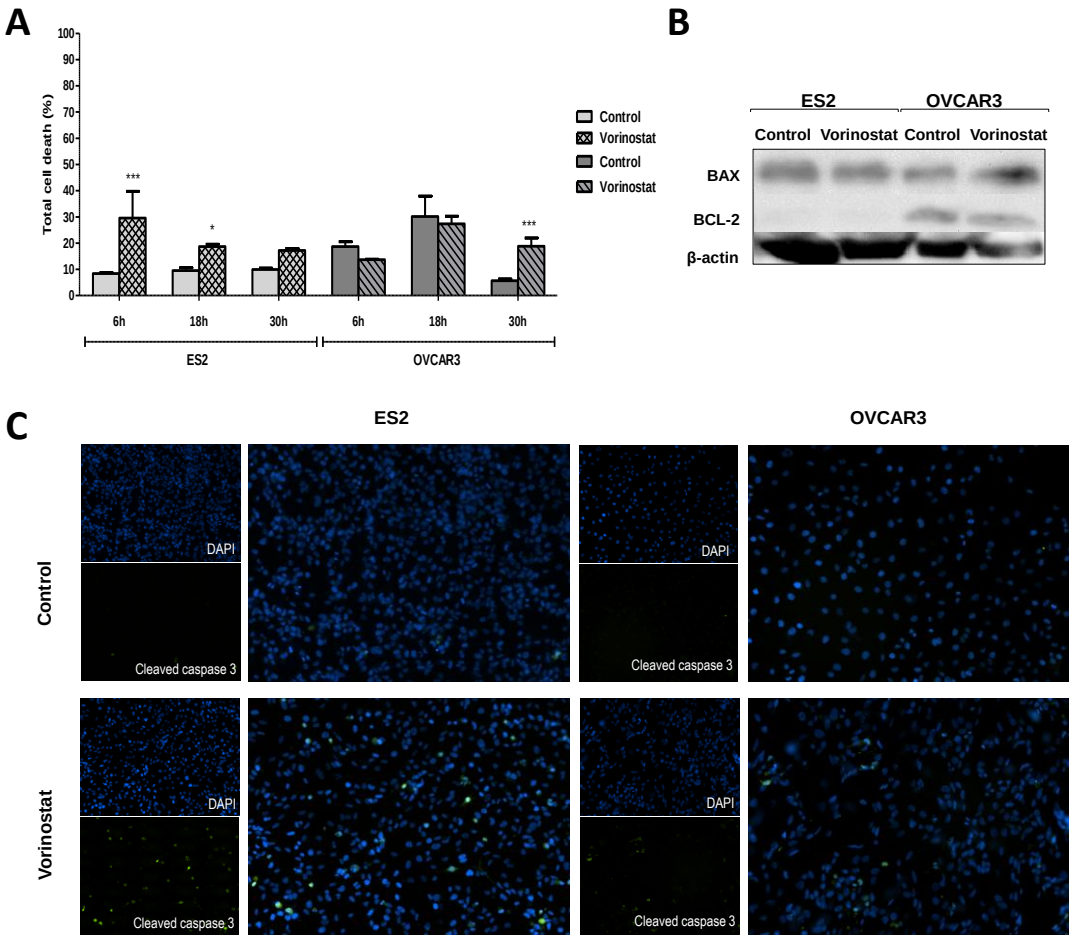

Figure 4. 4 - **Vorinostat increases cell death in clear cell carcinoma (ES2)**
A. Vorinostat induces death of ES2 cells at 6, 18 and 30h of exposure. This effect was observed in OVCAR3 cells under vorinostat exposure, only after 30h of treatment; **B.** The *ratio* BAX/BCL-2 is increased in ES2, after 30h of vorinostat exposure, confirming pro-apoptotic effect of vorinostat in CCC, and **C.** After 30h of exposure vorinostat increases the levels of cleaved caspase-3.

Since ES2 cells showed cell cycle arrest (Figure 4.1A and 4.1B) and increased cell death when exposed to vorinostat (Figure 4.4A), so it was mandatory to evaluate the effect of vorinostat exposure in HNF1β expression, once HNF1β is the key gene of CCC, contributing to cell survival and chemoresistance[72,402]. We observed that vorinostat exposure increased the expression of HNF1β in ES2 cells (Figure 4.5A and B) as well as the acetylation load of HNF1β (Figure 4.5B). As seen in Figure 4.5A, OVCAR3 does not express HNF1 β, even when exposed to vorinostat, so the following experiments were done only in ES2 cell line.

Interestingly, the levels of HNF1β mRNA also increase in vorinostat long term exposure of ES2 cells (Figure 4.5C).

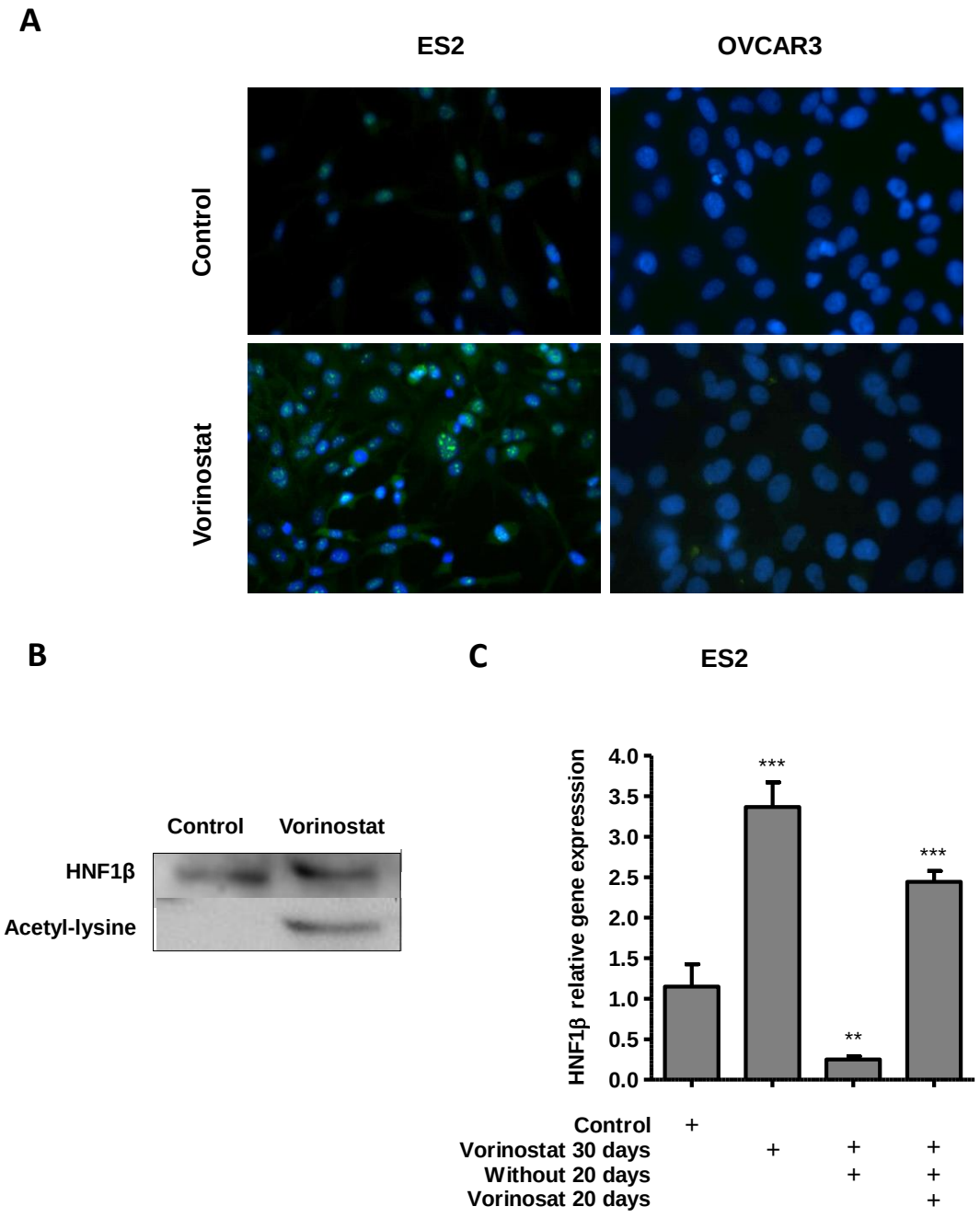

Figure 4. 5 - **Vorinostat exposure increase the levels of HNF1β in clear cell carcinoma (ES2), both in short and long term exposure**
A. In ES2, vorinostat increases the levels of HNF1β; **B.** Vorinostat increases the protein levels of HNF1β and its acetylation (in lysine residues), and **C.** Long term exposure to vorinostat increases the expression of HNF1β.

Discussion

As mentioned, CCC in advanced stages is characterized by a poor prognosis due to intrinsic resistance to conventional therapy[72]. Therefore, the discovery of new therapeutic alternatives is of absolute importance.

The emergence of HDACIs as therapeutic agents opened up novel perspectives for the treatment of cancer and particularly in ovarian cancer. In this work, we were able to document that vorinostat has different effects in ovarian cancer cell lines, CCC and HGSC. This result could be anticipated as these cancer cell lines derived from two different entities both in clinical and molecular terms.

Overall, it is known that vorinostat induces cell cycle arrest and apoptosis in EOC as described in other cancer contexts upon exposure to HDACIs[315,320,412]. Furthermore, the cell cycle arrest in G0/G1 phases is supported on the molecular level by the increased expression of p21, an inhibitor of cyclin dependent kinases (CDK)[414,415], thus not allowing the advance of cells throughout the cell cycle.

The p53 mutant variants present in the cell lines (CCC-ES2; C.722 C>T and HGSC-OVCAR3; C.743 G>A) used in this study were already described and these variants interfere with the p53 DNA binding capacity[416,417]. Gene CDKN1A (p21), is a main p53 target gene and the fact that p21 is increased in cells exposed to vorinostat, probably means that p53 is activating its transcription. The mutations in exon 7 of p53 codifies p53 variants that are protected from degradation, having an increased half-life time and accumulating in the cell[416,417]. As a tumor suppressor gene, it was expected a loss of function in mutant p53, however its special condition is well known and mutated p53 variants are characterized by oncogenic gain of function that can be patent for instance in its action as a dominant negative abrogating normal p53 function in the tetramer, or by interacting with new partners being able to regulate the expression of a new setting of genes that are favorable to cancer development and progression[418].

The dramatically increased levels of p53 in ES2 cells that are cultured free of vorinostat after a long term exposure to vorinostat can indicate that p53 p.S241F mutated variant (codified by C.722 C>T) plays a role in the survival of vorinostat

resistant cells at least in this cancer cell line. As p21 gene is also described to be a target of p73, a transcription factor belonging to p53 family that can overcome p53 function in cells with a mutated p53[419], it might be a possible explanation for p21 elevated levels.

Interference of HNF1β in cell cycle was already describe by Shigetomi et al.[402] where they demonstrate the involvement of HNF1β in cell cycle of ovarian CCC lines using HNF1β knockdown cell lines. The study suggested that drug resistance of CCC cell lines may be caused by sustained activation of the G2 checkpoint, through HNF1β overexpression. Asides from studying checkpoint kinase 1(CHK1), important in G2 checkpoint, no others proteins were investigated[402].

As demonstrated by our immunofluorescence experiments the HGSC cell line, OVCAR3 does not express HNF1β and therefore this type of carcinoma cannot help to explain the mechanism that cells use to survive through HNF1β action.

The most important aspect of this work was the finding of HNF1β acetylation induced by vorinostat. This finding can underly a mechanism of modulation/abrogation of HNF1β function, which is an advance in the understanding of the CCC biology. Since HNF1β has a pro-survival activity, this work showed that its acetylation can be a route of HDACIs action in CCC cells, affecting cell proliferation and viability.

Again, it became evident in this study that the action of HDACIs, although initially designed to affect the acetylation level of histones and therefore the conformation of chromatin; also affects the function of other proteins, which play crucial roles in cell function, since HDACs also deacetylate other proteins than histones. The HDACIs contribute for the overall increased levels of acetylation, interfering with proteins function[420] and the *turnover* of proteins, not only histones, by affecting the labeling of proteins to be degraded, similar to what it is described for p53[421–423]. Acetylation can interfere with the proteosomic degradation of ubiquitinated proteins. So far, HNF1β is not described as being regulated by ubiquitination (http://www.ncbi.nlm.nih.gov/ieb/research/acembly/av.cgi?db=human&term=HNF1B&submit=Go) but it may explain our results, since (Figure 5B) phosphorylation and ubiquitination are the same

mechanisms of regulation of p53 activity and degradation with which acetylation interferes[421–424].

Hence, this work also opens new perspectives for studies to be further developed in order to better understand the function of HNF1β, especially in the context of cancer, since HNF1β is consistently *de novo* expressed or overexpressed in CCC from different organs such as ovary, pancreas, kidney and liver[399,425–427].

Unfortunately, clinical trials testing HDACIs, that have been proven inconclusive, due to toxic effects, or have classified HDACIs as not suitable therapeutic agents for the treatment of EOC; were essentially carried out in EOC with no identification of the tumor histological type[324,374,428–430]. This practically prevented the adjustment and use of HDACIs to treat CCC which is undoubtedly the histological type of EOC that requires a more urgent effective therapeutic action and bears molecular trait that seems to be more susceptible to this therapy.

In light of our study, HDACIs are a group of drugs that could be a therapeutic alternative to the CCC. Possibly, its use also requires new strategies to deliver these drugs in a way to reduce the toxic effects already observed in clinical trials, since the structural changes are not indicated as they are inhibitors of the catalytic center of HDACs, and the toxic effects are adverse effects related to their specific function.

CHAPTER 5

Functional redundancy of the Notch pathway in ovarian cancer cell lines

Work presented in this chapter corresponds to the following publication:

Silva, F., Félix, A. & Serpa, J. Functional redundancy of the Notch pathway in ovarian cancer cell lines. *Oncol. Lett.* **12,** 2686–2691 (2016).

Abstract

Epithelial ovarian cancer is the most lethal gynecologic malignancy, despite advances in treatment. The most common histological type, high grade serous carcinoma (HGSC) is usually diagnosed at an advanced stage, and although this type of tumors frequently respond to surgery and platinum-based chemotherapy, they usually recur. Ovarian clear cell carcinoma (CCC) is an unusual histological type, which is known to be intrinsically chemoresistant and is associated with poor prognosis in advanced stages.

In recent years, genetic alterations and epigenetic modulation of signaling pathways have been reported in HGSC and CCC**,** including the overexpression of Notch pathway elements and histone deacetylases. Histone deacetylase inhibitors (HDACIs), including vorinostat (suberoylanilide hydroxamic acid), alter the transcription of genes involved in cell growth, survival and apoptosis, and have become an attractive therapeutic approach. However, no previous work has addressed the effect of HDACIs, and in particular vorinostat, on Notch signaling in ovarian cancer.

Therefore, the present study aimed to investigate the modulation of the Notch pathway by vorinostat in ovarian cancer. Using immunofluorescence and quantitative polymerase chain reaction, the present results revealed that vorinostat activated the Notch pathway in CCC and HGSC cell lines, through different Notch ligands. In CCC, the activation of Notch pathway appeared to occur through Delta-like (Dll) ligands 1, 2 and 3, whereas in HGSC Dll1 and Jagged 1 and 2 ligands were involved. The activation of Notch pathway by vorinostat, in CCC and HGSC cell lines, culminated in the increased expression of the same downstream transcription factors, hairy enhancer of split (*Hes1) 1 and 5, and Hes-related proteins 1* and *2.*

In conclusion, vorinostat modulates the expression of several downstream targets of the Notch pathway and independent Notch receptors and ligands that are expressed in HGSC and CCC. This upregulation of the Notch pathway may explain why vorinostat therapy fails in ovarian carcinoma treatment, as shown in certain clinical trials.

Keywords: ovarian cancer, Notch pathway, vorinostat

Introduction

Epithelial ovarian cancer (EOC) is the most lethal and the seventh most common gynecologic malignancy in women worldwide[3,4]. EOC represents 90% of ovarian malignant tumors[21] and it is an extremely heterogeneous group of neoplasms that exhibit a wide range of tumor morphology, clinical manifestations and underlying genetic alterations[25].

The most common histological type, high grade ovarian serous carcinoma (HGSC), is characterized by tumor protein 53 (TP53) mutations and breast cancer 1 and 2 dysfunction[31]. This type of tumor is aggressive and usually diagnosed at an advanced stage, and although HGSC frequently responds to surgery and platinum-based chemotherapy, it usually recurs[55].

Ovarian clear cell carcinoma (CCC) is a more unusual histotype of EOC, which is known to be intrinsically chemoresistant and is associated with poor prognosis in advanced stages[55]. Molecular alterations of CCC are not well known, presenting a challenge to treat this type of tumors. However, CCC is characterized by a unique histology, de novo expression of hepatocyte nuclear factor 1β transcription factor and somatic mutations of AT-rich interaction domain 1A gene, and loss of its expression[61,62].

In previous years, other genetic alterations and epigenetic modulation of signaling pathways have been reported in HGSC and CCC[64], including the overexpression of Notch pathway elements and histone deacetylases (HDAC)[339]. The Notch pathway has multiple roles in cell fate determination, since it regulates cell proliferation, differentiation, survival and apoptosis[135,136]. This signaling pathway is deregulated in human hematological malignancies and solid tumors[133,134], and it is also implicated in angiogenesis[431,432]. Notch signaling is a juxtacrine pathway composed by Notch receptors (Notch1-4) and two classes of ligands, Delta-like (Dll) 1, 3 and 4 and serrate-like Jagged1 and Jagged2[137–140].

Notch signaling is initiated by the binding of Delta/Jagged ligands to Notch receptors. Through several proteolytic cleavages, the Notch intracellular domain

(NICD) is released and activates the transcription of target genes, hairy enhancer of split (*Hes*) family proteins, *Hes*-related proteins (*Hey)*[143] as well as cell cycle regulators, including *p21*[135], *cyclin D1* and *3*[144], *c-myc*[145] and *human epidermal growth factor 2*[146].

Epigenetic alterations are also involved in the repression of tumor suppressor genes and promotion of tumorigenesis in ovarian cancers, and HDAC inhibitor (HDACI) drugs are an attractive therapeutic approach[286]. HDACIs inhibit cancer cell growth *in vitro* and *in vivo*, revert oncogene-transformed cell morphology, induce apoptosis, and enhance cell differentiation[279].

Vorinostat (suberoylanilide hydroxamic acid) is a HDACI[310] that was FDA approved in 2006 for the treatment of cutaneous T-cell lymphoma, and it has demonstrated interesting results in *in vitro* models of ovarian cancer[311]. However, to the best of our knowledge, there has been no previous study addressing the effect of HDACIs, and in particular of vorinostat, on Notch signaling on ovarian cancer.

Therefore, the aim of the present study was to investigate the modulation of the Notch pathway by vorinostat in ovarian cancer cell lines.

Material and Methods

Cell lines and cell culture conditions

CCC-ES2 (CRL-1978) and HGSC-OVCAR3 (HTB-161) cell lines were obtained from American Type Culture Collection (Manassas, VA, USA). The cells were incubated at 37°C in a humidified atmosphere containing 5% CO_2 in McCoy's 5A Modified Medium (Sigma-Aldrich, St. Louis, MO, USA), supplemented with 10% fetal bovine serum (FBS, S 0615, Invitrogen) and 1% antibiotic-antimycotic (AA) (Invitrogen™; Thermo Fisher Scientific, Inc., Waltham, MA, USA). The cells were cultured to 80-100% confluence prior to detachment by incubation with 1X 0.05% trypsin-EDTA (Invitrogen™; Thermo Fisher Scientific, Inc.) at room temperature. For the various assays, cell number was determined using a Bürker counting chamber. Vorinostat (catalog no. CAS 149647-78-9; Cayman Chemical, Ann Arbor, MI, USA) was used at 5 µM to treat cells.

Immunofluorescence

Procedure already described in Chapter 3.

The primary antibodies were as follows: rabbit polyclonal anti-human Notch1 extracellular (catalog no., ABS90, EMD Millipore, Billerica, MA, USA), rabbit monoclonal anti-Notch1 cleaved (catalog no. 1744, Cell Signaling, Inc., Danvers, MA, USA), rabbit polyclonal anti-Notch2, cleaved (catalog no., 07-1234, EMD Millipore) and rabbit polyclonal anti-Notch4 (catalog no., N5163; Sigma-Aldrich). The cells were incubated with Alexa Fluor® 488 goat anti-rabbit secondary antibody (catalog no., A-11008; Invitrogen™, Thermo Fisher Scientific, Inc.) for 2 h at room temperature. The slides were mounted in VECTASHIELD Anti-fade Mounting Medium with DAPI (catalog no., H-1200; Vector Laboratories, Inc., Burlingame, CA, USA) and examined by standard fluorescence microscopy using an Axio Imager microscope (Zeiss GmbH, Jena, Germany). Images were acquired with AxioVision software (version 4.5; Zeiss, GmbH) and processed with ImageJ software (version 1.44p; imagej.nih.gov/ij/).

Reverse transcription-quantitative polymerase chain reaction (qPCR).

Total RNA was isolated from cells cultured in complete McCoy's with or without (control condition) vorinostat, using RNeasy Mini Extraction Kit (catalog no., 74104, Qiagen, Inc., Valencia, CA, USA), according to the manufacture's protocol. Procedure already described in Chapter 3.

The primers sequences used were as follows: Notch1: TGGCGGGAAGTGTGAAGCGG (forward), GTGCGAGGCACGGGTTGGG (reverse), Notch2: CCATATGCTTCAGCCGGGATAC (forward), GTCTCACATTTCTGCCCTGTG (reverse), Notch3: CTGCAAGGACCGAGTCAATGG (forward), CGTCCACGTTGCGAT CACAC (reverse), Nocth4: CCACCTTTCACCTCTGCCTC (forward), ACCTCACAG TCTGGGCCTAT (reverse), Dll1: ATGCCTTCGGCCACTTCAC (forward), CACATCCAGGCAGGCAGAT (reverse), Dll3:GAACCCGTGTGCCAATGGAG (forward), GTAGGCAGAGTAGGGTCTG (reverse), Jagged1: CGGCTTTGCCATGTGCTT (forward), TCTTCCTCCATCCCTCTGTCA (reverse), Jagged2: GTCGTCATCCCCTTCCAGTTC (forward), CTCATTCGGGGTGGTATCGTT (reverse), Hey1: GAAGTTGCGCGTTATCTGAG (forward), GTTGAGATGCGAAACCAGTC (reverse), Hey2: TCGCCTCTCCACAATTCAG (forward), TGAATCCGCATGGGCAAACG (reverse), Hes1:

CGGAGGTGCTTCACTGTCAT (forward), ACGACACCGGATAAACCAAA (reverse), Hes5: GAGAAAAACC GACTGCGGAAG (forward), GACAGCCATCTCCAGGATGTC (reverse), Hes6: GAAGTGCTGGAGCTGACGG (forward), CGAGCAGATGGTTCAGGAGC (reverse). All samples were run in triplicate. Data were analyzed in SDS 2.4.1 software (Applied Biosystems; Thermo Fisher Scientific, Inc.) and the relative expression of each gene was quantified by comparative quantification cycle (Cq) method (ΔΔCt)[369] using hypoxanthine phosphoribosyltransferase gene (HPRT) as an endogenous reference gene.

Statistical analysis

Statistical analysis was performed using Student's t-test with GraphPad Prism software (version 5.03; GraphPad Software, Inc., La Jolla, CA, USA). $P<0.05$ was considered to indicate a statistically significant difference.

Results

Effects of vorinostat treatment on Notch signaling in ovarian cancer cells

In order to investigate the effect of HDACI vorinostat on the Notch signaling pathway, ES2 and OVCAR3 cell lines were exposed to vorinostat for various periods of time. The results demonstrated that vorinostat exposed ES2 cells express increased levels of Notch 2 ($P<0.010$), 3 and 4 ($P<0.001$) mRNAs, whereas Notch1 expression remained unchanged (Figure 5.1A). Increased levels of Notch1 NICD in control and vorinostat exposed cells was observed using immunofluorescence. In Fig. 5.1B, immunofluorescence revealed that vorinostat exposure increased Notch2 and 4 protein expression but not extracellular Notch1.

Concerning Notch ligands in ES2 cells, vorinostat induced an increased expression of Dll1, Dll3 and Dll4 ($P<0.001$), whereas Jagged1 and 2 levels remained the same compared to control cells (Figure 5.1C). The significant increase in mRNA levels of Notch downstream genes Hes1 ($P<0.010$), Hes5 ($P<0.001$), Hey1 ($P<0.01$), and Hey2 ($P<0.05$), in cells exposed to vorinostat, confirmed the activation of Notch pathway in this cell line (Figure 5.1D).

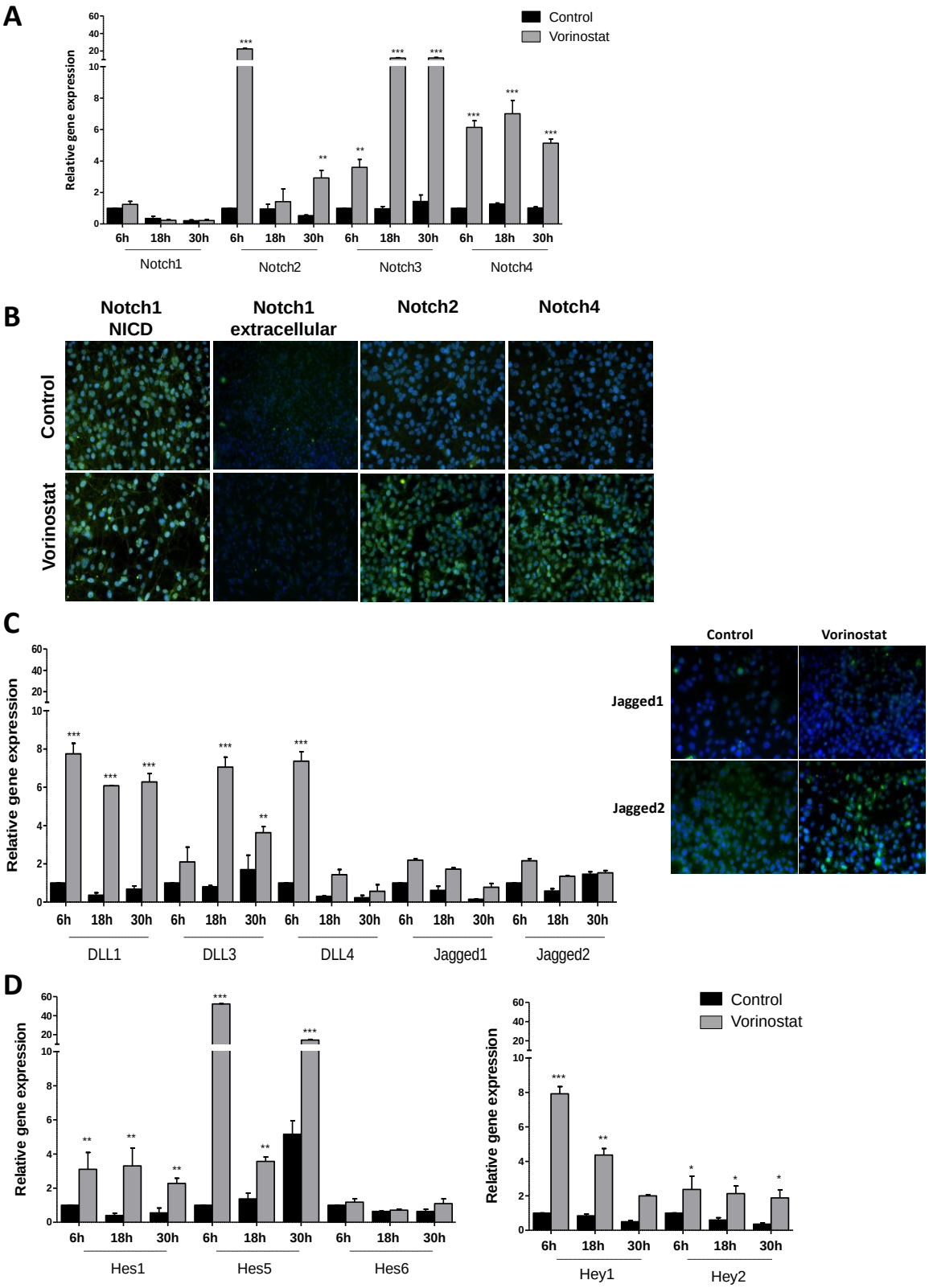

Figure 5.1 – **Vorinostat increases the expression of mRNA of Notch receptors, Delta/Jagged ligands and Hey/Hes downstream target genes**

Cells were grown in the absence and presence of vorinostat (5µM) and experimental conditions included exposures of 6, 18 and 30 hours, after starvation, with medium supplemented with 1% FBS; **A.** Notch receptors expression levels in ES2 cells. RQ-PCR showed that Notch2, Notch3 and Notch4 mRNAs are increased by vorinostat exposure, whereas Notch1 was not differentially expressed; **B.** Representative staining of Notch receptors by immunofluorescence. It was observed an increase of Notch2 and Notch4 protein after exposure to vorinostat (magnification 200x). Nuclei are stained with DAPI (blue), Notch receptors FITC (green); **C.** Notch ligands expression levels in ES2 cell line. RQ-PCR indicates that Dll1, Dll3, Dll4 mRNA expression levels in cells treated with vorinostat are higher than in cells without vorinostat. Jagged1 and Jagged2 mRNA expression levels were not significantly different; **D.** Notch downstream targets genes expression levels. RQ-PCR showed that Hes1, Hes5, Hey1 and Hey2 mRNA expression levels in cells treated with vorinostat are higher than in cells without vorinostat. Hes6 has similar expression in all conditions. The RQ-PCR was normalized to Hypoxanthine phosphoribosyltransferase gene (HPRT). Data are mean ± standard deviation of triplicates *p<0.05; **p<0.01; ***p ≤0.001.

In OVCAR3 cells, vorinostat also significantly increased Notch2, Notch3 and Notch4 (P<0.010), and slightly decreased Notch1 mRNA levels (Figure 5.2A). Protein expression of Notch2 and 4 was also higher in cells exposed to vorinostat; however, extracellular and NICD of Notch1 levels were not increased (Figure 5.2B). For Notch ligands, it was observed that there was a significant increase in Dll1 (P<0.001), Jagged1 and Jagged2 (P<0.001), mRNA levels in OVCAR3 cells exposed to vorinostat (Figure 5.2C), whereas Dll3 and 4 mRNA expression was not increased. Regarding Notch downstream targets, it was observed that vorinostat statistically increased *Hey1, Hey2* (p<0.001), *Hes1* (p<0.05), and *Hes5* (p<0.001), mRNA levels compared with control cells (Figure 5.2D); however, *Hes6* levels were not increased.

Overall, the present results revealed that vorinostat activated Notch pathway in CCC and HGSC cell lines; however, this activation was through a different expression panel of Notch ligands in the two cell lines. In CCC, the activation of Notch pathway appears to occur through Dll1, Dll2 and Dll3, whereas in HGSC Dll1 and Jagged 1 and 2 ligands families appear to be involved. Nevertheless, the present results revealed that the activation of Notch pathway by vorinostat, in CCC and HGSC cell lines, culminated in the increased expression of the same downstream targets, *Hey1, Hey2, Hes1* and *Hes5*.

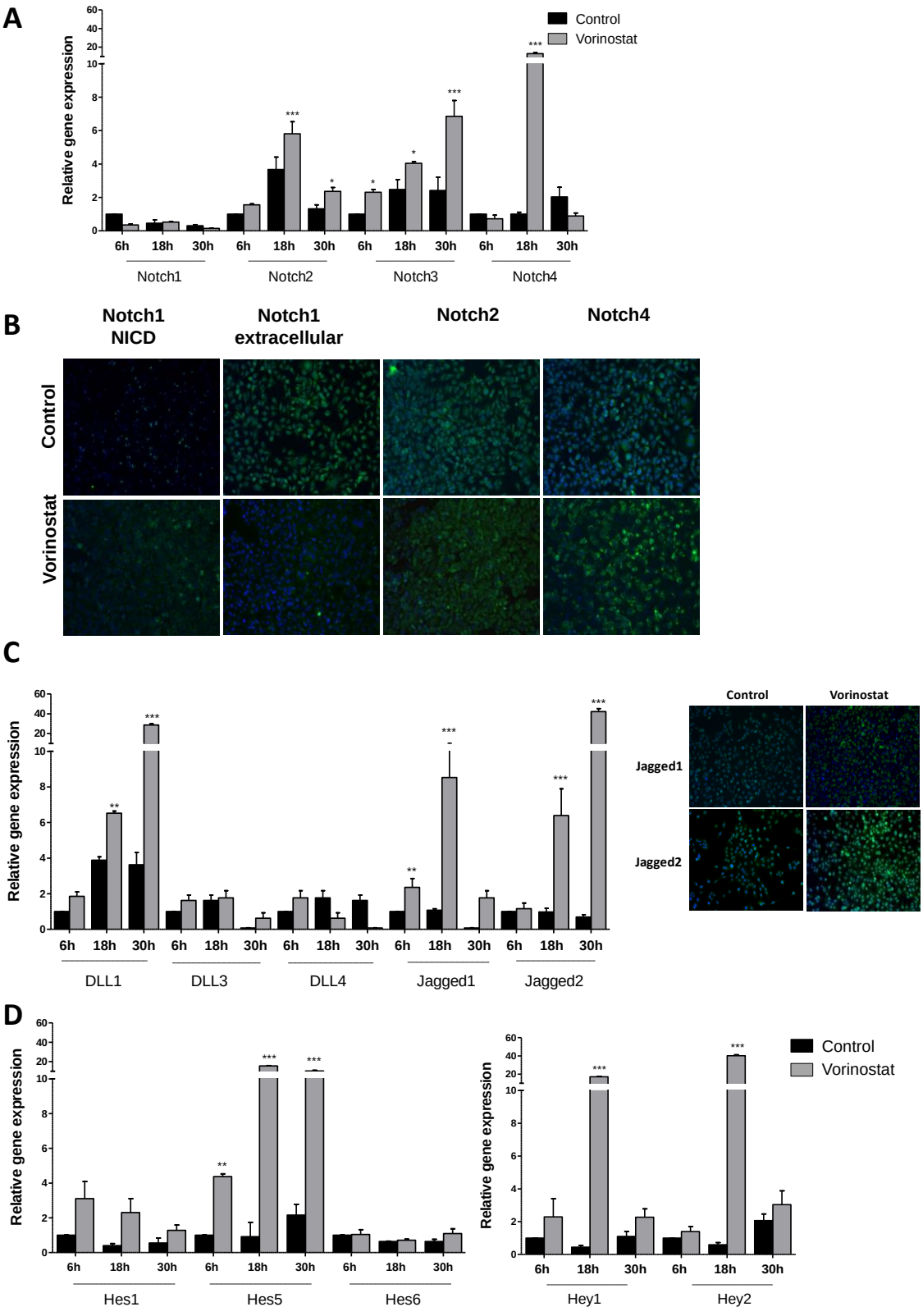

Figure 5. 2 – **Vorinostat increases the mRNA expression of Notch receptors, ligands and downstream targets in ovarian serous carcinoma OVCAR3 cell line**

The cells were grown in the absence and presence of vorinostat (5µM) for 6, 18 and 30 hours following starvation, with medium supplemented with 1% fetal bovine serum; **A.** Notch receptors expression levels in OVCAR3 cells. RQ-PCR indicated that Notch2, Notch3 and Notch4 mRNAs were increased following vorinostat exposure; **B.** Representative staining of Notch receptors by immunofluorescence. Vorinostat slightly increases the protein expression of Notch receptors 2 and 4, and decreased Notch1 expression following exposure to vorinostat (magnification 200x). Nuclei are stained with DAPI (blue), Notch receptors FITC (green); **C.** Notch ligands expression levels in OVCAR3 cell line. RQ-PCR showed that Dll1, Jagged1 and Jagged2 mRNA expression levels in cells treated with vorinostat are higher than in cells without vorinostat. Dll3 and Dell4 mRNA expression levels were not differentially express; **D.** Notch downstream targets genes expression levels. RQ-PCR showed that *Hes1, Hes5, Hey1* and *Hey2* mRNA expression levels in cells treated with vorinostat are higher than in cells without vorinostat. *Hes6* mRNA expression levels were not affected by vorinostat. The RQ-PCR was normalized to *Hypoxanthine phosphoribosyltransferase gene (HPRT).* Data are mean ± standard deviation of triplicates *p<0.05; **p<0.01; ***p ≤0.001.

Discussion

The Notch signaling pathway is an important cell signaling system that is activated in various types of cancer, including ovarian carcinomas[31,152,433]. Notch1 overexpression has been demonstrated in several studies to promote ovarian cancer cell proliferation[150,153,434] and this is primarily associated with increased levels of Notch1 NICD[150]. In the literature, Notch3 has also been demonstrated to be active in certain ovarian cancer cell lines and its overexpression was described in 20% of HGSC[148,151]. In addition, Notch3 was revealed to increase following tumor chemotherapy, and its overexpression is associated with tumor aggressiveness and poor prognosis of patients[151]. The present study aimed to investigate the effect of vorinostat, an HDAC inhibitor, on Notch signaling pathway in ovarian cancer cells. For this purpose, the present study used cell lines from two different histological types of EOC: HGSC, the most prevalent and aggressive EOC type; and CCC, which is a rare type of EOC that is highly resistant to chemotherapy[435].

No significant alteration in Notch1 mRNA levels following vorinostat exposure was identified in the two different ovarian cancer cell lines; however, high levels of cleaved Notch1 were detected in CCC cell line (ES2). In addition, Notch3 was demonstrated to be upregulated following vorinostat exposure in the two cell lines. Furthermore, the present study revealed that vorinostat activates the Notch pathway

through specific Notch ligands in CCC and HGSC cell lines; Dll1, 3 and 4 are activated in CCC, while Dll1 and Jagged1 and 2 are activated in HGSC. The present results are supported by a previous study that demonstrated altered Notch signaling in HGSC, due to increased expression of Jagged1 and 2 ligands[31,149].

The *Hes* and *Hey* gene families are the best characterized canonical Notch target genes, and the activation of Notch signaling upregulates their transcription[436], therefore *Hes* and *Hey* mRNA expression may be considered as markers for Notch activation. The present study demonstrated that *Hes* and *Hey* Notch target genes are overexpressed in EOC cells following exposure to vorinostat. The present data reveals that vorinostat induces the overexpression of *Hes* and *Hey* Notch target genes in EOC cells, due to Notch signaling activation. In addition, the redundancy of Notch, Delta and Jagged elements expressed in EOC cell lines was shown (Figure 3). Hence, no matter which panel of receptors or ligands is expressed on the cell membrane, the downstream target genes are always expressed in the presence of vorinostat. This upregulation can aid our understanding of the mechanism underlying the failure of vorinostat therapy in ovarian carcinoma.

In conclusion, the present findings illustrate the redundancy of Notch pathway in ovarian cancer, and suggest that disruption of histone acetylation may not be a useful therapeutic strategy in these carcinomas.

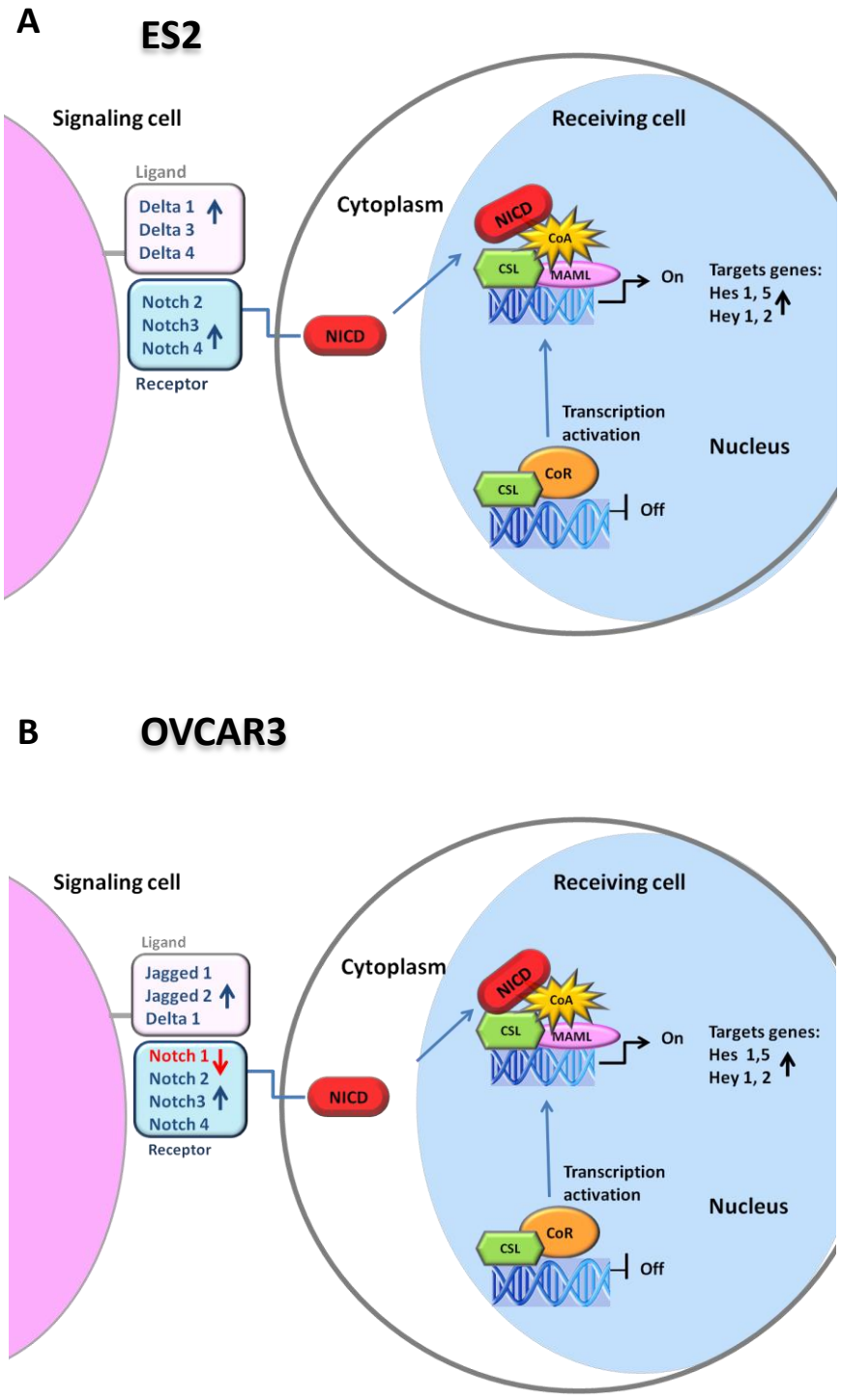

Figure 5. 3 - **Schematic representation of Notch pathway in ovarian cancer**
A. clear cell carcinoma ES2 and **B.** serous carcinoma OVCAR3 cells following exposure to vorinostat. NICD, Notch intracellular domain; CSL, Suppressor of Hairless; CoR, repressor; CoA, coactivator; MAML, mastermind-like proteins; Hes, hairy enhancer of split; Hey-related proteins.

CHAPTER 6

Establishment and Characterization of a novel ovarian high grade serous carcinoma cell line - IPO-SOC43

Manuscript in preparation

Abstract

Epithelial ovarian cancer (EOC) is an aggressive and lethal malignancy and novel EOC cell lines with detailed characterization are needed, to provide researchers helpful resources of diverse EOC to study biological processes and cancer experimental therapy.

The IPO-SOC43 cell line was established from the ascitic fluid of a patient with a diagnosis of high grade serous carcinoma (HGSC) of the ovary, previously treated with neoadjuvant chemotherapy. The cell immortalization was achieved as 2D cell culture and growth performed as 2D and 3D cell cultures. The morphological and molecular characterization of immortalized cells was done by immunocytochemistry, flow cytometry, cell proliferation and chromosomal Comparative Genomic Hybridization (cCGH).

Characterization studies confirmed that IPO-SOC43 cell line is of EOC origin and maintains morphological and molecular features of the primary tumor. cCGH analysis showed a complex profile with gains and losses of specific DNA regions in both primary ascitic fluid and cell line IPO-SOC43. The cell line was successfully grown in a 3D system which allows its future application in more complex assays than those performed in 2D models. IPO-SOC43 is available for public research and we hope it can contribute to enrich the *in vitro* models addressing EOC heterogeneity, being useful to investigate EOC and to develop new therapeutic modalities.

Keywords: high grade serous carcinoma (HGSC), cell line, 2D and 3D culture models, ovarian cancer.

Introduction

Cell lines provide a powerful model to clinical and basic research. *In vitro* models are suitable to study the molecular mechanisms underlying chemoresistance and cancer recurrence, being very helpful to clinical research, as the use of *in vitro* studies uncovered molecular pathways driving progression and metastatic spread of tumors[437,438].

As the development for precision medicine needs to account for tumor and microenvironment heterogeneity, the detailed characterization of *in vitro* models, representing the different histological and molecular types of ovarian cancer, is essential to accurate preclinical testing. There are at least 100 publicly available ovarian cancer cell lines but their origin and molecular characteristics are largely undescribed[439].

We described a new human high grade serous carcinoma (HGSC) cell line that represents the vast majority of ovarian carcinoma[73]. This tumor type is clinically aggressive, tumor relapse is frequent and most patients ultimately die due to the failure of current therapeutic regimes[73].

In this study, we presented the characteristics of immortalized cultured cells in two-dimensional (2D) monolayer culture and three-dimensional (3D) cell culture system, focusing on cell culture conditions, cell proliferation and the expression profile of biomarkers.

Material and Methods

Establishment of a primary cell line of ovarian carcinoma and culture conditions

In our study, 130 ovarian tumor samples and 30 ascitic fluid were collected and cultivated for primary cell culture. Tumor samples were diagnosed as serous (90), clear cell (3), endometrioid (33) and mucinous (4) ovarian carcinomas and ascites from patients with ovarian carcinoma (30).

A successful primary cell culture was established from the ascitic fluid obtained from a caucasian female patient diagnosed with ovarian carcinoma, at Instituto Português de Oncologia Francisco Gentil de Lisboa. The ascitic fluid was collected for therapeutic reasons and to cell culture, under patient's formal consent.

Clinical details were recorded and sample was assigned with a reference number to retain anonymity accordingly with the institutional approval for the research project, by our institutional Ethical Committee (UIC-772). This cell line was named IPO-SOC43.

Ascite-derived cells were isolated by centrifugation (1200 rpm, 2 minutes), and cells were stained with Giemsa for assessing the morphology of cells. Cells were also collected and suspended in culture medium, Dulbecco's Modified Eagle Medium (catalog no. 41965-039, Invitrogen™ Life Technologies), supplemented with 1% Antibiotic-Antimycotic (catalog no. 15240062, Invitrogen™ Life Technologies) and 10% FBS (catalog no. S0615, Invitrogen™ Life Technologies) and placed directly into culture with little manipulation at 37°C in an incubator with humidified atmosphere containing 5% CO_2. Adherent cells were observed after 48h and once cultures reach 80-90% confluency, cells were detached. At each passage, cells were washed with PBS, trypsinized with 0.05% trypsin-ethylenediamine-tetraacetic acid (EDTA) and maintained in culture. Cell counting of viable cells was performed using trypan blue exclusion method as described below. Immortalization occurred spontaneously after six months in continuous culture. The established cell line is maintained in culture in a 2D model for more than 100 passages. Cells, periodically, were collected and stored.

The ability of cells to survive and proliferate in low serum conditions was assessed by plating cells in T25 cm^2 flasks in DMEM supplemented with 1% FBS and cultured for 20 days. The medium was changed every three days. The experiments were performed in duplicate.

In summary, IPO-SOC43 was established from ascitic fluid of a patient diagnosed with HGSC (9 months after initial diagnosis) that was confirmed by histology.

Immunohistochemistry

Characterization of the tumor was performed on formalin fixed paraffin embedded tissue (FFPE) from the primary ovarian tumor and confirmed by immunohistochemistry with the standard technique. Briefly, 3µm sections were heated at 60°C for 60 minutes, deparaffinized in xylene and rehydrated in an ethanol decreasing gradient. Antigen retrieval was performed using boiling citrate buffer (0.01 M citric acid adjusted to pH 6.0) in a microwave for 10 min to retrieve antigens.

The sections were incubated with primary antibodies (see Table 6.1) for 60 min at room temperature, after washing, the incubation of secondary antibody Dako Real™, Envision™/HRP (ChemMate Envision Kit, K5007; DAKO, USA) was at room temperature for 30 min and were developed by Peroxidase/DAB. Sections were counterstained with Mayer's hematoxylin. Phosphate buffered saline was used as a negative control and selected tissues for each antibody were used as positive control.

Immunocytochemistry (ICC) and immunofluorescence

Antigen expression was searched in original ascitic fluid cells preserved in a cell block, in the established cell line and in the corresponding formalin-fixed paraffin embedded tumor, using the antibodies listed in Table 6.1.

IPO-SOC43 cells, in the exponential growth phase (2-3 days of growth) were removed from the surface of the flasks, cytospins prepared and the cell suspension, immediately fixed in ice-cold methanol at 4°C for 30 minutes and placed in polyethyleneglycol (PEG, P5402, Sigma-Aldrich) for 30 minutes and stored at room temperature (RT). Before ICC staining, PEG was removed by soaking in alcohol and incubated with several antibodies, indicated in Table 6.1. After incubation with primary antibody, slides were washed and then stained using Dako Real™, Envision™/HRP (ChemMate Envision Kit, K5007; DAKO, USA) at room temperature for 30 min and were developed by Peroxidase/DAB and counterstained with Mayer's hematoxylin and examined under a light microscope, Olympus Bx50F. Images were captured in Digital Microimaging Device (version 1.5, Leica Microsystems). Cytospin slides with no primary antibody were used as negative controls.

For immunofluorescence of the 2D cultures, permeabilization of cells was performed by incubation with 0.1% Triton X-100 for 10 min. Sections were blocked for 30 min with 0.2% FSG (fish skin gelatin). Appropriate amount of primary antibody was diluted in blocking solution and incubated for 2h at room temperature. Secondary antibody was diluted in 0.125% FSG and incubated for 1h at room temperature (Table 6.1). Sections were mounted with ProLong containing DAPI (Life Technologies). Samples were visualized using a fluorescence microscope (DMI6000 Leica Microsystems GmBH, Wetzlar, Germany).

For 3D cultures of IPO-SOC43 cells, aggregates in suspension were dehydrated using 30% sucrose solution overnight. The sucrose solution was removed and the samples were transferred in Tissue Teck OCT^{TM} (Sakura Finetek Europe B.V., Zoeterwoude, Netherlands) and stored at -80°C until cryosectioning in a cryostat (Cryostat I, Leica, Wetslar, Germany) to achieve sections of 10 µm thickness was performed. Immunofluorescence staining was then performed and visualized as indicated above for the 2D cultures.

Flow cytometry

Cells were collected to form a single cell suspension and washed in ice-cold phosphate buffered saline (PBS1X). Approximately, 1×10^6 cells were resuspended in 100 µl of ice cold PBS/BSA 0,1% (bovine serum albumin, Sigma) and primary antibodies, anti-pan cytokeratin-FITC (catalog no. ab52460, Abcam) and anti-human vimentin-APC (catalog no. IC2105A, R&D systems) were added and incubated for 60 minutes at 4°C in dark. At the end, cells labeled for the respective antigens were washed twice, centrifuged at 1200 rpm for 5 minutes, resuspended in 500 µl of PBS/BSA 0,1% and kept on ice until analysis. Appropriate controls have been used (unstained cells). Acquisition was performed in a FACScalibur (Becton Dickinson). Data were analyzed with FlowJo (http://flowjo.com/ version 1.44) software.

Table 6. 1 - **Antigens evaluated and antibodies used to characterize IPO-SOC43 cell line**

Antibody, clone, catalog number, source	Antigen	Function/location	Dilution	Positive control
Anti-Cytokeratin clone AE1/AE3, ISO53, Dako	cytokeratin type I and II	cytoskeleton intermediate filament	1:100	skin
Anti-β-catenin, sc-7199, Santa Cruz Biotechnology	β-catenin	transcription factor and E-cadherin interacting protein	1:1000	colon cancer
Anti-CA125 clone OC125, 325M, Cell Marque	mucin16 (MUC16) (Cancer antigen 125)	glycoprotein	1:150	ovarian cancer
Anti-cytokeratin clone Cam 5.2, 349205, BD Biosciences	cytokeratin type II	cytoskeleton	1:100	appendix
Anti-Calretinin clone DAK-Calret1, M7245, Dako	calretinin	calcium-binding protein	Predilute	mesothelioma
Anti-CK18 conjugated 488 F4772, Sigma-Aldrich	cytokeratin type I	cytoskeleton	1:100	appendix
Anti-Collagen IV Ab6586, Abcam	alpha 1 and 2 chains type IV collagen	basement membrane	1:10	appendix
Anti-E-cadherin 610181, BD Biosciences	E-cadherin	adherens junction protein	1:80	breast cancer
Anti-F-actin, 488 Phalloidin, Thermo Fisher	actin in the filamentous form	cytoskeleton	1:100	appendix
Anti-HNF1β HPA002083, Sigma-Aldrich	Hepatocyte nuclear factor 1β (HNF1β)	transcription factor	1:1000	kidney
Anti-Ki-67 ab16667, Abcam	nuclear protein in G1, S, M and G2 phase cell cycle	cell proliferation	1:150	tonsil
Anti-CINtec p16 clone E6H4, 725-4713 Ventana Medical System	p16INK4a protein	transcription factor cell cycle regulator	predilute	cervical cancer
Anti-p53 clone DO7, 453M, Cell Marque	p53	transcription factor cell cycle regulator	1:150	colon cancer
Anti-Vimentin clone 3B4, M7020, Dako and V6389, Sigma Aldrich	vimentin	Cytoskeleton, intermediate filament type III	1:150	appendix
Anti-WT1 clone 6F-H2, M3561, Dako	Wilm's tumor 1 factor	transcription factor	1:200	ovarian cancer

Proliferation curves

Cells obtained from 2D cultures were plated at a cell density of $1x10^4$ cells/well in a 12-well plate, in DMEM medium supplemented with 10% FBS and 1% antibiotic-antimycotic. Cell counting was determined by microscopy using the trypan blue exclusion method. Total number of viable cells was determined by counting the colorless cells in a Fuchs-Rosenthal hemocytometer chamber after incubation with a solution of 0,1%(v/v) of Trypan Blue dye (Gibco, Invitrogen Corporation, Paisley, UK) in PBS at regular time intervals (0 until 9 days). Each time point counting was performed

in triplicate and proliferation curves were plotted and doubling time was calculated according to the following formula:

$$\text{doubling time} = \frac{\text{duration}^* \log(2)}{\log(\text{final concentration}) - \log(\text{initial concentration})}$$

The crystal violet method was also used to determine the cell number. Cells were centrifuged for 5 min and then lysed using lysis solution (1% Triton X-100 in 0.1M citric acid), overnight at 37°C. Total cell number was determined after incubation with 0.1% (v/v) crystal violet in lysis solution. Nuclei density was assed using a Fuchs-Rosenthal hemocytometer and a microscope with phase contrast (DM IRB, Leica, Germany).

Wound healing assay

Cells were plated onto 12-well plates in DMEM medium supplemented of 10% FBS, and allowed to form a confluent monolayer. The cells were previously treated with 5µg/mL Mitomycin-C (Sigma), an antiproliferative agent, for 3 hours at 37°C in 5% CO_2. The monolayer was then scratched in a straight line with a pipette tip. Dethatched cells were removed by washing with PBS1X. Images of closure of the wound were captured at 0, 24, 48 and 72h after scratching.

Chromosomal Comparative genomic hybridization (cCGH)

Genomic DNA isolated from the ascitic fluid and derived cell line was done using DNA Purification Protocol for 1-2 Million Cells (Citogene® DNA isolation kit) according to manufacturer's protocol. cCGH technique was carried out according the method of the Kallioniemi et al.[440] adapted as previously described by Roque et al.[441].

For image analysis a Zeiss epifluorescence microscope linked to a Cytovision CGH software program (Cytovision version 7.4, Leica Biosystems, Richmond, USA) was used. For both ascitic cells DNA and derived cell line DNA, at least, 15 metaphases were acquired for the establishment of the cCGH profile. The green (test DNA) to red (reference DNA) fluorescence ratio along the length of the chromosomes was calculated. This high resolution cCGH version uses dynamic standard reference intervals based in the systematic variation seen in normal samples. When the dynamic standard reference intervals do not overlap the confidence limits, the software interprets as either a loss (red) or a gain (green) in the test DNA. Heterochromatic

regions in chromosomes 1, 9, 16 and Y, and the p arms of the acrocentric chromosomes were discarded from the analysis.

Polymerase chain reaction, Sanger sequencing and conformation sensitive capillary electrophoresis (CSCE)

The mutational status of TP53, BRCA1 and BRCA2 was evaluated as follow: genomic DNA was extracted using DNA Purification Protocol for 1-2 Million Cells (Citogene®DNA isolation kit) from cell line, according to manufacturer's protocol. Mutational analysis of *TP53* mutation was determinate by polymerase chain reaction (PCR) amplified products encompassing from exons 4, 5, 6, 7, 8 and 9 (Table 6.2) of the *TP53* gene (which arbor mutational hotspots).

The amplified PCR products were analyzed by electrophoresis, on a 2% (w/v) SEA KEM ® GTG ® agarose (50074, FMC BioProducts) gel (in TBE buffer 1x, diluted from TBE buffer 10 x, EC-860, National diagnostics) labelled with 0.05% (v/v) ethidium bromide 10 mg/ml (15585-011, Invitrogen), under UV (BioDocAnalyse Transilluminator, Biometra). DNA fragments with expected size were purified using Exonuclease I (20 U/µL) (catalog no. EN0582, ThermoFisher)/FastAP Thermo sensitive Alkaline Phosphatase (1 U/µL) (EF0651, ThermoFisher), according to the manufacturer's protocol. After purifying the DNA fragments were sequenced by automated sequencing.

Automated sequencing reacting products were purified with Illustra AutoSeq G-50 GFX (27-5340-03, GE Healthcare) according to manufacturer´s. Sequencing reaction was carried out in a T3000 thermocycler (Biometra), purified with AutoSeq G-50 dye terminator removal kit (27-5340-02, GE Healthcare Life Sciences), according to manufacturer's instructions and analyzed in an ABI Prism™ 3130 Genetic Analyzer (Applied Biosystems).

BRCA1 and *BRCA2* mutations were screened by CSCE (conformation sensitive capillary electrophoresis). This method is based on the principle that homoduplex and heteroduplex DNA have different mobility's when subjected to electrophoresis. All samples with an aberrant mobility were sequenced using BigDye Terminator cycle

sequencing kit v1.1 and DNA sequencing reactions were carried out on ABI Prism™ 3130 Genetic Analyzer (Applied Biosystems).

BRCA1 and *BRCA2* large rearrangements were determined by Multiplex Ligation-dependent Probe Amplification (MLPA) assay according to manufacturer's protocol. Amplification products were analyzed ABI Prism™ 3130 Genetic Analyzer (Applied Biosystems) using the GeneMapper software (Applied Biosystems) and data analysis was performed using Coffalyser software (MRC-Holland).

Table 6. 2 - **Primers for PCR of the *TP53* gene (Exons 4-9)**

Exon	Primer	Oligonucleotide sequence
4	forward	gacctggtcctctgactgct
4	reverse	caggcattgaagtctcatgg
5	forward	cgtgttccagttgctttatctg
5	reverse	gccagacctaagagcaatcagt
6	forward	ctcagatagcgatggtgagcag
6	reverse	cttaacccctcctcccagagac
7	forward	cctcatcttgggcctgtgtta
7	reverse	tggaagaaatcggtaagaggtg
8-9	forward	ccttactgcctcttgcttctc
8-9	reverse	cattttgagtgttagactggaaactt

Generation of 3D tumor cell spheroids in stirred-tank culture systems

Single cell suspensions of IPO-SOC43 cells (0.2 x 10^6 cell/mL) were inoculated in 125 mL of culture media in stirred-tank vessels with flat centered cap and angled side arms (Corning® Life Sciences) and cultured on a magnetic stirrer in an incubator at 37°C with humidified atmosphere containing 5% CO_2. Stirring rates of either 40 rpm or 60 rpm were tested. The culture media was the same used in the 2D cultures or supplemented with 10 µM of ROCK (Rho-associated coiled coil forming protein) inhibitor (highly potent, cell-permeable, and selective for ROCK I and II). Cultures were maintained for, at least, 72 hours.

Cell membrane integrity assay

Cell viability was evaluated using fluorescein diacetate (FDA; Sigma–Aldrich, Steinheim, Germany), an intracellular esterase substrate, at 10 µg/mL in PBS to label live cells, and TO-PRO-3 iodide (Invitrogen) at 1 µM in PBS to identify dead cells. Cultures were incubated for 5 min at RT with the fluorescent probes and then analyzed using a fluorescence microscope (DMI6000 Leica Microsystems GmBH, Wetzlar, Germany).

Spheroid morphometry

Aggregates were imaged in a fluorescence microscope (DMI6000, Leica Microsystems GmbH, Wetzlar, Germany). Ferret Diameter and the area of the aggregates were determined adjusting the threshold and applying the respective algorithm of FIJI open source software (Rasband, WS, ImageJ, U. S. National Institutes of Health, Bethesda, MD, USA, http://imagej.nih.gov/ij/, 1997–2012). In order to classify spheroid shape 'Shape Parameters' function of FIJI was used. The "solidity" function can be used as a measure of roughness of the spheroid surface and provides information about the regularity of the aggregate. A spheroid was considered as regular for solidity values higher than 0.9 on a scale from 0 to 1[442].

PicoGreen Assay

Total cell quantification of DNA was assessed in samples collected from 3D cultures and washed once with PBS. The pellet was resuspended in milliQ water, frozen in liquid N_2 and stored at -80°C until analysis. DsDNA quantification using Quant-iT™ PicoGreen® dsDNA Assay Kit (Life Technologies) was performed according to manufacturer's protocol. Briefly, samples were thawed and subsequently sonicated for 30 min. Appropriate dilutions of samples and dsDNA standard were prepared in Tris-EDTA buffer. Addition of Quant-iT™ PicoGreen® and incubation for 5 min was followed measurement of fluorescence (excitation 480 nm; emission 520 nm; Infinite 200 Pro NanoQuant, Life Science).

Results

Establishment of a primary culture

A successful primary cell culture was established from the ascitic fluid obtained from a caucasian female patient with 73 years old, diagnosed with ovarian high grade serous carcinoma, stage IIB (FIGO) with irressectable disease accordingly to imaging studies at Instituto Português de Oncologia Francisco Gentil de Lisboa. The patient underwent neoadjuvant standard chemotherapy (3 cycles), followed by surgery and was submitted to 3 more cycles. In the follow-up, 3 months after finishing chemotherapy, ascitic fluid was collected for therapeutic reasons and for cell culture, under patient's formal consent. The ascitic fluid was observed in cytospins and cell morphology assessed by Giemsa staining (Figure 6.1). Many cellular types were observed but malignant epithelial cells were predominant. These cells were present in large cell aggregates or isolated cells surrounded by inflammatory and mesothelial cells. Malignant cells expressed anti-cytokeratin type I and II (clone AE1/AE3) and CA125; vimentin was seldom positive in few malignant cells.

Establishment of the histological type of ovarian carcinoma

Residual tumor found in the ovary allowed the confirmation of the histotype as HGSC. Tumors cells aggregates show epithelial marker (cytokeratin), recognized by the antibody Cam 5.2. Mucin 16 (MUC16) recognized by anti-cancer antigen 125 (CA125) was observed in tumor cells (apical cell membrane). The cells showed strong nuclear staining for p53 and p16 protein and tumor cells aggregates were negative for WT1 and vimentin (VIM). Some tumor cells exhibit expression for calretinin (CALRET). Tumor tissue was negative for anti-HNF1β (Figure 6.2).

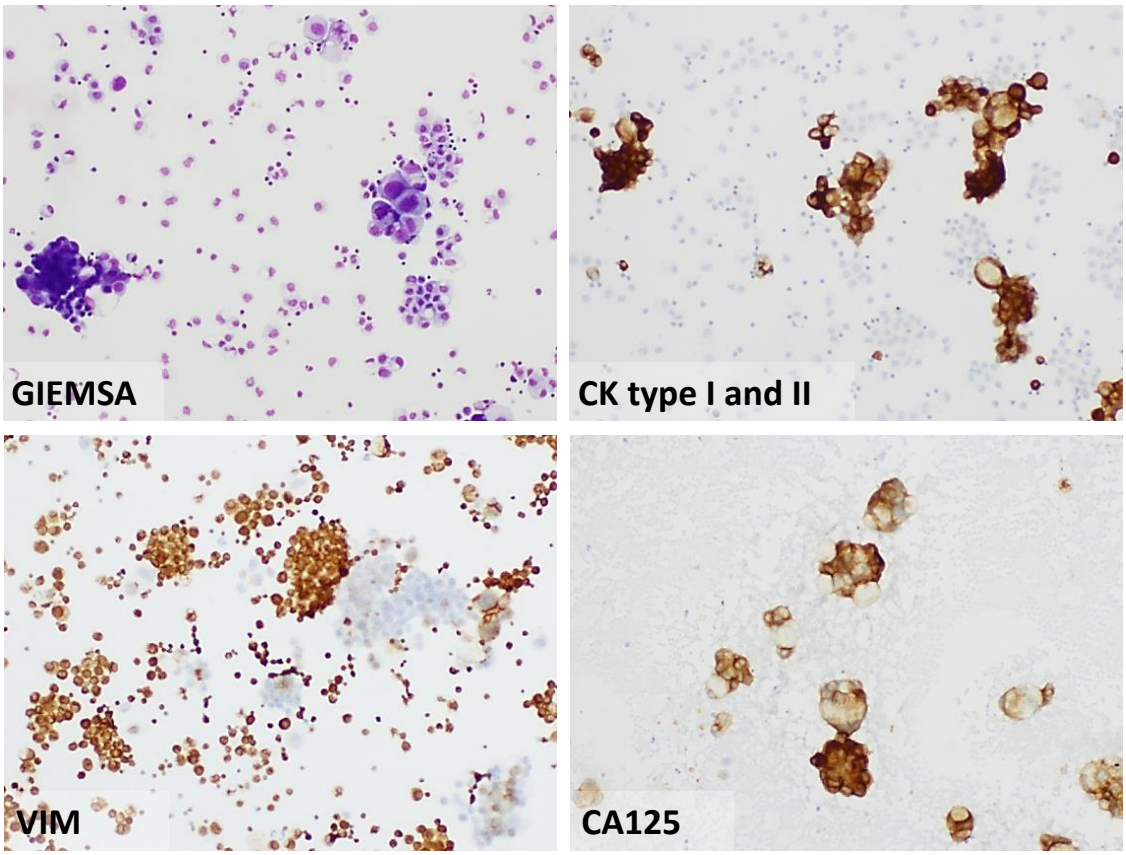

Figure 6. 1 – **Morphological characterization of cells from ascitic fluid**
Cells were collected by cytospins. Smears of cells stained with Giemsa show aggregates and isolated cells with irregular size, abundant cytoplasm and large nuclei, confirming the presence of malignant cells; Immunocytochemical characterization of cells was done using cytokeratin (CK) AE1/AE3 (neoplastic cells are positive); Vimentin (neoplastic cells are predominately negative, macrophages and mesothelial cells were positive) and CA125 (neoplastic cells were positive), 100x.

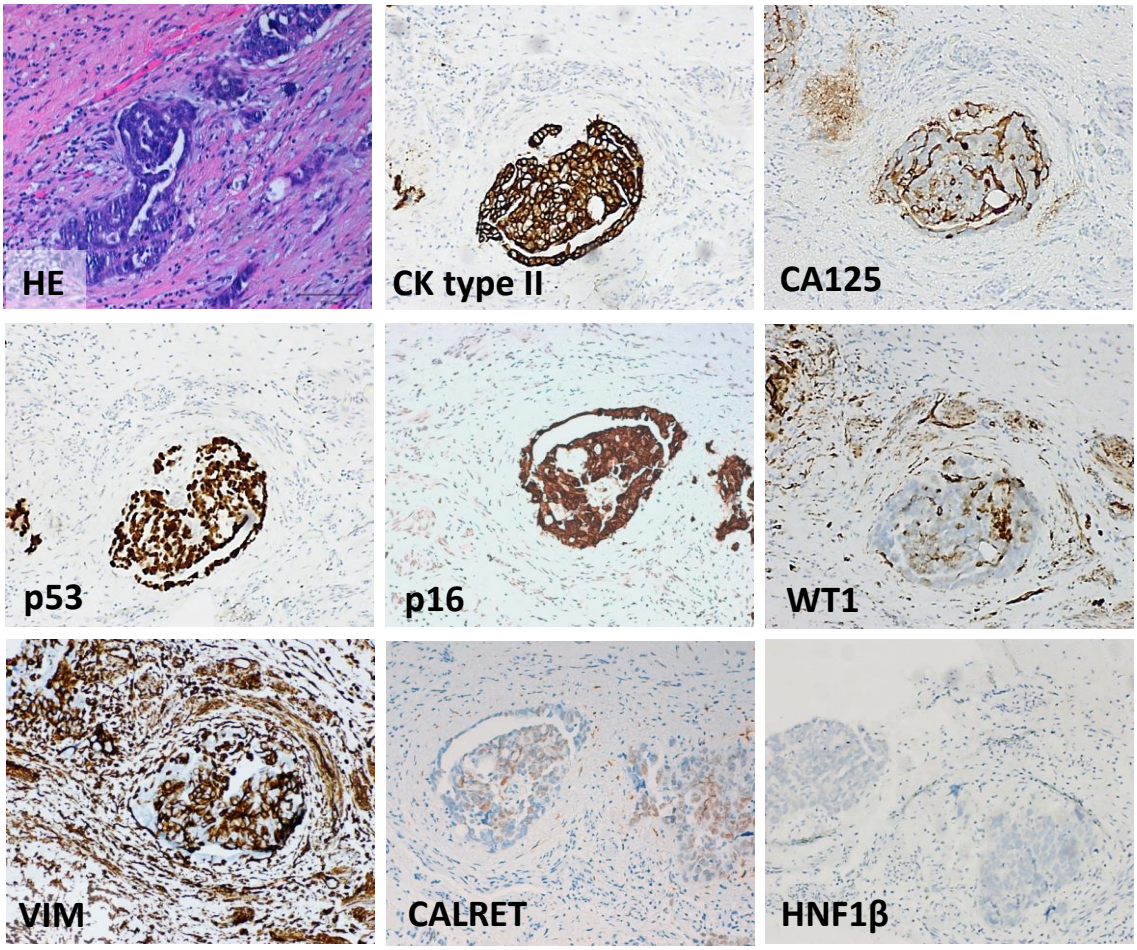

Figure 6. 2 - **Characterization of the primary ovarian carcinoma of the patient from whose ascitic fluid IPO-SOC43 was established**
Formalin fixed paraffin-embedded sections of patient tumor ovarian high grade serous carcinoma submitted to surgery and neoadjuvant chemotherapy (after 3rd cycle) stained with hematoxylin and eosin (H&E) and immunohistochemical staining. Tumor cells show positive expression of epithelial marker Cam 5.2 (CK type II). Apical cell membrane staining for CA125 in tumor cells. Cells exhibited nuclear positive expression for p53, p16 and WT1. Tumor cells were negative with vimentin (VIM), calretinin (CALRET) and HNF1β, 100x.

Expression of cell markers in IPO-SOC43 cell line

After spontaneous immortalization, cell line was characterized by a panel of markers in order to confirm its nature by flow cytometry and immunohistochemistry. Cytokeratin (epithelial cell marker) and vimentin (mesenchymal cell marker) expression were evaluated. The epithelial origin of the cell line, IPO-SOC43 was confirmed by flow cytometry, showing a high expression for cytokeratin (85% of cells) and low expression of vimentin (Figure 6.3).

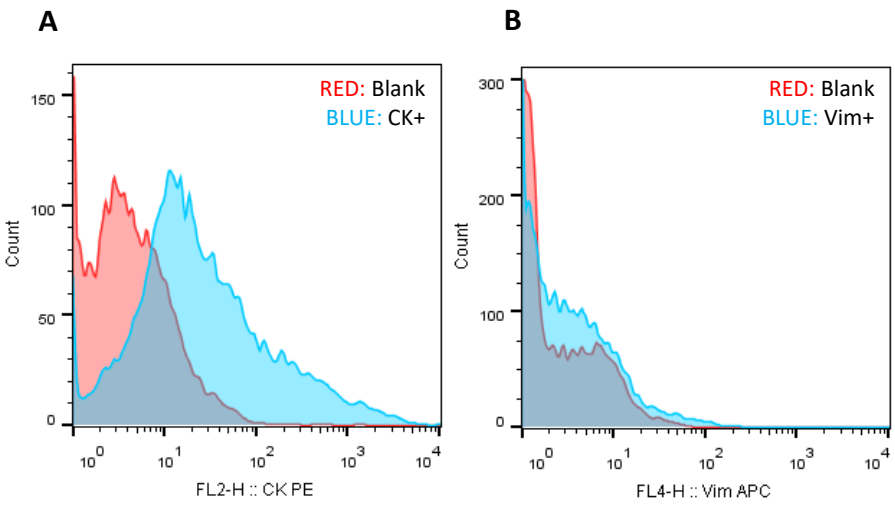

Figure 6. 3 - **Detection of cytokeratins and vimentin in IPO-SOC43 cell line by flow cytometry** Cells were positive to, **A.** anti-pan cytokeratin-FITC, and negative to **B.** anti-human vimentin-APC.

The epithelial nature of IPO-SOC43 cells was also confirmed by immunocytochemical analysis through positive expression of anti-cytokeratins type I and II (clone Cam 5.2 and AE1/AE3). Cells also show positive expression for vimentin and calretinin (Figure 6.4).

Expression of biological markers relevant in ovarian cancer

To further characterize this cell line we evaluated other biological markers such as the expression of cell cycle regulators and cell surface receptors relevant in ovarian carcinogenesis.

We observed that the majority of cells exhibit nuclear staining for p53, nuclear and cytoplasmic staining for $p16^{INK4a}$ protein, a cyclin-dependent kinase-4 (CDK4) inhibitor that is expressed in a limited range of normal tissues and tumors such as HGSC[443]. Cells exhibited nuclear expression of the Wilm's tumor 1 (WT1) protein and anti-cancer antigen 125 (Figure 6.4). The IPO-SOC43 cells were negative for HNF1β (data not showed in Figure 6.4).

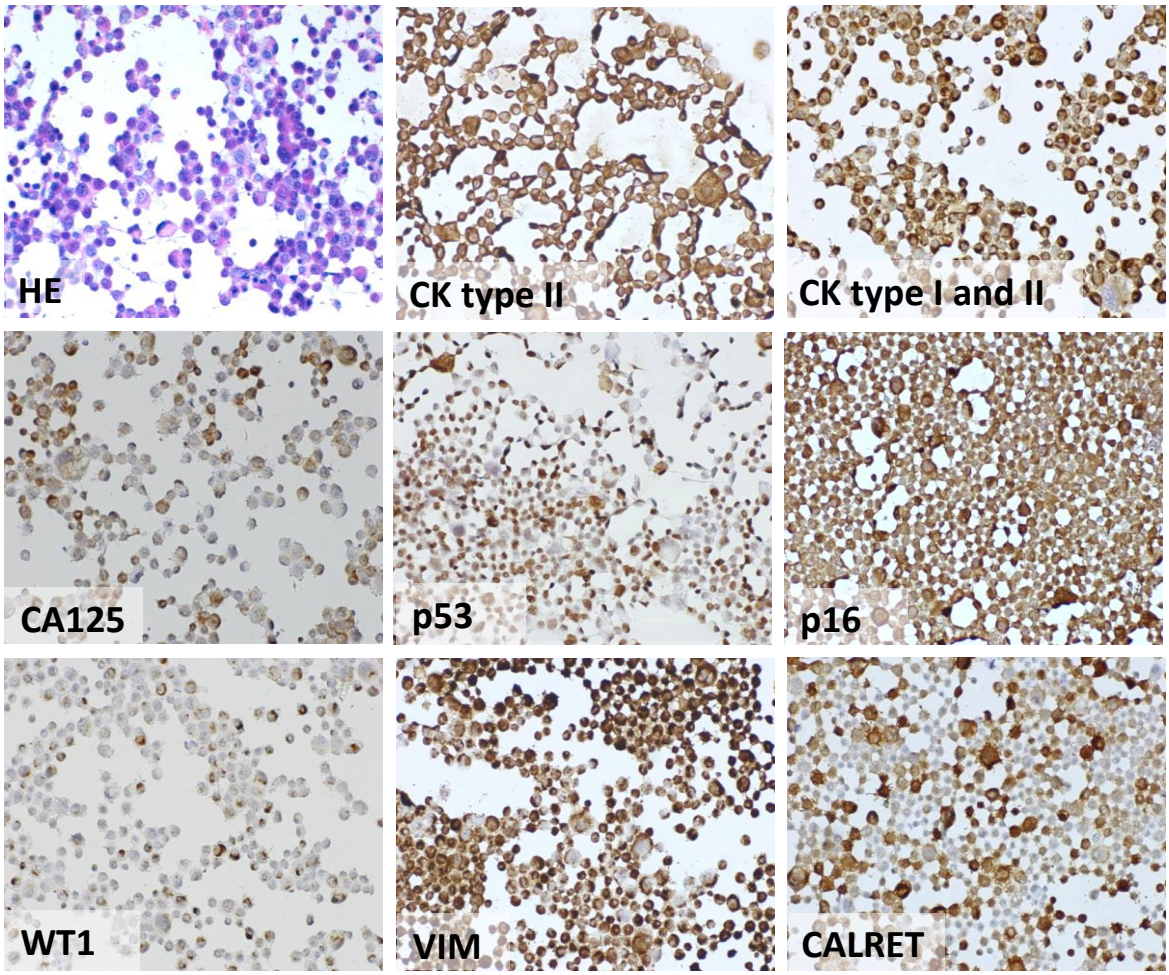

Figure 6. 4 - **Ovarian biomarkers in IPO-SOC43 cell line**
Cells were collected, prepared in cytospins and stained with hematoxylin and eosin (H&E) and several biomarkers were tested; cells show positive reaction with anti-cytokeratins (CK) type II (clone Cam 5.2) and type I and II (clone AE1/AE3). Cells exhibited protein expression for CA125, p53 and p16. Cells were negative for WT1, and some exhibited positive expression for vimentin (VIM) and calretinin (CALRET), 100x.

Other biological markers were also analyzed by immunofluorescence regarding cell-cell adhesion, cellular signaling, cell cycle status and tumor-stromal interactions as recreation of the tumor microenvironment is essential in cancer-related studies. We used immunofluorescence staining for cytokeratin 18, collagen IV, F-Actin, β-catenin, E-cadherin and Ki-67 (Figure 6.5).

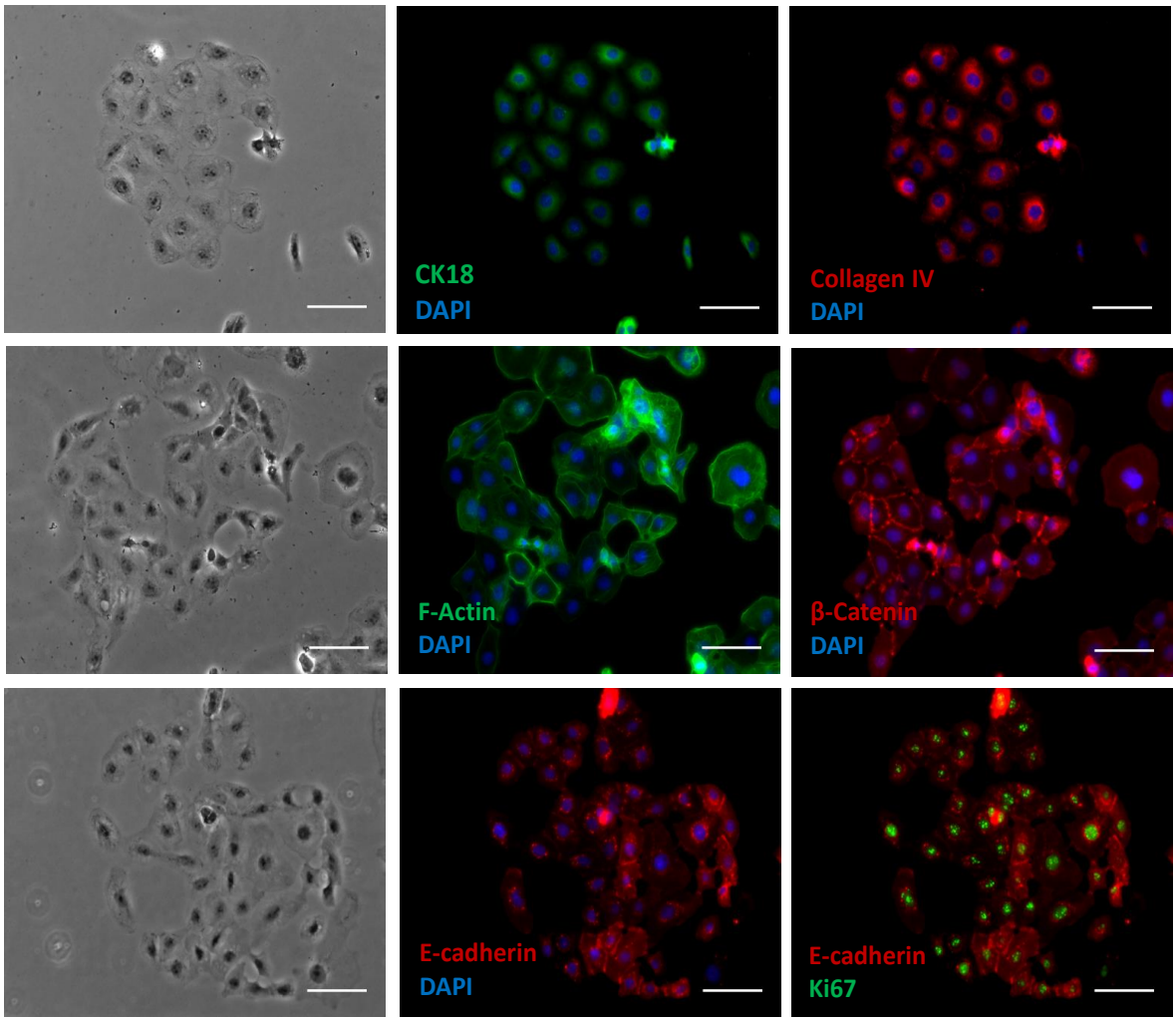

Figure 6. 5 - **Expression of biological markers in 2D cell culturing models in IPO-SOC43 cell line**
Cells exhibited positive expression for CK18, collagen IV, F-Actin, β-catenin, E-cadherin and Ki-67, 400x.

Cells showed positive expression for CK18, F-actin and collagen IV, a basement membrane component was detected in cytoplasm. Positive expression was observed for adherens junction protein E-cadherin and its partner β-catenin in cell membrane. Proliferation was evaluated by Ki-67 nuclear expression that was high, with more than 70% of cells exhibiting nuclear expression.

2D characterization of IPO-SOC43 cell line

The cells were able to adhere to the flask surface forming cell aggregates with polymorphic appearance. At first, cells had irregular size and shape, were vacuolated and had a very slow proliferation rate. However, after a low proliferation period of 2

months, outgrowths developed and a monolayer of epithelial cells with a pavement-like arrangement was established (Figure 6.6). At this time, cells were polygonal in shape and showed atypical nuclear features such as clusters of chromatin, thickened and convoluted nuclear membrane, and large nucleoli. Some multinucleated giant cells were also seen in cell culture.

These cells are growing without interruption for more than 40 months and with more than 100 serial passages, exhibiting a continuous, permanent and stable proliferation rate. This cell line can be maintained in DMEM only with 1% of FBS (Figure 6.6A).

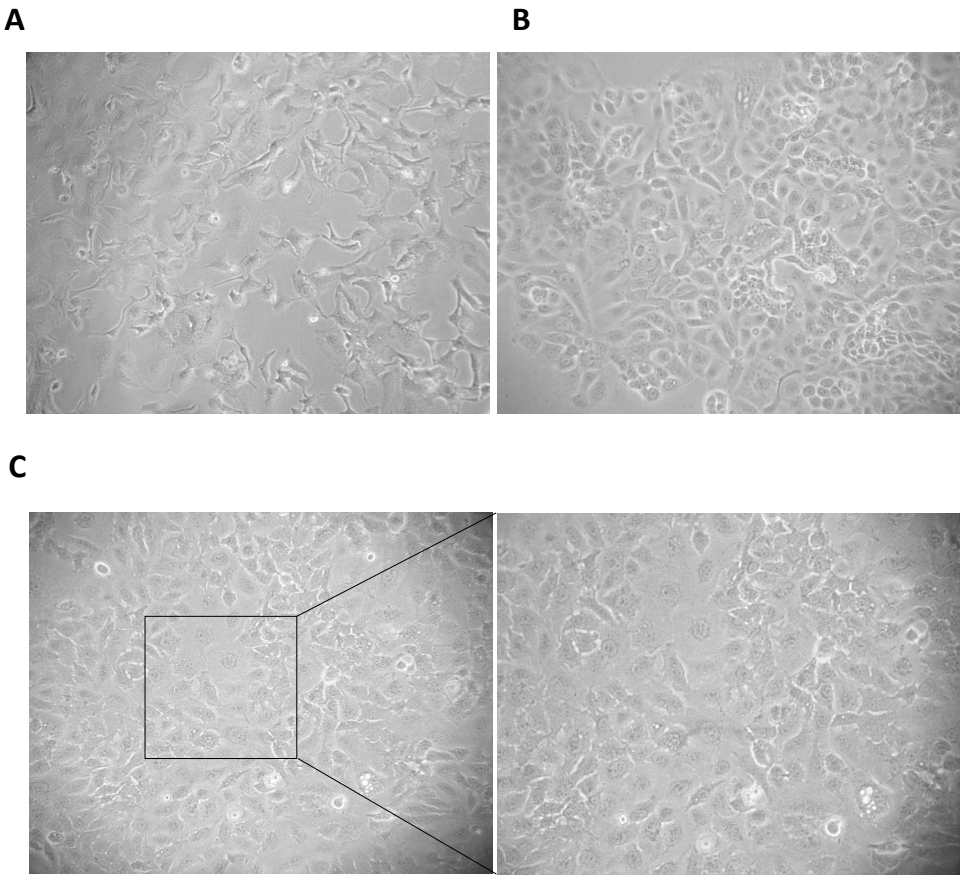

Figure 6. 6 - **Characterization of IPO-SOC43 cell line in 2D model**
The cell line presents cobblestone morphology or a pavement-like arrangement characteristic of epithelial cells in a confluent monolayer (cells with polygonal shape). **A.** Representative morphology of IPO-SOC43 cells in DMEM culture medium with 1% FBS, phase contrast microscopy, 100x. **B.** Representative morphological appearance of IPO-SOC43 cell line at passage 40, phase contrast microscopy, 100x; **C.** Representative morphology of IPO-SOC43 cells at passage 80, phase contrast microscopy, 100x and 200x.

Proliferation rate of IPO-SOC43 cell line

The proliferative characteristics of the cell line were assessed (Figure 6.7) and the cell line exhibited a slow proliferation rate and a doubling time (37,3 hours) with a proliferation rate of 1,86% in the initial 72 hours (3 days). Continuous growth (more than 100 passages), led us to believe that IPO-SOC43 cell line behaves as an immortalized cell line.

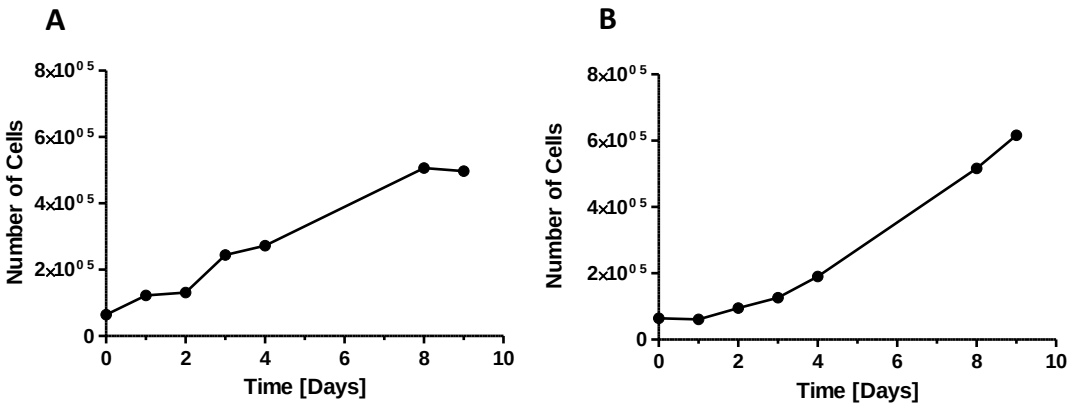

Figure 6. 7 - **Proliferation curve of IPO-SOC43 cell line**
A. Cell counting was determined by microscopy using the trypan blue exclusion method, and in **B.** nuclei counting was determined by crystal violet staining, at regular time intervals (1 to 9 days).

Migration properties of IPO-SOC43 cell line

The wound healing assay is a simple and reproducible method of measuring cell migration[444]. Scratch assays showed that the cell line have a low migration ability, taking 72h to close the wound area (Figure 6.8).

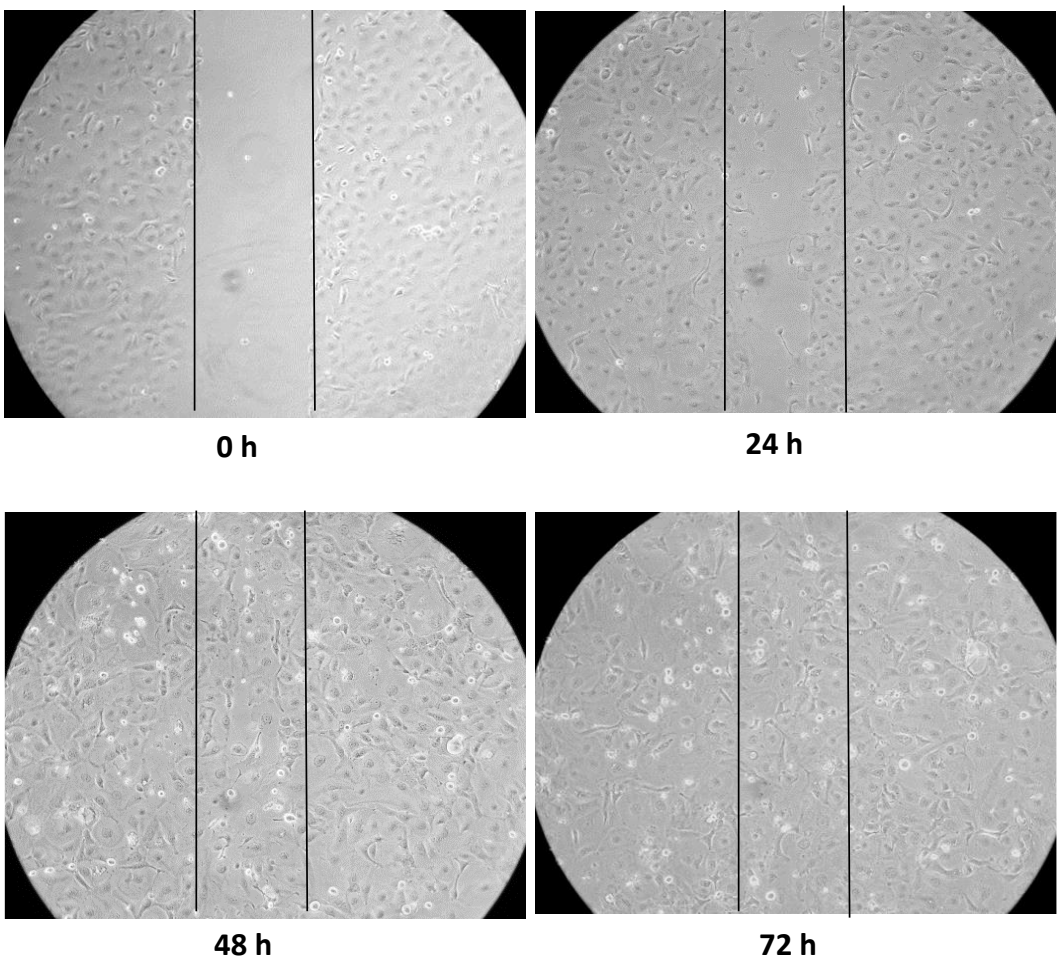

Figure 6. 8 - **Wound healing assay to determine the migration rate of IPO-SOC43.**
Representative images of wound-healing assays performed in IPO-SOC43 cell. Cells were plated onto a 12 well dish and treated with mitomycin-C. Wounds were generated and cells migrate filling the wound after 72h. Pictures were taken at 0 h, 24h, 48h and 72h after the scratch was performed (bright field microscopy), 100x.

Clonal selection was observed in IPO-SOC43 cells by cCGH

For the establishment of the genomic profile by cCGH analysis was performed in the DNA extracted from the original ascitic fluid cells and subsequently in the corresponding cell line, at passage twenty (p20, Figure 6.9B) and forty-two (p42, Figure 6.9C) after its initial establishment. We also tried to perform cCGH analysis with DNA extracted from paraffin sections of the primary tumor but the quality of the DNA was insufficient.

cCGH profiles showed gain and losses of chromosome regions as shown in Figure 6.9 and chromosome alterations are described in Table 6.3.

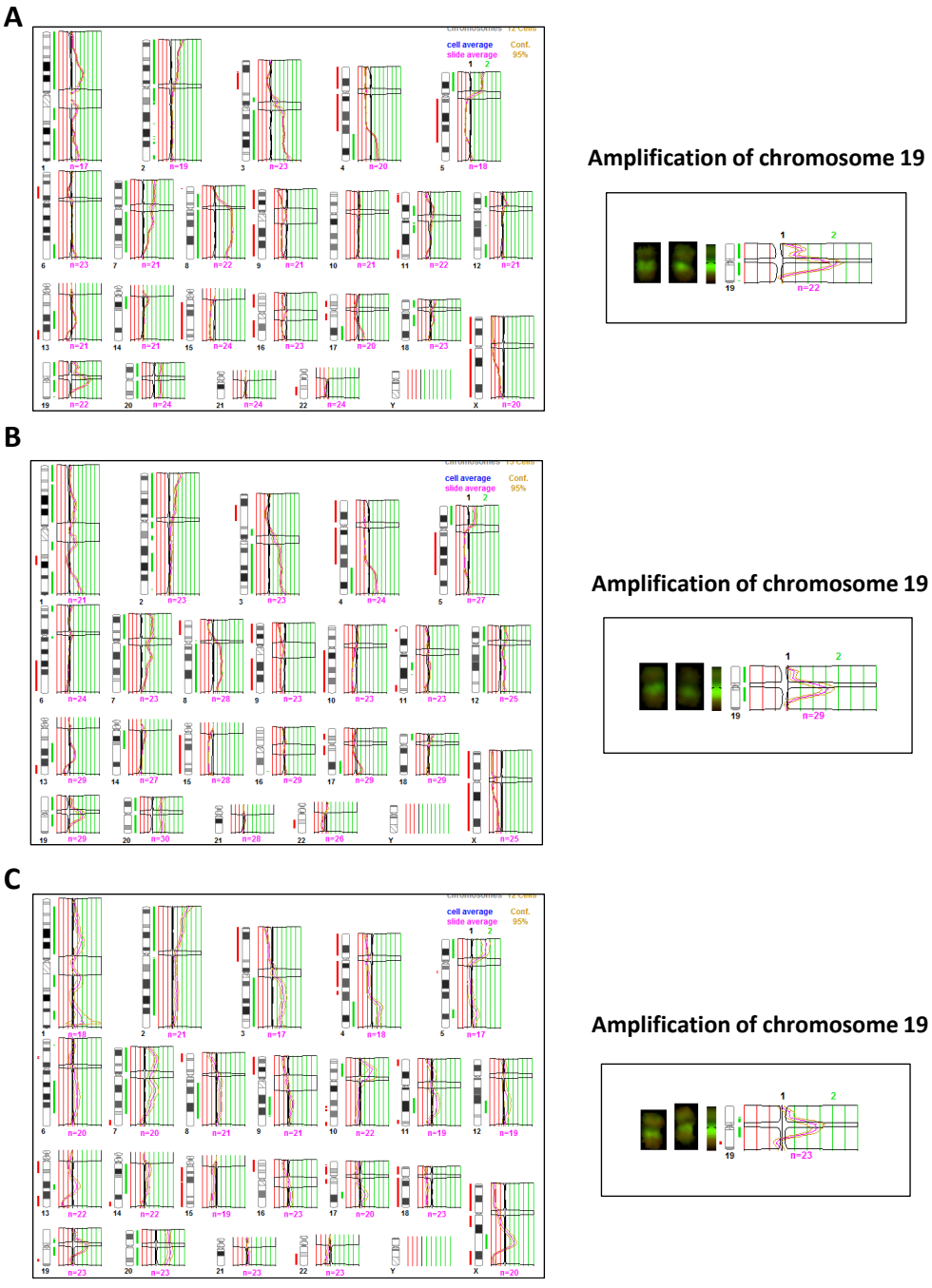

Figure 6. 9 - **cCGH profiles of cells from ascitic fluid and IPO-SOC43 cell line**
A. Cells from ascitic fluid; **B.** IPO-SOC43 cell line p20; **C.** and p42; Red lines indicate loss and green lines indicate gain of chromosomal regions.

As shown in Table 6.3 and Figure 6.9, tumor cells from ascitic fluid showed a complex genomic profile by cCGH with several gains, including amplifications, and losses of chromosome regions. The cell line cCGH profile was quite similar exhibiting most of the alterations present in the original ascetic fluid but also showing some *de novo* alterations.

Table 6. 3 - **Description of cCGH chromosome alterations in IPO-SOC43 cell line**

	Gain of entire chromosomes/partial gains of chromosome regions	**Loss of entire chromosomes/partial losses of chromosome regions**
Cells from ascitic fluid	20/ 1p34.3-q23, 1q31-q32.1, 1q32.3-q44, p25-p11.2, 3p12-q29, 4q28.q35, 5p15.3-p13, 7p22-q34, 8p21-q24.3 with amplification 8q11.2-q23, 11p14-p11.2, 12p12-p11.2, 13q21-q31, 14q11.2-q13, 17q24-q25, 18p11.3-p11.2, 18q12, 19p13.3-q13.2 with amplification 19q12-q13.1	9, 15, 16, X/ 3p24-p14, 4p16-q28, 5q11.2-q31, 6p22-p12, 11p15, 11q22-q25, 13q32-q34, 17p13-q21, 18q21.3-q23, 19q13.3-q13.4, 22q11.2-q13.
Cells passage twenty (p20)	7, 12, 20/ 1p36.3-q23, 1q32-q44, 2p25-q13, 2q21.1, 2q24-q32, 3p12-q29, 4q28.q35, 5p15.3, 8q11.2-q24.3, 11q13-q14, 13q21-q31, 14q11.2-q21, 17q22-q25, 18p11.3, 19p13.3-q13.2 with amplification of 19q13.1.	9, 15, X/ 1q25-q31, 3p23-p21, 4p16-q27, 5q11.2-q31.1, 6q21-q26, 8p23-p12, 10q11.2-q26, 11q23.3-q25, 13q32-q34, 17p12-q21.3, 22q12-q13.
Cells passage forty-two (p42)	20/ 1p36.1-p31, 1q22-q23, 1q41-q42, 2p25-p21, 3q13.1-q29, 4q28.q35, 5p15.3-p13, 5q32, 7p22-q31, 9q22-q31, 10p13-p12, 14q11.2-q13, 17q22, 19p13.1-q13.1 with amplification of 19q13.1, Xq21.3-q25	15, 18/ 1q31.1, 3p26-p13, 4p16-q27, 5q11.2-q22, 6p21.3-p12, 7q35-q36, 8p23-p12, 9p24-p13, 17p13-q21.1, 19q13.3, 22q12-q13, Xp22.3-q21.3, Xq25-q28

The cells from the ascetic fluid present alterations in TP53 gene, namely deletion of the region where TP53 gene is located, verified by cCGH (Figure 6.9).

Other alterations, also frequently found in ovarian cancer and also reported in TGCA[31], such as 1p36.3, 8q11.2 and 14q11.2 were observed in IPO-SOC43 cell line. The acquisition of changes not seen in the in the original ascitic fluid cells, possibly led to its spontaneous immortalization.

cCGH analysis of the cells from passage twenty showed gains of chromosome 7, 12 and 20 and partial gains on several chromosomes as reported in Table 6.3. The IPO-SOC43 cell line presented a total loss of chromosomes 9, 15 and X.

We also found that 19q 13.1 was amplified, this feature is maintained throughout all cell line passages and was reported in other studies[445,446].

In the passage 42, IPO-SOC43 showed gain of chromosome 20 and partial gains of 1p36.1-p31, 1q22-q23, 1q41-q42, 2p25-p21, 3q13.1-q29, 4q28.q35, 5p15.3-p13, 5q32, 7p22-q31, 9q22-q31, 10p13-p12, 14q11.2-q13, 17q22, 19p13.1-q13.1, Xq21.3-q25 and again amplification of 19q13.1 (Figure 6.9). Loss of chromosome 15 and 18 was observed, at this passage, and the cell line also maintained partial losses of some chromosome regions. cCGH analysis revealed that IPO-SOC43 cells at passage 42 contained more genetic changes than the original tumor cells from ascitic fluid, however these data are consistent with the acquisition of genetic change with cell line passage and clonal evolution.

Mutational status of *TP53*, *BRCA1* and *BRCA2* of IPO-SOC43 cell line

In order to further characterize the cell line, mutation analyses of *TP53* and *BRCA1* and BRCA*2* were performed. As mentioned above, IPO-SOC43 cell line has the deletion of the region where TP53 is located in the short arm of chromosome 17, detected by cCGH and indicating the loss of one allele (Figure 6.9). By automate Sanger sequencing a missense mutation in exon 5, codon 172 (p.V172F; GTT>TTT, c.514G>T) was detected in the other allele, with the substitution of Valin (Val) to phenylalanine (Phe), also identified in the hemizygotic histogram in Figure 6.10. This c.514G>T mutation in TP53 is associated with an advantage for tumor growth in a variety of neoplasms and it might have an pathophysiological effect, as reported in V80 COSMIC database (http://cancer.sanger.ac.uk/cosmic/mutation)[447–452]. Thus IPO-SOC43 cells do not have wild type p53 protein.

The *TP53* mutation status of IPO-SOC43 is consistent with IHC results, showing intense nuclear positivity for p53 protein, corresponding to aberrant expression mainly due to stabilization of the protein and a longer half-life[453].

Analysis of mutations in *BRCA1* and *BRCA2* genes was performed by CSCE. No mutation or polymorphism was identified in the *BRCA1* gene. Regarding *BRCA2* gene, three polymorphisms with no recognized clinical significance were identified: 5'UTR 1-26 G/A; p.N372H and p.V1269V.

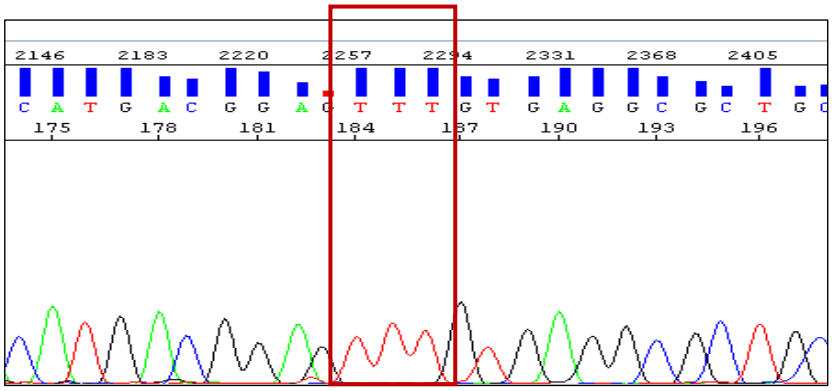

Figure 6. 10 - **Sanger sequencing histogram of TP53 exon 5**
IPO-SOC43 cell line has a mutation in codon 172 (p.V172F;GTT>TTT) on exon 5 in hemizygosity since the cell line has the loss of the short arm of chromosome 17 in one allele, resulting in substitution of Valin (Val) to phenylalanine (phe) (IARC TP53 mutation database).

Establishment and characteristics of 3D cell culture

3D cell cultures of IPO-SOC43 cells were established in stirred-tank culture systems. Two approaches were pursued to induce cell aggregation and compaction of cell aggregates: with and without ROCK inhibitor supplementation. We observed that IPO-SOC43 cells in 3D are heterogeneous and when cultured without ROCK inhibitor arranged in aggregates with irregular shape (grape-like shape, Figure 6.11). Addition of ROCK inhibitor improved cell aggregation reversibly as, when it was removed aggregates reacquired their original organization. On the other hand, cells with ROCK inhibitor maintained the conformation in aggregates (Figure 6.11); and after 72h of culture the levels of cell death were lower in aggregates with ROCK inhibitor than without it (Figure 6.11).

Culture progression was evaluated by measuring the area of the tumor aggregates. Cell aggregates had an average area of approximately 2761 ± 1986 μm^2 at day 1 of culture and 2970 ± 2401 μm^2 at day 3 (Figure 6.12A). We also assessed the cell concentration, by quantification of DNA and, after day 3, cell concentration decreased in 3D cultures (Figure 6.12B).

These results show that IPO-SOC43 cells are suitable to establish 3D cultures and to generate cell spheroids.

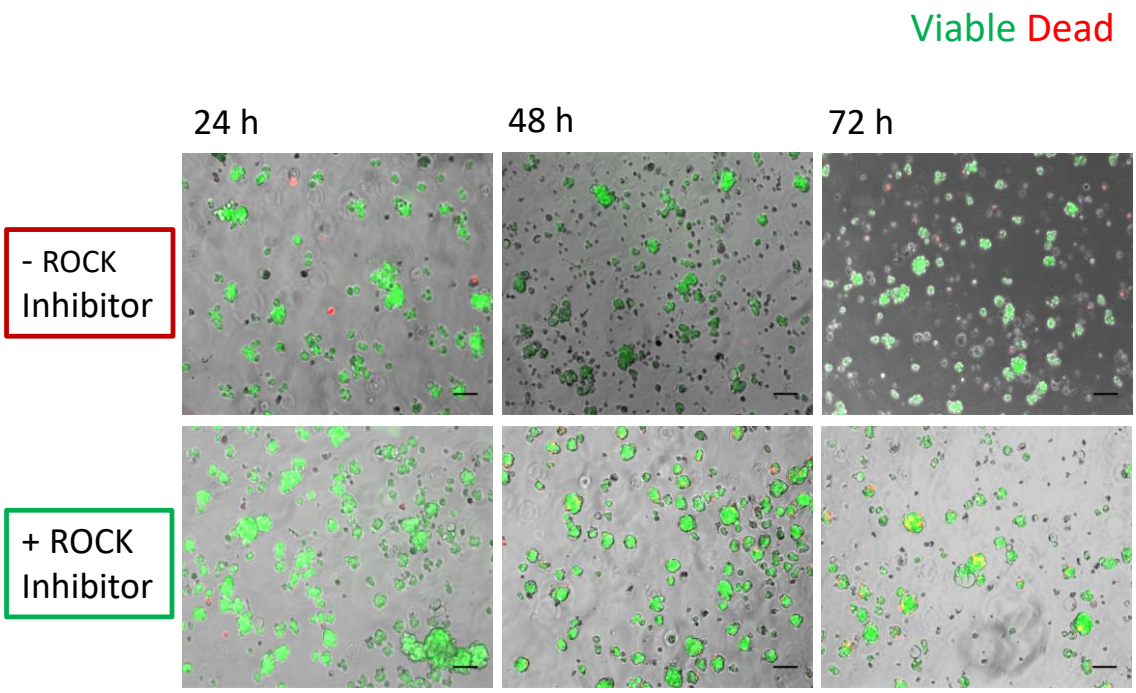

Figure 6. 11 - **Aggregation of IPO-SOC43 with and without ROCK Inhibitor in 3D culture system**
Aggregates in suspension were cultured on a magnetic stirrer (40 rpm) and supplemented with and without ROCK Inhibitor, during several time points. Aggregates with ROCK Inhibitor improves aggregation and after 72 hours most aggregated cells are still viable, scale bar 100 µm.

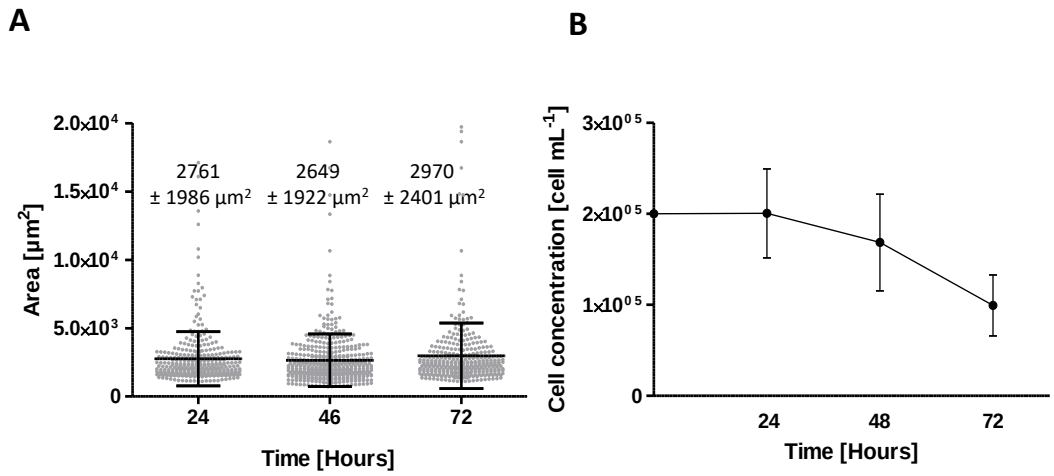

Figure 6. 12 - **3D Culture progression with measurement of aggregates area and growth curve of IPO-SOC43 cells with ROCK Inhibitor**
A. IPO-SOC43 aggregates area and **B.** growth curve, determined by PicoGreen analysis. Values are mean±SD. Area increased with culture time, but growth tends to be lower.

Regarding the imunoprofile of IPO-SOC43 cultured in 3D, cells express a similar profile as in 2D cell culture (Figure 6.13). Cells are positive for anti-cytokeratin type II (clone Cam 5.2), and CA125. Cells exhibit positive expression with p53 and are negative for WT1 as in 2D model and some cells express vimentin. IPO-SOC43 in 3D culture maintains the same biological markers (Figure 6.14) as cultured in 2D (Figure 6.5).

In 3D configuration, IPO-SOC43 cells exhibited loose aggregates. Cells continue to produce cytokeratin 18 and collagen IV. Cells exhibited β-catenin, mainly in the cytoplasm, and fewer cells exhibited positive expression for E-cadherin, with a more peripheral distribution in cell aggregates. Proliferation activity is maintained has seen by Ki67 positive staining (Figure 6.14).

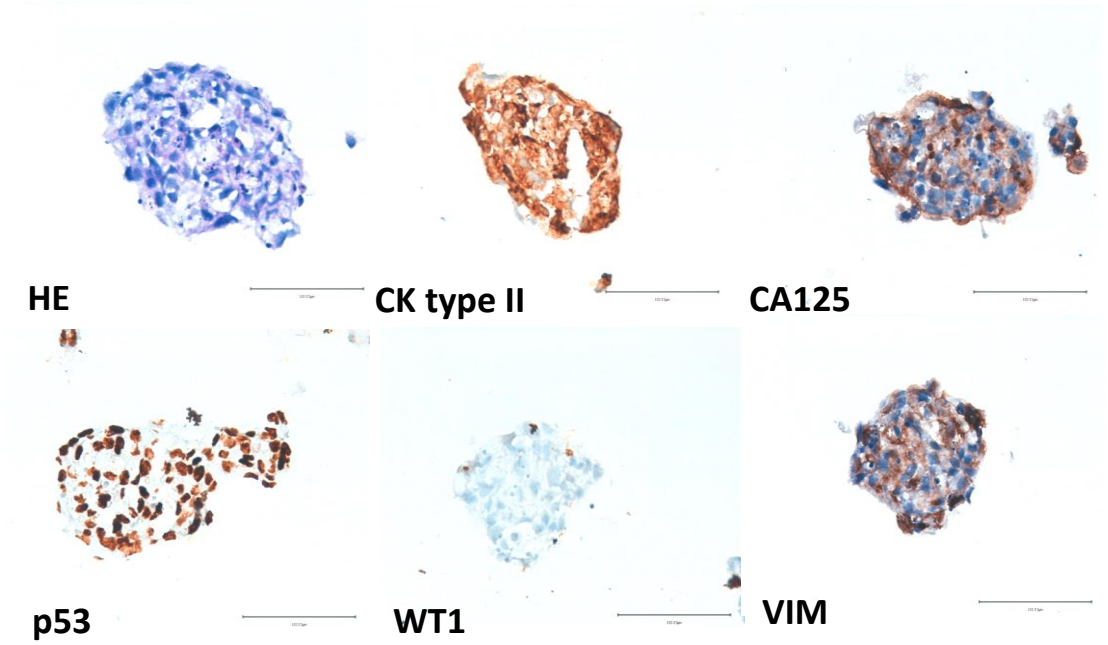

Figure 6. 13 - **Characterization of IPO-SOC43 cell line in 3D model**
Cryosections of 3D aggregates stained with hematoxylin and eosin (HE) and immunohistochemical staining panel. Cells show positive expression for cytokeratin (CK) type II (clone CAM 5.2), vimentin and p53. Cells were negative for WT1 and had positive expression for CA125, 400x.

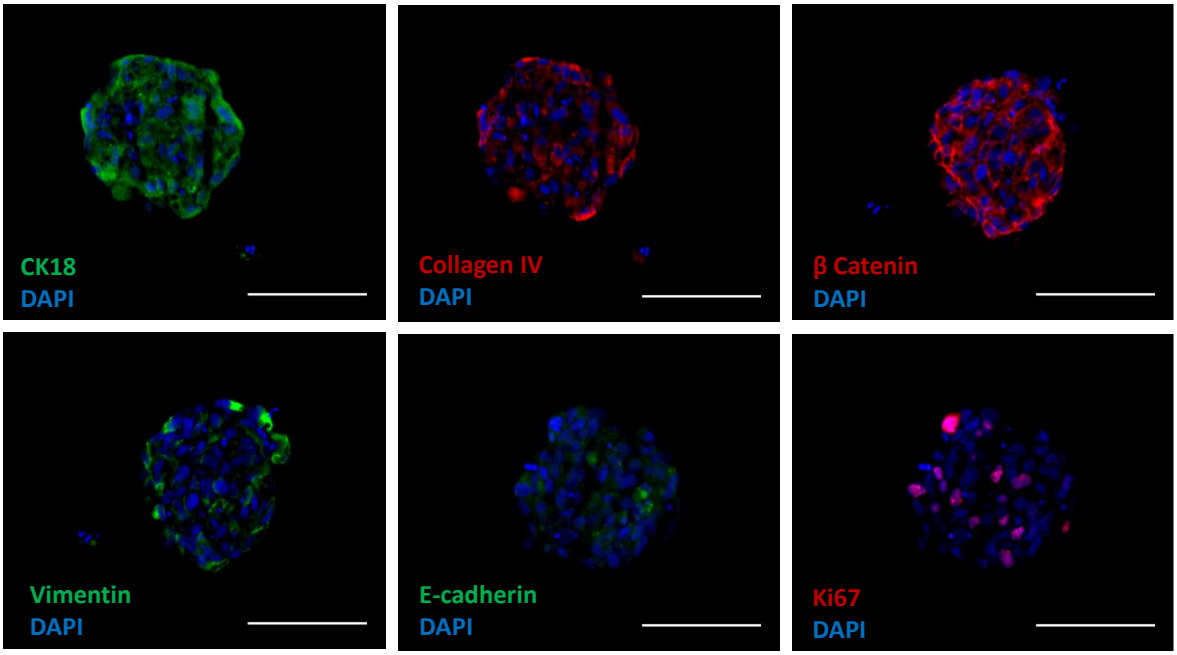

Figure 6. 14 - **Expression of biological markers relevant for the establishment of 3D cell culturing models in IPO-SOC43 cell line**
Cryosections of 3D aggregates show positive expression for CK18, collagen IV and β-catenin. Only few cells show positive expression for vimentin, E-cadherin and Ki-67, 400x.

Discussion

In this paper we characterized a new EOC cell line, IPO-SOC43 (*Instituto Português de Oncologia* - High Grade Serous Ovarian Carcinoma 43), established in our laboratory that can used as an important experimental tool in cancer research of EOC.

Cancer cell lines, besides their well-known limitations, are still useful *in vitro* models to study molecular mechanisms underlying cancer biology, chemoresistance and tumor recurrence, providing that they are well characterized[454]. There are many benefits in using primary cell cultures with little or no laboratory-induced transformation as the behavior of these cells reflects better the original tumor cells.

Our cell line was established from a patient (73 years old) receiving neoadjuvant chemotherapy treatment for advanced HGSC, not manageable by surgery up front. Ovarian cancer is recognized as a disease with distinct molecular backgrounds[28] and not a single clinical entity. Seventy percent of EOC are HGSC, making this tumor type an important research focus[455]. Although considerable progress has been made in cancer research, the survival rate of ovarian cancer has not improved over the past several decades[7], demonstrating the urgent need for understanding the mechanisms underlying the development of ovarian cancer.

In this study a detailed characterization of this cell line was done in order to establish the similarities and differences between the cell line and the original ascitic fluid[456].

The evaluation of the morphological features and immunohistochemistry confirm that the IPO-SOC43 cell line resembles the original cells from the ascitic fluid cells and also from the patient's ovarian primary tumor. The 2D model cell line expresses ovarian carcinoma markers and its epithelial origin has been confirmed by immunohistochemistry and immunofluorescence. Although a positive expression of vimentin was observed using techniques of immunocytochemistry, the result of flow cytometry indicates that the cell line does not express vimentin. We believe that the process of fixation of the cells can interfere with the antibody vimentin and this may explain the positive results by immunocytochemistry[457].

Dynamical chromosomal gains and losses in the cell line support the evidence of clonal selection. The cCGH profile of passage 42 of cell line showed less variability of numerical alterations apparently due to clonal adaptation to *in vitro* conditions and hopefully the stabilization of the cell line. Nevertheless, IPO-SOC43 cultured cells showed gains and losses similar to the parental cells as well as additional chromosomal alterations in clones compared with the parental cells suggesting that IPO-SOC43 cell line was undergoing clonal selection.

It is suggested that certain genetic alterations that emerge in a cancer cells confer a selective advantage over the others, and cancer progression results from the expansion of clone(s) that collectively acquires the following characteristics: self-sufficiency in growth signals, evasion to apoptosis, sustained angiogenesis, limitless replicate potential and capacity of tumor invasion and metastasis[458].

Through cCGH we verified that the cell line has the deletion of the region where TP53 is located in the short arm of chromosome 17 and IPO-SOC43 cells contains a missense mutation in *TP53* in exon 5, codon 172 (p.V172F;GTT>TTT, c.514G>T. This c.514G>T mutation is associated with an advantage for tumor growth in a variety of neoplasms and it might have an pathophysiological effect, as reported in V80 COSMIC database (http://cancer.sanger.ac.uk/cosmic/mutation)[447–452]. Thus IPO-SOC43 cells do not have wild type p53 protein.

IPO-SOC43 cell line harbors alterations in chromosome 19, specifically gain of chromosome regions 19p13.1-19q13.2 with amplification at 19q13.1, that has been reported as a frequent cytogenetic change observed in ovarian carcinomas by other studies[338,445,459]. We believe that our cell line may has become immortalized through these alterations as reported for other cell lines[338,445,459].

The study of the cCGH of our cell line revealed several other cytogenetic alterations that were already described as highly frequent in HGSC by Kim et al.[456], such as the gain of 1p36, Xq21 and loss of 8p23. The same authors claimed that gains of 5p15 and 14q11, and loss of 22q12, which we also find in IPO-SOC43 are associated to chemoresistant disease.

Finally, IPO-SOC43 cell line does not present *BRCA1* mutations although in *BRCA2* three polymorphisms were identified: 5'UTR 1-26 G/A; p.N372H and p.V1269V. These alterations are not associated with clinical significance.

In summary, the genetic main characteristics of this cell line match the "classical features" described by Cancer Genome Atlas Research Network (TGCA)[31] such as alterations in DNA regions copy number and *TP53* mutation (reported in 96% of cases).

3D cultures of tumor cell lines are considered to be better models than 2D for evaluation of tumor characteristics. For this reason we started by establishing a 3D culture of IPO-SOC43 and compared to the characteristics of neoplastic cells cultured in 2D culture. IPO-SOC43 cells in 2D were able to produce adhesion molecules such as E-cadherin and β-catenin; and extracellular matrix macromolecules as collagen IV. Their epithelial origin was proved by cytokeratin 18 positivity and expression of F-actin very similar with original tumor. Our cell line persists in 3D, in irregular and loose aggregates, and maintains the phenotypical features of the original tumor. This allow us to explore the advantages of the use of stirred-tank culture systems for 3D cultures in process scale-up over the standard two-dimensional (2D) static culture[460]; and by reproducing better the effects of the tissue microenvironment, including cell morphology, polarity and junctions.

In both models, we observed a similar proliferation activity (by Ki-67). In our 3D model, expression of adhesion molecules such as E-cadherin or extracellular matrix as collagen IV, indicates that cell aggregates maintained cell–cell interactions and expression of ECM components. We hope to use this 3D culture system in more complex assays, and to provide better and more complete answers regarding neoplastic cells and their microenvironment[460].

In conclusion, we describe the characteristic of an established cell line, IPO-SOC43, isolated from ascitic fluid of HGSC patient using different techniques and approaches (morphology, phenotype, genetic) and confirm its use as a stable cell line suitable to investigate on HGSC of ovary, fallopian tube and peritoneum.

CHAPTER 7

General Discussion

Epithelial ovarian cancer (EOC) is a heterogeneous disease composed by different histological types with distinctive patient outcomes[3–5]. EOC diagnosed while still limited to the ovaries, allow that 90% of patients can be cured with conventional surgery but cure rates decrease substantially after tumor dissemination to the pelvic organs or beyond the peritoneal cavity[2,26].

The standard chemotherapy procedure involving cytotoxic drugs has been established and optimized for ovarian cancer treatment (such as the combination of taxane and platinum); however, the overall cure rate has remained between 20-40% for the last 30 years[4,461–463]. Therefore, these therapeutic options are not effective, leading to therapy resistance and metastasis.

We focus our study in the most common histological type, high grade serous carcinoma (HGSC), usually diagnosed at an advanced stage, and although these tumors frequently respond to surgery and platinum-based chemotherapy, they usually recur[55]**;** and in ovarian clear cell carcinoma (CCC), less frequent histological type, known to be intrinsically chemoresistant and associated with poor prognosis in advanced stages[55]. New approaches are needed and epigenetic therapies raise as a possible route.

Histone deacetylases (HDACs) are responsible for many functions, they regulate the acetylation of a variety of histone and nonhistone proteins, controlling the regulation of transcription and function of genes involved in cell cycle control, proliferation, survival/cell death, DNA repair, differentiation and therapy[274,325,326]. Hence, HDACs expression is frequently altered in hematologic and solid tumor malignancies[329–331,334] and they can represent ideal targets for new therapeutic strategies.

In the perspective of better understanding the role of HDACs in ovarian carcinoma, we evaluated the expression profile of HDACs in our ovarian series, using immunohistochemistry (IHC). Although many studies have been carried out to elucidate the role of these enzymes in the context of ovarian cancer, their expression profile is still very ambiguous[325 464 339].

We evaluated the expression by immunohistochemistry of class I enzymes, HDAC1, 2, 3, and class II enzymes, HDAC4, 6 and phosphoHDAC4/5/7 in HGSC and CCC. The results in both EOC types, revealed that HDACs were significantly associated with the histological type of ovarian cancer. In HGSC, it was verified a high expression of HDAC1, 2, 3, 4, 6 and pHDAC4/5/7. Regarding evaluation of clinical parameters and cell cycle markers only HDAC1 expression was associated with p21 expression and HDAC3 was associated with disease stage at presentation in HGSC.

In CCC, high expression of HDAC1 and 2 was verified, whereas HDAC3 expression was only present in 30% of cases. Also the low expression of HDAC4 (in only 21% of cases) seems to be characteristic of this tumor type. In this cohort no other HDAC expression was associated with any of the analyzed molecular and clinical parameters.

As mentioned above, other studies report the expression of these enzymes in ovarian cancer, however, this is the first time the difference of HDACs expression profile between different histological types of ovarian carcinomas is highlighted.

However, since we show that HDACs are expressed in EOC at higher levels than in normal tissue counterparts, independently of which the enzyme is, we consider that HDACIs can be a putative therapeutic strategy for ovarian carcinoma.

Assuming that the expression profiles of HDACs were different between histological types we observed that HDACs are linked to the expression of cell cycle molecules as reported by other studies[296,299,325,421,465]. However, further investigation is required to clarify which of the identified biomarkers or whether they will ultimately be useful in the diagnosis and monitoring of patients with ovarian carcinomas.

Hence, we evaluated the effects of HDACI in proliferation and cell death in EOC cell lines with exposure to HDACI, DNA methyltransferases inhibitors (5-aza-dC) and conventional chemotherapy (carboplatin and paclitaxel). Our results report that HDAC inhibitors, butyric acid and vorinostat, induced cell death, mainly through apoptosis in ES2 cell line, confirmed by immunofluorescence of cleaved caspase 3 and the *ratio* of protein BAX/BCL-2 which increases after vorinostat exposure. Also, vorinostat and 5-aza-dC were able to potentiate the effect of chemotherapeutic drugs mainly in ES2 cell line (CCC), supporting that CCC treatment can benefit from combined chemical and

epigenetics directed therapy. Whereas in HGSC we verified that only tetra-combination of HDACIs, 5-aza-dC, carboplatin and paclitaxel would be profitable to induce cell death.

In this work it was interesting to note that vorinostat has differential effects between CCC and HGSC as it would be expected since they are different entities in clinical and molecular terms. Regrettably, clinical trials have been proven inconclusive or have classified HDACIs as not suitable therapeutic agents for the treatment of EOC, mainly due to toxic effects. Unfortunately, we cannot make a point on histological type response between our *in vitro* results and the literature on clinical assays, since the clinical trials were labeled as being carried out in EOC with no identification of the tumor histological type[324,374,428–430].

Further studies are needed to understand how and why the different cancer cell types respond to HDACIs differently and the mechanistic basis underlying resistance as well as the secondary and adverse effects in patients, in order to develop more effective and harmless HDACIs.

As mentioned above, CCC is an unique clinical, pathological and molecular entity within ovarian cancer, having HNF1β as a key pro-survival gene[400,401], being considered as responsible for cell survival, proliferation and chemoresistance[72,402]. So, we evaluated the effect of HDACI in HNF1β expression and CCC cells viability and the results showed that the increased levels of HNF1β by vorinostat induced cell cycle arrest and apoptosis in CCC cells. The increased expression of p21 supports the evidence observed of the cell cycle arrest in G0/G1 phases[414,415]. In our work we proved that increased levels of HNF1β by vorinostat is associated with cell cycle arrest and apoptosis in CCC cells. This observation was deeply related with increased acetylation load of HNF1β. The increased acetylation levels related to HDACIs exposure was already described for other proteins that are not histones, for example the tumor suppressor p53[421–424], although it is a completely new concept in HNF1β that we are currently experimentally depicting. However, since HNF1β has a pro-survival activity, this work showed that its acetylation can be a route of HDACIs action in CCC cells, altering its function in a way of decreasing cell proliferation and viability. Again it

becomes evident that the action of HDACIs, although initially they have been designed to affect the acetylation level of histones, also affects the function of other proteins which play crucial roles in cell function[420 421–423].

Together, our study provided new evidences of HNF1β role in CCC. Further studies are needed in order to unravel the function of HNF1β, especially in the context of cancer, since HNF1β is consistently *de novo* expressed or overexpressed in CCC from different organs such as ovarian, pancreas, kidney and liver[399,425–427].

At the light of our findings we can raise two more questions: 1) What is the role of HNF1β in tumor progression?, and 2) Would an acetylation of HNF1β-target therapy be efficient in clear cell carcinomas?

According to TGCA[31], genetic alterations and epigenetic modulation of signaling pathways have been reported in EOC**,** including the overexpression of Notch pathway elements and histone deacetylases. However, no previous work has addressed the effect of HDACIs, and in particular vorinostat, on Notch signaling in ovarian cancer.

In this PhD thesis we aimed to investigate the modulation of the Notch pathway by vorinostat, since it was already knew the involvement of Notch pathway in ovarian cancer biology[148,152,153,310,466]. With our study we revealed that vorinostat activated the Notch pathway in both CCC and HGSC cell lines, through different Notch elements. In CCC, the activation of Notch pathway appeared to occur through Delta-like (Dll) ligands 1, 2 and 3, whereas in HGSC Dll1 and Jagged 1 and 2 ligands were involved. Also, our results ensure the activation of Notch pathway in EOC cells by vorinostat because it induces the overexpression of *Hes* and *Hey* Notch target genes. Moreover, it was shown the redundancy of Notch, Delta and Jagged elements expressed in EOC cell lines; thus, whatever is the panel of receptor or ligands expressed on the cell membrane, the downstream target genes were always expressed in the presence of vorinostat. This upregulation can shed a light on the mechanism underlying the failure of vorinostat therapy in some ovarian carcinoma subsets, as shown on clinical trials[372,379,380]. Again, the fact that the published clinical trials do not present the results considering the histological type of tumor limits the confrontation of our results with the literature.

The final aim of this study was to establish and characterize a human cell line. We described a HGSC cell line (IPO-SOC43) immortalized without any induced transformation, which represents the most frequently occurring histopathological subtype of ovarian carcinomas, the HGSC.

The cell line is maintained in 2D and 3D model exhibiting protein expression profile similar to the primary tumor. The expression of adhesion molecules indicating that the established cells closely mimic the natural environment found *in vivo,* resembling the primary tumor.

The cell line arbors some classical features described by TGCA[31], such as alterations in DNA copy number, *TP53* mutation and *BRCA2* mutation. The IPO-SOC43 cell line established is a suitable model to investigate the molecular mechanisms underlying the progression, treatment, resistance and recurrence of HGSC. We hope this new cell line can contribute to enlarge the panel of cell lines uncovering ovarian cancer heterogeneity, however, considering *in vitro* models and the development of cell technology some questions remain to be answered: Do 3D models have an advantage on 2D models, giving a more real picture of an ovarian cancer?, and Can 3D models be useful tools to predict sensitivity to therapy, allowing an accurate screening of drugs to be used individually in each patient- precision medicine?

Conclusions

In this study, our results confirmed previous reports that HDACs are expressed in ovarian cancer, involved in tumor progression and cancer metastasis and the epigenetic changes found could potentially serve as biomarkers for disease progression. The research of class I and II of HDACs expression profiles evidenced their association with different histological types of ovarian cancer. Moreover, we demonstrated that HDACIs inhibit cell proliferation and induced cell death in ovarian clear cell carcinoma (CCC) and in high grade serous carcinoma (HGSC), especially in combined therapy with 5-aza-dC, carboplatin and/or paclitaxel. Our data specified some of the putative mechanisms for apoptosis induced by HDACIs. Also, we reported in CCC, that acetylation of HNF1β can be a way of modulating its function, turning its

action from pro-survival to anti-survival upon exposure to vorinostat or other HDACI. So, the description of HNF1β acetylation can constitute a mechanism of modulation/abrogation of HNF1β pro-survival function in CCC, which can contribute for the design of a new CCC therapy.

Furthermore, we reported that vorinostat modulates the expression of downstream targets of the Notch pathway whatever is the panel of Notch receptor or ligands expressed in EOC cell lines. Hence, the downstream target genes are always expressed in the presence of vorinostat. This regulation may explain the mechanism underlying the failure of vorinostat therapy in ovarian carcinoma, but our results did not show a route to impair Notch pathway in ovarian cancer by using HDACIs.

In the course of this work, we demonstrated the successful establishment of a cell line of HGSC, cultured in 2D and 3D, without lab immortalization, which can be a new tool to study ovarian cancer biology. So far, due to the high heterogeneity of EOC the existing models have been insufficient to accurately mimic all disease cases. This new cell line will contribute to enrich the current panel of cell lines available for scientific and clinical use. Moreover, *in vitro* models, transient/perishable or stable/immortalized, will be for sure the most suitable tools to select more efficient drugs and predict chemoresistance allowing an increasingly individualized medicine, in which cells of a patient can be manipulated *in vitro* to select a more beneficial therapeutic program.

In conclusion, our findings reinforced the putative efficiency of HDACs in a combined therapy to treat ovarian cancer and we believe this thesis work contributes with new molecular insights on how HDACIs disturbs the biological functioning of these two different histological types of ovarian cancer (CCC and HGSC) and opens new directions for research and therapeutic intervention and precision medicine.

Future Perspectives

In the last decade, the surgical approach and the standardization of chemotherapeutic modalities have slightly improved survival of epithelial ovarian cancer (EOC) patients, however EOC still has a poor prognosis. Since the histological types of EOC corresponds to different diseases, future developments in the understanding of these diseases and treatment should focus on histology and its specific molecular alterations.

Based on the fact that histone deacetylases (HDACs) expression is increased in EOC, the research presented in this thesis contributes with some inputs to disclose the molecular mechanisms underlying the action of histone deacetylases inhibitors (HDACIs) in EOC. We reported that the expression profile of HDAC, class I (HDAC1, 2, 3) and class II (HDAC4, 6 and phosphoHDAC4/5/7) in ovarian cancer is intimately associated with the histological type. Considering this, in the future it would be interesting to perform *in vitro* knockdown studies aiming the relevance of each HDAC in the different histological types of EOC, to disclose their real role as epigenetic biomarkers.

This thesis open up for a wide range of further investigation to explore the role of HDACs in cancer cells pathophysiology that might have an impact on cancer therapy. Clear cell carcinoma (CCC) is by far the most interesting and challenging EOC biological model.

Regarding the HNF1β in CCC, we showed that Vorinostat induces both the increased of HNF1β levels and its acetylation load concomitantly with a decreased cell survival. This evidence is new since high levels of HNF1β are correlated to increased cell survival. So, the meaning of HNF1β acetylation must be clarified in order to know the role of HDACs and/or other deacetylases in the modulation of HNF1β function as well as their relevance in CCC biology. Moreover, our group have shown recently that HNF1β regulates the production of glutathione (GSH) which constitutes a mechanism of resistance to carboplatin. Hence, HNF1β is still a very interesting gene/protein which function deserves to be depicted in cancer, not only in EOC but also in other malignancies presenting its overexpression or de novo expression. The partnership

established by HNF1β and other molecular elements, such as p53 and BAF250a (encoded by ARID1A) is for sure a challenge.

In our study it was not possible to include *TP53* wild type CCC cell lines but it would be interesting to evaluate how the function of HNF1β is affected (abrogated or potentiated) by p53. Since HNF1β is a pro-survival gene in CCC and TP53 mutation is uncommon in CCC, we believe the modulation of the action of HNF1β will be rather different than in TP53 mutated CCC cell lines.

ARID1A is a gene that codifies BAF250a protein that belongs to a chromatin remodeling complex and has recently been pointed out as a marker for CCC. In our cohort we saw a perfect match between HNF1β and BAF250 expression and their interaction remain unknown in CCC biology. Disclosing their relationship we can go forth into a relevant step to understand CCC unique biological behavior.

The redundancy of epigenetic modulation of Notch pathway elements by Vorinostat in EOC was also shown, indicating that Notch pathway is really central in EOC carcinogenesis and progression and this fundamented by the way their elements are able to overcome each other functions and sustain the expression of downstream targets. In this point, it would be interesting to find a way other than through HDACS to effectively disturb Notch pathway in EOC.

The results *in vitro* proved that there is benefits of combined therapy, using drugs with action of epigenetic modulation and conventional therapy. Future analyses of both primary and relapse tumors from the same patient would be an ideal way to study chemotherapy resistance in EOC as well as new combined therapeutic regimes. However, since secondary surgery is rarely performed, ascitic fluid which is collected for a palliative purpose can be a good alternative to collect cancer cells, as we have shown with the establishment of a primary cell line from a HGSC patient. Additionally, *ex vivo* transient experiments using tumor explants can be an useful approach to be optimized in order to serve as a screening platform to analyze individualized responses of patients to therapy.

REFERENCES

1. Seyfried, T. N. & Shelton, L. M. Cancer as a metabolic disease. *Nutr. Metab. (Lond).* **7,** 7 (2010).
2. Who. World cancer factsheet. *World Heal. Organ.* **2012,** 4 (2014).
3. Reinhardt, M. J. Gynecologic tumors. *Recent Results Cancer Res.* **170,** 141–50 (2008).
4. Bast, R. C., Hennessy, B. & Mills, G. B. The biology of ovarian cancer: new opportunities for translation. *Nat. Rev. Cancer* **9,** 415–28 (2009).
5. Jayson, G. C., Kohn, E. C., Kitchener, H. C. & Ledermann, J. A. Ovarian cancer. *The Lancet* **384,** (2014).
6. Ferlay, J. *et al.* Cancer incidence and mortality patterns in Europe: Estimates for 40 countries in 2012. *Eur. J. Cancer* **49,** 1374–1403 (2013).
7. Bray, F., Ren, J.-S. S., Masuyer, E. & Ferlay, J. Global estimates of cancer prevalence for 27 sites in the adult population in 2008. *Int. J. Cancer* **132,** 1133–1145 (2013).
8. Hough, C. D. *et al.* Large-scale serial analysis of gene expression reveals genes differentially expressed in ovarian cancer. *Cancer Res.* **60,** 6281–7 (2000).
9. Hennessy, B. T., Coleman, R. L. & Markman, M. Ovarian cancer. *Lancet* **374,** 1371–82 (2009).
10. Mungenast, F. & Thalhammer, T. Estrogen Biosynthesis and Action in Ovarian Cancer. *Front. Endocrinol. (Lausanne).* **5,** 1–12 (2014).
11. Siegel, R., Naishadham, D. & Jemal, A. Cancer statistics, 2012. *CA. Cancer J. Clin.* **62,** 10–29 (2012).
12. ROR-Centro, I. P. de O. de C. F. G.-E. *Registo Oncológico Nacional 2008*. (2014).
13. Liu, C.-M. Cancer of the ovary. *N. Engl. J. Med.* **352,** 1268-9-9 (2005).
14. Risch, H. A. *et al.* Population BRCA1 and BRCA2 mutation frequencies and cancer penetrances: a kin-cohort study in Ontario, Canada. *J. Natl. Cancer Inst.* **98,** 1694–706 (2006).
15. Aysal, A. *et al.* Ovarian Endometrioid Adenocarcinoma. *Am. J. Surg. Pathol.* **36,** 163–172 (2012).
16. de Pauw, A. *et al.* [Hereditary forms of ovarian cancer]. *Bull. Cancer* **99,** 453–62 (2012).
17. Couch, F. J., Nathanson, K. L. & Offit, K. Two decades after BRCA: setting paradigms in personalized cancer care and prevention. *Science* **343,** 1466–70 (2014).
18. Koornstra, J. J. *et al.* Management of extracolonic tumours in patients with Lynch syndrome. *Lancet. Oncol.* **10,** 400–8 (2009).
19. Beral, V., Doll, R., Hermon, C., Peto, R. & Reeves, G. Ovarian cancer and oral contraceptives: collaborative reanalysis of data from 45 epidemiological studies including 23,257 women with ovarian cancer and 87,303 controls. *Lancet* **371,** 303–14 (2008).

20. Gadducci, A., Biglia, N., Cosio, S., Sismondi, P. & Genazzani, A. R. Gynaecologic challenging issues in the management of BRCA mutation carriers: oral contraceptives, prophylactic salpingo-oophorectomy and hormone replacement therapy. *Gynecol. Endocrinol.* **26,** 568–577 (2010).

21. Siegel, R., Naishadham, D. & Jemal, A. Cancer statistics, 2013. *CA. Cancer J. Clin.* **63,** 11–30 (2013).

22. Kurman, R. J. & Shih, I.-M. Pathogenesis of ovarian cancer: lessons from morphology and molecular biology and their clinical implications. *Int. J. Gynecol. Pathol.* **27,** 151–60 (2008).

23. Kurman, R. J. & Shih, I.-M. Molecular pathogenesis and extraovarian origin of epithelial ovarian cancer--shifting the paradigm. *Hum. Pathol.* **42,** 918–31 (2011).

24. Kurman, R. J. & Shih, I.-M. The Dualistic Model of Ovarian Carcinogenesis Revisited, Revised, and Expanded. (2016). doi:10.1016/j.ajpath.2015.11.011

25. Smolle, E. *et al.* Targeting signaling pathways in epithelial ovarian cancer. *Int. J. Mol. Sci.* **14,** 9536–55 (2013).

26. Prat, J. Ovarian carcinomas: five distinct diseases with different origins, genetic alterations, and clinicopathological features. *Virchows Arch.* **460,** 237–49 (2012).

27. Cho, K. R. & Shih, I.-M. Ovarian cancer. *Annu. Rev. Pathol.* **4,** 287–313 (2009).

28. Shih, I.-M. & Kurman, R. J. Ovarian Tumorigenesis. *Am. J. Pathol.* **164,** 1511–1518 (2004).

29. Landen, C. N., Birrer, M. J. & Sood, A. K. Early Events in the Pathogenesis of Epithelial Ovarian Cancer. *J. Clin. Oncol.* **26,** 995–1005 (2008).

30. Kurman, R. J. & Shih, I.-M. The origin and pathogenesis of epithelial ovarian cancer: a proposed unifying theory. *Am. J. Surg. Pathol.* **34,** 433–43 (2010).

31. Cancer Genome Atlas Research Network. Integrated genomic analyses of ovarian carcinoma. *Nature* **474,** 609–15 (2011).

32. Jones, P. M. & Drapkin, R. Modeling High-Grade Serous Carcinoma: How Converging Insights into Pathogenesis and Genetics are Driving Better Experimental Platforms. *Front. Oncol.* **3,** 217 (2013).

33. Karst, A. M. & Drapkin, R. Ovarian Cancer Pathogenesis: A Model in Evolution. *J. Oncol.* **2010,** 1–13 (2010).

34. WG., M. Morphological subtypes of ovarian carcinoma: a review with emphasis on new developments and pathogenesis. *Pathology* (2011).

35. Gershenson, D. M. *et al.* Clinical behavior of stage II-IV low-grade serous carcinoma of the ovary. *Obstet. Gynecol.* **108,** 361–8 (2006).

36. Burotto, M., Chiou, V. L., Lee, J.-M. & Kohn, E. C. The MAPK pathway across different malignancies: a new perspective. *Cancer* **120,** 3446–56 (2014).

37. Köbel, M. *et al.* Ovarian carcinoma subtypes are different diseases: implications for biomarker studies. *PLoS Med.* **5,** e232 (2008).

38. Malpica, A. *et al.* Grading ovarian serous carcinoma using a two-tier system. *Am. J. Surg. Pathol.* **28,** 496–504 (2004).

39. Singer, G. *et al.* Patterns of p53 mutations separate ovarian serous borderline tumors and low- and high-grade carcinomas and provide support for a new model of ovarian carcinogenesis: a mutational analysis with immunohistochemical correlation. *Am. J. Surg. Pathol.* **29,** 218–24 (2005).

40. Köbel, M. *et al.* A limited panel of immunomarkers can reliably distinguish between clear cell and high-grade serous carcinoma of the ovary. *Am. J. Surg. Pathol.* **33,** 14–21 (2009).

41. Nakayama, K. *et al.* Amplicon profiles in ovarian serous carcinomas. *Int. J. Cancer* **120,** 2613–7 (2007).

42. Patch, A.-M. *et al.* Whole–genome characterization of chemoresistant ovarian cancer. *Nature* **521,** 489–494 (2015).

43. Bayani, J. *et al.* Parallel analysis of sporadic primary ovarian carcinomas by spectral karyotyping, comparative genomic hybridization, and expression microarrays. *Cancer Res.* **62,** 3466–76 (2002).

44. Wiegand, K. C. *et al.* ARID1A mutations in endometriosis-associated ovarian carcinomas. *N. Engl. J. Med.* **363,** 1532–43 (2010).

45. Prat, J. Pathology of the Ovary. (2004).

46. Lee, K., Tavassoli, F., Prat, J. & Dietel, M. Surface epithelial-stromal tumours. *World Heal. Organ. …* (2003).

47. Sato, N. *et al.* Loss of heterozygosity on 10q23.3 and mutation of the tumor suppressor gene PTEN in benign endometrial cyst of the ovary: possible sequence progression from benign endometrial cyst to endometrioid carcinoma and clear cell carcinoma of the ovary. *Cancer Res.* **60,** 7052–6 (2000).

48. Palacios, J. & Gamallo, C. Mutations in the {beta}-Catenin Gene (CTNNB1) in Endometrioid Ovarian Carcinomas. *Cancer Res.* **58,** 1344–1347 (1998).

49. Lu, K. H. & Daniels, M. Endometrial and ovarian cancer in women with Lynch syndrome: update in screening and prevention. *Fam. Cancer* **12,** 273–277 (2013).

50. Gras, E. *et al.* Microsatellite instability, MLH-1 promoter hypermethylation, and frameshift mutations at coding mononucleotide repeat microsatellites in ovarian tumors. *Cancer* **92,** 2829–36 (2001).

51. Moreno-Bueno, G. *et al.* beta-Catenin expression pattern, beta-catenin gene mutations, and microsatellite instability in endometrioid ovarian carcinomas and synchronous endometrial carcinomas. *Diagn. Mol. Pathol.* **10,** 116–22 (2001).

52. Wiegand, K. C. *et al.* Loss of BAF250a (ARID1A) is frequent in high-grade endometrial carcinomas. *J. Pathol.* **224,** 328–33 (2011).

53. Yamamoto, S., Tsuda, H., Takano, M., Tamai, S. & Matsubara, O. Loss of ARID1A protein expression occurs as an early event in ovarian clear-cell carcinoma development and frequently coexists with PIK3CA mutations. *Mod. Pathol. an Off. J. United States Can. Acad. Pathol. Inc* **25,** 615–24 (2012).

54. Prat, J. New insights into ovarian cancer pathology. *Ann. Oncol.* **23,** (2012).

55. del Carmen, M. G., Birrer, M. & Schorge, J. O. Clear cell carcinoma of the ovary: a review of the literature. *Gynecol. Oncol.* **126,** 481–90 (2012).

56. Sugiyama, T. *et al.* Clinical characteristics of clear cell carcinoma of the ovary: a distinct histologic type with poor prognosis and resistance to platinum-based chemotherapy. *Cancer* **88,** 2584–9 (2000).

57. Jones, S. Frequent Mutations of Chromatin Remodeling Gene ARID1A in Ovarian. *Biochemistry* **228,** 228–231 (2010).

58. Shigetomi, H. *et al.* The role of components of the chromatin modification machinery in carcinogenesis of clear cell carcinoma of the ovary (Review). *Oncol. Lett.* **2,** 591–597 (2011).

59. Katagiri, A. *et al.* Loss of ARID1A expression is related to shorter progression-free survival and chemoresistance in ovarian clear cell carcinoma. *Mod. Pathol. an Off. J. United States Can. Acad. Pathol. Inc* **25,** 282–8 (2012).

60. Campbell, I. G. *et al.* Mutation of the PIK3CA gene in ovarian and breast cancer. *Cancer Res.* **64,** 7678–81 (2004).

61. Guan, B., Wang, T.-L. & Shih, I.-M. ARID1A, a factor that promotes formation of SWI/SNF-mediated chromatin remodeling, is a tumor suppressor in gynecologic cancers. *Cancer Res.* **71,** 6718–27 (2011).

62. Ayhan, A. *et al.* Loss of ARID1A expression is an early molecular event in tumor progression from ovarian endometriotic cyst to clear cell and endometrioid carcinoma. *Int. J. Gynecol. Cancer* **22,** 1310–5 (2012).

63. Press, J. Z. *et al.* Ovarian carcinomas with genetic and epigenetic BRCA1 loss have distinct molecular abnormalities. *BMC Cancer* **8,** 17 (2008).

64. Kotsopoulos, I. C. *et al.* Serous ovarian cancer signaling pathways. *Int. J. Gynecol. Cancer* **24,** 410–7 (2014).

65. Banerjee, S. & Kaye, S. B. New strategies in the treatment of ovarian cancer: current clinical perspectives and future potential. *Clin. Cancer Res.* **19,** 961–8 (2013).

66. Yamaguchi, K. *et al.* Epigenetic determinants of ovarian clear cell carcinoma biology. *Int. J. cancer* **135,** 585–97 (2014).

67. Kato, N., Sasou, S. & Motoyama, T. Expression of hepatocyte nuclear factor-1beta (HNF-1beta) in clear cell tumors and endometriosis of the ovary. *Mod. Pathol.* **19,** 83–9 (2006).

68. Kobayashi, H. *et al.* The role of hepatocyte nuclear factor-1beta in the pathogenesis of clear cell carcinoma of the ovary. *Int. J. Gynecol. Cancer* **19,** 471–9 (2009).

69. Cuff, J. *et al.* Integrative bioinformatics links HNF1B with clear cell carcinoma and tumor-associated thrombosis. *PLoS One* **8,** e74562 (2013).

70. Terasawa, K. *et al.* Epigenetic inactivation of TCF2 in ovarian cancer and various cancer cell lines. *Br. J. Cancer* **94,** 914–21 (2006).

71. Kato, N., Tamura, G. & Motoyama, T. Hypomethylation of hepatocyte nuclear factor-1beta (HNF-1beta) CpG island in clear cell carcinoma of the ovary. *Virchows Arch.* **452,** 175–80 (2008).

72. Lopes-Coelho, F. *et al.* HNF1β drives glutathione (GSH) synthesis underlying intrinsic carboplatin resistance of ovarian clear cell carcinoma (OCCC). *Tumor Biol.* **37,** 4813–4829 (2016).

73. Kurman, R. J., International Agency for Research on Cancer. & World Health Organization. *WHO classification of tumours of female reproductive organs*. (International Agency for Research on Cancer, 2014).

74. Rodríguez, I. M. & Prat, J. Mucinous tumors of the ovary: a clinicopathologic analysis of 75 borderline tumors (of intestinal type) and carcinomas. *Am. J. Surg. Pathol.* **26,** 139–52 (2002).

75. Lee, K. R. & Scully, R. E. Mucinous tumors of the ovary: a clinicopathologic study of 196 borderline tumors (of intestinal type) and carcinomas, including an evaluation of 11 cases with 'pseudomyxoma peritonei'. *Am. J. Surg. Pathol.* **24,** 1447–64 (2000).

76. Silverberg, S. G. *et al.* Borderline ovarian tumors: key points and workshop summary. *Hum. Pathol.* **35,** 910–7 (2004).

77. Heinzelmann-Schwarz, V. A. *et al.* A distinct molecular profile associated with mucinous epithelial ovarian cancer. *Br. J. Cancer* **94,** 904–913 (2006).

78. Cuatrecasas, M., Villanueva, A., Matias-Guiu, X. & Prat, J. K-ras mutations in mucinous ovarian tumors: a clinicopathologic and molecular study of 95 cases. *Cancer* **79,** 1581–6 (1997).

79. Twombly, R. Cancer Killer May Be 'Silent' No More. *JNCI J. Natl. Cancer Inst.* **99,** 1359–1361 (2007).

80. Winter, W. E. *et al.* Prognostic Factors for Stage III Epithelial Ovarian Cancer: A Gynecologic Oncology Group Study. *J. Clin. Oncol.* **25,** 3621–3627 (2007).

81. Smith, L. H. *et al.* Ovarian cancer: Can we make the clinical diagnosis earlier? *Cancer* **104,** 1398–1407 (2005).

82. Roett, M. A. & Evans, P. Ovarian Cancer : An Overview. **80,** (2009).

83. Høgdall, E. V. S. *et al.* CA125 expression pattern, prognosis and correlation with serum CA125 in ovarian tumor patients. From The Danish 'MALOVA' Ovarian Cancer Study. *Gynecol. Oncol.* **104,** 508–15 (2007).

84. Badgwell, D. & Bast, R. C. Early detection of ovarian cancer. *Dis. Markers* **23,** 397–410 (2007).

85. Barakat, R., Berchuck, A., Markman, M. & Randall, M. E. *Principles and Practice of Gynecologic Oncology*. (Lippincott Williams & Wilkins, 2013).

86. Ricardo, S. *et al.* Detection of glyco-mucin profiles improves specificity of MUC16 and MUC1 biomarkers in ovarian serous tumours. *Mol. Oncol.* **9,** 503–12 (2015).

87. Schummer, M. *et al.* Comparative hybridization of an array of 21,500 ovarian cDNAs for the discovery of genes overexpressed in ovarian carcinomas. *Gene* **238,** 375–85 (1999).

88. Drapkin, R. *et al.* Human epididymis protein 4 (HE4) is a secreted glycoprotein that is overexpressed by serous and endometrioid ovarian carcinomas. *Cancer Res.* **65,** 2162–9 (2005).

89. Hellström, I. *et al.* The HE4 (WFDC2) protein is a biomarker for ovarian carcinoma. *Cancer Res.* **63,** 3695–700 (2003).

90. Moore, R. G. *et al.* The use of multiple novel tumor biomarkers for the detection of ovarian carcinoma in patients with a pelvic mass. *Gynecol. Oncol.* **108,** 402–8 (2008).

91. Moore, R. G. *et al.* A novel multiple marker bioassay utilizing HE4 and CA125 for the prediction of ovarian cancer in patients with a pelvic mass. *Gynecol. Oncol.* **112,** 40–46 (2009).

92. Huhtinen, K. *et al.* Serum HE4 concentration differentiates malignant ovarian tumours from ovarian endometriotic cysts. *Br. J. Cancer* **100,** 1315–9 (2009).

93. Van Holsbeke, C. *et al.* Ultrasound methods to distinguish between malignant and benign adnexal masses in the hands of examiners with different levels of experience. *Ultrasound Obstet. Gynecol.* **34,** 454–61 (2009).

94. Lacey, J. V. *et al.* Ovarian Cancer Screening in Women With a Family History of Breast or Ovarian Cancer. *Obstet. Gynecol.* **108,** 1176–1184 (2006).

95. Robboy, S. J. *Robboy's Pathology of the Female Reproductive Tract*. (Elsevier Health Sciences, 2009).

96. Gubbels, J. A., Claussen, N., Kapur, A. K., Connor, J. P. & Patankar, M. S. The detection, treatment, and biology of epithelial ovarian cancer. *J. Ovarian Res.* **3,** 8 (2010).

97. Ozols, R. F. Phase III Trial of Carboplatin and Paclitaxel Compared With Cisplatin and Paclitaxel in Patients With Optimally Resected Stage III Ovarian Cancer: A Gynecologic Oncology Group Study. *J. Clin. Oncol.* **21,** 3194–3200 (2003).

98. Armstrong, D. K. *et al.* Intraperitoneal cisplatin and paclitaxel in ovarian cancer. *N. Engl. J. Med.* **354,** 34–43 (2006).

99. Le Page, C., Huntsman, D. G., Provencher, D. M. & Mes-Masson, A.-M. Predictive and Prognostic Protein Biomarkers in Epithelial Ovarian Cancer: Recommendation for Future Studies. *Cancers (Basel).* **2,** 913–954 (2010).

100. Siddik, Z. H. Cisplatin: mode of cytotoxic action and molecular basis of resistance. *Oncogene* **22,** 7265–79 (2003).

101. Kelland, L. The resurgence of platinum-based cancer chemotherapy. *Nat. Rev. Cancer* **7,** 573–84 (2007).

102. van der Vijgh, W. J. Clinical pharmacokinetics of carboplatin. *Clin. Pharmacokinet.* **21,** 242–61 (1991).

103. Boulikas, T. & Vougiouka, M. Cisplatin and platinum drugs at the molecular level. (Review). *Oncol. Rep.* **10,** 1663–82

104. Jamieson, E. R. & Lippard, S. J. Structure, Recognition, and Processing of Cisplatin-DNA Adducts. *Chem. Rev.* **99,** 2467–98 (1999).

105. Todd, R. C. & Lippard, S. J. Inhibition of transcription by platinum antitumor compounds. *Metallomics* **1,** 280–91 (2009).

106. Knox, R. J., Friedlos, F., Lydall, D. A. & Roberts, J. J. Mechanism of cytotoxicity of anticancer platinum drugs: evidence that cis-diamminedichloroplatinum(II) and cis-diammine-(1,1-cyclobutanedicarboxylato)platinum(II) differ only in the kinetics of their interaction with DNA. *Cancer Res.* **46,** 1972–9 (1986).

107. Rixe, O. *et al.* Oxaliplatin, tetraplatin, cisplatin, and carboplatin: spectrum of activity in drug-resistant cell lines and in the cell lines of the National Cancer Institute's Anticancer Drug Screen panel. *Biochem. Pharmacol.* **52,** 1855–65 (1996).

108. Gligorov, J. & Lotz, J. P. Preclinical pharmacology of the taxanes: implications of the differences. *Oncologist* **9 Suppl 2,** 3–8 (2004).

109. Cragg, G. M. Paclitaxel (Taxol): a success story with valuable lessons for natural product drug discovery and development. *Med. Res. Rev.* **18,** 315–31 (1998).

110. Bharadwaj, R. & Yu, H. The spindle checkpoint, aneuploidy, and cancer. *Oncogene* **23,** 2016–27 (2004).

111. Brito, D. A., Yang, Z. & Rieder, C. L. Microtubules do not promote mitotic slippage when the spindle assembly checkpoint cannot be satisfied. *J. Cell Biol.* **182,** 623–629 (2008).

112. Ganguly, A., Yang, H. & Cabral, F. Paclitaxel-dependent cell lines reveal a novel drug activity. *Mol. Cancer Ther.* **9,** 2914–23 (2010).

113. Zhou, J. & Giannakakou, P. Targeting Microtubules for Cancer Chemotherapy. *Curr. Med. Chem. Agents* **5,** 65–71 (2005).

114. Yasuda, M. *et al.* [Dose finding study of paclitaxel and carboplatin for ovarian cancer (JKTB)]. *Gan To Kagaku Ryoho.* **28,** 493–8 (2001).

115. Dumontet, C. & Jordan, M. A. Microtubule-binding agents: a dynamic field of cancer therapeutics. *Nat. Rev. Drug Discov.* **9,** 790–803 (2010).

116. Alexandre, J. *et al.* Accumulation of hydrogen peroxide is an early and crucial step for paclitaxel-induced cancer cell death both in vitro and in vivo. *Int. J. Cancer* **119,** 41–8 (2006).

117. Ramanathan, B. Resistance to Paclitaxel Is Proportional to Cellular Total Antioxidant Capacity. *Cancer Res.* **65,** 8455–8460 (2005).

118. Di Nicolantonio, F. *et al.* Cancer cell adaptation to chemotherapy. *BMC Cancer* **5,** 78 (2005).

119. Lloyd, K. L. *et al.* Prediction of resistance to chemotherapy in ovarian cancer: a systematic review. *BMC Cancer* **15,** 117 (2015).

120. Xia, C. *et al.* Reactive oxygen species regulate angiogenesis and tumor growth through vascular endothelial growth factor. *Cancer Res.* **67,** 10823–30 (2007).

121. Lee, J. M. Inhibition of p53-dependent apoptosis by the KIT tyrosine kinase: regulation of mitochondrial permeability transition and reactive oxygen species generation. *Oncogene* **17,** 1653–62 (1998).

122. Storz, P. Reactive oxygen species in tumor progression. *Front. Biosci.* **10,** 1881–96 (2005).

123. Rhee, S. G., Bae, Y. S., Lee, S.-R. & Kwon, J. Hydrogen Peroxide: A Key Messenger That Modulates Protein Phosphorylation Through Cysteine Oxidation. *Sci. Signal.* **2000,** pe1-pe1 (2000).

124. Brozovic, A., Ambriović-Ristov, A. & Osmak, M. The relationship between cisplatin-induced reactive oxygen species, glutathione, and BCL-2 and resistance to cisplatin. *Crit. Rev. Toxicol.* **40,** 347–59 (2010).

125. Wondrak, G. T. Redox-directed cancer therapeutics: molecular mechanisms and opportunities. *Antioxid. Redox Signal.* **11,** 3013–69 (2009).

126. Gottesman, M. M., Fojo, T. & Bates, S. E. Multidrug resistance in cancer: role of ATP-dependent transporters. *Nat. Rev. Cancer* **2,** 48–58 (2002).

127. Szakács, G., Paterson, J. K., Ludwig, J. A., Booth-Genthe, C. & Gottesman, M. M. Targeting multidrug resistance in cancer. *Nat. Rev. Drug Discov.* **5,** 219–34 (2006).

128. Gonçalves, A. *et al.* Resistance to Taxol in lung cancer cells associated with increased microtubule dynamics. *Proc. Natl. Acad. Sci. U. S. A.* **98,** 11737–42 (2001).

129. Kavallaris, M. *et al.* Taxol-resistant epithelial ovarian tumors are associated with altered expression of specific beta-tubulin isotypes. *J. Clin. Invest.* **100,** 1282–1293 (1997).

130. Abdullah, L. N. & Chow, E. K.-H. Mechanisms of chemoresistance in cancer stem cells. *Clin. Transl. Med.* **2,** 3 (2013).

131. Saldanha, S. N. & Tollefsbol, T. O. Pathway modulations and epigenetic alterations in ovarian tumorbiogenesis. *J. Cell. Physiol.* **229,** 393–406 (2014).

132. Perdigoto, C. N. & Bardin, A. J. Sending the right signal: Notch and stem cells. *Biochim. Biophys. Acta* **1830,** 2307–22 (2013).

133. Nickoloff, B. J., Osborne, B. A. & Miele, L. Notch signaling as a therapeutic target in cancer: a new approach to the development of cell fate modifying agents. *Oncogene* **22,** 6598–608 (2003).

134. Aster, J. C. & Blacklow, S. C. Targeting the Notch Pathway: Twists and Turns on the Road to Rational Therapeutics. *J. Clin. Oncol.* **30,** 2418–2420 (2012).

135. Ranganathan, P., Weaver, K. L. & Capobianco, A. J. Notch signalling in solid tumours: a little bit of everything but not all the time. *Nat. Rev. Cancer* **11,** 338–51 (2011).

136. Takebe, N., Nguyen, D. & Yang, S. X. Targeting notch signaling pathway in cancer: clinical development advances and challenges. *Pharmacol. Ther.* **141,** 140–9 (2014).

137. Fleming, R. J., Purcell, K. & Artavanis-Tsakonas, S. The NOTCH receptor and its ligands. *Trends Cell Biol.* **7,** 437–41 (1997).

138. Lendahl, U. A growing family of Notch ligands. *Bioessays* **20,** 103–7 (1998).

139. Gray, G. E. *et al.* Human ligands of the Notch receptor. *Am. J. Pathol.* **154,** 785–94 (1999).

140. Yamaguchi, E. *et al.* Expression of Notch ligands, Jagged1, 2 and Delta1 in antigen presenting cells in mice. *Immunol. Lett.* **81,** 59–64 (2002).

141. Logeat, F. *et al.* The Notch1 receptor is cleaved constitutively by a furin-like convertase. *Proc. Natl. Acad. Sci. U. S. A.* **95,** 8108–12 (1998).

142. Fortini, M. E. Gamma-secretase-mediated proteolysis in cell-surface-receptor signalling. *Nat. Rev. Mol. Cell Biol.* **3,** 673–84 (2002).

143. Kao, H. Y. *et al.* A histone deacetylase corepressor complex regulates the Notch signal transduction pathway. *Genes Dev.* **12,** 2269–77 (1998).

144. Ronchini, C. & Capobianco, A. J. Induction of cyclin D1 transcription and CDK2 activity by Notch(ic): implication for cell cycle disruption in transformation by Notch(ic). *Mol. Cell. Biol.* **21,** 5925–34 (2001).

145. Weng, A. P. *et al.* c-Myc is an important direct target of Notch1 in T-cell acute lymphoblastic leukemia/lymphoma. *Genes Dev.* **20,** 2096–109 (2006).

146. Hirose, H. *et al.* Notch pathway as candidate therapeutic target in Her2/Neu/ErbB2 receptor-negative breast tumors. *Oncol. Rep.* **23,** 35–43 (2010).

147. Yamaguchi, H., Chang, S.-S., Hsu, J. L. & Hung, M.-C. Signaling cross-talk in the resistance to HER family receptor targeted therapy. *Oncogene* **33,** 1073–1081 (2013).

148. Park, J. T. *et al.* Notch3 gene amplification in ovarian cancer. *Cancer Res.* **66,** 6312–8 (2006).

149. Jung, S. G. *et al.* Prognostic significance of Notch 3 gene expression in ovarian serous carcinoma. *Cancer Sci.* **101,** 1977–83 (2010).

150. Hopfer, O., Zwahlen, D., Fey, M. F. & Aebi, S. The Notch pathway in ovarian carcinomas and adenomas. *Br. J. Cancer* **93,** 709–718 (2005).

151. Park, J. T. *et al.* Notch3 overexpression is related to the recurrence of ovarian cancer and confers resistance to carboplatin. *Am. J. Pathol.* **177,** 1087–94 (2010).

152. McAuliffe, S. M. *et al.* Targeting Notch, a key pathway for ovarian cancer stem cells, sensitizes tumors to platinum therapy. *Proc. Natl. Acad. Sci. U. S. A.* **109,** E2939-48 (2012).

153. Rose, S. L., Kunnimalaiyaan, M., Drenzek, J. & Seiler, N. Notch 1 signaling is active in ovarian cancer. *Gynecol. Oncol.* **117,** 130–133 (2010).

154. Wang, M., Wu, L., Wang, L. & Xin, X. Down-regulation of Notch1 by gamma-secretase inhibition contributes to cell growth inhibition and apoptosis in ovarian cancer cells A2780. *Biochem. Biophys. Res. Commun.* **393,** 144–149 (2010).

155. Yap, T. A., Carden, C. P. & Kaye, S. B. Beyond chemotherapy: targeted therapies in ovarian cancer. *Nat. Rev. Cancer* **9,** 167–181 (2009).

156. Longuespée, R. *et al.* Ovarian cancer molecular pathology. *Cancer Metastasis Rev.* **31,** 713–732 (2012).

157. Toss, A. *et al.* Ovarian Cancer: Can Proteomics Give New Insights for Therapy and Diagnosis? *Int. J. Mol. Sci.* **14,** 8271–8290 (2013).

158. Pohl, G. *et al.* Inactivation of the mitogen-activated protein kinase pathway as a potential target-based therapy in ovarian serous tumors with KRAS or BRAF mutations. *Cancer Res.* **65,** 1994–2000 (2005).

159. Janku, F. *et al.* PI3K/AKT/mTOR inhibitors in patients with breast and gynecologic malignancies harboring PIK3CA mutations. *J. Clin. Oncol.* **30,** 777–82 (2012).

160. Li, H., Zeng, J. & Shen, K. PI3K/AKT/mTOR signaling pathway as a therapeutic target for ovarian cancer. *Arch. Gynecol. Obstet.* **290,** 1067–1078 (2014).

161. Edkins, S. *et al.* Recurrent KRAS codon 146 mutations in human colorectal cancer. *Cancer Biol. Ther.* **5,** 928–32 (2006).

162. Harris, T. J. R. & McCormick, F. The molecular pathology of cancer. *Nat. Rev. Clin. Oncol.* **7,** 251–65 (2010).

163. Li, H.-T., Lu, Y.-Y., An, Y.-X., Wang, X. & Zhao, Q.-C. KRAS, BRAF and PIK3CA mutations in human colorectal cancer: relationship with metastatic colorectal cancer. *Oncol. Rep.* **25,** 1691–7 (2011).

164. Stewart, C. J. R. *et al.* KRAS mutations in ovarian low-grade endometrioid adenocarcinoma: association with concurrent endometriosis. *Hum. Pathol.* **43,** 1177–83 (2012).

165. Lee, S., Choi, E.-J., Jin, C. & Kim, D.-H. Activation of PI3K/Akt pathway by PTEN reduction and PIK3CA mRNA amplification contributes to cisplatin resistance in an ovarian cancer cell line. *Gynecol. Oncol.* **97,** 26–34 (2005).

166. Dobbin, Z. C. & Landen, C. N. The Importance of the PI3K/AKT/MTOR Pathway in the Progression of Ovarian Cancer. *Int. J. Mol. Sci.* **14,** 8213–27 (2013).

167. Cantley, L. C. & Neel, B. G. New insights into tumor suppression: PTEN suppresses tumor formation by restraining the phosphoinositide 3-kinase/AKT pathway. *Proc. Natl. Acad. Sci. U. S. A.* **96,** 4240–5 (1999).

168. Meng, Q., Xia, C., Fang, J., Rojanasakul, Y. & Jiang, B.-H. Role of PI3K and AKT specific isoforms in ovarian cancer cell migration, invasion and proliferation through the p70S6K1 pathway. *Cell. Signal.* **18,** 2262–71 (2006).

169. Yan, X., Fraser, M., Qiu, Q. & Tsang, B. K. Over-expression of PTEN sensitizes human ovarian cancer cells to cisplatin-induced apoptosis in a p53-dependent manner. *Gynecol. Oncol.* **102,** 348–55 (2006).

170. Paige, A. J. & Brown, R. Pharmaco(epi)genomics in ovarian cancer. *Pharmacogenomics* **9,** 1825–1834 (2008).

171. Blanco-Aparicio, C., Renner, O., Leal, J. F. M. & Carnero, A. PTEN, more than the AKT pathway. *Carcinogenesis* **28,** 1379–86 (2007).

172. Manning, B. D. & Cantley, L. C. AKT/PKB signaling: navigating downstream. *Cell* **129,** 1261–74 (2007).

173. Datta, S. R. *et al.* Survival factor-mediated BAD phosphorylation raises the mitochondrial threshold for apoptosis. *Dev. Cell* **3,** 631–43 (2002).

174. Wullschleger, S., Loewith, R. & Hall, M. N. TOR signaling in growth and metabolism. *Cell* **124,** 471–84 (2006).

175. Mabuchi, S., Hisamatsu, T. & Kimura, T. Targeting mTOR signaling pathway in ovarian cancer. *Curr. Med. Chem.* **18,** 2960–8 (2011).

176. No, J. H. *et al.* Activation of mTOR signaling pathway associated with adverse prognostic factors of epithelial ovarian cancer. *Gynecol. Oncol.* **121,** 8–12 (2011).

177. Ho, K. K., Myatt, S. S. & Lam, E. W.-F. Many forks in the path: cycling with FoxO. *Oncogene* **27,** 2300–11 (2008).

178. Liang, J. *et al.* PKB/Akt phosphorylates p27, impairs nuclear import of p27 and opposes p27-mediated G1 arrest. *Nat. Med.* **8,** 1153–60 (2002).

179. Liang, J. & Slingerland, J. M. Multiple roles of the PI3K/PKB (Akt) pathway in cell cycle progression. *Cell Cycle* **2,** 339–45 (2003).

180. Roy, S. K., Srivastava, R. K. & Shankar, S. Inhibition of PI3K/AKT and MAPK/ERK pathways causes activation of FOXO transcription factor, leading to cell cycle arrest and apoptosis in pancreatic cancer. *J. Mol. Signal.* **5,** 10 (2010).

181. Zanella, F., Link, W. & Carnero, A. Understanding FOXO, new views on old transcription factors. *Curr. Cancer Drug Targets* **10,** 135–46 (2010).

182. Kajihara, T. *et al.* Differential Expression of FOXO1 and FOXO3a Confers Resistance to Oxidative Cell Death upon Endometrial Decidualization. *Mol. Endocrinol.* (2013).

183. Sunters, A. *et al.* Paclitaxel-induced nuclear translocation of FOXO3a in breast cancer cells is mediated by c-Jun NH2-terminal kinase and Akt. *Cancer Res.* **66,** 212–20 (2006).

184. Sunters, A. *et al.* FoxO3a transcriptional regulation of Bim controls apoptosis in paclitaxel-treated breast cancer cell lines. *J. Biol. Chem.* **278,** 49795–805 (2003).

185. Hui, R. C.-Y. *et al.* Doxorubicin activates FOXO3a to induce the expression of multidrug resistance gene ABCB1 (MDR1) in K562 leukemic cells. *Mol. Cancer Ther.* **7,** 670–8 (2008).

186. Francis, R. E. *et al.* FoxM1 is a downstream target and marker of HER2 overexpression in breast cancer. *Int. J. Oncol.* **35,** 57–68 (2009).

187. Krol, J. *et al.* The transcription factor FOXO3a is a crucial cellular target of gefitinib (Iressa) in breast cancer cells. *Mol. Cancer Ther.* **6,** 3169–79 (2007).

188. Fernandez de Mattos, S. *et al.* FoxO3a and BCR-ABL Regulate cyclin D2 Transcription through a STAT5/BCL6-Dependent Mechanism. *Mol. Cell. Biol.* **24,** 10058–10071 (2004).

189. Birkenkamp, K. U. *et al.* FOXO3a induces differentiation of Bcr-Abl-transformed cells through transcriptional down-regulation of Id1. *J. Biol. Chem.* **282,** 2211–20 (2007).

190. Myatt, S. S. & Lam, E. W.-F. The emerging roles of forkhead box (Fox) proteins in cancer. *Nat. Rev. Cancer* **7,** 847–59 (2007).

191. Wilson, M. S. C., Brosens, J. J., Schwenen, H. D. C. & Lam, E. W.-F. FOXO and FOXM1 in cancer: the FOXO-FOXM1 axis shapes the outcome of cancer chemotherapy. *Curr. Drug Targets* **12,** 1256–66 (2011).

192. Kwok, J. M.-M. *et al.* FOXM1 confers acquired cisplatin resistance in breast cancer cells. *Mol. Cancer Res.* **8,** 24–34 (2010).

193. Mencalha, A. L., Binato, R., Ferreira, G. M., Du Rocher, B. & Abdelhay, E. Forkhead box M1 (FoxM1) gene is a new STAT3 transcriptional factor target and is essential for proliferation, survival and DNA repair of K562 cell line. *PLoS One* **7,** e48160 (2012).

194. Yang, C. *et al.* Inhibition of FOXM1 transcription factor suppresses cell proliferation and tumor growth of breast cancer. *Cancer Gene Ther.* **20,** 117–24 (2013).

195. Wang, Z. *et al.* FoxM1 is a Novel Target of a Natural Agent in Pancreatic Cancer. *Pharm. Res.* **27,** 1159–1168 (2010).

196. Kinross, K. M. *et al.* In vivo activity of combined PI3K/mTOR and MEK inhibition in a Kras(G12D);Pten deletion mouse model of ovarian cancer. *Mol. Cancer Ther.* **10,** 1440–9 (2011).

197. Abe, A. *et al.* PIK3CA overexpression is a possible prognostic factor for favorable survival in ovarian clear cell carcinoma. *Hum. Pathol.* **44,** 199–207 (2013).

198. Huang, J. *et al.* Frequent genetic abnormalities of the PI3K/AKT pathway in primary ovarian cancer predict patient outcome. *Genes. Chromosomes Cancer* **50,** 606–18 (2011).

199. Rivlin, N., Brosh, R., Oren, M. & Rotter, V. Mutations in the p53 Tumor Suppressor Gene: Important Milestones at the Various Steps of Tumorigenesis. *Genes Cancer* **2,** 466–74 (2011).

200. Kandoth, C. *et al.* Mutational landscape and significance across 12 major cancer types. *Nature* **502,** 333–9 (2013).

201. Hammond, E. M. & Giaccia, A. J. The role of p53 in hypoxia-induced apoptosis. *Biochem. Biophys. Res. Commun.* **331,** 718–25 (2005).

202. Hoffman, W. H., Biade, S., Zilfou, J. T., Chen, J. & Murphy, M. Transcriptional repression of the anti-apoptotic survivin gene by wild type p53. *J. Biol. Chem.* **277,** 3247–57 (2002).

203. Vogelstein, B., Lane, D. & Levine, A. J. Surfing the p53 network. *Nature* **408,** 307–10 (2000).

204. Bartel, F. *et al.* Both germ line and somatic genetics of the p53 pathway affect ovarian cancer incidence and survival. *Clin. Cancer Res.* **14,** 89–96 (2008).

205. de Graeff, P. *et al.* Modest effect of p53, EGFR and HER-2/neu on prognosis in epithelial ovarian cancer: a meta-analysis. *Br. J. Cancer* **101,** 149–59 (2009).

206. Gadducci, A., Cosio, S., Tana, R. & Genazzani, A. R. Serum and tissue biomarkers as predictive and prognostic variables in epithelial ovarian cancer. *Crit. Rev. Oncol. Hematol.* **69,** 12–27 (2009).

207. Canevari, S., Gariboldi, M., Reid, J. F., Bongarzone, I. & Pierotti, M. A. Molecular predictors of response and outcome in ovarian cancer. *Crit. Rev. Oncol. Hematol.* **60,** 19–37 (2006).

208. Knudson, A. G. & Jr. Mutation and cancer: statistical study of retinoblastoma. *Proc. Natl. Acad. Sci. U. S. A.* **68,** 820–3 (1971).

209. Sigal, A. & Rotter, V. Oncogenic mutations of the p53 tumor suppressor: the demons of the guardian of the genome. *Cancer Res.* **60,** 6788–93 (2000).

210. Chène, P. In vitro analysis of the dominant negative effect of p53 mutants. *J. Mol. Biol.* **281,** 205–9 (1998).

211. Kern, S. E. *et al.* Oncogenic forms of p53 inhibit p53-regulated gene expression. *Science* **256,** 827–30 (1992).

212. Unger, T., Mietz, J. A., Scheffner, M., Yee, C. L. & Howley, P. M. Functional domains of wild-type and mutant p53 proteins involved in transcriptional regulation, transdominant inhibition, and transformation suppression. *Mol. Cell. Biol.* **13,** 5186–94 (1993).

213. Harris, S. L. & Levine, A. J. The p53 pathway: positive and negative feedback loops. *Oncogene* **24,** 2899–2908 (2005).

214. Piette, J., Neel, H. & Maréchal, V. Mdm2: keeping p53 under control. *Oncogene* **15,** 1001–10 (1997).

215. Manfredi, J. J. The Mdm2-p53 relationship evolves: Mdm2 swings both ways as an oncogene and a tumor suppressor. *Genes Dev.* **24,** 1580–9 (2010).

216. Marks, J. R. *et al.* Overexpression and mutation of p53 in epithelial ovarian cancer. *Cancer Res.* **51,** 2979–84 (1991).

217. Havrilesky, L. *et al.* Prognostic significance of p53 mutation and p53 overexpression in advanced epithelial ovarian cancer: a Gynecologic Oncology Group Study. *J. Clin. Oncol.* **21,** 3814–25 (2003).

218. Tai, Y. T. *et al.* BAX protein expression and clinical outcome in epithelial ovarian cancer. *J. Clin. Oncol.* **16,** 2583–90 (1998).

219. Ziółkowska-Seta, I. *et al.* TP53, BCL-2 and BAX analysis in 199 ovarian cancer patients treated with taxane-platinum regimens. *Gynecol. Oncol.* **112,** 179–84 (2009).

220. Ozer, H. *et al.* Immunohistochemistry with apoptotic-antiapoptotic proteins (p53, p21, bax, bcl-2), c-kit, telomerase, and metallothionein as a diagnostic aid in benign, borderline, and malignant serous and mucinous ovarian tumors. *Diagn. Pathol.* **7,** 124 (2012).

221. Reles, A. *et al.* Correlation of p53 mutations with resistance to platinum-based chemotherapy and shortened survival in ovarian cancer. *Clin. Cancer Res.* **7,** 2984–97 (2001).

222. Rose, S. L. *et al.* The impact of p53 protein core domain structural alteration on ovarian cancer survival. *Clin. Cancer Res.* **9,** 4139–44 (2003).

223. Skirnisdóttir, I., Seidal, T., Gerdin, E. & Sorbe, B. The prognostic importance of p53, bcl-2, and bax in early stage epithelial ovarian carcinoma treated with adjuvant chemotherapy. *Int. J. Gynecol. Cancer* **12,** 265–76 (2002).

224. Tan, D. S. P. & Kaye, S. Ovarian clear cell adenocarcinoma: a continuing enigma. *J. Clin. Pathol.* **60,** 355–60 (2007).

225. Yamaguchi, K. *et al.* Identification of an ovarian clear cell carcinoma gene signature that reflects inherent disease biology and the carcinogenic processes. *Oncogene* **29,** 1741–52 (2010).

226. Bach, I., Mattei, M. G., Cereghini, S. & Yaniv, M. Two members of an HNF1 homeoprotein family are expressed in human liver. *Nucleic Acids Res.* **19,** 3553–9 (1991).

227. Horikawa, Y. *et al.* Mutation in hepatocyte nuclear factor-1 beta gene (TCF2) associated with MODY. *Nat. Genet.* **17,** 384–5 (1997).

228. Tsuchiya, A. *et al.* Expression profiling in ovarian clear cell carcinoma: identification of hepatocyte nuclear factor-1 beta as a molecular marker and a possible molecular target for therapy of ovarian clear cell carcinoma. *Am. J. Pathol.* **163,** 2503–12 (2003).

229. Shen, H. *et al.* Epigenetic analysis leads to identification of HNF1B as a subtype-specific susceptibility gene for ovarian cancer. *Nat. Commun.* **4,** 1628 (2013).

230. Bali, A. *et al.* Cyclin D1, p53, and p21Waf1/Cip1 expression is predictive of poor clinical outcome in serous epithelial ovarian cancer. *Clin. Cancer Res.* **10,** 5168–77 (2004).

231. Barbieri, F. *et al.* Overexpression of cyclin D1 is associated with poor survival in epithelial ovarian cancer. *Oncology* **66,** 310–5 (2004).

232. Hashimoto, T. *et al.* Cyclin D1 predicts the prognosis of advanced serous ovarian cancer. *Exp. Ther. Med.* **2,** 213–219 (2011).

233. Sherr, C. J. Cancer cell cycles. *Science* **274,** 1672–7 (1996).

234. Gallagher, M. F. *et al.* Suppression of cancer stemness p21-regulating mRNA and microRNA signatures in recurrent ovarian cancer patient samples. *J. Ovarian Res.* **5,** 2 (2012).

235. Hindley, C. & Philpott, A. Co-ordination of cell cycle and differentiation in the developing nervous system. *Biochem. J.* **444,** 375–82 (2012).

236. Milde-Langosch, K., Hagen, M., Bamberger, A.-M. & Löning, T. Expression and prognostic value of the cell-cycle regulatory proteins, Rb, p16MTS1, p21WAF1, p27KIP1, cyclin E, and cyclin D2, in ovarian cancer. *Int. J. Gynecol. Pathol.* **22,** 168–74 (2003).

237. Oudit, G. Y. *et al.* The role of phosphoinositide-3 kinase and PTEN in cardiovascular physiology and disease. *J. Mol. Cell. Cardiol.* **37,** 449–71 (2004).

238. Anttila, M. A. *et al.* p21/WAF1 expression as related to p53, cell proliferation and prognosis in epithelial ovarian cancer. *Br. J. Cancer* **79,** 1870–8 (1999).

239. Schmider-Ross, A. *et al.* Cyclin-dependent kinase inhibitors CIP1 (p21) and KIP1 (p27) in ovarian cancer. *J. Cancer Res. Clin. Oncol.* **132,** 163–70 (2006).

240. Sharma, S., Kelly, T. K. & Jones, P. A. Epigenetics in cancer. *Carcinogenesis* **31,** 27–36 (2010).

241. Kanwal, R. & Gupta, S. Epigenetic modifications in cancer. *Clin. Genet.* **81,** 303–11 (2012).

242. Jones, P. A. & Baylin, S. B. The epigenomics of cancer. *Cell* **128,** 683–92 (2007).

243. Lopez, J., Percharde, M., Coley, H. M., Webb, a & Crook, T. The context and potential of epigenetics in oncology. *Br. J. Cancer* **100,** 571–577 (2009).

244. Nguyen, H. T., Tian, G. & Murph, M. M. Molecular epigenetics in the management of ovarian cancer: are we investigating a rational clinical promise? *Front. Oncol.* **4,** 71 (2014).

245. Marks, P. *et al.* Histone deacetylases and cancer: causes and therapies. *Nat. Rev. Cancer* **1,** 194–202 (2001).

246. Seeber, L. M. S. & van Diest, P. J. Epigenetics in ovarian cancer. *Methods Mol. Biol.* **863,** 253–69 (2012).

247. Watson, J. Watson J.D., et al. Molecular Biology of the Gene (5th edition, 2004)b.pdf. *BioScience* **16,** 209 (2004).

248. Kouzarides, T. Chromatin modifications and their function. *Cell* **128,** 693–705 (2007).

249. Clark, S. J. & Melki, J. DNA methylation and gene silencing in cancer: which is the guilty party? *Oncogene* **21,** 5380–7 (2002).

250. Gardiner-Garden, M. & Frommer, M. CpG islands in vertebrate genomes. *J. Mol. Biol.* **196,** 261–82 (1987).

251. Lund, A. H. & van Lohuizen, M. Epigenetics and cancer. *Genes Dev.* **18,** 2315–35 (2004).

252. Jones, P. A. & Baylin, S. B. The fundamental role of epigenetic events in cancer. *Nat. Rev. Genet.* **3,** 415–28 (2002).

253. Baylin, S. B. & Chen, W. Y. Aberrant gene silencing in tumor progression: implications for control of cancer. *Cold Spring Harb. Symp. Quant. Biol.* **70,** 427–33 (2005).

254. Horak, P. *et al.* Contribution of epigenetic silencing of tumor necrosis factor-related apoptosis inducing ligand receptor 1 (DR4) to TRAIL resistance and ovarian cancer. *Mol. Cancer Res.* **3,** 335–43 (2005).

255. Baldwin, R. L. *et al.* BRCA1 promoter region hypermethylation in ovarian carcinoma: a population-based study. *Cancer Res.* **60,** 5329–33 (2000).

256. Hilton, J. L. *et al.* Inactivation of BRCA1 and BRCA2 in ovarian cancer. *J. Natl. Cancer Inst.* **94,** 1396–406 (2002).

257. McCoy, M. L., Mueller, C. R. & Roskelley, C. D. The role of the breast cancer susceptibility gene 1 (BRCA1) in sporadic epithelial ovarian cancer. *Reprod. Biol. Endocrinol.* **1,** 72 (2003).

258. Strathdee, G. *et al.* Primary ovarian carcinomas display multiple methylator phenotypes involving known tumor suppressor genes. *Am. J. Pathol.* **158,** 1121–7 (2001).

259. Wang, C. *et al.* Expression of BRCA1 protein in benign, borderline, and malignant epithelial ovarian neoplasms and its relationship to methylation and allelic loss of the BRCA1 gene. *J. Pathol.* **202,** 215–23 (2004).

260. Yang, H.-J., Liu, V. W. S., Wang, Y., Tsang, P. C. K. & Ngan, H. Y. S. Differential DNA methylation profiles in gynecological cancers and correlation with clinico-pathological data. *BMC Cancer* **6,** 212 (2006).

261. Bol, G. M. *et al.* Methylation profiles of hereditary and sporadic ovarian cancer. *Histopathology* **57,** 363–70 (2010).

262. Rathi, A. *et al.* Methylation profiles of sporadic ovarian tumors and nonmalignant ovaries from high-risk women. *Clin. Cancer Res.* **8,** 3324–31 (2002).

263. Kontorovich, T., Cohen, Y., Nir, U. & Friedman, E. Promoter methylation patterns of ATM, ATR, BRCA1, BRCA2 and p53 as putative cancer risk modifiers in Jewish BRCA1/BRCA2 mutation carriers. *Breast Cancer Res. Treat.* **116,** 195–200 (2009).

264. Chan, K. Y. K., Ozçelik, H., Cheung, A. N. Y., Ngan, H. Y. S. & Khoo, U.-S. Epigenetic factors controlling the BRCA1 and BRCA2 genes in sporadic ovarian cancer. *Cancer Res.* **62,** 4151–6 (2002).

265. Blasi, M. F. *et al.* A human cell-based assay to evaluate the effects of alterations in the MLH1 mismatch repair gene. *Cancer Res.* **66,** 9036–44 (2006).

266. Jiricny, J. & Nyström-Lahti, M. Mismatch repair defects in cancer. *Curr. Opin. Genet. Dev.* **10,** 157–61 (2000).

267. Murphy, M. A. & Wentzensen, N. Frequency of mismatch repair deficiency in ovarian cancer: a systematic review This article is a US Government work and, as such, is in the public domain of the United States of America. *Int. J. Cancer* **129,** 1914–22 (2011).

268. Zhang, H. *et al.* Expression and promoter methylation status of mismatch repair gene hMLH1 and hMSH2 in epithelial ovarian cancer. *Aust. N. Z. J. Obstet. Gynaecol.* **48,** 505–9 (2008).

269. Watanabe, Y. *et al.* A change in promoter methylation of hMLH1 is a cause of acquired resistance to platinum-based chemotherapy in epithelial ovarian cancer. *Anticancer Res.* **27,** 1449–52

270. Tam, K. F. *et al.* Methylation profile in benign, borderline and malignant ovarian tumors. *J. Cancer Res. Clin. Oncol.* **133,** 331–341 (2006).

271. Fu, S. *et al.* Phase 1b-2a study to reverse platinum resistance through use of a hypomethylating agent, azacitidine, in patients with platinum-resistant or platinum-refractory epithelial ovarian cancer. *Cancer* **117,** 1661–1669 (2011).

272. Fang, F. *et al.* A phase 1 and pharmacodynamic study of decitabine in combination with carboplatin in patients with recurrent, platinum-resistant, epithelial ovarian cancer. *Cancer* **116,** 4043–4053 (2010).

273. Lehrmann, H., Pritchard, L. L. & Harel-Bellan, A. Histone acetyltransferases and deacetylases in the control of cell proliferation and differentiation. *Adv. Cancer Res.* **86,** 41–65 (2002).

274. Gallinari, P., Di Marco, S., Jones, P., Pallaoro, M. & Steinkühler, C. HDACs, histone deacetylation and gene transcription: from molecular biology to cancer therapeutics. *Cell Res.* **17,** 195–211 (2007).

275. Richon, V. M., Garcia-Vargas, J. & Hardwick, J. S. Development of vorinostat: current applications and future perspectives for cancer therapy. *Cancer Lett.* **280,** 201–10 (2009).

276. Lee, J.-H., Choy, M. L. & Marks, P. A. Mechanisms of resistance to histone deacetylase inhibitors. *Adv. Cancer Res.* **116,** 39–86 (2012).

277. Hyun-Jung Kim, S.-C. B. Histone deacetylase inhibitors: molecular mechanisms of action and clinical trials as anti-cancer drugs. *Am. J. Transl. Res.* **3,** 166 (2011).

278. Richon, V. M. Targeting histone deacetylases: development of vorinostat for the treatment of cancer. *Epigenomics* **2,** 457–65 (2010).

279. Bolden, J. E., Peart, M. M. J. & Johnstone, R. R. W. Anticancer activities of histone deacetylase inhibitors. *Nat. Rev. Drug Discov.* **5,** 769–84 (2006).

280. Bolden, J., Peart, M. & Johnstone, R. Anticancer activities of histone deacetylase inhibitors. *Nat. Rev. Drug Discov.* (2006).

281. Marks, P. A. & Dokmanovic, M. Histone deacetylase inhibitors: discovery and development as anticancer agents. *Expert Opin. Investig. Drugs* **14,** 1497–511 (2005).

282. Dokmanovic, M., Clarke, C. & Marks, P. A. Histone deacetylase inhibitors: overview and perspectives. *Mol. Cancer Res.* **5,** 981–9 (2007).

283. Blander, G. & Guarente, L. The Sir2 family of protein deacetylases. *Annu. Rev. Biochem.* **73,** 417–35 (2004).

284. Luo, J. *et al.* Negative control of p53 by Sir2alpha promotes cell survival under stress. *Cell* **107,** 137–48 (2001).

285. Firestein, R. *et al.* The SIRT1 deacetylase suppresses intestinal tumorigenesis and colon cancer growth. *PLoS One* **3,** e2020 (2008).

286. Takai, N. & Narahara, H. Histone deacetylase inhibitor therapy in epithelial ovarian cancer. *J. Oncol.* **2010,** 458431 (2010).

287. Dokmanovic, M. & Marks, P. A. Prospects: histone deacetylase inhibitors. *J. Cell. Biochem.* **96,** 293–304 (2005).

288. Mercurio, C., Minucci, S. & Pelicci, P. G. Histone deacetylases and epigenetic therapies of hematological malignancies. *Pharmacol. Res.* **62,** 18–34 (2010).

289. Piekarz, R. L. & Bates, S. E. Epigenetic modifiers: basic understanding and clinical development. *Clin. Cancer Res.* **15,** 3918–26 (2009).

290. Burgess, A. *et al.* Histone deacetylase inhibitors specifically kill nonproliferating tumour cells. *Oncogene* **23,** 6693–701 (2004).

291. Chambers, A. E. *et al.* Histone acetylation-mediated regulation of genes in leukaemic cells. *Eur. J. Cancer* **39,** 1165–75 (2003).

292. Mitsiades, C. S. *et al.* Transcriptional signature of histone deacetylase inhibition in multiple myeloma: biological and clinical implications. *Proc. Natl. Acad. Sci. U. S. A.* **101,** 540–5 (2004).

293. Glaser, K. B. Defining the role of gene regulation in resistance to HDAC inhibitors--mechanisms beyond P-glycoprotein. *Leuk. Res.* **30,** 651–2 (2006).

294. Richon, V. M., Sandhoff, T. W., Rifkind, R. A. & Marks, P. A. Histone deacetylase inhibitor selectively induces p21WAF1 expression and gene-associated histone acetylation. *Proc. Natl. Acad. Sci. U. S. A.* **97,** 10014–9 (2000).

295. Vidal, A. & Koff, A. Cell-cycle inhibitors: three families united by a common cause. *Gene* **247,** 1–15 (2000).

296. Gui, C.-Y., Ngo, L., Xu, W. S., Richon, V. M. & Marks, P. A. Histone deacetylase (HDAC) inhibitor activation of p21WAF1 involves changes in promoter-associated proteins, including HDAC1. *Proc. Natl. Acad. Sci. U. S. A.* **101,** 1241–6 (2004).

297. Xu, W.-S., Perez, G., Ngo, L., Gui, C.-Y. & Marks, P. A. Induction of polyploidy by histone deacetylase inhibitor: a pathway for antitumor effects. *Cancer Res.* **65,** 7832–9 (2005).

298. Archer, S. Y., Meng, S., Shei, A. & Hodin, R. A. p21(WAF1) is required for butyrate-mediated growth inhibition of human colon cancer cells. *Proc. Natl. Acad. Sci. U. S. A.* **95,** 6791–6 (1998).

299. Hitomi, T., Matsuzaki, Y., Yokota, T., Takaoka, Y. & Sakai, T. p15(INK4b) in HDAC inhibitor-induced growth arrest. *FEBS Lett.* **554,** 347–50 (2003).

300. Minucci, S. & Pelicci, P. G. Histone deacetylase inhibitors and the promise of epigenetic (and more) treatments for cancer. *Nat. Rev. Cancer* **6,** 38–51 (2006).

301. Xu, Y. Regulation of p53 responses by post-translational modifications. *Cell Death Differ.* **10,** 400–3 (2003).

302. Zhao, Y. *et al.* Inhibitors of histone deacetylases target the Rb-E2F1 pathway for apoptosis induction through activation of proapoptotic protein Bim. *Proc. Natl. Acad. Sci. U. S. A.* **102,** 16090–5 (2005).

303. Ashkenazi, A. Targeting death and decoy receptors of the tumour-necrosis factor superfamily. *Nat. Rev. Cancer* **2,** 420–30 (2002).

304. Nakata, S. *et al.* Histone deacetylase inhibitors upregulate death receptor 5/TRAIL-R2 and sensitize apoptosis induced by TRAIL/APO2-L in human malignant tumor cells. *Oncogene* **23,** 6261–71 (2004).

305. Insinga, A. *et al.* Inhibitors of histone deacetylases induce tumor-selective apoptosis through activation of the death receptor pathway. *Nat. Med.* **11,** 71–6 (2005).

306. Jiang, X. & Wang, X. Cytochrome C-mediated apoptosis. *Annu. Rev. Biochem.* **73,** 87–106 (2004).

307. Rosato, R. R. & Grant, S. Histone deacetylase inhibitors: insights into mechanisms of lethality. *Expert Opin. Ther. Targets* **9,** 809–24 (2005).

308. Shao, Y., Gao, Z., Marks, P. A. & Jiang, X. Apoptotic and autophagic cell death induced by histone deacetylase inhibitors. *Proc. Natl. Acad. Sci. U. S. A.* **101,** 18030–5 (2004).

309. Kim, Y. K. *et al.* Histone deacetylase inhibitor apicidin-mediated drug resistance: involvement of P-glycoprotein. *Biochem. Biophys. Res. Commun.* **368,** 959–64 (2008).

310. Richon, V. M. Cancer biology: mechanism of antitumour action of vorinostat (suberoylanilide hydroxamic acid), a novel histone deacetylase inhibitor. *Br. J. Cancer* **95,** S2–S6 (2006).

311. Cooper, A. L. *et al.* In vitro and in vivo histone deacetylase inhibitor therapy with suberoylanilide hydroxamic acid (SAHA) and paclitaxel in ovarian cancer. *Gynecol. Oncol.* **104,** 596–601 (2007).

312. Serpa, J. *et al.* Butyrate-rich colonic microenvironment is a relevant selection factor for metabolically adapted tumor cells. *J. Biol. Chem.* **285,** 39211–23 (2010).

313. Rajendran, P., Williams, D. E., Ho, E. & Dashwood, R. H. Metabolism as a key to histone deacetylase inhibition. *Crit. Rev. Biochem. Mol. Biol.* **46,** 181–99 (2011).

314. Rodríguez-Paredes, M. & Esteller, M. Cancer epigenetics reaches mainstream oncology. *Nat. Med.* 330–339 (2011). doi:10.1038/nm.2305

315. Frew, A. J., Johnstone, R. W. & Bolden, J. E. Enhancing the apoptotic and therapeutic effects of HDAC inhibitors. *Cancer Lett.* **280,** 125–33 (2009).

316. Deroanne, C. F. *et al.* Histone deacetylases inhibitors as anti-angiogenic agents altering vascular endothelial growth factor signaling. *Oncogene* **21,** 427–36 (2002).

317. Cohen, L. A. *et al.* Suberoylanilide hydroxamic acid (SAHA), a histone deacetylase inhibitor, suppresses the growth of carcinogen-induced mammary tumors. *Anticancer Res.* **22,** 1497–504 (2002).

318. Butler, L. M. *et al.* Suberoylanilide hydroxamic acid, an inhibitor of histone deacetylase, suppresses the growth of prostate cancer cells in vitro and in vivo. *Cancer Res.* **60,** 5165–5170 (2000).

319. He, L.-Z. *et al.* Histone deacetylase inhibitors induce remission in transgenic models of therapy-resistant acute promyelocytic leukemia. *J. Clin. Invest.* **108,** 1321–1330 (2001).

320. Lindemann, R. K. *et al.* Analysis of the apoptotic and therapeutic activities of histone deacetylase inhibitors by using a mouse model of B cell lymphoma. *Proc. Natl. Acad. Sci. U. S. A.* **104,** 8071–6 (2007).

321. Kerr, J. S. *et al.* Nonclinical Safety Assessment of the Histone Deacetylase Inhibitor Vorinostat. *Int. J. Toxicol.* **29,** 3–19 (2009).

322. Lane, A. A. & Chabner, B. A. Histone deacetylase inhibitors in cancer therapy. *J. Clin. Oncol.* **27,** 5459–68 (2009).

323. Siegel, D. *et al.* Vorinostat in solid and hematologic malignancies. *J. Hematol. Oncol.* **2,** 31 (2009).

324. Kelly, W. K. & Marks, P. A. Drug insight: Histone deacetylase inhibitors--development of the new targeted anticancer agent suberoylanilide hydroxamic acid. *Nat. Clin. Pract. Oncol.* **2,** 150–7 (2005).

325. Hayashi, A. *et al.* Type-specific roles of histone deacetylase (HDAC) overexpression in ovarian carcinoma: HDAC1 enhances cell proliferation and HDAC3 stimulates cell migration with downregulation of E-cadherin. *Int. J. Cancer* **127,** 1332–46 (2010).

326. Ahmad, M. *et al.* Understanding histone deacetylases in the cancer development and treatment: an epigenetic perspective of cancer chemotherapy. *DNA Cell Biol.* **31 Suppl 1,** S62-71 (2012).

327. Ropero, S. & Esteller, M. The role of histone deacetylases (HDACs) in human cancer. (2007). doi:10.1016/j.molonc.2007.01.001

328. Jiao, F. *et al.* Aberrant expression of nuclear HDAC3 and cytoplasmic CDH1 predict a poor prognosis for patients with pancreatic cancer. *Oncotarget* **7,** 16505–16 (2016).

329. Müller, B. M. *et al.* Differential expression of histone deacetylases HDAC1, 2 and 3 in human breast cancer - overexpression of HDAC2 and HDAC3 is associated with clinicopathological indicators of disease progression. *BMC Cancer* **13,** 215 (2013).

330. Schneider, G., Krämer, O. H., Schmid, R. M. & Saur, D. Acetylation as a Transcriptional Control Mechanism—HDACs and HATs in Pancreatic Ductal Adenocarcinoma. *J. Gastrointest. Cancer* **42,** 85–92 (2011).

331. Sangha, R., Lara, P. N., Mack, P. C. & Gandara, D. R. Beyond antiepidermal growth factor receptors and antiangiogenesis strategies for nonsmall cell lung cancer: exploring a new frontier. *Curr. Opin. Oncol.* **21,** 116–23 (2009).

332. Bots, M. & Johnstone, R. W. Rational combinations using HDAC inhibitors. *Clin. Cancer Res.* **15,** 3970–7 (2009).

333. Khan, O. & La Thangue, N. B. Drug Insight: histone deacetylase inhibitor-based therapies for cutaneous T-cell lymphomas. *Nat. Clin. Pract. Oncol.* **5,** 714–26 (2008).

334. Duvic, M. *et al.* Phase 2 trial of oral vorinostat (suberoylanilide hydroxamic acid, SAHA) for refractory cutaneous T-cell lymphoma (CTCL). *Blood* **109,** 31–9 (2007).

335. Chen, S. *et al.* The anti-tumor effects and molecular mechanisms of suberoylanilide hydroxamic acid (SAHA) on the aggressive phenotypes of ovarian carcinoma cells. *PLoS One* **8,** e79781 (2013).

336. Hrzenjak, A. *et al.* Histone deacetylase inhibitor vorinostat suppresses the growth of uterine sarcomas in vitro and in vivo. *Mol. Cancer* **9,** 49 (2010).

337. Slingerland, M., Guchelaar, H.-J. & Gelderblom, H. Histone deacetylase inhibitors: an overview of the clinical studies in solid tumors. *Anticancer. Drugs* **25,** (2014).

338. Micci, F. *et al.* Genomic profile of ovarian carcinomas. *BMC Cancer* **14,** 315 (2014).

339. Jin, K. L. *et al.* Expression profile of histone deacetylases 1, 2 and 3 in ovarian cancer tissues. *J. Gynecol. Oncol.* **19,** 185–90 (2008).

340. Cristea, M., Han, E., Salmon, L. & Morgan, R. J. Practical considerations in ovarian cancer chemotherapy. *Ther. Adv. Med. Oncol.* **2,** 175–87 (2010).

341. Park, S. Y. *et al.* Histone deacetylases 1, 6 and 8 are critical for invasion in breast cancer. *Oncol. Rep.* **25,** 1677–81 (2011).

342. Brunmeir, R., Lagger, S. & Seiser, C. Histone deacetylase HDAC1/HDAC2-controlled embryonic development and cell differentiation. *Int. J. Dev. Biol.* **53,** 275–89 (2009).

343. Luo, Y. *et al.* Trans-regulation of histone deacetylase activities through acetylation. *J. Biol. Chem.* **284,** 34901–10 (2009).

344. Wilson, A. J. *et al.* HDAC4 promotes growth of colon cancer cells via repression of p21. *Mol. Biol. Cell* **19,** 4062–75 (2008).

345. Rey, M., Irondelle, M., Waharte, F., Lizarraga, F. & Chavrier, P. HDAC6 is required for invadopodia activity and invasion by breast tumor cells. *Eur. J. Cell Biol.* **90,** 128–35 (2011).

346. Ozdağ, H. *et al.* Differential expression of selected histone modifier genes in human solid cancers. *BMC Genomics* **7,** 90 (2006).

347. Kong, Y. *et al.* Histone deacetylase cytoplasmic trapping by a novel fluorescent HDAC inhibitor. *Mol. Cancer Ther.* **10,** 1591–9 (2011).

348. Zeng, L.-S. *et al.* Overexpressed HDAC4 is associated with poor survival and promotes tumor progression in esophageal carcinoma. *Aging (Albany. NY).* **8,** 1236–1248 (2016).

349. Giaginis, C. *et al.* Histone deacetylase (HDAC)-1, −2, −4 and −6 expression in human pancreatic adenocarcinoma: associations with clinicopathological parameters, tumor proliferative capacity and patients' survival. *BMC Gastroenterol.* (2015). doi:10.1186/s12876-015-0379-y

350. Shen, Y.-F., Wei, A.-M., Kou, Q., Zhu, Q.-Y. & Zhang, L. Histone deacetylase 4 increases progressive epithelial ovarian cancer cells via repression of p21 on fibrillar collagen matrices. *Oncol. Rep.* **35,** 948–54 (2015).

351. Boyault, C. *et al.* HDAC6 controls major cell response pathways to cytotoxic accumulation of protein aggregates. *Genes Dev.* **21,** 2172–81 (2007).

352. Shan, B. *et al.* Requirement of HDAC6 for transforming growth factor-beta1-induced epithelial-mesenchymal transition. *J. Biol. Chem.* **283,** 21065–73 (2008).

353. Tsunoda, K. *et al.* Nucleus accumbens-associated 1 contributes to cortactin deacetylation and augments the migration of melanoma cells. *J. Invest. Dermatol.* **131,** 1710–9 (2011).

354. Matsuyama, A. *et al.* In vivo destabilization of dynamic microtubules by HDAC6-mediated deacetylation. *EMBO J.* **21,** 6820–31 (2002).

355. Kawaguchi, Y. *et al.* The deacetylase HDAC6 regulates aggresome formation and cell viability in response to misfolded protein stress. *Cell* **115,** 727–38 (2003).

356. Matthias, P., Yoshida, M. & Khochbin, S. HDAC6 a new cellular stress surveillance factor. *Cell Cycle* **7,** 7–10 (2008).

357. Lee, Y.-S. *et al.* The cytoplasmic deacetylase HDAC6 is required for efficient oncogenic tumorigenesis. *Cancer Res.* **68,** 7561–9 (2008).

358. Sakuma, T. *et al.* Aberrant expression of histone deacetylase 6 in oral squamous cell carcinoma. *Int. J. Oncol.* **29,** 117–24 (2006).

359. Santo, L. *et al.* Preclinical activity, pharmacodynamic, and pharmacokinetic properties of a selective HDAC6 inhibitor, ACY-1215, in combination with bortezomib in multiple myeloma. *Blood* **119,** 2579–89 (2012).

360. Takai, N. *et al.* Human ovarian carcinoma cells: histone deacetylase inhibitors exhibit antiproliferative activity and potently induce apoptosis. *Cancer* **101,** 2760–70 (2004).

361. Glozak, M. A. & Seto, E. Histone deacetylases and cancer. *Oncogene* **26,** 5420–5432 (2007).

362. Juan, L.-J. *et al.* Histone Deacetylases Specifically Down-regulate p53-dependent Gene Activation*. (2000). doi:10.1074/jbc.M000202200

363. West, A. C. *et al.* An intact immune system is required for the anticancer activities of histone deacetylase inhibitors. *Cancer Res.* **73,** (2013).

364. Akasaka, K. *et al.* Loss of class III beta-tubulin induced by histone deacetylation is associated with chemosensitivity to paclitaxel in malignant melanoma cells. *J. Invest. Dermatol.* **129,** 1516–26 (2009).

365. Konecny, G. E. & Kristeleit, R. S. PARP inhibitors for BRCA1/2-mutated and sporadic ovarian cancer: current practice and future directions. *Br. J. Cancer* **115,** 1157–1173 (2016).

366. Chung, C. & Lee, R. An update on current and emerging therapies for epithelial ovarian cancer: Focus on poly(adenosine diphosphate-ribose) polymerase inhibition and antiangiogenesis. *J. Oncol. Pharm. Pract.* (2016). doi:10.1177/1078155216657165

367. Mann, B. S., Johnson, J. R., Cohen, M. H., Justice, R. & Pazdur, R. FDA Approval Summary: Vorinostat for Treatment of Advanced Primary Cutaneous T-Cell Lymphoma. *Oncologist* **12,** 1247–1252 (2007).

368. Mossman, D., Kim, K.-T. & Scott, R. J. Demethylation by 5-aza-2'-deoxycytidine in colorectal cancer cells targets genomic DNA whilst promoter CpG island methylation persists. *BMC Cancer* **10,** 366 (2010).

369. Livak, K. J. & Schmittgen, T. D. Analysis of relative gene expression data using real-time quantitative PCR and the 2(-Delta Delta C(T)) Method. *Methods* **25,** 402–8 (2001).

370. Elmore, S. Apoptosis: a review of programmed cell death. *Toxicol. Pathol.* **35,** 495–516 (2007).

371. Wirawan, E., Vanden Berghe, T., Lippens, S., Agostinis, P. & Vandenabeele, P. Autophagy: for better or for worse. *Cell Res.* **22,** 43–61 (2012).

372. Modesitt, S. C. & Parsons, S. J. In vitro and in vivo histone deacetylase inhibitor therapy with vorinostat and paclitaxel in ovarian cancer models: does timing matter? *Gynecol. Oncol.* **119,** 351–7 (2010).

373. Diyabalanage, H. V. K., Granda, M. L. & Hooker, J. M. Combination therapy: histone deacetylase inhibitors and platinum-based chemotherapeutics for cancer. *Cancer Lett.* **329,** 1–8 (2013).

374. Matulonis, U. *et al.* Phase I study of combination of vorinostat, carboplatin, and gemcitabine in women with recurrent, platinum-sensitive epithelial ovarian, fallopian tube, or peritoneal cancer. *Cancer Chemother. Pharmacol.* **76,** 417–23 (2015).

375. Aghajanian, C. *et al.* OCEANS: A Randomized, Double-Blind, Placebo-Controlled Phase III Trial of Chemotherapy With or Without Bevacizumab in Patients With Platinum-Sensitive Recurrent Epithelial Ovarian, Primary Peritoneal, or Fallopian Tube Cancer. *J Clin Oncol* **30,** (2012).

376. Meehan, R. S. *et al.* New treatment option for ovarian cancer: PARP inhibitors. *Gynecol. Oncol. Res. Pract.* **3,** 3 (2016).

377. Benafif, S. & Hall, M. An update on PARP inhibitors for the treatment of cancer. *Onco. Targets. Ther.* **8,** 519–28 (2015).

378. Singh, B. N. *et al.* Preclinical studies on histone deacetylase inhibitors as therapeutic reagents for endometrial and ovarian cancers. *Future Oncol.* **7,** 1415–28 (2011).

379. Olsen, E. A. *et al.* Phase IIB Multicenter Trial of Vorinostat in Patients With Persistent, Progressive, or Treatment Refractory Cutaneous T-Cell Lymphoma. *J. Clin. Oncol.* **25,** 3109–3115 (2007).

380. Modesitt, S. C. *et al.* A phase II study of vorinostat in the treatment of persistent or recurrent epithelial ovarian or primary peritoneal carcinoma: a Gynecologic Oncology Group study. *Gynecol. Oncol.* **109,** 182–6 (2008).

381. Xu, W. S., Parmigiani, R. B. & Marks, P. A. Histone deacetylase inhibitors: molecular mechanisms of action. *Oncogene* **26,** 5541–52 (2007).

382. Mottamal, M., Zheng, S., Huang, T. L. & Wang, G. Histone Deacetylase Inhibitors in Clinical Studies as Templates for New Anticancer Agents. *Molecules* **20,** 3898–3941 (2015).

383. Al-Yacoub, N. *et al.* Apoptosis induction by SAHA in cutaneous T-cell lymphoma cells is related to downregulation of c-FLIP and enhanced TRAIL signaling. *J. Invest. Dermatol.* **132,** 2263–74 (2012).

384. Luu, T. H. *et al.* A phase II trial of vorinostat (suberoylanilide hydroxamic acid) in metastatic breast cancer: a California Cancer Consortium study. *Clin. Cancer Res.* **14,** 7138–42 (2008).

385. Dupéré-Richer, D. *et al.* Vorinostat-induced autophagy switches from a death-promoting to a cytoprotective signal to drive acquired resistance. *Cell Death Dis.* **4,** e486 (2013).

386. Hou, W., Han, J., Lu, C., Goldstein, L. A. & Rabinowich, H. Autophagic degradation of active caspase-8: a crosstalk mechanism between autophagy and apoptosis. *Autophagy* **6,** 891–900 (2010).

387. Lum, J. J. *et al.* Growth Factor Regulation of Autophagy and Cell Survival in the Absence of Apoptosis. *Cell* **120,** 237–248 (2005).

388. Chen, M.-Y. *et al.* Decitabine and suberoylanilide hydroxamic acid (SAHA) inhibit growth of ovarian cancer cell lines and xenografts while inducing expression of imprinted tumor suppressor genes, apoptosis, G2/M arrest, and autophagy. *Cancer* **117,** 4424–38 (2011).

389. Martin, T. A., Ye, L., Sanders, A. J., Lane, J. & Jiang, W. G. Cancer Invasion and Metastasis: Molecular and Cellular Perspective. (2013).

390. Quail, D. F. & Joyce, J. A. Microenvironmental regulation of tumor progression and metastasis. *Nat. Med.* **19,** 1423–37 (2013).

391. Sonnemann, J. *et al.* Comparative evaluation of the treatment efficacy of suberoylanilide hydroxamic acid (SAHA) and paclitaxel in ovarian cancer cell lines and primary ovarian cancer cells from patients. *BMC Cancer* **6,** 183 (2006).

392. Pectasides, D., Pectasides, E., Psyrri, A. & Economopoulos, T. Treatment Issues in Clear Cell Carcinoma of the Ovary: A Different Entity? *Oncologist* **11,** 1089–1094 (2006).

393. Kim, A. *et al.* Enhanced expression of Annexin A4 in clear cell carcinoma of the ovary and its association with chemoresistance to carboplatin. *Int. J. Cancer* **125,** 2316–22 (2009).

394. Angelucci, A. *et al.* Suberoylanilide hydroxamic acid partly reverses resistance to paclitaxel in human ovarian cancer cell lines. *Gynecol. Oncol.* **119,** 557–63 (2010).

395. Dietrich, C. S. *et al.* Suberoylanilide hydroxamic acid (SAHA) potentiates paclitaxel-induced apoptosis in ovarian cancer cell lines. *Gynecol. Oncol.* **116,** 126–130 (2010).

396. Nolan, L., Johnson, P. W. M., Ganesan, a, Packham, G. & Crabb, S. J. Will histone deacetylase inhibitors require combination with other agents to fulfil their therapeutic potential? *Br. J. Cancer* **99,** 689–94 (2008).

397. Fantin, V. R. & Richon, V. M. Mechanisms of resistance to histone deacetylase inhibitors and their therapeutic implications. *Clin. Cancer Res.* **13,** 7237–42 (2007).

398. Fujiwara, K., Shintani, D. & Nishikawa, T. symposium article Clear-cell carcinoma of the ovary. *Ann. Oncol.* **27,** 1–3 (2016).

399. Gounaris, I. & Brenton, J. D. Molecular pathogenesis of ovarian clear cell carcinoma. *Futur. Oncol.* **11,** 1389–1405 (2015).

400. Lim, D., Ip, P. P. C., Cheung, A. N. Y., Kiyokawa, T. & Oliva, E. Immunohistochemical Comparison of Ovarian and Uterine Endometrioid Carcinoma , Endometrioid Carcinoma. *Am J Surg Pathol* **39,** 1061–1069 (2015).

401. Kao, Y., Lin, M., Lin, W., Jeng, Y. & Mao, T. Utility of hepatocyte nuclear factor-1 b as a diagnostic marker in ovarian carcinomas with clear cells. *Histopathology* **61,** 760–8 (2012).

402. Shigetomi, H., Sudo, T. & Shimada, Þ. K. Inhibition of Cell Death and Induction of G2 Arrest Accumulation in Human Ovarian Clear Cells by HNF-1 A Transcription Factor Chemosensitivity Is Regulated by Checkpoint Kinase CHK1. *Int. J. Gynecol. Cancer* **24,** 838–843 (2014).

403. Park, S. J. *et al.* SAHA , an HDAC inhibitor , overcomes erlotinib resistance in human pancreatic cancer cells by modulating E-cadherin. *Tumor Biol.* **37,** 4323–30 (2015).

404. Ou, W. *et al.* HDACi inhibits liposarcoma via targeting of the MDM2-p53 signaling axis and PTEN , irrespective of p53 mutational status. *Oncotarget* **6,** 10510–10520 (2015).

405. Diss, E., Nalabothula, N., Nguyen, D., Chang, E. & Kwok, Y. VorinostatSAHA Promotes Hyper-Radiosensitivity in Wild Type p53 Human Glioblastoma Cells. *J Clin Oncol Res.* **2,** 1–16 (2014).

406. Liang, C.-C., Park, A. Y. & Guan, J.-L. In vitro scratch assay: a convenient and inexpensive method for analysis of cell migration in vitro. *Nat. Protoc.* **2,** 329–33 (2007).

407. Lin, C. *et al.* Valproic acid resensitizes cisplatin-resistant ovarian cancer. *Cancer Sci* | **99,** 1218–1226 (2008).

408. Yang, Y. *et al.* Initial characterization of the glutamate-cysteine ligase modifier subunit Gclm(-/-) knockout mouse. Novel model system for a severely compromised oxidative stress response. *J. Biol. Chem.* **277,** 49446–52 (2002).

409. Marks, P. A., Richon, V. M. & Rifkind, R. A. Histone Deacetylase Inhibitors : Inducers of Differentiation or Apoptosis of Transformed Cells. *J. Natl. Cancer Inst.* **92,** 2–8 (2000).

410. Chen, Z. *et al.* Induction and superinduction of growth arrest and DNA damage gene 45 (GADD45) a and b messenger RNAs by histone deacetylase inhibitors trichostatin A (TSA) and butyrate in SW620 human colon carcinoma cells. *Cancer Lett.* **188,** 127–140 (2002).

411. Ogryzko, V. V, Hirai, T. H., Russanova, V. R., Barbie, D. A. & Howard, B. H. Human Fibroblast Commitment to a Senescence-Like State in Response to Histone Deacetylase Inhibitors Is Cell Cycle Dependent. *Mol. Cell. Biol.* **16,** 5210–5218 (1996).

412. Silva, G., Cardoso, B. A., Belo, H. & Almeida, A. M. Vorinostat induces apoptosis and differentiation in myeloid malignancies: genetic and molecular mechanisms. *PLoS One* **8,** e53766 (2013).

413. Cardoso, B. A., Belo, H., Barata, J. T. & Almeida, A. M. The Bone Marrow-Mediated Protection of Myeloproliferative Neoplastic Cells to Vorinostat and Ruxolitinib Relies on the Activation of JNK and PI3K Signalling Pathways. *PLoS One* **10,** e0143897 (2015).

414. Fischer, M., Quaas, M., Steiner, L. & Engeland, K. The p53-p21-DREAM-CDE/CHR pathway regulates G2/M cell cycle genes. *Nucleic Acids Res.* **44,** 164–174 (2016).

415. Gartel, A. L. & Radhakrishnan, S. K. Lost in Transcription : p21 Repression , Mechanisms , and Consequences. *Cancer Res.* **65,** 3980–3985 (2005).

416. Lozano, G. The oncogenic roles of p53 mutants in mouse models. *Curr. Opin. Genet. Dev.* **17,** 66–70 (2007).

417. Weisz, L., Oren, M. & Rotter, V. Transcription regulation by mutant p53. *Oncogene* **53,** 2202–2211 (2007).

418. Strano, S. *et al.* Mutant p53 : an oncogenic transcription factor. *Oncogene* **53,** 2212–2219 (2007).

419. Papers, J. B. C. *et al.* Cyclin-dependent Kinases Phosphorylate p73 at Threonine 86 in a Cell Cycle-dependent Manner and Negatively Regulate p73 *. *J. Biol. Chem.* **278,** 27421–27431 (2003).

420. Das, C. & Kundu, T. K. Critical Review Transcriptional Regulation by the Acetylation of Nonhistone Proteins in Humans – A New Target for Therapeutics. *Life* **57,** 137–148 (2005).

421. Condorelli, F. *et al.* Inhibitors of histone deacetylase (HDAC) restore the p53 pathway in neuroblastoma cells. *Br. J. pharmocology* **153,** 657–668 (2008).

422. Luo, J. *et al.* Acetylation of p53 augments its site-specific DNA binding both in vitro and in vivo. *PNAS* **101,** 2259–2264 (2004).

423. Brooks, C. L. & Ã, W. G. Ubiquitination , phosphorylation and acetylation : the molecular basis for p53 regulation. *Curr. Opin. Cell Biol.* **15,** 164–171 (2003).

424. Yang, X.-J. & Seto, E. Lysine acetylation: codified crosstalk with other posttranslational modifications. *Mol. Cell* **31,** 449–461 (2008).

425. Yu, D. D., Guo, S. W., Jing, Y. Y., Dong, Y. L. & Wei, L. X. A review on hepatocyte nuclear factor - 1beta and tumor. *Cell Biosci.* **5,** 1–8 (2015).

426. Hnf-b, D. *et al.* Downregulation of HNF-1B in Renal Cell Carcinoma Is Associated With Tumor Progression and Poor Prognosis. *Urology* **76,** 507.e6-507.e11 (2010).

427. Chen, M. *et al.* Decitabine and suberoylanilide hydroxamic acid (SAHA) inhibit growth of ovarian cancer cell lines and xenografts while inducing expression of imprinted tumor suppressor genes, apoptosis, G2/M arrest and autophagy. *Cancer* **117,** 4424–4438 (2012).

428. Mendivil, A. A. *et al.* Increased incidence of severe gastrointestinal events with first-line paclitaxel, carboplatin, and vorinostat chemotherapy for advanced-stage epithelial ovarian, primary peritoneal, and fallopian tube cancer. *Int. J. Gynecol. Cancer* **23,** 533–9 (2013).

429. Modesitt, S. C., Sill, M., Hoffman, J. S. & Bender, D. P. A phase II study of vorinostat in the treatment of persistent or recurrent epithelial ovarian or primary peritoneal carcinoma : A Gynecologic Oncology Group study. *Gynecol. Oncol.* **109,** 182–186 (2008).

430. Kelly, W. K. *et al.* Phase I Clinical Trial of Histone Deacetylase Inhibitor : Suberoylanilide Hydroxamic Acid Administered Intravenously 1. *Clin. Cancer Res.* **9,** 3578–3588 (2003).

431. Li, J.-L. & Harris, A. L. Notch signaling from tumor cells: A new mechanism of angiogenesis. *Cancer Cell* **8,** 1–3 (2005).

432. Dufraine, J., Funahashi, Y. & Kitajewski, J. Notch signaling regulates tumor angiogenesis by diverse mechanisms. *Oncogene* **27,** 5132–5137 (2008).

433. Bolós, V., Grego-Bessa, J. & de la Pompa, J. L. Notch Signaling in Development and Cancer. *Endocr. Rev.* **28,** 339–363 (2007).

434. Capaccione, K. M. & Pine, S. R. The Notch signaling pathway as a mediator of tumor survival. *Carcinogenesis* **34,** 1420–30 (2013).

435. Tan, D. S. P., Miller, R. E. & Kaye, S. B. New perspectives on molecular targeted therapy in ovarian clear cell carcinoma. *Br. J. Cancer* **108,** 1553–1559 (2013).

436. Iso, T., Kedes, L. & Hamamori, Y. HES and HERP families: multiple effectors of the Notch signaling pathway. *J. Cell. Physiol.* **194,** 237–55 (2003).

437. Feldmann, G., Rauenzahn, S. & Maitra, A. In vitro models of pancreatic cancer for translational oncology research. *Expert Opin. Drug Discov.* **4,** 429–443 (2009).

438. Santo, V. E. *et al.* Drug screening in 3D in vitro tumor models: overcoming current pitfalls of efficacy read-outs. *Biotechnol. J.* **12,** 1600505 (2017).

439. Beaufort, C. M. *et al.* Ovarian cancer cell line panel (OCCP): clinical importance of in vitro morphological subtypes. *PLoS One* **9,** e103988 (2014).

440. Kallioniemi, O. P. *et al.* Optimizing comparative genomic hybridization for analysis of DNA sequence copy number changes in solid tumors. *Genes. Chromosomes Cancer* **10,** 231–43 (1994).

441. Roque, L., Rodrigues, R., Pinto, A., Moura-Nunes, V. & Soares, J. Chromosome imbalances in thyroid follicular neoplasms: a comparison between follicular adenomas and carcinomas. *Genes. Chromosomes Cancer* **36,** 292–302 (2003).

442. Santo, V. E. *et al.* Adaptable stirred-tank culture strategies for large scale production of multicellular spheroid-based tumor cell models. *J. Biotechnol.* **221,** 1–12 (2016).

443. O'Neill, C. J. & McCluggage, W. G. p16 expression in the female genital tract and its value in diagnosis. *Adv. Anat. Pathol.* **13,** 8–15 (2006).

444. Cory, G. *Cell Migration*. *Methods in molecular biology (Clifton, N.J.)* **769,** (Humana Press, 2011).

445. Pejovic, T. *et al.* Chromosome aberrations in 35 primary ovarian carcinomas. *Genes, Chromosom. Cancer* **4,** 58–68 (1992).

446. Bolton, K. L. *et al.* Common variants at 19p13 are associated with susceptibility to ovarian cancer. *Nat. Genet.* **42,** 880–4 (2010).

447. Boersma, B. J. *et al.* Association of Breast Cancer Outcome With Status of p53 and MDM2 SNP309. *JNCI J. Natl. Cancer Inst.* **98,** 911–919 (2006).

448. Berg, M. *et al.* DNA Sequence Profiles of the Colorectal Cancer Critical Gene Set KRAS-BRAF-PIK3CA-PTEN-TP53 Related to Age at Disease Onset. *PLoS One* **5,** e13978 (2010).

449. Aquilina, G. *et al.* Mismatch Repair and p53 Independently Affect Sensitivity to N-(2-chloroethyl)-N'-cyclohexyl-N-nitrosourea. *Clin. Cancer Res.* **6,** (2000).

450. Siddik, Z. H., Mims, B., Lozano, G. & Thai, G. Independent pathways of p53 induction by cisplatin and X-rays in a cisplatin-resistant ovarian tumor cell line. *Cancer Res.* **58,** 698–703 (1998).

451. Zanjirband, M., Edmondson, R. J. & Lunec, J. Pre-clinical efficacy and synergistic potential of the MDM2-p53 antagonists, Nutlin-3 and RG7388, as single agents and in combined treatment with cisplatin in ovarian cancer. *Oncotarget* **7,** 40115–40134 (2016).

452. Xie, X., Lozano, G. & Siddik, Z. H. Heterozygous p53V172F mutation in cisplatin-resistant human tumor cells promotes MDM4 recruitment and decreases stability and transactivity of p53. *Oncogene* **35,** 4798–4806 (2016).

453. Cadwell, C. & Zambetti, G. P. The effects of wild-type p53 tumor suppressor activity and mutant p53 gain-of-function on cell growth. *Gene* **277,** 15–30 (2001).

454. Jacob, F., Nixdorf, S., Hacker, N. F. & Heinzelmann-Schwarz, V. A. Reliable in vitro studies require appropriate ovarian cancer cell lines. *J. Ovarian Res.* **7,** 60 (2014).

455. Köbel, M. *et al.* Differences in tumor type in low-stage versus high-stage ovarian carcinomas. *Int. J. Gynecol. Pathol.* **29,** 203–11 (2010).

456. Kim, S. W. *et al.* Analysis of chromosomal changes in serous ovarian carcinoma using high-resolution array comparative genomic hybridization: Potential predictive markers of chemoresistant disease. *Genes. Chromosomes Cancer* **46,** 1–9 (2007).

457. Bancroft, J. D., Layton, C. (Histologist) & Suvarna, S. K. *Bancroft's theory and practice of histological techniques*.

458. Hanahan, D. & Weinberg, R. A. Hallmarks of cancer: the next generation. *Cell* **144,** 646–74 (2011).

459. Micci, F. *et al.* Array-CGH analysis of microdissected chromosome 19 markers in ovarian carcinoma identifies candidate target genes. *Genes Chromosom. Cancer* **49,** 1046–1053 (2010).

460. Estrada, M. F. *et al.* Modelling the tumour microenvironment in long-term microencapsulated 3D co-cultures recapitulates phenotypic features of disease progression. *Biomaterials* **78,** 50–61 (2016).

461. He, Z.-Y. *et al.* Ovarian cancer treatment with a tumor-targeting and gene expression-controllable lipoplex. *Sci. Rep.* **6,** 23764 (2016).

462. Katsumata, N. *et al.* Long-term results of dose-dense paclitaxel and carboplatin versus conventional paclitaxel and carboplatin for treatment of advanced epithelial ovarian, fallopian tube, or primary peritoneal cancer (JGOG 3016): a randomised, controlled, open-label trial. *Lancet. Oncol.* **14,** 1020–6 (2013).

463. Stark, D. *et al.* Standard chemotherapy with or without bevacizumab in advanced ovarian cancer: quality-of-life outcomes from the International Collaboration on Ovarian Neoplasms (ICON7) phase 3 randomised trial. *Lancet. Oncol.* **14,** 236–43 (2013).

464. Weichert, W. *et al.* Expression of class I histone deacetylases indicates poor prognosis in endometrioid subtypes of ovarian and endometrial carcinomas. *Neoplasia* **10,** 1021–7 (2008).

465. Wagner, T., Brand, P., Heinzel, T. & Krämer, O. H. Histone deacetylase 2 controls p53 and is a critical factor in tumorigenesis. *Biochim. Biophys. Acta* **1846,** 524–538 (2014).

466. Groeneweg, J. W., Foster, R., Growdon, W. B., Verheijen, R. H. & Rueda, B. R. Notch signaling in serous ovarian cancer. *J. Ovarian Res.* **7,** 95 (2014).